AFOSR - TR - 76 - 0513

Form Approved
Budget Bureau No. 22-R0293

DEPARTMENT OF GEOLOGICAL SCIENCES
210 KIMBALL HALL
CORNELL UNIVERSITY
ITHACA, NEW YORK 14853

AD A024344

FINAL REPORT

to

AIR FORCE OFFICE OF SCIENTIFIC RESEARCH

from

CORNELL UNIVERSITY

DEPARTMENT OF GEOLOGICAL SCIENCES

Title of Proposal: Integrated Geophysical and Geological Study of Earthquakes in Normally Aseismic Areas

Sponsored by: Advanced Research Projects Agency
ARPA Order No. 1827

Program Code: 4F10

Effective Date of Contract: 1 March 1973

Contract Expiration Date: 31 Dec 1975

Amount of Contract Dollars: $210,218

Contract Number: AFOSR 73-2494

Principal Investigators: Jack E. Oliver
(607) 256-2877

Bryan L. Isacks
(607) 256-2307

1976

256p.

DDC
RECEIVED
MAY 12 1976
B

Jack E. Oliver
Principal Investigator

AIR FORCE OFFICE OF SCIENTIFIC RESEARCH (AFSC)
NOTICE OF TRANSMITTAL TO DDC
This technical report has been reviewed and is approved for public release IAW AFR 190-12 (7b).
Distribution is unlimited.
A. D. BLOSE
Technical Information Officer

AF-AFOSR-2494-73
ARPA Order-1827

Bryan L. Isacks
Principal Investigator

402 984

DISCLAIMER NOTICE

THIS DOCUMENT IS THE BEST QUALITY AVAILABLE.

COPY FURNISHED CONTAINED A SIGNIFICANT NUMBER OF PAGES WHICH DO NOT REPRODUCE LEGIBLY.

Unclassified

SECURITY CLASSIFICATION OF THIS PAGE (When Data Entered)

REPORT DOCUMENTATION PAGE

READ INSTRUCTIONS BEFORE COMPLETING FORM

1. REPORT NUMBER: AFOSR - TR - 76 - 0513
2. GOVT ACCESSION NO.
3. RECIPIENT'S CATALOG NUMBER

4. TITLE (and Subtitle)
Integrated Geophysical and Geological Study of Earthquakes in Normally Aseismic Areas

5. TYPE OF REPORT & PERIOD COVERED
Final

6. PERFORMING ORG. REPORT NUMBER

7. AUTHOR(s)
Jack E. Oliber and Bryan L. Isacks
Compiled by James York

8. CONTRACT OR GRANT NUMBER(s)
AFOSR 73-2494

9. PERFORMING ORGANIZATION NAME AND ADDRESS
Cornell University
Ithaca, New York 14853

10. PROGRAM ELEMENT, PROJECT, TASK AREA & WORK UNIT NUMBERS
Program Element Code 62701E
Project-Task AO 1827-5

11. CONTROLLING OFFICE NAME AND ADDRESS
ARPA
1400 Wilson Boulevard
Arlington, Virginia 22209

12. REPORT DATE
1976

13. NUMBER OF PAGES
247

14. MONITORING AGENCY NAME & ADDRESS (if different from Controlling Office)
AFOSR/NP
Bolling AFB, Bldg. 410
Wash DC 20332

15. SECURITY CLASS. (of this report)
Unclassified

15a. DECLASSIFICATION DOWNGRADING SCHEDULE

16. DISTRIBUTION STATEMENT (of this Report)

17. DISTRIBUTION STATEMENT (of the abstract entered in Block 20, if different from Report)
Approved for public release; distribution unlimited.

18. SUPPLEMENTARY NOTES
TECH, OTHER

19. KEY WORDS (Continue on reverse side if necessary and identify by block number)
Intraplate tectonics, vertical movements, Quaternary faulting, releveling, tide gauges, LANDSAT, eastern United States, China

20. ABSTRACT (Continue on reverse side if necessary and identify by block number)
Information from precise leveling, sea level observations, geomorphology, photogeology, the sedimentary record, igneous activity, faulting, and theoretical geomechanics are brought to bear on understanding intraplate tectonics, especially in the eastern United States and China. Releveling data indicate vertical movements much faster than average geologic rates and possible movements on concealed faults. Intraplate faulting in the eastern U.S. and China extend the seismic record through Quaternary and earlier times.

DD FORM 1 JAN 73 1473 EDITION OF 1 NOV 65 IS OBSOLETE

Unclassified

ACCESSION for
NTIS White Section
DDC Buff Section
UNANNOUNCED
JUSTIFICATION
BY
DISTRIBUTION/AVAILABILITY CODES
Dist. AVAIL. and/or SPECIAL
A

TECHNICAL REPORT SUMMARY

Technical Problem

Although a consistent and relatively successful theoretical and empirical framework has been developed for understanding seismicity near lithospheric plate boundaries, earthquakes occurring within these boundaries remain a little understood phenomenon. Intraplate earthquakes are less common than seismic events in active tectonic regions, but they are known to reach large magnitudes. The fact that propagation of seismic energy is more efficient in at least some intraplate regions coupled with the general lack of engineering precautions against the occurrence of nearby earthquakes in these regions dramatically increases the potential destructiveness of a large intraplate event. In addition to the implications for seismic hazard evaluation, the general lack of knowledge concerning intraplate seismicity makes discrimination of such events from nuclear explosions very difficult. The problem which this study addresses is therefore to correlate what is known about intraplate seismicity, and to apply old and new research techniques to this study in order to develop a better understanding of the characteristics of the events.

General Method

In order to circumvent the limitations placed on studies of intraplate seismicity by the infrequent occurrence of such earthquakes, data from sources outside of seismology must be incorporated and evaluated in a study such as this one. Collection and synthesis of information from precise leveling, theoretical geomechanics, sea level observations, geomorphology, photogeology, the sedimentary record, igneous activity and faulting have been undertaken. Several literature reviews on related subjects have been completed. A complete data set of elevation change measurements for the eastern United States has been prepared in cooperation with the National Geodetic Survey. This leveling data has

been used to provide valuable information on vertical crustal movements in the eastern United States. Theoretical computations have been used to derive physical models of the forces which may be responsible for these leveling derived movements. The study group in photogeology has obtained and analyzed ERTS (now LANDSAT) and SKYLAB photographs of Eurasia and the United States. Special U-2 missions have been flown to provide detailed coverage of regions of particular interest in the United Staes. Mapping of photo features has been integrated with available seismic fault plane solutions, seismicity patterns, and in situ stress measurements. Field excursions were undertaken to verify and identify features indicated in aerial photographs of the eastern United States, as well as to investigate areas of particular interest as suggested by leveling and seismic studies.

In addition to the detailed research concerning the eastern United States, considerable effort has been directed at another intraplate region, China. In attempting to study the seismicity of intraplate regions one finds that mainland China is ideally suited for this type of investigation because of its relatively high seismic activity and large number of destructive earthquakes. In addition, the recorded history of Chinese earthquakes goes back much farther than any other area in the world, thus making China the best location for the study of time variations earthquake activity. Seismicity maps covering various time periods and magnitude ranges have been made. The use of the ERTS imagery and geomorphology permit one to determine recent crustal movements and to better define the tectonic structure of China. Based on the ERTS imagery, Quaternary faults in China have been mapped. Study of individual earthquake series and their aftershocks were carried out in order to define fault trends and to investigate the space, time, and magnitude variations along these zones of weakness. Such studies will help to determine the cause of the larger earthquakes such as the 1966 series near Hsing-t'ai in an area that was previously thought to be seismically inactive.

In order to evaluate the generality of the conclusions reached in the detailed research concerning the eastern United States and China, results of similar studies in other regions, particularly in Japan, Europe,

and the Soviet Union, were examined so that any fundamental relationships common to all areas can be discerned and contrasts understood.

Technical Results

Our efforts toward understanding normally aseismic regions with an integrated, interdisciplinary approach have focused on two geographic areas, with specific programs under each:

(1) Eastern United States
   (a) Cretaceous and Cenozoic faults and their relation to known seismicity
   (b) regional synthesis of vertical movements from releveling data
   (c) comparisons of releveling data and tide gauge measurements
   (d) local studies where releveling data suggests possible near-surface fault movements
   (e) possible systematic errors in releveling

(2) China
   (a) using ERTS imagery and seismicity data to study seismotectonics
   (b) relocating events in a earthquake swarm to determine the fault plane
   (c) Quaternary faulting in Taiwan

Cretaceous and Cenozoic faulting in eastern North America: Summary

Because Cretaceous and Cenozoic faulting occurred after the last major tectonic event in eastern North America, such faulting was produced in a normally aseismic region. Seismic data accumulate slowly in such regions, so data on faulting are valuable for understanding intraplate tectonics. Dating fault movement usually depends on the presense of Cretaceous and younger sediments or features such as glacial striations. Because such sediments are absent from most of eastern North America, intraplate surface faulting is probably much more abundant than reported here (see Appendix A). Furthermore, there have not been systematic field investigations for such faulting except in small areas. The known distribution of the faulting shows some correlation with

seismic regions such as the central Mississippi River valley and the Appalachians. However, some faults occur in areas with virtually no historic seismicity, implying that caution should be used in applying the historic record to determine future seismicity.

Recent Vertical Crustal Movements in the Eastern U.S.: Summary

Leveling data collected by the National Geodetic Survey have been used to construct regional and local profiles of apparent vertical crustal movement in the eastern United States. These profiles have been found to correlate with geological structure, suggesting that these structures may represent areas of crustal instability. Large regions of the eastern U.S. seem to exhibit coherent patterns of vertical crustal movement; for example, the Appalachians are presently rising with respect to the coastal areas, the Atlantic and Gulf Coastal Plains are subsiding relative to the continental interior, and the central U.S. is tilting down toward the east. See Appendix B for further discussion.

Recent Vertical Crustal Movements from Leveling and Sea Level Measurement Along the East Coast of the U.S.: Summary.

Sea level measurements indicate relative vertical crustal movements in the Atlantic coastal regions. Comparisons of sea level measurements with leveling results were used to investigate possible error sources in the two methods. Differences in sea-level measurements between separate locations may indicate possible short-term crustal movements (i.e. periods on the order of 100 years). In spite of the inherent uncertainties in both sea level and leveling results, we find that the apparent crustal movements indicated by these methods probably reflect real earth movements and provide important information on the tectonic processes operating in the eastern U.S. The results of this study are presented more fully in Appendix C. Although this region is called "aseismic", these results indicate that it is far from being "inactive".

Fault Movement and Leveling Data: Summary

When near surface faults suffer displacement with a significant vertical component (due either to earthquakes or gradual slip), one would expect to see relatively steep tilts in the surface deformation pattern derived from repeated levelings across active faults.

One of the most striking examples in the leveling data of the eastern United States which resembles fault displacement was noted in western Kentucky, just inside the Mississippi Embayment. After a detailed study of the data and the region, it was concluded that a fault here is indeed a plausible explanation of the anomalous movement seen in the leveling data. See Appendix D for a detailed discussion of these results.

The Refraction Error in Precise Leveling: Summary

Changes in the index of refraction of light, caused mainly by changes in air temperature, may cause systematic errors in leveling. Comparisons of two levelings with different errors will result in apparent, but unreal, vertical movements. Because our work is in part concerned with leveling data, the possible effect of such an error was investigated theoretically. Preliminary results with simple temperature gradients suggest that this error is not significant, but all possible temperature gradients have not been investigated thoroughly. See Appendix E for a detailed discussion of these results.

Seismicity and Quaternary Faulting in China: Summary

With newly made mosiacs of LANDSAT (formerly ERTS) imagery of China, criteria were developed to distinguish lineaments on the imagery that probably represent Quaternary faults. By analysis of LANDSAT imagery, large strike-slip faults in western China were noted for the first time. Both the map of faults and newly compiled seismicity maps show a change in tectonics from eastern to western China. As has been previously proposed, it appears that the tectonics in western China are dominated by the effects

of the collision of the India and Eurasia plates. A mosiac of small plates, as has been proposed for some other regions of diffuse seismicity, is not apparent for China. As in some other intraplate areas, Paleozoic mountain ranges still have minor seismicity associated with them. Detailed discussion on the seismotectonics of China is in Appendix F.

Investigation of the 1966 Earthquake Series in Northern China Using the Method of Joint Epicenter Determination: Summary

A series of destructive earthquakes occurred in northern China during March 1966 in an area with no previous instrumentally located seismicity. Examination of LANDSAT-1 imagery revealed evidence of recent surface faulting in this and other nearby regions of northern China. The method of "Joint Epicenter Determination" (JED) was used to relocate the epicenters of the earthquakes. These locations, along with published fault plane solutions, historical earthquake records, and LANDSAT-1 imagery are in very good agreement with the published field investigations that reported the earthquakes to have occurred along a large right-lateral strike-slip fault zone. The sense of motion on this strike-slip feature appears to be related to an extensional stress system oriented NNW-SSE in the region of the Shansi Graben and the North China Plain. Details of this report are in Appendix G.

Quaternary Faulting in Eastern Taiwan: Summary

Several recent hypotheses suggest that the intraplate seismicity within China is related to the tectonic activity along nearby plate boundaries. One poorly understood nearby plate boundary lies in Taiwan. There has been conflicting evidence on what type of boundary this is. Whether two plates converge here or slide by one another might change the predicted stress pattern within China. Therefore, geologic field work, partially supported by the AFOSR, was undertaken in Taiwan to help resolve this problem. A detailed report is attached as Appendix H. The main conclusion is that there has been a complicated combination of convergent and strike-slip motion in Taiwan over at least the past few million years.

APPENDIX A

CRETACEOUS AND CENOZOIC FAULTING IN EASTERN NORTH AMERICA

James E. York

Jack E. Oliver

Department of Geological Sciences

Cornell University

Ithaca, New York 14853

ABSTRACT

Observations of Cretaceous and Cenozoic faulting in eastern North America provide evidence of modest intraplate tectonic activity in this region. Thrust and gravity faults are found; strike-slip movement is not demonstrable but could have occurred in some cases. Fault movements are dated by offset Cretaceous, Tertiary, and Quaternary sediments, Cretaceous kimberlites, and Pleistocene glacial striations. Observed Cretaceous and Cenozoic displacements range from about 1 mm to several tens of meters. The faults are found in the central Mississippi River valley, the southeastern United States, the northeastern United States, and eastern Canada. Correlations between historic seismicity, fault plane solutions, and the Cretaceous and Cenozoic faulting in the central Mississippi River valley and the southeastern United States suggest a close causal relationship. The quality of the correlation between historic seismicity and Cretaceous and Cenozoic faulting in the northeastern United States and eastern Canada varies considerably from area to area, and hence the relation there between Cretaceous and Cenozoic faulting and contemporary seismotectonics is uncertain.

Sharp offsets in loosely consolidated sediments, the presence of slickensides and fault gouge, and the involvement of Precambrian or Paleozoic bedrock provide the best evidence that faulting was associated

with tectonic earthquakes. The displacement of near-surface deposits implies that surface faulting has occurred, although it has not been documented for modern earthquakes in eastern North America. In at least some cases displacements have occurred along pre-existing faults. The number and amounts of Cretaceous and Cenozoic movements on each fault has not been determined, but in at least one case the short time span available for movement suggests that an earthquake of about magnitude 6 was associated with the displacement. The largest Cretaceous and Cenozoic displacements must represent more than one movement.

The presence of both thrust and gravity faults and the inconsistent trends of the faults imply that stresses that vary spatially and/or temporally, rather than a single stress field acting steadily throughout the entire North America plate, are responsible for causing this intraplate tectonic activity. Key words: faults, seismotectonics, intraplate tectonics, eastern North America.

INTRODUCTION

Several large earthquakes have occurred in eastern North America during the past few hundred years. They include the 1663 St. Lawrence Valley earthquake (maximum Modified Mercalli Intensity X, Smith, 1962), the 1811-1812 series of earthquakes near New Madrid, Missouri (maximum intensity XII, Fuller, 1912), the 1886 Charleston, South Carolina earthquake (maximum intensity X, Dutton, 1889), and the 1929 earthquake near the Grand Banks of Newfoundland (magnitude 7, Smith, 1966). Many smaller but sometimes damaging shocks have also been felt (Fig. 1). Eastern North America does not include a major plate boundary, and simple plate tectonics theory does not account for deformation in the interior of the North American plate. Thus this area and some other intraplate

Fig. 1

areas are in that sense anomalous, and should be studied to provide a basic understanding of the earthquake phenomenon there.

Because the seismicity of eastern North America is not high, conventional seismological data such as the space-time-magnitude relationships of earthquakes and their focal mechanisms accumulate slowly; hence other sources of information are especially valuable. A complementary source of information is the geologic evidence for prehistoric earthquake activity. This geologic evidence consists mainly of observation of Cretaceous and Cenozoic faulting, the subject of this paper.

None of the faults discussed here can be considered as major tectonic features during the Cretaceous and Cenozoic. The San Andreas fault system in southern California has had displacements totaling nearly 300 km since late Miocene time (Crowell, 1973). The faulting discussed here is minor in comparison. However, in the absence of such large active faults in eastern North America, the Cretaceous and Cenozoic faulting represents a non-trivial record of crustal movements in an intraplate area.

PREVIOUS INVESTIGATIONS

Previous investigations of seismotectonics in eastern North America have attempted to relate contemporary tectonics to Paleozoic and Mesozoic tectonic features (Woollard, 1958, 1969; Fox, 1970), to stress measurements (Sbar and Sykes, 1973), to releveling measurements (Bollinger, 1973a; Brown and Oliver, in preparation), and to seismic wave travel time anomalies (Fletcher and others, 1974). Oliver and others (1970) summarized the occurrences and possible causes of post-glacial faulting in the northeastern United States and eastern Canada.

Few authors have dealt with the relationship between surface faulting

and earthquakes in eastern North America for several reasons. Firstly, there have been no reported cases of surface faulting during historic earthquakes in this region, except for some gravity faulting in unconsolidated sediments during the New Madrid earthquakes. Secondly, there are no known major faults with evidence of large scale movements since the Triassic. In more seismically active regions, such as California, instances of surface faulting during historic earthquakes and abundant evidence for Quaternary movement on major faults have led to extensive studies that help elucidate the tectonics of these regions (for example, Allen and others, 1965).

During the course of geological investigations, several authors have found evidence for Cretaceous and Cenozoic faulting in eastern North America (for example, see Fig. 2). Their reports, plus the success of studies correlating faults and seismicity in other regions, prompted the present field and literature search for Cretaceous and Cenozoic faulting.

Fig. 2

DESCRIPTION OF FAULTING

Data on known occurrences of exposed examples of Cretaceous and Cenozoic faulting in eastern North America is summarized with the appropriate references in Table 1 and Figure 3. At each locality listed in Table 1 there is only a single, usually manmade, exposure. The faults usually cannot be traced unambiguously over long distances because of the lack of a modern fault scarp or lack of differential erosion along the faults. To be included in Table 1, the fault must have been found by either a geologist who reported the fault in the available literature or the authors. This qualification usually implies that the fault must be exposed and must have occurred near the ground surface. In addition,

Table 1

Fig. 3

the fault must offset rocks or other features datable as Cretaceous or younger. Thus there very likely are large numbers of faults in eastern North America with Cretaceous and Cenozoic movement that are not included in Table 1.

Evidence for Cretaceous and Cenozoic faulting that would not qualify a fault for entry in Table 1 comes from reports of faults based on fault plane solutions for earthquakes (Street and others, 1974), seismic reflection profiles (Jacobeen, 1972), projected abrupt changes in Cretaceous or Cenozoic stratigraphy as well log data might indicate, escarpments (Fisk, 1944), lineations on aerial photography (Fisk, 1944) or satellite images (Withington, 1973), and other more speculative criteria. Some of these, especially the fault plane solutions, may represent Cretaceous or Cenozoic faulting, but we include here only cases where fault displacement has been observed and do not include cases based on interpretation of other data.

The gravity faults of the Gulf Coastal Plain are also not included even though some such faults are thought to have minor earthquakes and surface movement associated with them (Fisk, 1944, p. 33; Kehle, 1970). These are growth faults and do not seem to apply directly to the problem of why large earthquakes occur in eastern North America. Gravity faults exposed only in unconsolidated sediments are also not included, as such faults may be the result of local slumping.

Some characteristics of the faults described in Table 1 suggest that an earthquake was associated with fault movement, although there is no archeological or historical evidence to suggest that movement on any of the faults discussed here occurred during historic earthquakes. Firstly, observations that most of the faults form sharp dislocations in

unconsolidated sediments (for example, Fig. 4) suggest that a sudden movement caused the offset. If the displacements were the result of creep on a fault in the bedrock, a wider and more disordered zone would probably be formed in the unconsolidated sediments above the bedrock. Secondly, it can be seen that, in most cases, the fault is observed to cut Paleozoic or Precambrian bedrock. These observations show that the faults are not limited to the near-surface unconsolidated sediments. These two characteristics suggest, but do not prove, that the fault displacements observed at the surface resulted from the rapid upward propagation of faulting. It appears reasonable to assume that an earthquake accompanied this faulting.

Another characteristic of many of the Cretaceous and Cenozoic faults is the presence of fault gouge and slickensides. While gouge and slickensides are also characteristic of many known earthquake faults, they are not conclusive evidence in support of the association of earthquakes with movements on the Cretaceous and Cenozoic faults. They are, however, suggestive of this association.

It is desirable to distinguish between tectonic earthquakes and those caused by gravity-driven mass movements such as landslides. Landslides commonly include gravity faulting, and thrust faulting may occur at the toe of a landslide. However, there is no evidence in the present landscape to suggest that landslides caused any of the faults in Table 1, and involvement of the bedrock is further evidence against this association in some cases. Therefore, most of the faults in Table 1 probably represent tectonic effects.

Assuming that earthquakes were associated with movements on the faults, very rough estimates of the magnitudes of these earthquakes could, in principle, be made. Since we have no estimates of the lengths or

depths of the faults, we can deal only with displacements. Bonilla and Buchanan (1970) developed a relationship between magnitude and maximum fault displacement based on historic earthquakes with measured ground surface displacements and known magnitudes. Most of these earthquakes occurred in areas of higher seismicity than that of eastern North America, but let us assume their relationship applies to this area as well. For thrust faults, they find average surface displacements of about 3 m for a magnitude 8 earthquake, 1 m for a magnitude 7 earthquake, and 0.5 m for a magnitude 6 earthquake. They also find that surface displacements are usually not observed for earthquakes with magnitudes less than 6, although this observation could be caused by difficulty in detecting small surface displacements. Because one magnitude 7 earthquake is probably more destructive than two magnitude 6 earthquakes at the same locality, the determination of the number and amounts of movements that caused the displacements listed in Table 1 is of considerable significance. Unfortunately, there are usually no data on the number and amounts of movement. Although some of the displacements listed in Table 1 may represent just one movement, the larger ones, several tens of meters, probably represent more than one movement, because such large displacements are rarely associated with single earthquakes.

At the second Drewrys Bluff locality (Fig. 4) of Table 1, surface faulting of 0.6 m during a short interval in the Cretaceous can be demonstrated. Here faulted Cretaceous sediments of silt, sand, and peat are overlain by unfaulted, or at least much less offset, Cretaceous conglomerate. This relationship indicates that faulting occurred contemporaneously with sedimentation and at the surface. There was about one half meter of fault movement between the deposition of the sand, silt, and peat and the deposition of the conglomerate. This movement could

well have occurred in one earthquake, in which case the displacement of about one half meter suggests the earthquake had a magnitude of about 6. For the other faults in Table 1, the ages of fault movements cannot be bracketed by such a short time span.

IMPLICATIONS FOR CRETACEOUS AND CENOZOIC TECTONICS

In order to study only intraplate tectonics, the effects of faulting in eastern North America that were associated with the initial opening of ocean basins must be avoided. The initial opening of the Atlantic Ocean is dated as late Triassic and early Jurassic along most of eastern North America (Pitman and Talwani, 1972); hence, Cretaceous and Cenozoic tectonic activity in this region can be classified as intraplate tectonics. The rifting in the Baffin Bay-Labrador Sea area and along east Greenland is dated as Cretaceous and Tertiary (Pitman and Talwani, 1972). For this reason reported Cenozoic faults in west Greenland (Koch, 1929) are not included in this study; these faults displace Tertiary basalts. The age and mechanism of formation of the Gulf of Mexico and the Mississippi Embayment is less certain than those of the above two regions. However, the major faulting associated with the formation of the Mississippi Embayment can be dated as post-Carboniferous and pre-Cretaceous (King, 1951); hence the Cretaceous and Cenozoic faulting there can be classified as intraplate faulting.

The most recent movements on the faults described here can usually be dated only as younger than faulted Cretaceous, Tertiary, or Pleistocene sediments. For the faults listed in Table 1 only at the Drewrys Bluff locality described above can a lower limit to the age of faulting be found. Thus, although all the faulting described in Table 1 represents Cretaceous and Cenozoic tectonic activity, the precise time

of faulting may be quite different for different faults.

The Cretaceous and Cenozoic faults provide information on several aspects of intraplate tectonics in eastern North America. The first is the question of whether new faults are being formed in rocks of pre-Cretaceous age or whether old faults are being reactivated. Fox (1970) reported that most earthquakes in eastern North America occur in areas with known faulting, although the age of faulting can usually be dated only as Paleozoic or younger. Page and others (1968) have suggested that minor seismic activity along the New Jersey-New York border may be associated with the Ramapo fault, a Triassic graben border fault. At two localities in Table 1 the faults can be shown to be reactivated faults, because the displacement in the bedrock is greater than the displacement in the overlying Cretaceous and younger sediments. The first locality is near Greenwood, Virginia, whre the fault occurs in a major shear zone (Nelson, 1962) that is Paleozoic in age. The second locality is Pumpkin Hollow, New York. Here and at most other postglacial fault localities described by Oliver and others (1970) the faults occur along cleavage surfaces of slates. Offsets of small scale banding at Pumpkin Hollow and also at Halifax, Nova Scotia (Oliver and others, 1970) show that the fault had previous displacements larger than those of the scarps. Another case of a reactivated fault is reported to be near Smithland in western Kentucky (Rhoades and Mistler, 1941) but is not included in Table 1 because the fault plane is not exposed. At the Smithland locality, about 300 m of vertical movement is indicated by changes in elevation of rock units across a northeast-southwest trending fault, and only 40 to 50 m of this movement is Cretaceous or younger. At most localities in Table 1 the limited extent of exposed bedrock does not provide sufficient information to determine whether the fault is new or reactivated, but it is possible that all of the faulting in Table 1 occurred along preexist-

ing faults.

The second aspect of intraplate tectonics about which the Cretaceous and Cenozoic faulting gives evidence is the state of stress in part of the North American plate. Sbar and Sykes (1973) summarized data from in situ stress measurements and from earthquake fault plane solutions. They find evidence for east to northeast trending horizontal compressive stresses higher than would be expected from the lithostatic load, over an area from west of the Appalachian orogenic belt to the middle of the continent and from southern Illinois to southern Ontario. Within the Appalachians they do not find consistent trends. Using many more fault plane solutions, Street and others (1974) find a complicated stress pattern in the central United States. The data on Cretaceous and Cenozoic faulting do not show a consistent direction of maximum compressive stress axes for Cretaceous and Cenozoic time in the part of eastern North America covered by the data (Fig. 3). Thus, to whatever extent surface faulting is indicative of crustal stress, the data discussed here indicate that the stress system causing intraplate seismicity has varied spatially or temporally or both.

The faulting may also provide information on contemporary tectonics. In more seismically active regions, such as California, a fault which has not moved since the Cretaceous may often be considered as having no relation to contemporary tectonics. However, in eastern North America, earthquakes which occurred in, say, the early Tertiary are just as much a mystery as modern earthquakes. Understanding this paleoseismicity may be helpful in understanding contemporary tectonics, because both represent intraplate tectonic activity. Before discussing the relation of the faults in Table I to contemporary tectonics, two cases of faulting that may not be related to the present tectonic regime will be mentioned. Firstly, the faults

that offset Cretaceous kimberlites (dated by Zartman and others, 1967) may be associated with stresses that were active only near the time of intrusion. The second case is that of the postglacial faults described by Oliver and others (1970). These postglacial faults, which are in the northeastern United States and eastern Canada, usually occur along the cleavage surfaces of slates, have small displacements, usually less than a few centimeters, and are numerous. The field data on these postglacial faults appear to favor expansion of the rocks and subsequent rotation of the cleavage planes as the cause of faulting (Oliver and others, 1970). This expansion might have been caused by removal of the late Pleistocene ice load (Lawson, 1911). Although there is some seismicity in the region where these postglacial faults occur in the Appalachian Foldbelt, modern seismicity is virtually absent near similar occurrences in western Ontario. The varying quality of the correlation of these faults with historic seismicity suggests that the deformation is complete, although Sbar and Sykes (1973) do report cases of deformation of man-made structures in New York State and surrounding areas that indicate the continued presence of high stresses. Thus the relation of these postglacial faults to contemporary seismotectonics is still an open question.

The remainder of this discussion is limited to two regions, the central Mississippi River valley and the southeastern United States, where the correlation of Cretaceous and Cenozoic faulting with modern seismicity is better. Both regions have experienced moderate seismic activity in historic time (Fig. 1), and some trends of seismicity in these regions may be seen (Fig. 1). A first glance at Figure 1 reveals that small earthquakes occur throughout most of the eastern North America. However, most of the larger earthquakes occur along certain trends. One trend is along the Appalachian foldbelt. A parallel trend, without

apparent tectonic control, appears from the head of the Mississippi Embayment to the St. Lawrence Valley. Cross trends are seen in the northeastern United States-eastern Canada area and in South Carolina. Minor cross trends are present in the Mississippi Embayment region and in Virginia. In the following sections the trends of the faults will be compared with the seismic trends, with trends of major pre-Cretaceous fault zones and with fault plane solutions.

Central Mississippi River Valley

Historically, the central Mississippi River valley has been one of the most seismically active areas in eastern North America (Fig. 1). The data on the Cretaceous and Cenozoic faulting in this region (Fig. 5) suggest that this high activity had been characteristic of this region earlier in Cenozoic time also. This suggestion is based on three observations. Firstly, the density of Cretaceous and Cenozoic faults in this region is greater than in other areas of comparable size which are also covered with Cretaceous and younger sediments. Secondly, the magnitude of displacement on some of these faults is much greater than on most Cretaceous and Cenozoic faults in other parts of eastern North America. Thirdly, some post-Cretaceous tilting of sediments and formation of clastic dikes can be dated as pre-Pleistocene (Rhoades and Mistler, 1941).

Most of the faults shown in Figure 5 are only seen to involve unconsolidated sediments and hence cannot be shown to be continuations of faults in the basement. However, there are at least two cases where the consolidated Paleozoic sediments are also involved in the faulting. The first fault is at the Benton, Missouri locality (Table 1). This fault is not exposed but is based on well logs from 3 wells drilled by three different drilling companies (Grokskopf, 1955). In each well a sequence of Cretaceous and Ordovician sediments overlies another

sequence of Cretaceous and Ordovician sediments. This relationship indicates that a thrust fault is present between the two sequences. Assuming that the three fault locations determined from the well data represent the same fault, one obtains an east-west trending fault with a 1 degree dip to the south. This extremely low dip suggests that the assumption of one fault is in error and that two or three faults are present. The second fault that involves Paleozoic rocks trends northeast near Smithland in western Kentucky (Rhoades and Mistler, 1941) and is discussed above. Mateker and others (1968) also mention a northeast trending fault that cuts Paleozoic and Cretaceous rocks. Therefore, although some of the faults described in the Mississippi Embayment could be only surficial faults in unconsolidated sediments, at least some represent extensions of faults from Paleozoic rocks into younger sediments.

There are no major fault zones known in the Cretaceous and younger sediments of the Mississippi Embayment, but major fault zones do exist north of the embayment. Because of the lack of Cretaceous and younger sediments north of the embayment, fault movements there cannot easily be dated, except as post-Cretaceous, because they trend into the embayment and are there covered by Cretaceous sediments. The New Madrid fault zone is the major fault zone that is truncated by the Mississippi Embayment. This fault zone trends northeast from the northern end of the embayment (Heyl and others, 1965). The other fault zone that is truncated by the embayment is the Ste. Genevieve fault zone. This fault zone trends northwest from the northern end of the embayment (Heyl and others, 1965). The seismic trends (Fig. 1) also show a major northeast trend and a minor northwest cross trend. The fault plane solutions of Street and others (1974) show mostly northeast trending faults in the area of the exposed New Madrid fault zone and along its projection southwestward beneath

the embayment. Street and others (1974) also report west and northwest trending faults in southeast Missouri. Four of the Cretaceous and Cenozoic faults of Table 1 are subparallel to the northeast trend (Fig. 5). Faults at three localities in Table 1 are subparallel to the northwest trend (Fig. 5). The correlations of Cretaceous and Cenozoic fault strikes and fault plane solutions with pre-Cretaceous fault zones suggest that the pre-Cretaceous faults are being reactivated. The correlations of Cretaceous and Cenozoic fault strikes with historic seismic trends and with fault plane solutions suggest that the northeast and northwest trends are real and that these seismic trends had been active earlier in Cretaceous and Cenozoic time.

Southeastern United States

There are three main seismic trends in the southeastern United States. One is in the Appalachian orogenic belt and is parallel to the trend of the belt. The earthquakes in this trend occur mainly in the Blue Ridge and Valley and Ridge provinces (Fox, 1970). The other two trends are transverse and are in the Piedmont and Coastal Plain provinces in South Carolina and in Virginia (Fig. 1). The Quantico and Drewrys Bluff faults (Table 1) trend nearly east-west and are in the transverse seismic zone in Virginia. Some of the other Cretaceous and Cenozoic faults are subparallel to the Appalachian structures (Fig. 6), but this correlation is not highly convincing. This poor correlation may be caused by the complicated structure of the Appalachians or by the complicated nature of intraplate tectonics.

The Crystal River, Florida fault may be connected with movement on the Ocala uplift (Vernon, 1951). The region of the Ocala uplift is an area of minor seismic activity (Fig. 1), although, as elsewhere in eastern North America, the correlation between earthquakes and specific faults is uncertain.

The Deep River, North Carolina locality includes several gravity faults that offset Pliocene(?) high level surficial deposits, Mesozoic dikes, and earlier faults (Reinemund, 1955). These faults are within a Triassic graben. Quaternary gravity faulting with displacements of about 0.2 m has also been reported in Middlesex County, New Jersey (Ries and others, 1904; Salisbury and Knapp, 1917) in the Coastal Plain above other Triassic basin. Here only unconsolidated Quaternary sediments were seen to be faulted, and hence this locality is not included in Table 1. Gravity faulting was also indicated in northern New Jersey by a composite fault plane solution (Sbar and others, 1970). The continuation or reactivation of gravity faulting in Cenozoic time suggests that extensional stresses are important in contemporary tectonics, if this faulting is tectonic in origin and not merely slumping.

Two of the localities in Table 1 represent previously unreported faults. The second Drewrys Bluff, Virginia, entry in Table 1 represents three minor faults in addition to the one described (Fig. 4). All are located in the cliff along the south bank of the James River next to Fort Darling (a historical monument). Over a vertical distance of about 2 m, the dip of the main fault decreases towards the surface from 45 to 30 degrees, and the fault splays upward into several branches. Fault gouge is present, but no slickensides were observed.

The second previously unreported fault is about 2 km east of Saluda, Polk County, North Carolina (the third entry at this locality in Table 1). This fault is exposed in a road cut on the north side of country road 1122 approximately 1.2 km east of the intersection of country road 1122 and 1142. Here weathered migmatite has been thrust over reddish colluvium. No slickensides were found. Since the lower nonconformity between the colluvium and the migmitite is not exposed, only a minimum displacement

of 4 m can be determined.

CONCLUSIONS

A major unsolved problem in seismotectonics is lack of understanding of the processes responsible for generating the stresses that cause intraplate seismicity. Possible causes of these stresses include the effects of varying lithospheric thicknesses caused by isostatically compensated topography (Jeffreys, 1959; Artyushkov, 1974), erosion and subsequent isostatic uplift of the Appalachians, sedimentation in and subsequent depression of the Mississippi Embayment, and other vertical movements perhaps induced by lateral temperature and compositional variations that cause flow in the asthenosphere. Because both gravity and thrust faults are found, and because the strikes of the faults vary considerably, one must invoke stresses that vary spatially and/or temporally.

In regions of major active plate boundaries in continental areas, preexisting faults are usually reactivated during earthquakes, and faulting sometimes extends to the ground surface. These two characteristics of faulting have not been documented for modern earthquakes in eastern North America, and the question arises whether or not this lack of documentation is caused by the short time period of observations. The data on Cretaceous and Cenozoic intraplate faulting described here suggests that it is caused by the short time period of observations. Firstly, in some cases this intraplate faulting occurs along preexisting weaknesses. Secondly, the fact that the faults usually cut surficial deposits suggests that surface faulting has occurred. The lack of induration of these sediments suggests that they were not deeply buried, faulted, and then uplifted. Another indication of surface faulting in two cases is the decreasing dip of the fault plane as it approaches the surface. Finally, the correlations of the trends of the Cretaceous and Cenozoic

faulting in the central Mississippi River valley and in the southeastern United States with historic seismicity, with fault plane solutions, and with older fault zones suggest that the Cretaceous and Cenozoic faulting and contemporary seismotectonics in these regions have similar causes. Thus one may suppose that features of the Cretaceous and Cenozoic faulting, such as reactivation of pre-existing faults and surface faulting, will characterize some modern earthquakes.

The distribution of Cretaceous and Cenozoic faulting described here represents only a small sample of the faults that moved during this time period. Probably not all fault movements came near enough to the ground surface to be exposed at present. Furthermore, the inability to date many young fault movements and the lack of sufficient exposures to find the young movements that are datable surely keep many examples of Cretaceous and Cenozoic faulting from being identified. Therefore many more cases of Cretaceous and Cenozoic faulting very likely exist in eastern North America. Also, because the distribution of Cretaceous and younger sediments, which are usually needed to date the young fault movements, has varied throughout time as these sediments are deposited and eroded, the distribution of the Cretaceous and Cenozoic faulting described here is a function of the location of young sediment cover as well as a function of seismicity. Still, in the southeastern United States and central Mississippi River valley, the Cretaceous and Cenozoic faults are found only in areas that have experienced some historic seismicity. Thus, in these regions, there is some support to the suggestion that the seismicity is associated with faulting.

No data on Cretaceous and Cenozoic faulting have been found to help elucidate the tectonics around Charleston, South Carolina. This lack of data is possibly caused by the thickness (more than 1000 m) of Coastal Plain sediments here, because fault movements in the basement

rocks may not remain as sharp breaks throughout this thickness of sediments. Whether such large earthquakes may occur elsewhere in the Coastal Plain or at other locations in eastern North America that have experienced little historic seismicity, or whether these large earthquakes will reoccur only near previous historic locations, is still not known. Faults such as those illustrated in Figures 2 and 4 may suggest that earthquakes with a magnitude of about 6 can be expected to occur along the Appalachian trend of seismicity, but this point is not proved, and the frequency of such shocks is not well determined. The data suggest that caution should be applied before predicting future seismicity entirely on the basis of the historical seismic record.

ACKNOWLEDGEMENTS

We thank M. Barazangi, W. Haxby, E. Harrison, B. Isacks, and C. Stephens for critically reviewing the manuscript. J. Ni drafted the figures.

This research was supported by the Advanced Research Projects Agency of the Department of Defense and was monitored by the Air Force Office of Scientific Research under Contract No. AFOSR- 73-2494. Cornell University Department of Geological Sciences Contribution No. 564.

REFERENCES CITED

Allen, C.R., St. Amand, P., Richter, C.F., and Nordquist, J.M., 1965, Relationship between seismicity and geologic structure in the southern California region: Seism. Soc. Am. Bull., v. 58, p. 1183-1186.

Artyushkov, E.V., 1974, Can the earth's crust be in a state of isostacy?: J. Geophys. Res., v. 79, p. 741-752.

Bollinger, G.A., 1973a, Seismicity and crustal uplif in the southeastern United States: Am. Jour. Sci., v. 273-A, p. 396-408.

Bollinger, G.A., 1973b, Seismicity of the southeastern United States: Seism. Soc. Am. Bull., v. 63, p. 1785-1808.

Bonilla, M.G., and Buchanan, J.M., 1970, Interim report on worldwide historic surface faulting: U.S. Geol. Survey Open File Report, 32 p.

Carr, M.S., 1950, The District of Columbia: its rocks and their geologic history: U.S. Geol. Survey Bull. 967, 59 p.

Cederstrom, D.J., 1945, Geology and groundwater resources of the Coastal Plain in southeastern Virginia: Virginia Geol. Survey Bull. 63, 384 p.

Coffman, J.L., and von Hake, C.A., editors, 1973, Earthquake history of the United States: Environmental Data Service, National Oceanic and Atmospheric Administration, U.S. Dept. of Commerce, Publication 41-1 (revised edition, through 1970), 208 p.

Conley, J.F., and Drummond, K.M., 1965, Faulted alluvial and colluvial deposits along the Blue Ridge Front near Saluda, North Carolina: Southeastern Geology, v. 7, p. 35-39.

Crowell, J.C., 1973, Problems concerning the San Andreas fault system in southern California, in Proceedings of the conference on tectonic

problems of the San Andreas fault system: Stanford University Publications, Geological Sciences, v. 13, p. 125-135.

Darton, N.H., 1939, Gravel and sand deposits of eastern Maryland: U.S. Geol. Survey Bull. 906-A, 42 p.

Docekal, J., 1970, Earthquakes of the stable interior with emphasis on the midcontinent, v. 2: Ph.D. thesis, Univ. of Nebraska, 332 p.

Dryden, A.L., Jr., 1932, Faults and joints in the Coastal Plain of Maryland: Jour. of the Washington Academy of Sciences, v. 22, p. 469-472.

Dutton, C.E., 1889, The Charleston earthquake of August 31, 1886: U.S. Geol. Survey Ann. Rept. 1887-88, p. 203-528.

Farrar, W., and McManamy, L., 1937, The geology of Stoddard County, Missouri: Missouri Geol. Survey and Water Resources Biennial Report 59, Appendix 6, 92 p.

Fenneman, N.M., 1946, Physical Divisions of the United States [map]: U.S. Geol. Survey.

Fisk, H.N., 1944, Geological investigation of the alluvial valley of the lower Mississippi River: Vicksburg, Mississippi, Mississippi River Commission, 78 p.

Fletcher, J.P., Sbar, M.L., and Sykes, L.R., 1974, Seismic zones and travel time anomalies in eastern North America related to fracture zones active in the early opening of the Atlantic [abs.]: Trans. Am. Geophys. Union, v. 55, p. 447.

Fox, F.L., 1970, Seismic geology of the eastern United States: Assoc. Eng. Geologists Bull., v. 7, p. 21-43.

Fuller, M.L., 1912, The New Madrid earthquake: U.S. Geol. Survey Bull. 494, 119 p.

Grohskopf, J.G., 1955, Subsurface geology of the Mississippi Embayment of southeast Missouri: Missouri Geol. Survey and Water Resources, v. 37, series 2, 133 p.

Heyl, A.V., Brock, M.R., Jolly, J.L., and Wells, C.E., 1965, Regional structure of the southeast Missouri and Illinois-Kentucky mineral districts: U.S. Geol. Survey Bull. 1202-B, 20 p.

Hudson, G.H., and Cushing, H.P., 1931, The dike invasions of the Champlain Valley, New York: New York State Museum Buil. 286, p. 81-117.

Jacobeen, F.H., Jr., 1972, Seismic evidence for high angle reserve faulting in the coastal plain of Prince Georges and Charles County, Maryland: Maryland Geol. Survey Information Circular No. 13, 21 p.

Jeffreys, H., 1959, The earth (fourth edition): London, Cambridge Univ. Press, 420 p.

Kehle, R.O., 1970, Earth movements: an increasing problem in the cities, in American Geological Institute Short Course Lecture Notes on Environmental Geology: Falls Church, Virginia, American Geological Institute, 78 p.

King, P.B., 1951, The tectonics of middle North America: Princeton, New Jersey, Princeton University press, 203 p.

King, P.B., 1969, Tectonic map of North America [map]: U.S. Geol. Survey.

Koch, L., 1929, Stratigraphy of Greenland: Meddeleser om Grønland, v. 73, pt. 2, p. 205-320.

Lawson, A.C., 1911, On some postglacial faults near Banning, Ontario: Seism. Soc. Am. Bull., v. 1, p. 159-166.

Mateker, E.J., Jr., Tikrity, S., and Phelan, M., 1968, Earthquake epicenters and subsurface geology in the Mississippi Valley [abs.]: Trans. Am. Geophys. Union, v. 49, p. 290.

Matson, G.C., 1905, Peridotite dikes near Ithaca, New York: Jour. Geology, v. 13, p. 264-275.

Nelson, W.A., 1962, Geology and mineral resources of Albemarle County: Virginia Geol. Survey Bull. 77, 92 p.

O'Connor, B.J., Carpenter, R.H., Paris, T.A., Hartley, M.E., and Denman, H.E., 1974, Recently discovered faults in the central Savannah River area [abs.]: Georgia Academy of Sciences Bull., v. 32, p. 15.

Oliver, J., Johnson, T., and Dorman, J., 1970, Postglacial faulting and seismicity in New York and Quebec: Canadian Jour. of Earth Sciences, v. 7, p. 579-590.

Page, R.A., Molnar, P.H., and Oliver, J., 1968, Seismicity in the vicinity of the Ramapo fault, New Jersey - New York: Seism. Soc. Am. Bull. v. 58, p. 681-687.

Pitman, W.C., III, and Talwani, M., 1972, Sea-floor spreading in the North Atlantic: Geol. Soc. America Bull., v. 83, p. 619-649.

Reinemund, J.A., 1955, Geology of the Deep River Coal Field, North Carolina: U.S. Geol. Survey Prof. Paper 246, 159 p.

Rhoades, R., and Mistler, A.J., 1941, Post-Appalachian faulting in western Kentucky: Am. Assoc. Petroleum Geologists Bull., v. 25, p. 2046-2056.

Ries, H., Kummel, H.B., and Knapp, G.N., 1904, The clays and clay industry of New Jersey: New Jersey Geol. Survey, State Geologist's Final Report Series, v. 6, 548 p.

Salisbury, R.D., and Knapp, G.N., 1917, The Quaternary formations of southern New Jersey: New Jersey Geol. Survey, State Geologist's Final Report Series, v. 8, 218 p.

Sbar, M.L., Rynn, J.M.W., Gumper, F.J., and Lahr, J.C., 1970, An earthquake sequence and focal mechanism solution, Lake Hopatcong, northern New Jersey: Seism. Soc. Am. Bull., v. 60, p. 1231-1243.

Sbar, M.L., and Sykes, L.R., 1973, Contemporary compressive stress and seismicity in eastern North America: an example of intraplate tectonics: Geol. Soc. America Bull., v. 84, p. 1861-1882.

Smith, W.E.T., 1962, Earthquakes of eastern Canada and adjacent areas, 1534-1927: Dominion Observatory Publications, v. 26, p. 271-301.

Smith, W.E.T., 1966, Earthquakes of eastern Canada and adjacent areas, 1928-1959: Dominion Observatory Publications, v. 32, p. 87-121.

Street, R.L., Herrman, R.B., and Nuttli, O.W., 1974, Earthquake mechanisms in central United States: Science, v. 184, p. 1285-1287.

Thompson, Z., 1853, Appendix to Thompson's History of Vermont: Burlington, Vermont, Z. Thompson, 64 p.

United States Earthquakes, 1928-1971, [annual issues]: Washington, D.C., U.S. Dept. of Commerce.

Vernon, R.O., 1951, Geology of Citrus and Levy Countries, Florida: Florida Geological Survey Bull. 33, 256 p.

White, W.A., 1952, Post-Cretaceous faults in Virginia and North Carolina: Geol. Soc. America Bull., v. 63, p. 745-748.

Withington, C.F., 1973, Lineaments in coastal plain sediments as seen in ERTS imagery, in Symposium on significant results obtained from the Earth Resources Technology Satellite-1: Washington, D.C., National Aeronautics and Space Administration, p. 517-521.

Woollard, G.P., 1958, Areas of tectonic activity in the United States as indicated by earthquakes epicenters: Trans. Am. Geophys. Union, v. 39, p. 1135-1150.

Woollard, G.P., 1969, Tectonic activity in North America as indicated by earthquakes, in The earth's crust and upper mantle: Am. Geophys. Union Mon. 13, p. 125-133.

Zartman, R.E., Brock, M.R., Heyl, A.V., and Thomas, H.H., 1967, K-Ar and Rb-Sr ages of some alkalic intrusive rocks from central and eastern United States: Am. Jour. Sci., v. 265, p. 848-870.

ILLUSTRATIONS

Figure 1. Distribution of reported earthquakes in eastern North America from historical and instrumental data (Bollinger, 1973b; Coffman and von Hake, 1973; Docekal, 1970; Smith, 1962, 1966; United States Earthquakes, 1928-1971). Because of the uncertainties in pre-1928 epicenter locations, two maps are presented. (1A) Earthquake epicenters 1534-1971. (1B) Earthquake epicenters 1928-1971. Tectonic provinces are from King (1969).

Figure 2. Fault in Washington, D.C., offsetting Precambrian schist, Pleistocene terrace gravel, and Pleistocene loam. Displacement appears to be about 1 m. Fault is no longer exposed. From Darton (1939).

Figure 3. Cretaceous and Cenozoic faults in eastern North America. Data from table 1 and three more representative postglacial fault locations (Ontario, Quebec, and Nova Scotia) from Oliver and others (1970). Line segments show strikes of faults; short cross segment indicates a vertical fault, D on downthrown side; circles show faults with unreported strikes; R indicates reverse faults; N indicates normal fault; pointed barbs indicate reverse faults; straight hachures indicate normal faults; barbs and hachures are on down dip side of faults; hourglass symbols show fault zones where fault strikes vary within limits shown; small square between four short line segments indicates a horizontal fault. Tectonic provinces are from King (1969).

Figure 4. Cretaceous fault at Drewrys Bluff, Virginia. The banded sediments exposed above the colluvium are loosely consolidated, interbedded silt, sand, and peat. A conglomerate unconformably overlies the faulted sediments. Dip-slip displacement is about 0.6 m; strike-slip displacement is unknown. Two geological hammers provide scales. Photographed by David Prowell, U.S. Geological Survey.

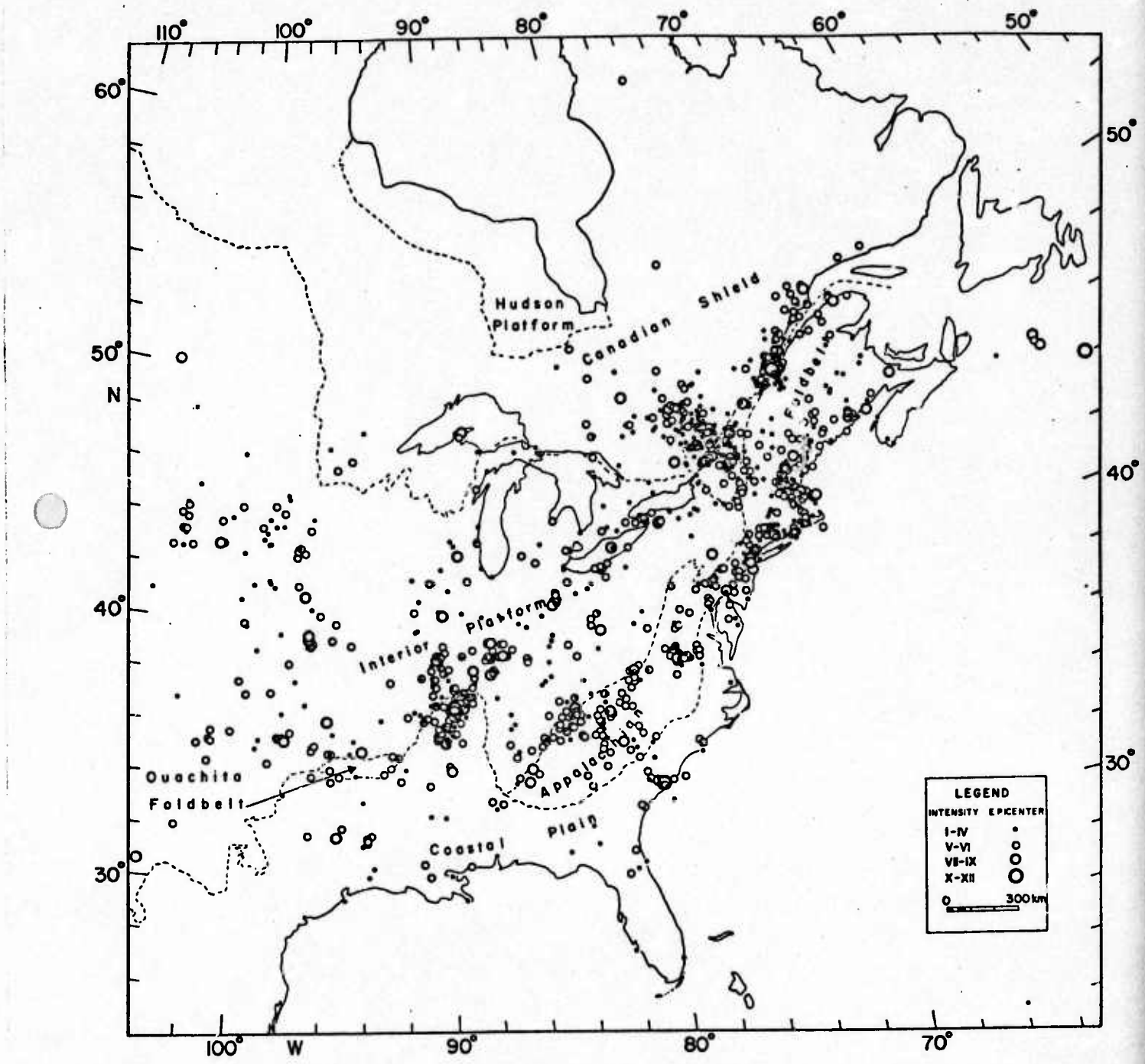
Figure 5. Distribution of Cretaceous and Cenozoic faults in the central Mississippi River valley. Data are from Table 1. Symbols are as in Figure 3. Physical divisions are from Fenneman (1946).

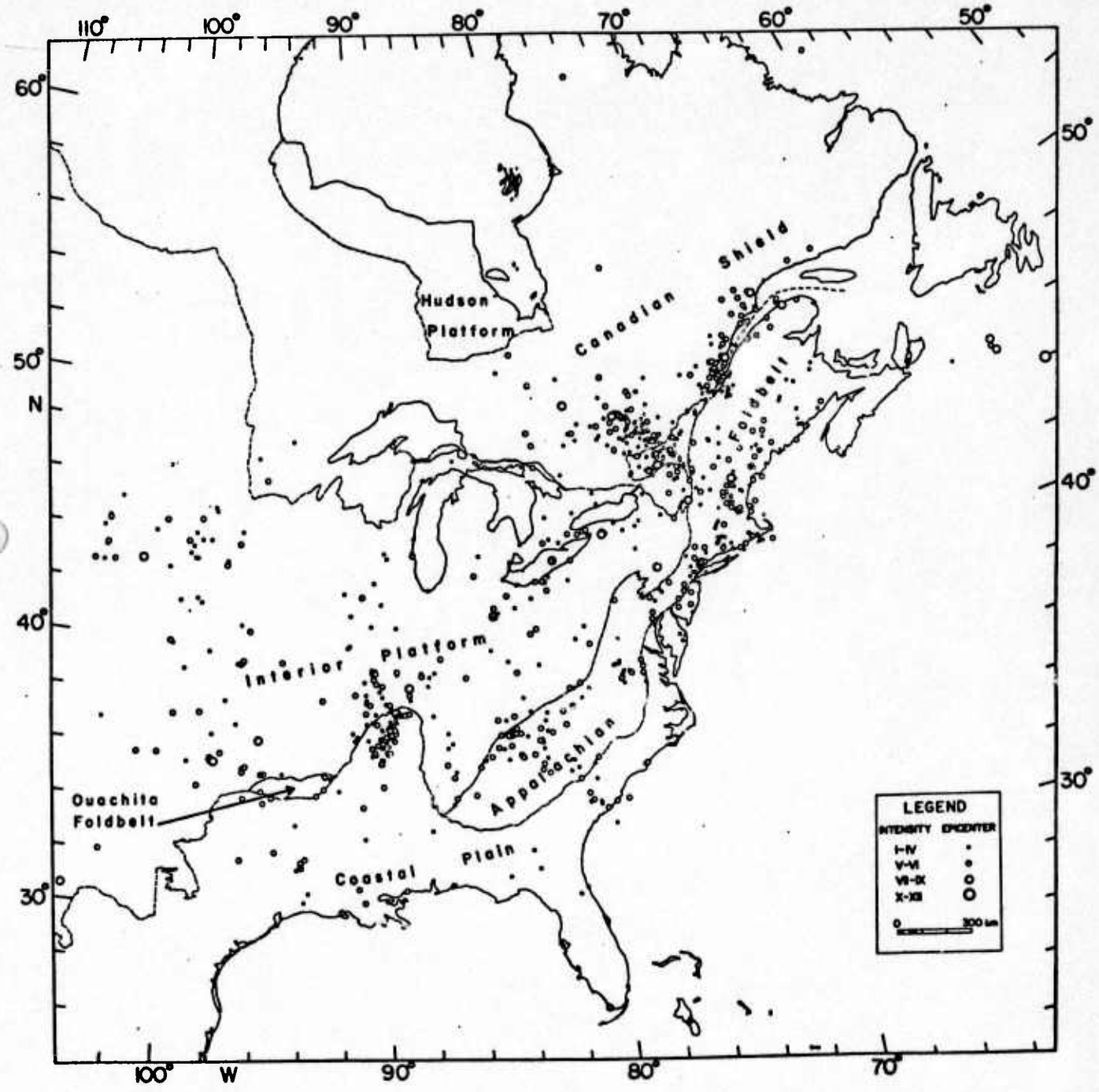
Figure 6. Distribution of Cretaceous and Cenozoic faults in the southeastern United States. Data are from Table 1. Symbols are as in Figure 3. Physical divisions are from Fenneman (1946).

TABLE 1. DESCRIPTIONS OF FAULTS

Locetion	Type of feult*	Strike	Dip	Displecement (metsrs)	Youngest feultsd rocks	Observed 1974	Litereture reference
Belsir, Georgis	R	N20E	58-80 E	>1	Creteceous sedimsnts §	-	O'Connor snd others(1974)
Benton, Kentucky	V	N45E	90	0.3	Pliocens(?) terracs grevsls	-	Rhoedes snd Mistler(1941)
Benton, Miseouri	R	-	-	>15	Creteceous sedimente§	-	Grohskopf (1955)
Bloomfield, Miseouri	-	N55W to N30W to NS	-	3-6	Tertiery sediments	-	Grohskopf (1955)
Bloomfisld, Missouri	-	N50W to NS to N30E	-	3-6	Tertisry sediments	-	Grohekopf (1955)
Buckhorn Croasroede, North Carolina†	R	N51E	48 NW	0.3	Cretaceous sediments§	-	White(1952)
Burlington, Vermont	-	-	-	0.9	Cretaceous kimberlits§	-	Thompson (1853, p. 53)
Clifton Forge, Virginis†	V	N25W	90 (E side down)	5-6	Tertiery grevsls§	X	White(1952)
Commercs, Miseouri	-	-	-	-	Pliocsns(?) grevsls	-	Grohekopf (1955)
Crystsl River, Florids†	-	N45W	-	-	Eocene limeetohe	-	Vsrnon(1951)
Desp River, North Cerolina	N	-	-	>0.5	Pliocene(?) ssdiments	-	Reinemund (1955)
Drewrys Bluff, Virginie†	R	-	>50	<0.5	Crstsceous ssdimente	-	Cederstrom (1945)
Drewrys Bluff, Virginis	R	N65E	45 S	0.6	Crsteceous eediments	X	
Grsnd Rivere, Kentucky	V	N18E	90 (E side down)	-	Creteceous sediments	-	Rhoedes end Mietler(1941)
Gresnwood, Virginia†	R	N20E	57 E	1.5	Pleietocsns terrece grevsls§	X	Neleon(1962)
Hillsboro, Virginis	-	-	>45	0.9	Tertiery grsvels	-	White(1952)
Hydro, North Carolina†	R	N40E	50 NW	5	Tertiery gravels§	X	Whits(1952)
Idslie, Mieeouri	-	N45W	-(NE sids down)	20	Tertiery sediments	-	Ferrar snd McManamy(1937)
Idelia, Missouri	-	N55E	-	>15	Pliocens(?) grsvels	-	Grohskopf (1955)
Kentucky Dam, Kentucky	V	N60E	90	>30	Crstaceous sediments	-	Rhoedee snd Mietler(1941)
Ludlowvills, New York	H	-	-	0.6	Cretscsous kimberlits§	-	Matson(1905)
Pumpkin Hollow, New York†#	R	N40E	65 SE	.05	Plsistocens glsciel striations§	X	Oliver end othere(1970)
Quantico, Virginis†	R	N75W	50 S	0.25	Cretaceous sediments	X	Cederstrom (1945)
Saluds, North Carolina	N	N80E	11 S	>0.5	Queternery(?) terrsce grsvels§	-	Conlsy snd Drummond (1965)
Ssluds, North Cerolina	N	N8E	67 E	>5	Qusternery(?) colluvium§	-	Conley end Drummond (1965)
Salude, North Carolina	R	N40W	20 NE	>4	Qusternery(?) colluvium§	X	
Teughannock Falls, New York	H	-	-	0.5	Creteceous kimberlite§	-	Matson(1905)
Upper Marlboro, Marylend	R	-	-	>0.3	Plsistocsne ssdiments	-	Dryden(1932)
Velcour Islend, New York	-	NS	-	-	Creteceous kimberlite§	-	Hudson end Cushing(1931)
Vslcour Ielend, New York	-	N50E	-	-	Crstecsoue kimbsrlits§	-	Hudson and Cushing(1931)
Washington, D.C.	-	-	-(E side down)	>2	Cretaceous sediments§	-	Carr(1950)
Washington, D.C.†	R	-	>60	-1	Pleistocsne terrece grsvels§	-	Derton(1939)
Washington, D.C.	R	N5W	60 W	>2	Creteceous sediments§	X	Carr(1950)

* R (reverse), N (normal), V (vertical), H (horizontel)
† Photograph of feult is published in the literature reference.
§ Peleozoic or Precambrian bedrock is also exposed and offset by the fault.
# This locality is representetive of many postglacial faults listed in the litereture reference.


110°
100°
90°
80°
70°
60°
50°
60°
50°
40°
30°
N
Hudson Platform
Canadian Shield
Foldbelts
Interior Platform
Appalachian
Ouachita Foldbelt
Coastal Plain
LEGEND
INTENSITY EPICENTER
I-IV
V-VI
VII-IX
X-XII
0 300 km
100° W
90°
80°
70°


110°
100°
90°
80°
70°
60°
50°
60°
50°
N
40°
30°
100° W
90°
80°
70°
Hudson Platform
Canadian Shield
Foldbelt
Interior Platform
Appalachian
Ouachita Foldbelt
Coastal Plain
LEGEND
INTENSITY
EPICENTER
I-IV
V-VI
VII-IX
X-XII
0
300 km

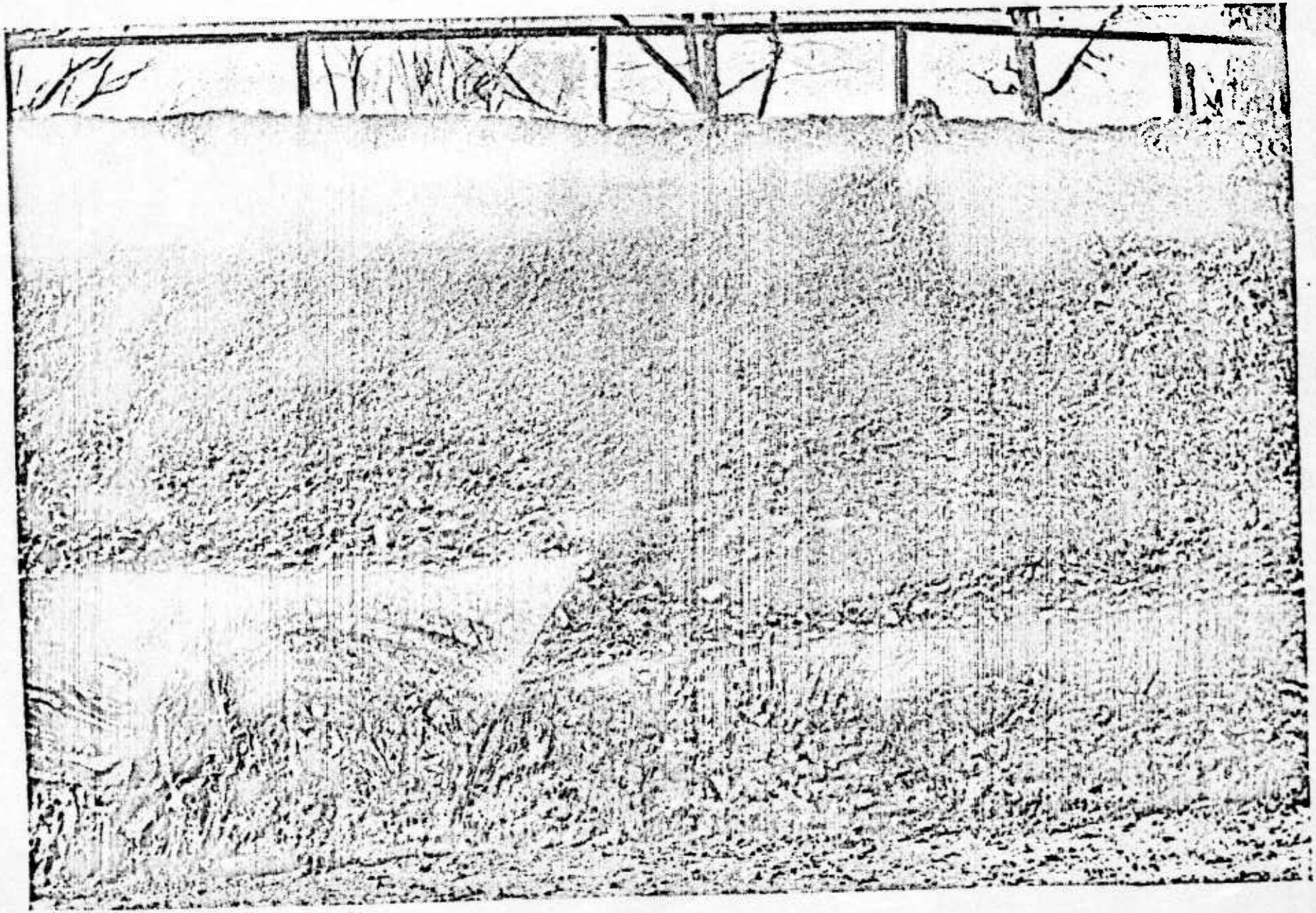
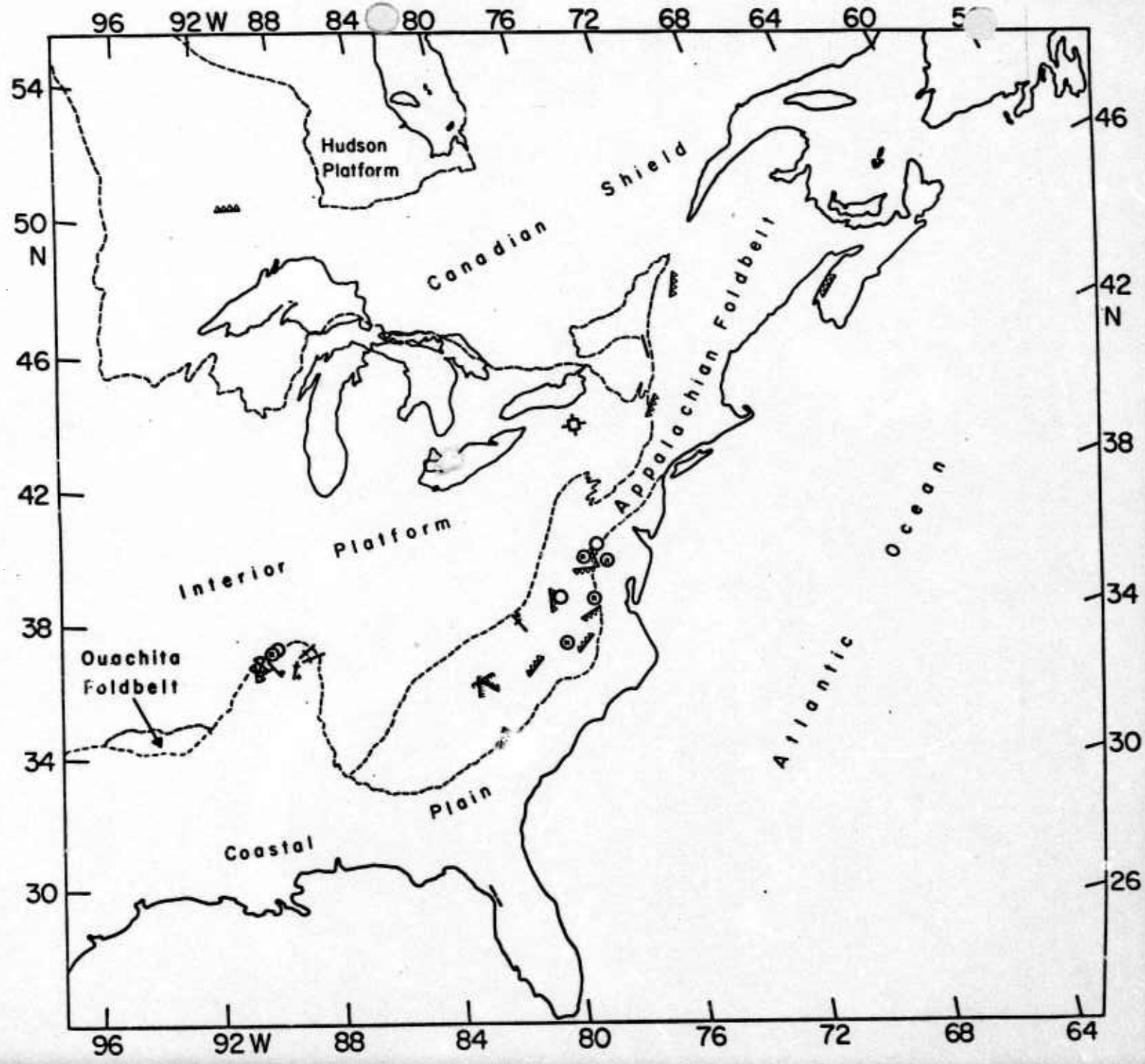


Fig. 2


96
92W
88
84
80
76
72
68
64
60
54
50
N
46
42
38
34
30
46
42
N
38
34
30
26
Hudson
Platform
Canadian Shield
Appalachian Foldbelt
Interior Platform
Ouachita
Foldbelt
Coastal
Plain
Atlantic
Ocean



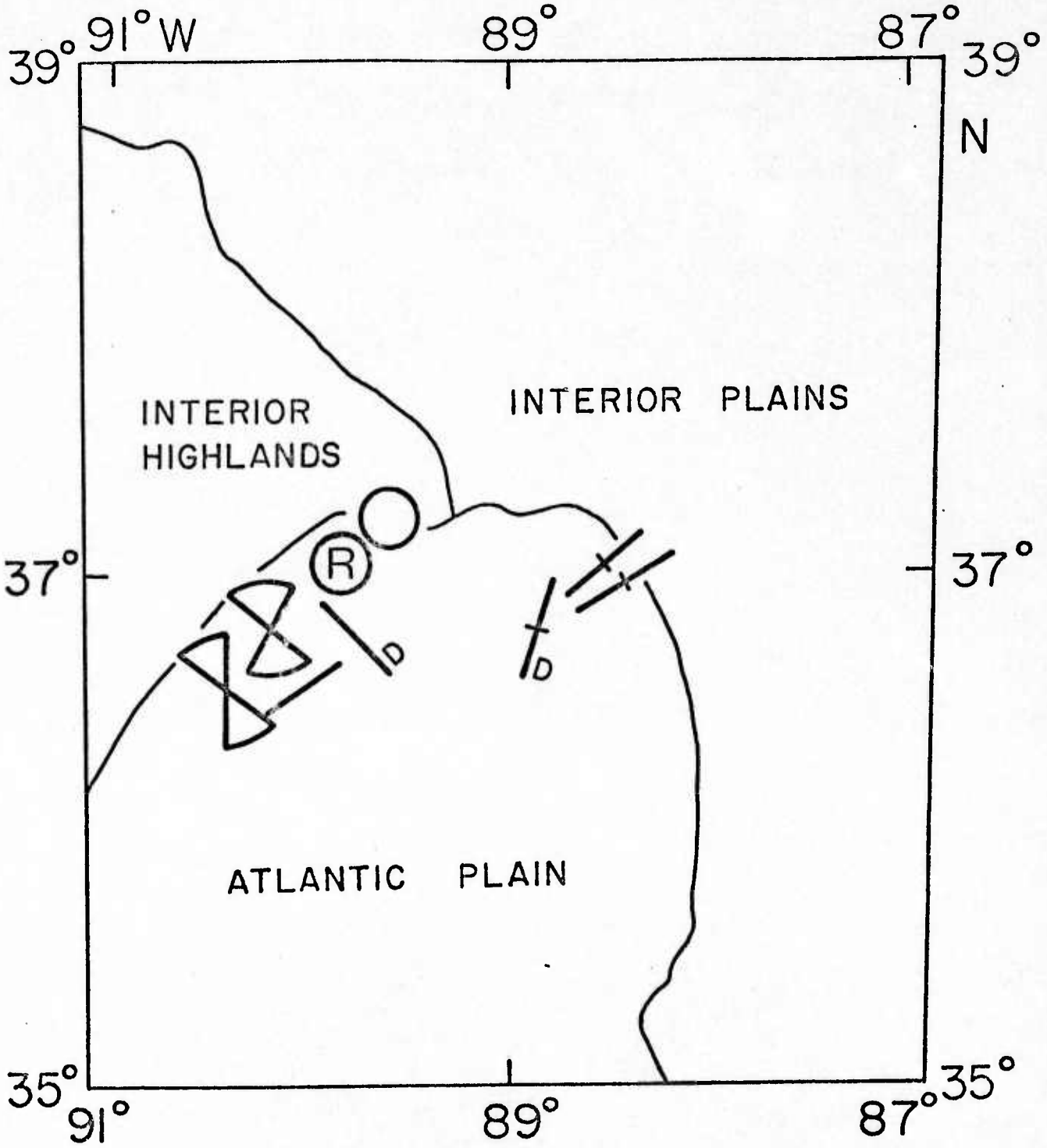

39°
91° W
89°
87°
39°
N
INTERIOR
HIGHLANDS
INTERIOR PLAINS
37°
R
D
D
37°
ATLANTIC PLAIN
35°
91°
89°
87°
35°

Fig. 5

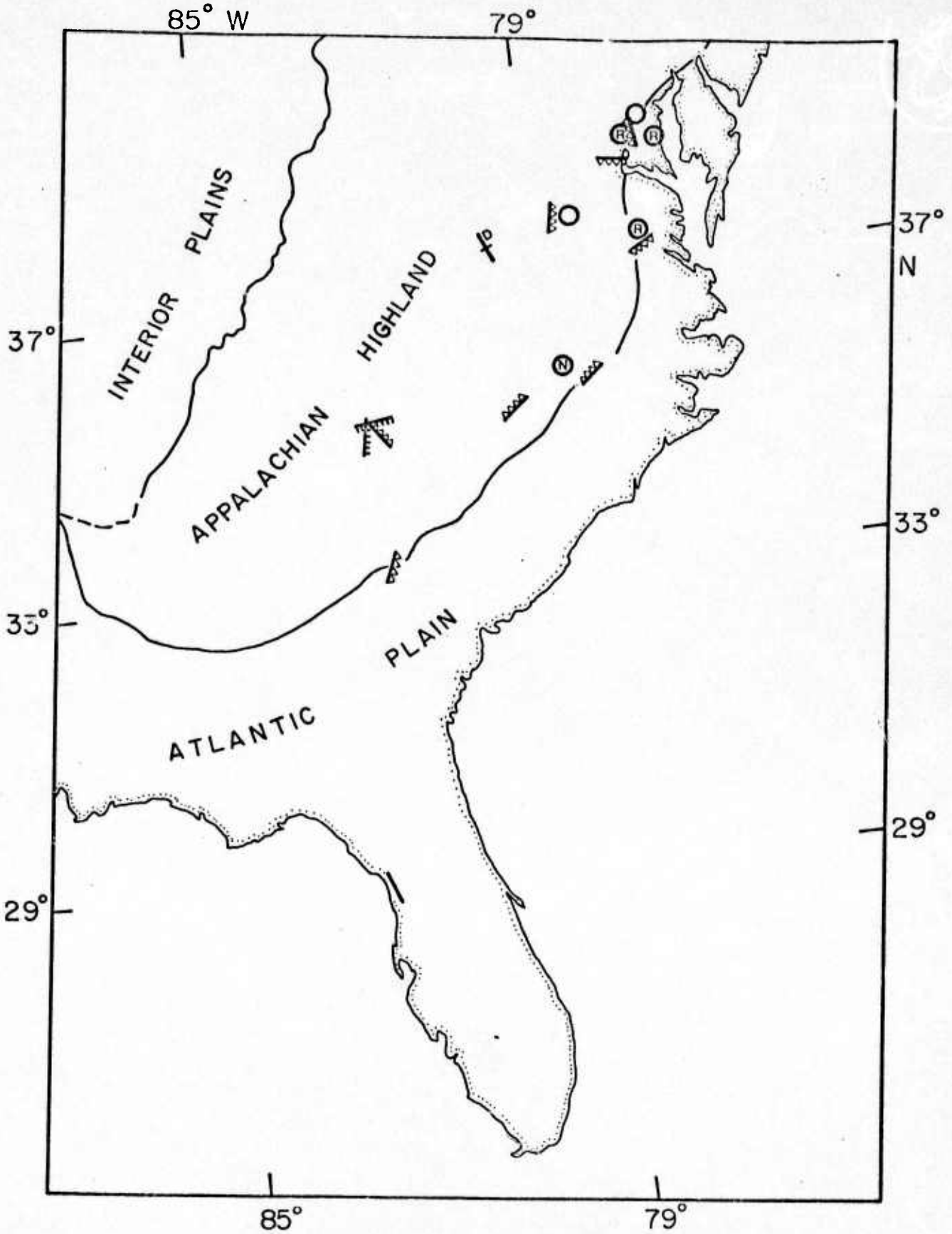

85° W
79°
37° N
37°
33°
29°
INTERIOR PLAINS
APPALACHIAN HIGHLAND
ATLANTIC PLAIN
85°
79°

Fig. 4

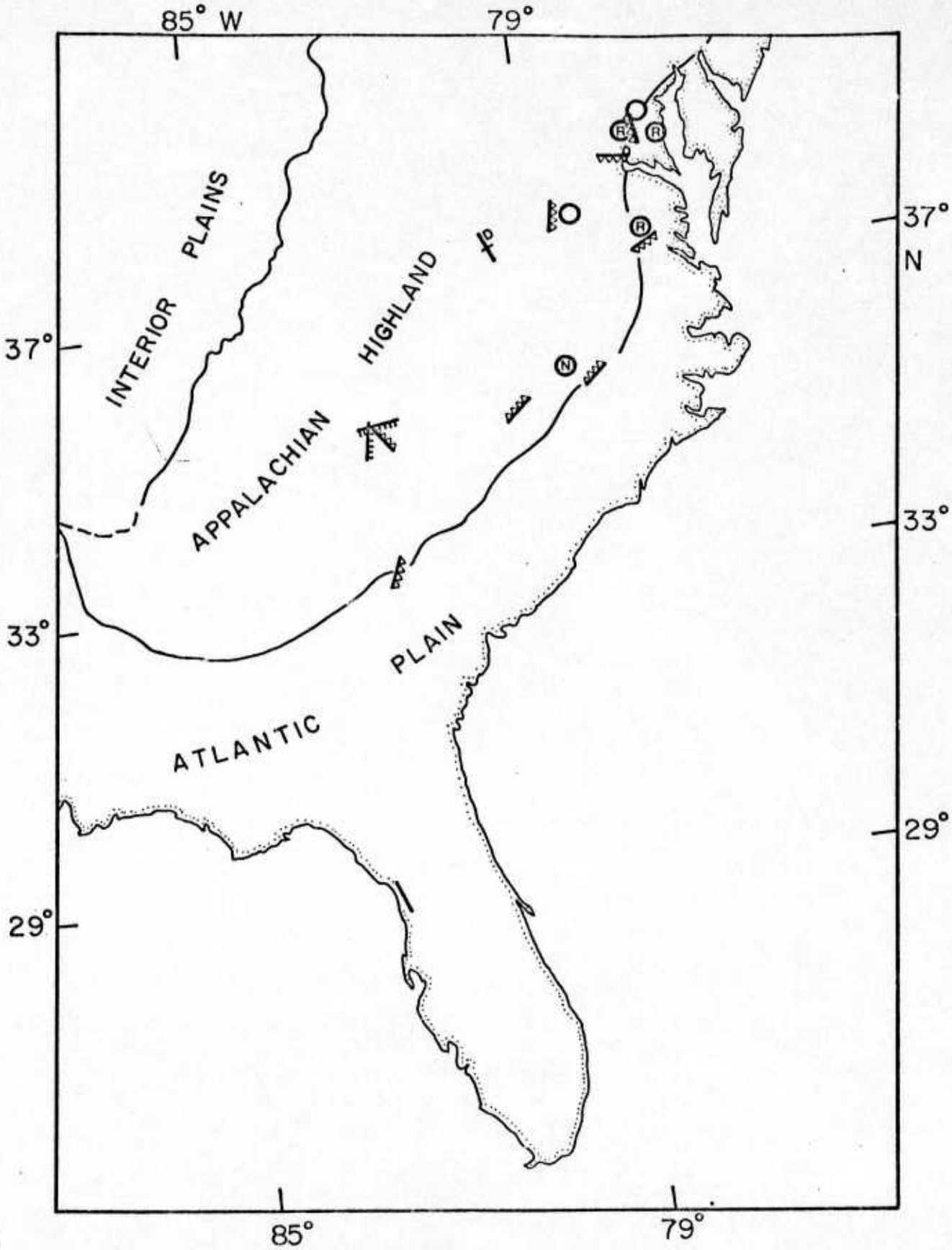

85° W
79°
37°
N
33°
29°
INTERIOR PLAINS
APPALACHIAN HIGHLAND
ATLANTIC PLAIN
R
R
R
N

Fig. 4

Vertical Crustal Movements From Leveling Data and Their Relation to Geologic Structure in the Eastern United States

LARRY D. BROWN AND JACK E. OLIVER

Department of Geological Sciences, Cornell University, Ithaca, New York 14853

Through analysis of leveling data, rates of relative vertical motion have been determined for points of a grid of profiles over much of the eastern United States. The rates are commonly too large to be attributed to leveling errors and therefore must reflect true earth movements. With some exceptions, modern movements appear to be related to earlier Phanerozoic trends, but the rates of modern movements are much larger than average rates over the past 130 m.y. Thus movements are either episodic or oscillatory about a long-term trend. If oscillatory, the periods must be less than about 10^6 yr and may be much smaller. The spatial patterns of the rates of relative motion, or tilts, can be correlated with certain geological features. The Atlantic and Gulf coastal plains are tilting downward away from the continental interior. Along a profile from Savannah, Georgia, to Philadelphia, Pennsylvania, the Atlantic Coastal Plain is also tilting downward to the north, with a perturbation at the Cape Fear arch. The Appalachian Highlands are rising relative to the Atlantic Coast at rates of up to 6 mm/yr. The pattern of maxima and minima in relative velocities along the profiles crossing the Appalachian Highlands province suggests elongated zones of relative uplift and subsidence paralleling either the Appalachian drainage divide or the trend of Appalachian structure. The maxima correlate strongly with topographic highs. There is a suggestion of correlation of modern seismicity with extremes of relative velocities in the Appalachian Highlands province. The Interior Plains are tilting downward to the east at a rate of 2×10^{-8} rad/yr, the implication being that glacial rebound is not an important factor south of the Great Lakes at the present time. The wavelength between successive zones of relative uplift in the Appalachian Highlands is about 300 km, suggesting that at least the entire thickness of the lithosphere is involved, and probably the asthenosphere as well. Possible explanations for these phenomena include the effects of hydrologic variations, phase transitions in the lower crust and/or the upper mantle, asthenospheric currents driven by ocean and ice loads or plate motions, and stresses derived from nonequilibrium crustal loads or crustal unloading by erosion.

INTRODUCTION

The purpose of this study is to relate data from precise leveling to various geological and geophysical parameters in the hope of learning more of the deformation and deformational processes affecting the earth's crust. The area focused upon is the eastern United States, for which leveling data have been collected and were generously made available by the National Geodetic Survey (NGS) of the National Ocean Survey (formerly the U.S. Coast and Geodetic Survey). The analysis and approach used here differ somewhat from those of many previous studies in that emphasis is placed on the leveling data alone and on the relative velocities (or tilt rates over finite segments) determined from those data. It is this information that is related to geological parameters. Commonly, leveling information is adjusted by warping the leveled surface to fit sea level measurements at certain common points and to obtain internal consistency within the level net. From differences of two such adjusted surfaces, 'absolute' velocities (really relative to sea level) can be obtained. This method has the advantage of reducing, hopefully, the effect of cumulative errors in leveling, but may introduce new sources of error in the form of ambiguous sea level measurements, nonsynchroneity of observations, excessive smoothing, and other effects, so that warping may obscure information of value in the study of geological phenomena. For these reasons only information from relative velocity and tilt rate data is used here. Furthermore, only larger wavelength movements were examined in order to minimize the influence of local (< 50 km) nontectonic processes (e.g., groundwater withdrawal, compaction due to man-made loads).

Copyright © 1976 by the American Geophysical Union.

Six continuous profiles of relative velocity have been prepared from NGS data. These profiles cross virtually all of the major structural provinces in the eastern United States. From these profiles several features not previously reported may be seen, as well as others that are common to most studies of leveling data. In many cases, but not all, modern relative movement is in accord with the direction of movement indicated by the geological record for part or all of the Phanerozoic. Thus the Atlantic and Gulf coastal plains are tilting seaward and the Appalachians are rising. As has been found elsewhere, the rates of movement, however, are larger than those deduced from the geological evidence. In fact, they are so large (note that 1 mm/yr = 1 km/m.y.) that they could not continue without change for long (say one or a few million years) without unreasonable deformation of the earth's surface. Thus there are two possible conclusions. Either the leveling data are in error and hence misleading, or else contemporary movements are episodic or oscillatory, perhaps about some long-term trend. A substantial analysis of errors in leveling has been made, both here and elsewhere, and it is highly unlikely that such errors can explain the observations; hence it seems certain that real motion of the crust is being observed. That the pattern of movements shows some correlation with topographic and geological features is additional strong evidence that surveying errors are not predominant.

Once episodic or oscillatory motion of the crust is established, it becomes important to understand this phenomenon, for the movements may be related to lithosphere-asthenosphere dynamics and hence informative on a variety of geological problems such as plate motions, basin and dome deformation, epeirogeny, and earthquake occurrence within lithospheric plates.

Of special interest are the results of this study that suggest

elongate zones of relative uplift and subsidence paralleling the Appalachian drainage divide or, as an alternative interpretation, the trend of Appalachian structure. The wavelengths involved, on the order of 300 km, are typical of lithosphere-asthenosphere phenomena. The evidence for such features is not so complete as one might like because of the wide spacings between profiles, but the possibility that this pattern of movements and similar patterns in other areas might be measured is an exciting one, for the patterns are a likely clue to the mechanism.

The background and capabilities of precise leveling as a tool for the study of crustal movements are first considered. The sources of error in leveling are examined, and the methods of analysis used for this study are discussed. The remainder of the paper is devoted to the presentation and interpretation of the results of correlating the vertical crustal movements deduced from leveling data with geologic structure in the eastern United States.

MEASUREMENTS OF CRUSTAL MOVEMENT USING PRECISE LEVELING

The use of precise leveling to investigate crustal movements dates from engineering studies of building settlement in the mid-nineteenth century [*Werner*, 1970]. Leveling has proven valuable in the study of areas where fluid withdrawal, sediment compaction, and mining operations are significantly affecting surface stability. In the United States there are several areas where such factors are causing significant economic concern. For example, the Houston-Galveston area is subsiding due to water withdrawal and sediment compaction at rates up to 90 mm/yr relative to local sea level [*Small*, 1960; *Gabrysch*, 1969; *Poland and Davis*, 1969]. Groundwater withdrawal is also responsible for subsidence in several parts of the San Joaquin valley at rates in excess of 300 mm/yr relative to local sea level [*Poland and Davis*, 1956; *Small*, 1961; *Holdahl*, 1969]. Such large rates are rare, but these effects must, of course, be taken into account in studies of crustal mobility.

Leveling has also been used successfully to measure vertical movements believed to be associated with major earthquakes. Levelings before and after the 1964 Alaskan earthquake [*Small and Wharton*, 1969], the 1959 Hebgen Lake, Montana, earthquake [*Myers and Hamilton*, 1964], and the 1954 Dixie Valley earthquakes [*Whitten*, 1957] have revealed vertical crustal movements on the order of 1–5 m, accompanying independently measured fault displacements up to 10 m. Similar but smaller magnitude movements have been measured by leveling in Japan, New Zealand, Australia, and Hungary [*Mescherikov*, 1968; *Lensen*, 1971; *Lensen and Otway*, 1971; *Gordon*, 1971]. Recent work suggests that both premonitory vertical movements and postearthquake fault slip are amenable to study by precise leveling [*Miyabe*, 1955; *Hagiwara*, 1964; *Tsubokawa and Nagasawa*, 1966; *Lensen and Otway*, 1971; *Rikitake*, 1972; *Castle et al.*, 1974; *Savage and Church*, 1974].

Leveling has also been used to study the deformation processes initiated by the imposition and removal of large crustal loads. The filling of large reservoirs has been shown to cause significant elevation changes in the immediate and surrounding vicinities [*Longwell*, 1960; *Carder and Small*, 1948; *Sleigh et al.*, 1969]. The effects of unloading Pleistocene lakes [*Crittenden*, 1963] as well as the retreat of glacial ice sheets [*Kaariainen*, 1953] have been investigated by means of precise leveling. The determination of recent uplift of the earth's crust in Finland probably represents the best leveling study of large scale vertical movement to date [*Kaariainen*, 1953, 1966; *Kukkamaki*, 1955].

Although the use of precise leveling in studies of secular vertical crustal movements is not new in the United States [*Small*, 1963; *Meade*, 1971], the method has received much more attention in Europe and Japan [e.g., *Mescherikov*, 1959; *Beloussov*, 1962; *Rezanov and Zarudny*, 1962; *Gerasimov*, 1967; *Riives*, 1973; *Miyabe*, 1952; *Miyabe et al.*, 1966]. Much of this work is summarized in the form of contour maps of adjusted velocities of vertical crustal movement [*Miyabe et al.*, 1966; *Mescherikov*, 1973]. Other regions where similar studies have been undertaken include the Alps [*Levallois*, 1972; *Schaer and Jeanrichard*, 1974], the Negev of Israel [*Karcz and Kafri*, 1971, 1973], the Himalayas [*Chugh*, 1974], and the Canadian shield [*Vanicek and Hamilton*, 1972]. These studies indicate that while leveling can be used effectively to measure secular vertical crustal movements, the results tend to be varied, and as yet no comprehensive mechanism for driving these movements has been found. Comparison of results from many parts of the world [*Mizoue*, 1967; *Beloussov et al.*, 1974] shows that the magnitudes of these movements tend to be consistent (i.e., tilt rates on the order of 10^{-6}–10^{-7} rad/yr) with orogenic zones generally being characterized by larger rates and shorter wavelengths than platform regions. The results of this study support these observations.

The more convincing studies deal with movements of large magnitude and/or movements for which reasonable causative mechanisms have been found. When the magnitude of the movements approaches the accuracy limit of the leveling process itself, it becomes extremely difficult to discriminate actual crustal movement from possible leveling errors. The cost of leveling in terms of both time and money virtually prohibits the frequent repetition of leveling over large distances. Lack of knowledge about the periodicity of recent vertical crustal movements introduces the strong possibility of aliasing in the results of leveling determinations of movements. For example, if the time interval of leveling coincides with the natural period of the movement, the net measure of crustal movement will be zero regardless of its actual amplitude. Few studies exist in which the discontinuous record of movements determined by precise leveling can be compared unambiguously with results obtained by independent, continuous methods, e.g., tiltmeter surveys [*Kasahara*, 1973]. For these reasons it is important to understand the leveling process and its limits when attempting to apply its results to geological and geotectonic problems.

U.S. LEVEL NETWORK

The establishment of an accurate net of reference points for elevation determinations in the United States began in 1878 when the U.S. Coast and Geodetic Survey initiated work on a transcontinental line of first-order leveling. By 1929, the level net had been extended to include approximately 45,000 miles (72,000 km) of first-order leveling. To make measurement in the net internally consistent under the assumption of crustal stability, a series of least squares adjustments were performed in 1899, 1903, 1907, 1912, 1927, and 1929. More recent data have been accommodated by supplementary adjustments to the 1929 general adjustment [*USCGS*, 1961]. Maintenance and development of the Vertical Control Net of the United States is carried out by the NGS.

During releveling of portions of the U.S. net, it became apparent that the assumption of crustal stability upon which adjustment procedures are based was not valid, at least in certain areas. Horizontal distance measurements (triangula-

tion) after the 1906 San Francisco earthquake clearly demonstrated the instability of the earth's crust [*Bowie*, 1928]. Analyses of triangulation data by C. A. Whitten, B. K. Meade, and others have since provided valuable data on the recent horizontal movements associated with the San Andreas fault system [*Whitten*, 1948, 1949, 1956; *Whitten and Claire*, 1960; *Meade*, 1948, 1965, 1966]. Likewise, *Small* [1961, 1963, 1966], *Holdahl* [1969, 1973*a*, *b*], and *Holdahl and Morrison* [1973] have pointed out that significant changes in elevation also occur in many areas in the United States.

In keeping with the goals of the Commission on Recent Crustal Movements of the International Association of Geodesy [*CRCM*, 1962, 1966, 1968], the NGS is actively amassing a bank of elevation change data to facilitate study of recent vertical crustal movements. Another objective being pursued by the NGS is the compilation of maps of recent vertical crustal movements for the United States. Although such maps provide the best representation of movements from a statistical viewpoint, they have a number of weaknesses when used to infer possible geologic processes. Among these weaknesses are the assumption of constant velocity of movement over the time period of the measurement and the wide variations in the spatial density of the data, with corresponding loss of detail during smoothing procedures. By examining data that are unbiased by the limitations of statistical assumptions, some of the ambiguities inherent in maps of adjusted vertical velocity values can be avoided [*Bendefy*, 1966].

In order to interpret leveling data with confidence it is necessary to understand the methods of observation and analysis in some depth and to give careful consideration to the errors that might arise at each step of the procedure. There may be considerable variation in quality from one set of data to the next, and poor data must be eliminated or downgraded. The leveling data used here were studied in considerable detail, as described in the next section.

Leveling Procedure

Figure 1 illustrates the basic technique of precise leveling. In essence it involves establishing a horizontal reference surface and making a measurement of the difference in height between two reference points (bench marks) [see *Bomford*, 1971, for details]. The instrument used by the NGS for most of its work, until recently, was the Fischer first-order level, in which the line of sight was made normal to the plumb line by adjustment of a very sensitive level bubble. Modern instruments rely on an automatic leveling system. Both types depend on the relative uniformity of the local geoid. Spatial geoid variations are not ordinarily a problem in elevation change measurements, however, since the wavelengths of significant gravity anomalies are usually much larger than the length of a measurement interval. Any small systematic error introduced by ignoring gravity anomalies will cancel when subtracting elevation differences. Short-wavelength gravity anomalies should contribute only random error. Temporal changes in the gravity field change the shape of the reference geoid and therefore affect measurements of vertical crustal movement. Corrections for such effects require a knowledge of the secular gravity variation as well as the geometry and density changes of the source region, none of which are known quantities at present. It is implicitly assumed in this paper that the geoid remains sufficiently constant for the times of leveling and releveling to justify neglecting the effects of secular gravity variations. This assumption appears to be valid for the movements considered here, if one considers the magnitudes of the gravity changes needed to significantly affect leveling. It should be noted that crustal movements also give rise to gravity variations which will affect leveling results. The effect causes the leveling measurement of the magnitude of elevation change to be smaller than the actual elevation change magnitude; however, the effect is small and will be neglected. The measuring rods are made of invar, whose coefficient of thermal expansion is small and well-known. The most common type of bench mark used by the NGS is a bronze tablet set into a bell-shaped concrete post 3–5 ft (1–1.5 m) long and buried in the ground with its top flush with the surface [*Rappleye*, 1948]. The ability of the bench marks to hold their position relative to the crust upon which they are located determines to a large extent the usefulness of elevation change measurements for crustal movement studies. *Rappleye* [1948] describes the criteria used by the NGS in placing bench marks. Rock outcrops are preferred, but necessity often dictates the choice of less stable positions. Small bridges and curbs are examples of structures where bench marks are sometimes placed which are subject to large nontectonic disturbances. Local soil compaction due to nearby buildings has been found to be a common problem near cities for certain types of bench marks [*Uspenskii*, 1961, 1967; *Lutsar et al.*, 1973]. Frost heaving can cause relative uplift of bench marks on the order of several decimeters over a period of 15–20 yr if they are not secured below the frost level [*Uspenskii*, 1961]. Field tests and inspections have shown that the majority of bench marks are not significantly affected by such factors [*Ellingwood and Holdahl*, 1972; *Lilienberg and Setunskaya*, 1969]. Unstable bench marks are easily recognized by their unusually large and singular movements.

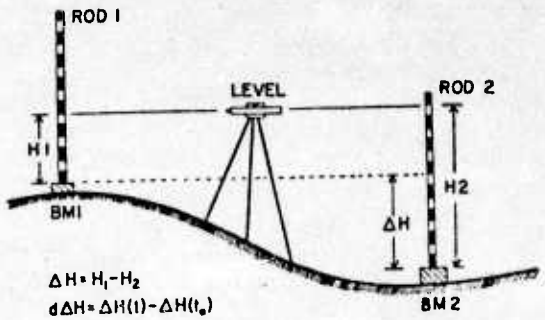


Fig. 1. Technique of precise leveling, defining the quantities ΔH (elevation difference) and $d\Delta H$ (relative elevation change).

The distance between bench marks is about 1 mile (1.6 km), while the distance between leveling rods for each setup of the instrument is about 100 m. An average rate of progression for leveling work is about 3 km per day. Leveling designated as first-order is double run, i.e., the measurement of Δh is performed twice, once going from BM1 to BM2 and again going from BM2 to BM1. The difference between the two determinations gives an estimate of the precision of the work. Second-order leveling is also double run in many cases.

Errors

The largest difficulty in evaluating elevation changes by precise leveling lies in determining the influence of leveling errors on the measurement of elevation. Leveling is susceptible to errors which are varied in type as well as magnitude. These errors may be classified as blunders, random errors, or systematic errors.

Blunders, such as reading a rod 1 m or 1 dm wrong or misrecording a value, are usually revealed in the discrepancies between forward and backward leveling or in the overall cir-

cuit misclosures because of their unusually large values. They are nearly always eliminated before elevations are computed. For this reason they are not normally a serious problem in interpreting elevation changes.

Random errors are propagated as the square root of the number of measurements made. Since the lengths of the setups are usually about the same, the random error is expressed in terms of the square root of the distance leveled, i.e., $m_L = m \cdot L^{1/2}$, where m_L (in millimeters) is the standard deviation of an elevation difference determined over a distance L (in kilometers) from a reference point, and m is the standard deviation of leveling over unit distance. The quantity m can be determined from the discrepancies between forward and backward levelings [*Bomford*, 1971]. The allowable deviations between forward and backward levelings as of 1961 for the NGS are shown in Table 1. Recently the NGS has adopted $m = 1.0$ for its high-precision work. The data used in this study are derived mainly from first-order leveling, supplemented by some second-order results. In practice, it is found that the standard deviations of leveling are usually smaller than the values which can be deduced from the tolerance limits given in Table 1. *Holdahl* [1973*a*] gives estimates of m for NGS leveling completed within given periods for which different types of instrumentation and procedures were used (Table 2). The standard deviations of the relative velocities used in this paper were calculated according to the following relation [*Holdahl*, 1973*a*]:

$$m_v = [(m_t^2 + m_{t_0}^2) \cdot L]^{1/2}/(t - t_0) \qquad (1)$$

where m_v is the standard deviation of relative velocity v with respect to a reference point at distance L (kilometers) in millimeters per year, m_t is the standard deviation of leveling over unit distance at time t (years), and m_{t_0} is the standard deviation of leveling over unit distance at time t_0. Values for m_t and m_{t_0} are taken from Table 2. Sources of random error are covered in *Rappleye* [1948], *Bomford* [1971], and others and will not be discussed here. For the purposes of this study, the effect of random errors are accounted for in the parameter m_v.

The most serious types of error with respect to elevation change measurements are systematic. Systematic errors occur with predominantly the same sign and accumulate with the first power of distance. Systematic errors may show themselves in the misclosures of leveling circuits and thus can be eliminated by least squares adjustments. Some types of systematic error do not appear in closing errors and are therefore the most troublesome when evaluating leveling-derived elevation changes. Errors accumulating with height or latitude are of this type. An error of 0.03 mm in a 3-m rod would give an error of 1 mm per 100 m of elevation change. NGS rods are checked regularly to insure that the rod lengths are known to better than 1 part in 10^3. *Kaarianinen* [1966] reports that rod length changes over short intervals of time appear to be on this order or smaller. A significant source of elevation-correlated error arises from refraction effects. *Bomford* [1971] reports that these errors, worst on long easy grades, could amount to 20 mm per 100 m of elevation change. Inspection of the theoretical refraction correction of *Kukkamaki* [1938, 1939] indicates that 20 mm per 100 m of elevation change is abnormally large and probably represents an upper limit to the magnitude of this error. Since the refraction is predominantly of the same sign during normal working hours, the effect of refraction should be cancelled, at least in part, when taking the difference of two elevation values. Furthermore, randomization of weather conditions over the time period of leveling should reduce the systematic influence of refraction. *Hytonen* [1967] reports an average refraction effect during the second leveling of Finland of only 6 mm per 100 m of rise. *Holdahl* [1974], using the theoretical formulas of Kukkamaki, found the refraction error on a California line to be less than 4 mm per 100 m of rise.

Tidal forces have also been shown to affect leveling results. These errors are negligible on an east-west line [*Bomford*, 1971; *Holdahl*, 1974] but may accumulate significantly on a north-south line. At most the astronomical correction is 0.1 mm/km [*Holdahl*, 1974], corresponding to a tilt of about 0.3×10^{-8} rad/yr for a 30-yr time interval. Earth tides and ocean loading are generally thought to be negligible as far as measurement of secular trends is concerned [*Bomford*, 1971], although *Simonsen* [1966] reported tidal tilts due to earth tides, ocean loading, and the attraction of water on the order of 4×10^{-8} rad/yr. It seems unlikely, however, that such tilts could affect leveling systematically for long distances. *Thurm* [1971] examined the influence of refraction, lunisolar tides, and thermal rod changes on a level net in the Elbe river valley and concluded that the corrections for these factors did not significantly affect elevation change measurements.

Leveling procedures are designed to minimize or eliminate the influence of these and other sources of systematic error, such as instrument maladjustment, nonverticality of rods, and sinking or rising of rods and instruments. Other sources of error, such as gravity anomalies or atmospheric pressure changes, are probably negligible in elevation change measure-

TABLE 1. Specifications for Precise Leveling Done by the U.S. Coast and Geodetic Survey [*USCGS*, 1961]

	Order of Leveling			
	First	Second (Class 1)	Second (Class 2)	Third
Spacing of lines and cross lines, miles	60 (96.6)	25–35 (40.2–56.3)	6 (9.7)	Not specified
Average spacing of permanently marked bench marks along lines, miles, not to exceed	1 (1.6)	1 (1.6)	1 (1.6)	3 (4.8)
Length of sections, miles	0.5–1 (0.8–1.6)	0.5–1 (0.8–1.6)	0.5–1 (0.8–1.6)	Not specified
Check between forward and backward running between fixed elevations or loop closures*, not to exceed	4 mm$(L)^{1/2}$	8.4 mm$(L)^{1/2}$	8.4 mm$(L)^{1/2}$	12 mm$(L)^{1/2}$

Numbers in parentheses are metric equivalents.
* Where L is in kilometers.

TABLE 2. Estimates of the Standard Deviation m of Precise Leveling Completed During Certain Time Periods

Time Period	First Order*, mm	Second Order*, mm
Prior to 1900	2.5	5.0
1900–1916	2.0	4.0
1917–1955	1.5	3.0
1956 to present	1.0	2.0

From *Holdahl* [1973a].
* If distance is measured in kilometers.

ments [*Leont'ev*, 1967; *Bomford*, 1971; *Isacks et al.*, 1973]. It should be emphasized, however, that knowledge of sources of error in leveling and their influence is by no means complete [*Bomford*, 1971]; however, to invoke unknown sources of error in order to explain away measured elevation changes is unwarranted and completely ad hoc at the present time. Routine office corrections applied to the field observations include corrections for the deviations in individual rod lengths, the thermal expansion or contraction of the rods, and residual collimation error [*Holdahl*, 1973*a*].

In an attempt to eliminate systematic errors from the leveling data, least squares adjustments are often performed. The result of such a process yields a set of adjusted elevations obtained by eliminating circuit misclosures in accordance with the laws of probability. The data used in preparing adjusted elevations usually span large time intervals, and thus any real vertical crustal movements are treated as errors. Elevation change calculations based on such data may therefore give very distorted patterns of vertical crustal movement. To avoid this problem, a number of methods have been worked out to adjust elevation change measurements [*Gale*, 1970; *Vanicek and Hamilton*, 1972; *Holdahl*, 1973*b*; *Vanicek and Christodulidis*, 1974]. Most of these methods depend on the assumption of constant rates of elevation change. *Vanicek and Hamilton* [1972] have questioned the normality of the error distributions involved, while Figure 2 demonstrates the weakness in the assumption of constant velocity. In order to minimize possible distortions due to adjustment procedures, only observed elevations incorporating routine office corrections are used in this study.

Data Analysis

The data examined in this paper were furnished, courtesy of the NGS, from the bank of elevation change data recently established at the Vertical Network Branch. The data format consists of tabulated and plotted values of relative elevation change between successive levelings along the same route (profile). The relative elevation changes are obtained by subtracting the elevation difference Δh between a given bench mark and some reference bench mark (usually the first) at some reference time from the same difference measured at some other time, i.e.,

$$d\Delta h = \Delta h(t) - \Delta h(t_0) \tag{2}$$

which is equivalent to summing the sequential intervening values of elevation change, i.e.,

$$d\Delta h_n = \sum_{i=1}^{n} d\Delta h_i \tag{3}$$

Relative velocities are obtained by dividing the relative elevation changes by the time interval over which they have occurred, i.e., only average velocities can be calculated. For simplicity, the duration of the leveling (which may be several months) is taken to be negligible in comparison with the time interval between levelings. It should be emphasized that the elevation changes and velocities used in this paper are relative to some reference point, usually arbitrarily chosen. It is the pattern of movement rather than the absolute values which is of primary importance. The problem of assigning absolute values is essentially one of least squares adjustment of leveling data with sea level changes, usually provided by tide gage measurements. Such absolute movement values, while representing an attempt to eliminate the effect of some types of errors, inherit the uncertainties of the assumptions involved in the adjustment procedures as well as those associated with sea level measurements [*Gutenberg*, 1941; *Bloom*, 1967; *Higgins*, 1965; *Emery and Uchupi*, 1972]. Figure 3 shows the lines of leveling in the elevation change data base of the NGS which are examined in this paper, as well as some supplementary data not yet incorporated into the base. Almost 40,000 km of the Vertical Control Net have been releveled in the eastern United States. The quality of this information and its suitability for discerning vertical movements of different wavelengths varies widely. Some profiles have effective bench mark densities of one per kilometer while other profiles have only one usable bench mark every 100 km. In order to provide a semiquantitative measure of the relative overall quality, each profile was assigned a quality factor. The criteria used in assigning a quality factor were as follows: the amount of scatter the bench mark density, the length of the time interval between levelings (longer time intervals given higher rating), and consistency in trend between successive releveling. The last two

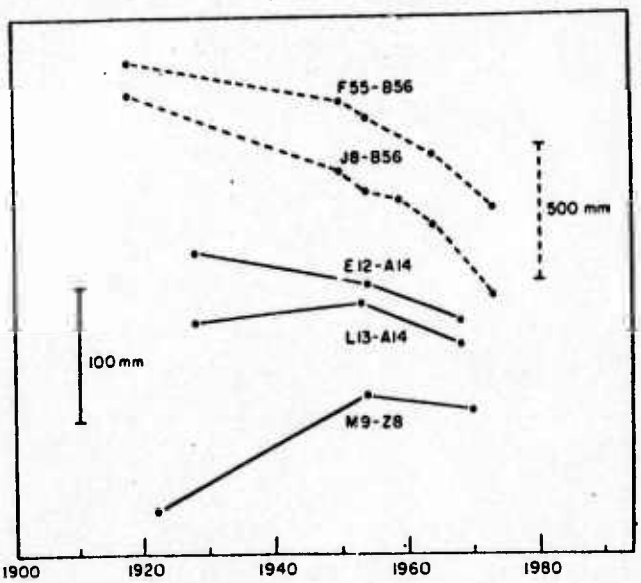


Fig. 2. Relative elevation changes for selected pairs of bench marks. For example, the upper curve depicts the movement of bench mark F55 relative to B56, using the dashed scale. Note nonlinearity in the two lower curves the direction of movement reverses with time.

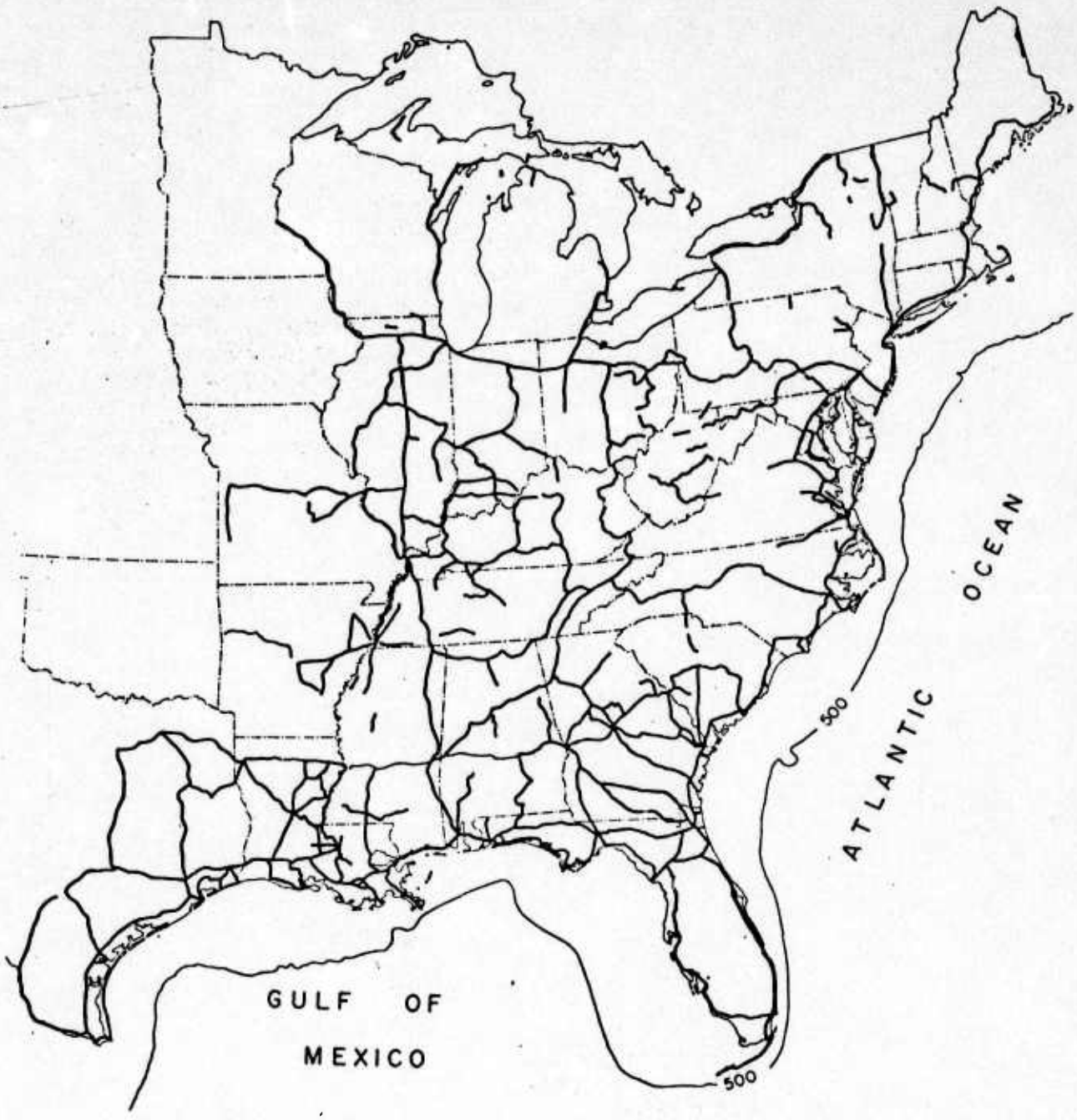


Fig. 3. Map showing routes of releveling in the eastern United States for which elevation change data have been compiled.

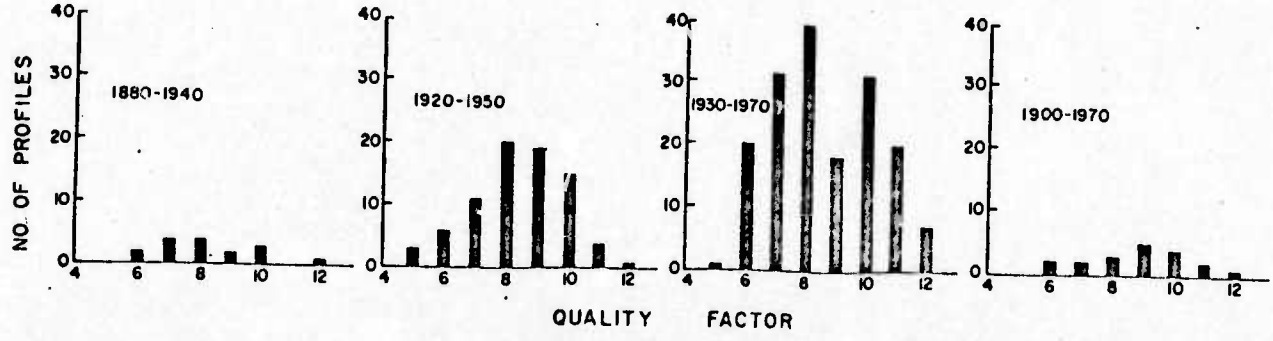


Fig. 4. Quality distribution of elevation change data according to the approximate time interval subtended by levelings. See text for discussion.

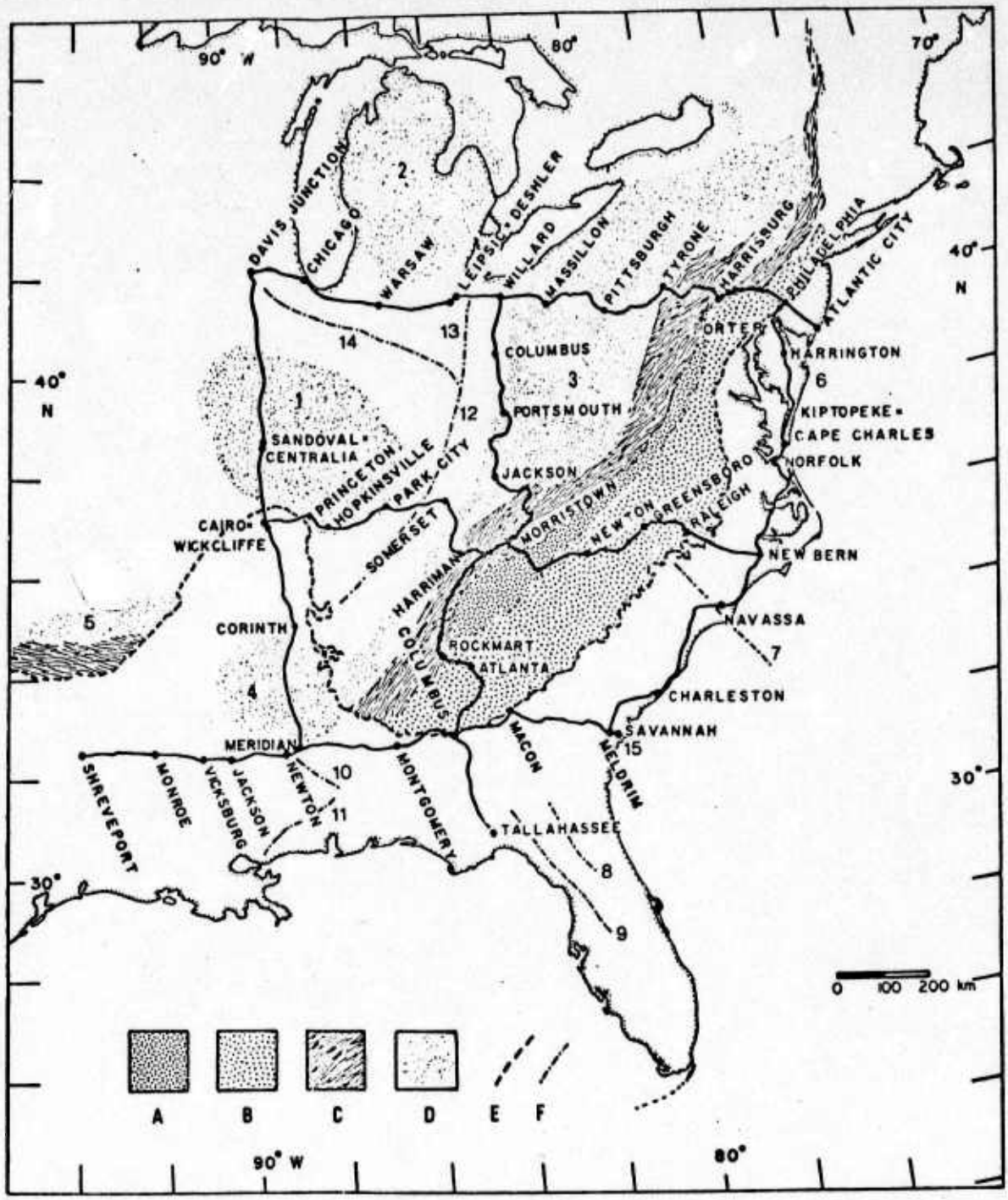


Fig. 5. Index map for relative velocity profiles shown in Figures 7–12. Physiographic provinces after *Fenneman* [1946]; geologic structure after *King* [1969*b*] and *Murray* [1961]. The symbols are defined as follows: A, Blue Ridge; B, Piedmont; C, Valley and Ridge; D, interior basins; E, inner limit of the Coastal Plain; F, structural high; 1, Illinois basin; 2, Michigan basin; 3, Appalachian foreland basin; 4, Black Warrior basin; 5, Ouachita foreland basin; 6, Chesapeake-Delaware embayment; 7, Cape Fear arch; 8, Peninsular arch; 9, Ocala uplift; 10, Hatchetigbee anticline; 11, Wiggins uplift; 12, Cincinnati arch; 13, Findlay arch; 14, Kankakee arch; 15, Southeast Georgia basin.

criteria depend in part on the assumption of constant rates of elevation change, an assumption which has already been questioned (Figure 2). However, since unambiguous multiple relevelings are not common, the influence of this assumption on the distribution of quality factors is small. Each profile, designated in accordance with the NGS data base, is rated 1, 2, or 3 for each criteria (3 being the highest), and the ratings summed. Figure 4 shows the result of such a rating for elevation change data classified according to the periods most closely subtended by the leveling interval of the profiles. The overall quality appears to be consistently high regardless of the times of leveling. Sufficient data of comparable quality are therefore presently available to make a meaningful analysis of regional differences in patterns of recent vertical crustal movements. In this paper an attempt was made to utilize the best measurements available for a given region.

When interpreting elevation change measurements it is often useful to work with the data in terms of tilts or tilt rates. Tilt rates are especially useful when comparing measurements of relative velocities with corresponding values of propagated error. Whereas the velocities and error referred to in this paper are relative, tilt rates are absolute. Tilt rates are calculated

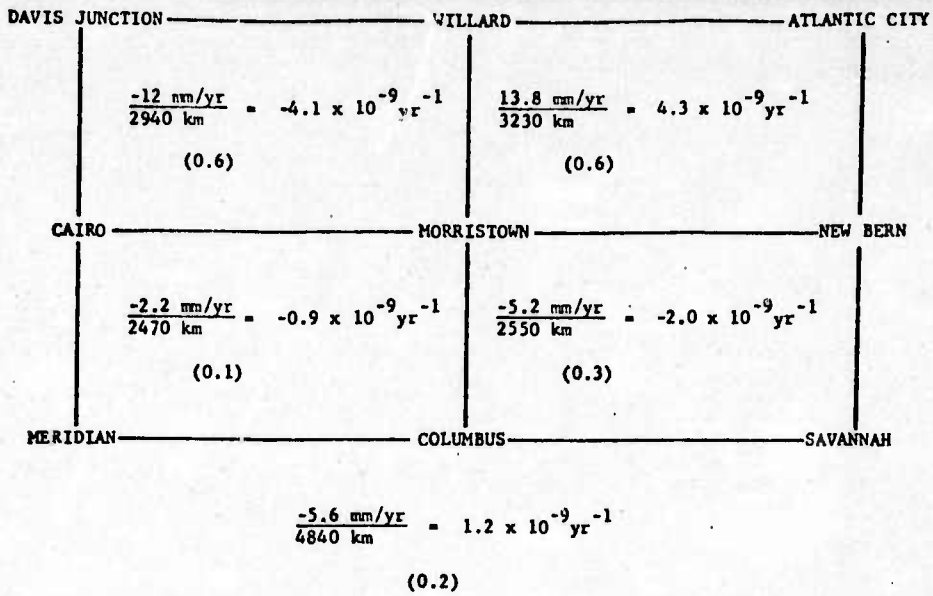


Fig. 6. Circuit misclosures computed from the profiles in Figures 7–12. The blocks represent the quadrants enclosed by the routes in Figure 5, with Davis Junction represented by the upper left corner. The numerator is the magnitude of the relative velocity misclosure, while the denominator is the length of the circuit. Also shown is the misclosure calculated as a tilt rate and (in parentheses) as a standard deviation of leveling. The bottom figures refer to the perimeter of the net.

from the slopes of relative velocity versus distance curves, i.e., $\tau = \Delta v/\Delta x$. Since the routes along which the leveling is actually done are neither direct nor horizontal lines, the tilt rates calculated in this manner are merely apparent, the actual values being greater than or equal to the apparent values. In the worst case this effect is as great as 25%, but it is usually much less than 10% and hence negligible. The measured component of tilt varies with the strike of the leveling route. Values of τ for the lines shown in Figure 3 range from 10^{-9} to 10^{-6} rad/yr. The larger values of τ are generally limited to areas where large-magnitude nontectonic processes are dominant, such as the Houston-Galveston region. Outside such areas, tilt rates appear to cluster between 10^{-8} and 10^{-7} rad/yr. The polarity of the tilt will be noted by the direction which is relatively subsiding, i.e., an eastward tilt is equivalent to a tilt down to the east.

In order to provide a representation of regional vertical crustal movements free of possible unwarranted distortion by adjustment procedures, six long profiles of relative velocity were compiled from shorter segments in the NGS data base. The only assumption involved is that there are no discontinuities in the relative velocity curves at the junction point. Figure 5 shows the routes of leveling as well as the major physiographic provinces and tectonic structures which are crossed [*Fenneman*, 1946; *King*, 1969*b*]. The cities mark, in general, the junction points of the elevation change profiles used. The designations in the NGS data base are used with only minor exceptions. It should be emphasized that different segments were leveled and releveled at different times (Tables 3*a*–3*f*), therefore the profiles are inhomogeneous with respect

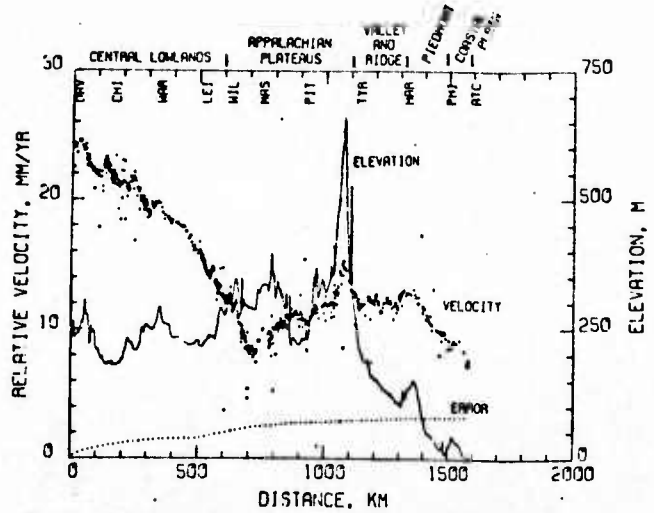


Fig. 7. Profile A, Davis Junction, Illinois, to Atlantic City, New Jersey. The points depict the relative velocities, the solid line gives the absolute elevations, and the lower dashed line represents the estimate of standard deviation relative to the starting point of the profile. Movements may be considered significant where the slope of the relative velocity curve exceeds the slope of the error propagation curve. The position of each reference point shown in Figure 5 is labeled at the top of the figure. Only relative velocities are depicted, i.e., the velocity values at $x = 0$ are arbitrary and chosen for scaling convenience only.

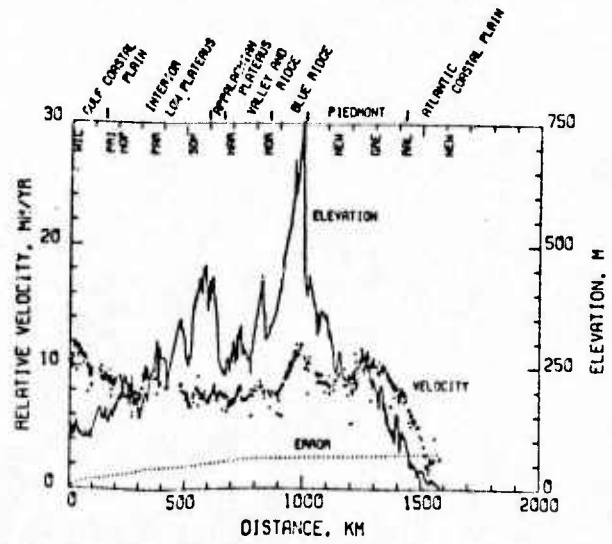


Fig. 8. Profile B, Wickcliffe, Kentucky, to New Bern, North Carolina. Symbols are defined in Figure 7.

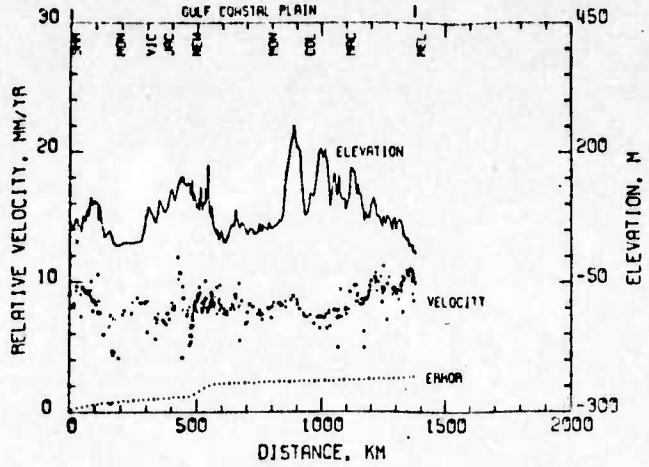


Fig. 9. Profile C, Shreveport, Louisiana, to Meldrim, Georgia. Symbols are defined in Figure 7.

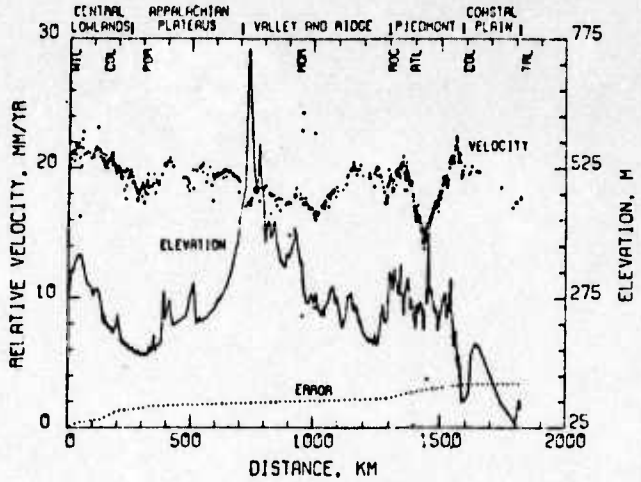


Fig. 11. Profile E, Willard, Ohio, to north of Tallahassee, Florida. Symbols are defined in Figure 7.

to time. Any attempt to compare trends among the several segments should therefore be made cautiously.

Figure 6 is a schematic diagram of the leveling routes with misclosures of the various circuits shown, as well as the corresponding contributions that these errors would make to tilt rates in the circuit if the closing errors were distributed homogeneously throughout the length of the circuit. Such a distribution is simplistic in that most of the error may be concentrated in only a few of the segments involved. Adjustment procedures try to account for such factors by various weighting schemes [*Vanicek and Hamilton*, 1972; *Holdahl and Morrison*, 1973], but lack of knowledge about the nature of the movements involved leaves the validity of these schemes open to question. In any case, the important point is that the tilt rates calculated from these misclosures are an order of magnitude smaller than the tilt rates indicated by the leveling data. If one were to attribute the misclosures to the propagation of random errors, the required standard deviations m_0 (also shown in Figure 6) are well within the limits estimated in Table 2. Thus the error curves in Figures 7–12 appear to be valid estimates of the errors to be expected in the relative velocity curves.

Figures 7–12 are profiles of vertical crustal movement which sample virtually all of the major tectonic provinces in the eastern United States. Pertinent facts related to these profiles are listed in Tables 3*a* through 3*f*. All of the profiles are plotted on the same scale for easy comparison. In addition to the curve of relative velocities, represented by points (each point representing an individual bench mark), the absolute elevations (relative to sea level) determined for each bench mark are shown as solid lines. These elevation profiles follow leveling routes, which are usually located along the smallest gradient available, often corresponding to railway routes and river courses, and therefore are normally not direct traverses across physiographic provinces. The error curves (dotted lines) represent the propagated random error estimated from the values of m in Table 2 using (1). The ordinate of the curve at a given distance x represents the standard deviation of relative velocity at that distance with respect to the initial bench mark in the profile. In order to evaluate the significance of any segment within the profile, the magnitude of the slopes of the relative velocity should be compared to the error curves. In general, velocity gradients which exceed the error gradients can be considered significant. Abbreviations of the names of the reference cities shown in Figure 5 are plotted at their respective positions along the profile route. In many cases, results from more than one releveling are available for segments of these profiles. The choice of which profile to use was based on several criteria. Profile segments with larger quality factors were given priority. An attempt was made to match segments whose times of leveling and releveling were similar in order to minimize the effect of nonlinear movements. Segments over which successive levelings are separated by very small time

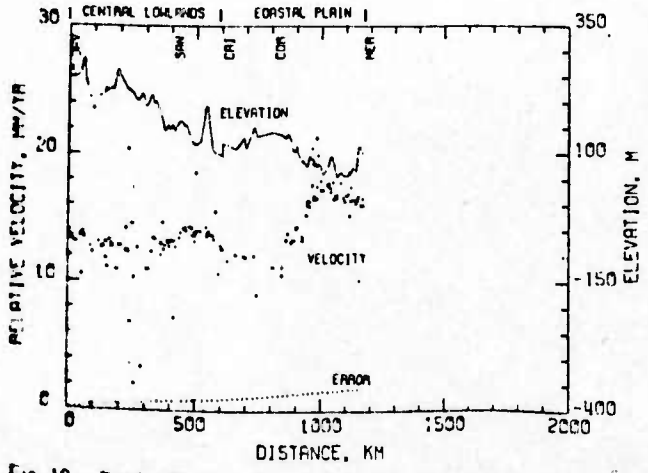


Fig. 10. Profile D, Davis Junction, Illinois, to Meridian, Mississippi. Symbols are defined in Figure 7.

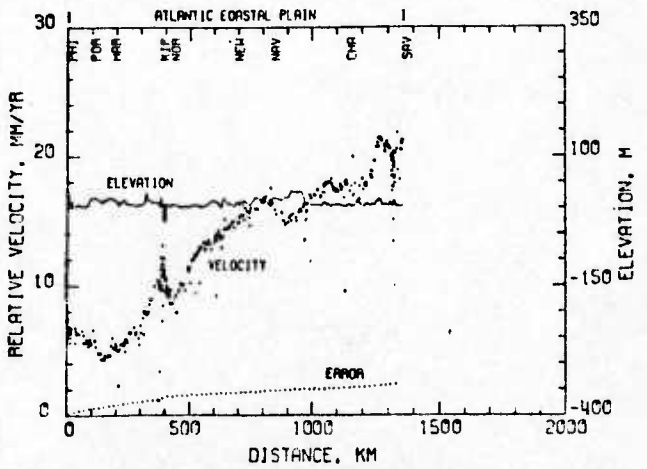


Fig. 12. Profile F, Philadelphia, Pennsylvania, to Savannah Beach, Georgia. Symbols are defined in Figure 7.

TABLE 3*a*. Background Data for Relative Velocity Profile A in Figure 7

Segment End Point	Distance From Davis Junction, km	Time Interval	*t*, years
Chicago	148	1947–1969.5	22.5
•	130	1947–1968.8	21.8
Warsaw	328	1946–1968.8	22.8
Leipsic-Deshler	504	1930–1968.8	38.8
Willard	607	1954–1968.6	14.6
•	718	1954–1967.5	13.5
Massillon	731	1934–1967.5	33.5
•	777	1934–1969.9	32.9
•	869	1950–1966.9	16.9
Pittsburgh	910	1941–1966.8	25.9
•	1095	1941–1966.8	25.8
Tyrone	1119	1934–1966.8	32.8
Harrisburg	1309	1941–1966.7	25.7
Philadelphia	1484	1929–1966.6	37.6
Atlantic City	1585	1924–1964.8	40.8

• Intermediate location.

TABLE 3*b*. Background Data for Relative Velocity Profile B in Figure 8

Segment End Point	Distance From Wickcliffe, km	Time Interval	*t*, years
•	94	1947–1968.7	21.7
Princeton	144	1934–1968.7	34.7
Hopkinsville	197	1949–1968.9	19.9
•	252	1940–1968.6	28.6
Park City	340	1954–1968.6	14.6
Somerset	504	1928–1968.6	40.6
Harriman	666	1950–1968.6	18.6
•	749	1950–1967.9	17.9
Morristown	826	1935–1967.9	32.9
•	1100	1935–1967.9	32.8
Newton	1117	1932–1967.8	35.8
•	1194	1932–1967.8	35.8
Greensboro	1275	1935–1967.8	32.8
Raleigh	1408	1935–1967.9	32.9
New Bern	1588	1935–1968	33

• Intermediate location.

TABLE 3*c*. Background Data for Relative Velocity Profile C in Figure 9

Segment End Point	Distance From Shreveport, km	Time Interval	*t*, years
Monroe	172	1938–1969.1	31.1
Vicksburg	292	1934–1961.1	35.1
Jackson	363	1935–1968.9	33.9
Newton	475	1935–1968.9	33.9
•	562	1961–1968.3	7.3
•	620	1943.8–1968.3	24.5
Montgomery	781	1933–1968.5	35.3
Columbus	931	1933–1968.3	35.3
Macon	1096	1917–1958	41
•	1312	1934.8–1962	27.2
Meldrim	1378	1934.8–1955	20.2

• Intermediate location.

TABLE 3*d*. Background Data for Relative Velocity Profile D in Figure 10

Segment End Point	Distance From Davis Junction, km	Time Interval	*t*, years
Sandoval-Centralia	411	1920–1969.8	49.8
Cairo-Wickcliffe	605	1922–1969.9	47.9
Corinth	810	1889–1948	59
Meridian	1173	1935–1961.0	26.0

TABLE 3e. Background Data for Relative Velocity Profile E in Figure 11

Segment End Point	Distance From Willard, km	Time Interval	t, years
Columbus	139	1934–1967.7	33.7
*	215	1954–1967.8	13.8
Portsmouth	294	1943–1967.8	39.8
*	354	1956–1967.8	11.8
Jackson	536	1928–1967.8	39.8
Morristown	926	1930–1967.6	37.6
Rockmart	1291	1935–1967.9	32.9
Atlanta	1378	1959–1968.5	9.5
Columbus	1587	1958–1968.3	10.3
Tallahassee	1820	1916–1958	42

* Intermediate location.

TABLE 3f. Background Data for Relative Velocity Profile F in Figure 12

Segment End Point	Distance From Philadelphia, km	Time Interval	t, years
*	17	1929–1964.7	35.7
Porter	94	1932–1964.7	33.7
Harrington	175	1931–1963.0	32.0
Kiptopeke	376	1935–1963.0	28.0
*	408	1963–1972.4	9.4
Norfolk	420	1952–1972.4	20.4
New Bern	683	1932–1963	31
Navassa	831	1932–1963.2	31.2
Charleston	1138	1932.8–1963.0	30.2
*	1238	1933–1961	28
Savannah Beach	1355	1933–1955	22

* Intermediate location.

intervals were avoided unless no other measurements were available. In general, the trends shown in Figures 7–12 are supported, at least in sign, by the additional relevelings available. A notable exception is the segment from Raleigh, North Carolina, to New Bern, North Carolina (*b* in Figure 13), which shows eastward tilting (i.e., down to the east) between 1935 and 1968 and westward tilting between 1897 and 1935. Although the elevation changes on the earlier profile lie well within the range one might expect from random error, those of the later profile do not; hence the rate of elevation change must have been significantly different for the two observation periods. Another exception occurs in the segment between Macon, Georgia, and Savannah, Georgia (*a* in Figure 13), which shows an eastward tilt between 1917 and 1935 and a westward tilt between 1935 and 1962, a reversal with time opposite to that in the previous example. These two examples demonstrate that these movements do not have constant velocities. If they represent true crustal movement, the period of these movements could be on the order of the time intervals between levelings.

RESULTS

An inspection of Figures 5 and 7–12 reveals a marked correspondence between the shape of the relative velocity curves and the regional geologic structure along the leveling route. Consistent patterns can be recognized for the Coastal Plain, the Appalachian Highlands, and the Interior Plains, following the terminology of *Fenneman* [1946].

Coastal Plain

The dominant characteristic of the Coastal Plain province, especially pronounced in the Atlantic section, is a consistent tilt down toward the ocean. This tilt can be seen in Figures 7, 8, and 11, but not in Figure 9. It can also be seen in other leveling lines of the NGS data base that traverse the Coastal Plain (Figure 13); 14 of 15 profiles of this data base show oceanward tilting. Two of these, however, indicate a reversal in the direction of tilting between successive relevelings (*a* and *b* in Figure 13). One of these lines (*a* in Figure 13, which is part of profile C) and a line that shows a net tilt down toward the continental interior (*c* in Figure 13) are located in a region of historic and recent seismicity [*Bollinger*, 1972; *Coffman and von Hake*, 1973]. The oceanward tilts correspond to the general oceanward decrease in elevation across the Coastal Plain, the possibility thus being raised that elevation-correlated errors (e.g., rod miscalibration or refraction) dominate the trends. Since the error has an equal chance of occurring in either the original leveling or the subsequent releveling, one would expect such errors to yield apparent tilts both toward and away from the coast. Furthermore, the magnitude of the



Fig. 13. Selected routes of elevation change profiles which cross the Coastal Plains and parts of the Interior Plains. (See text.)

correlation between the relative velocity and the elevation curves appears to be greater than that which one would expect from rod error or refraction effects (Figure 14). Figure 12, showing the results of releveling from north to south along the coast, indicates that there is considerable variation in vertical movement along the Atlantic Coastal Plain. The dominant feature is a very large northward tilt of the Atlantic Coastal Plain between Harrington, Delaware, and Savannah, Georgia. The virtually flat topography along this line eliminates elevation-correlated errors as an influence. Being a north-south line, it is susceptible to the accumulation of tidal errors. However, the tilt rates along this line ($\sim 2 \times 10^{-8}$ rad/yr) are significantly larger than those attributable to tidal error ($\sim 2 \times 10^{-9}$ rad/yr). A large part of this tilt may be attributed to absolute subsidence of the Chesapeake-Delaware embayment (Figure 5) relative to sea level, as indicated by adjustments of leveling and tide gage data in the area by the NGS [*Holdahl*, 1973*a*; *Holdahl and Morrison*, 1973; *Balazs*, 1974]. The tilt rate drops off rapidly at the Cape Fear arch (Figure 5), which indicates that the arch is acting as a hinge line. Leveling between New Bern, North Carolina, and Charleston, South Carolina (Figures 5 and 12) indicates relative uplift at the Cape Fear arch. The pattern of movement suggests three alternative interpretations. (1) a domelike relative uplift centered offshore, i.e., the direction of tilt reverses as the line of leveling alternately approaches and retreats from the coast line at the arch, which is consistent with the behavior one would expect if leveling first toward, then away from the crest of an actively doming structure; (2) a corresponding circular subsidence centered inland; or (3) a narrow relative subsidence trough extending inland transverse to the coast which just happens to coincide with the change in direction of leveling. The general oceanward tilt of the Coastal Plain argues against the second alternative, and probability argues against the third, making relative uplift offshore at the Cape Fear arch the most likely possibility. Localized uplifts are also seen to occur at Kiptopeke, Virginia, and Savannah, Georgia. Releveling extending to the south and west of Savannah, Georgia, indicates that the relative uplift in this area is also domelike in nature. There is no additional releveling in the area of Cape Charles, Virginia, to suggest the three-dimensional nature of movement there.

In contrast to the large movements shown in Figure 12 for the Atlantic Coastal Plain, the profile (Figure 9) that parallels the Gulf coast (Figure 5) shows relative stability. The dominant feature in this profile is the relative uplift of the Savannah (Meldrim) area. Other than this trend, only very localized movements are inferred, such as the relative subsidence of the Monroe, Louisiana, area, possibly reflecting natural gas production nearby [*Louisiana Geological Survey*, 1973]. Small peaks in relative velocity can be seen near Shreveport, Louisiana, and west of Columbus, Georgia. The segment in Figure 10 from Corinth, Mississippi, to Meridian, Mississippi, indicates significant uplift of the northeastern part of Mississippi relative to the central United States region.

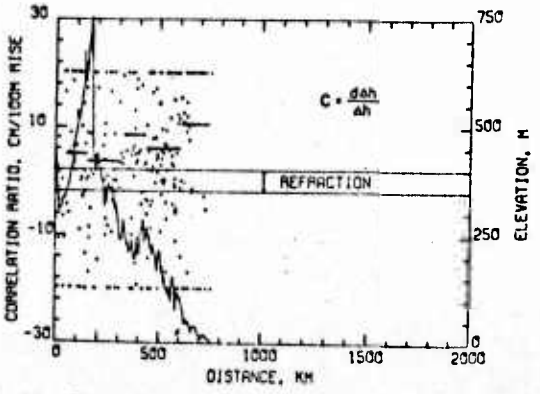


Fig. 14. Plot of correlation ratio of elevation change to elevation difference as a function of distance from Morristown, Tennessee, eastward along profile B. The maximum values to be expected due to refraction errors are shown. Solid line represents absolute elevation along profile. The short horizontal bars depict the net or 'average' value of c for that particular segment.

Holdahl [1973*b*] has prepared a map of the Gulf Coast region from an adjustment of leveling and tide gage data (Figure 15). In addition to the oceanward tilt characteristic of the Coastal Plain this map locates centers of subsidence relative to sea level (without the eustatic term) in the Houston-Galveston region and part of the Mississippi delta region in Louisiana. Widespread fluid withdrawal may explain these features, although sediment compaction may also be involved in the Mississippi delta region. Two prominent features of this map which do not appear to be associated with fluid withdrawal are a domelike uplift centered over southwest Alabama and an eastward tilting of the Florida peninsula. Due to its large magnitude, it is unlikely that the Alabama movement can be attributed to distortion due to the adjustment procedure.

The question naturally arises as to the relationship of these movements with geologic structure and their consistency with long-term trends indicated by the geologic record. The Mesozoic and Cenozoic structural trends in the Chesapeake-Delaware embayment appear to reflect underlying Paleozoic structures [*Murray*, 1961]. The area has been structurally low since the Cretaceous, although the absence of certain major sedimentary rock sequences indicates intermittent uplift [*Murray*, 1961]. The Cape Fear arch represents the southern boundary of the embayment and is a distinct northwest-trending basement ridge which gradually merges with the pre-Cretaceous surface near the fall line [*Bonini*, 1955; *Ferenczi*, 1959]. The sediment thickness, as indicated by depth to basement, decreases as one traverses the arch [*Berry*, 1951].

The oceanward tilt of the Coastal Plains (both Atlantic and Gulf) also correlates in general with the increase of sediment thickness toward the ocean [*Spangler*, 1950; *Spangler and Peterson*, 1950; *Drake et al.*, 1959; *Murray*, 1961; *Maher*, 1968; *Uchupi*, 1970]. The increase in the magnitude of relative subsidence with increasing sediment thickness suggests that a sediment compaction mechanism might be responsible. However, the large tilt rates measured by releveling seem to preclude compaction due solely to overburden pressure as a reasonable mechanism [*Weller*, 1959; *Rieke and Chilingarian*, 1974]. On the other hand, near-surface compaction due to groundwater variations may be significant. *Poland and Davis* [1956] presented strong evidence linking subsidence to fluid withdrawal and the subsequent reduction in artesian pressure and compaction of clays. They found surface level changes of about 1 m for every 20 m of water level decline in the San Joaquin valley. Similar results have been found in the Houston-Galveston region where the average groundwater pumping rate in 1964 was 411 million gal./day (1.6×10^9 l/day) [*Gabrysch*, 1969]. In contrast, pumping rates near the routes of releveled profiles in the Atlantic Coastal Plain exceed 72 million gal./day (2.7×10^8 l/day) only at Savannah, Georgia, and Philadelphia, Pennsylvania [*USGS*, 1970]. Furthermore, surface movements due to groundwater withdrawal tend to be localized rather than regional [*Small*, 1961]. The scatter in relative velocity values at Savannah,

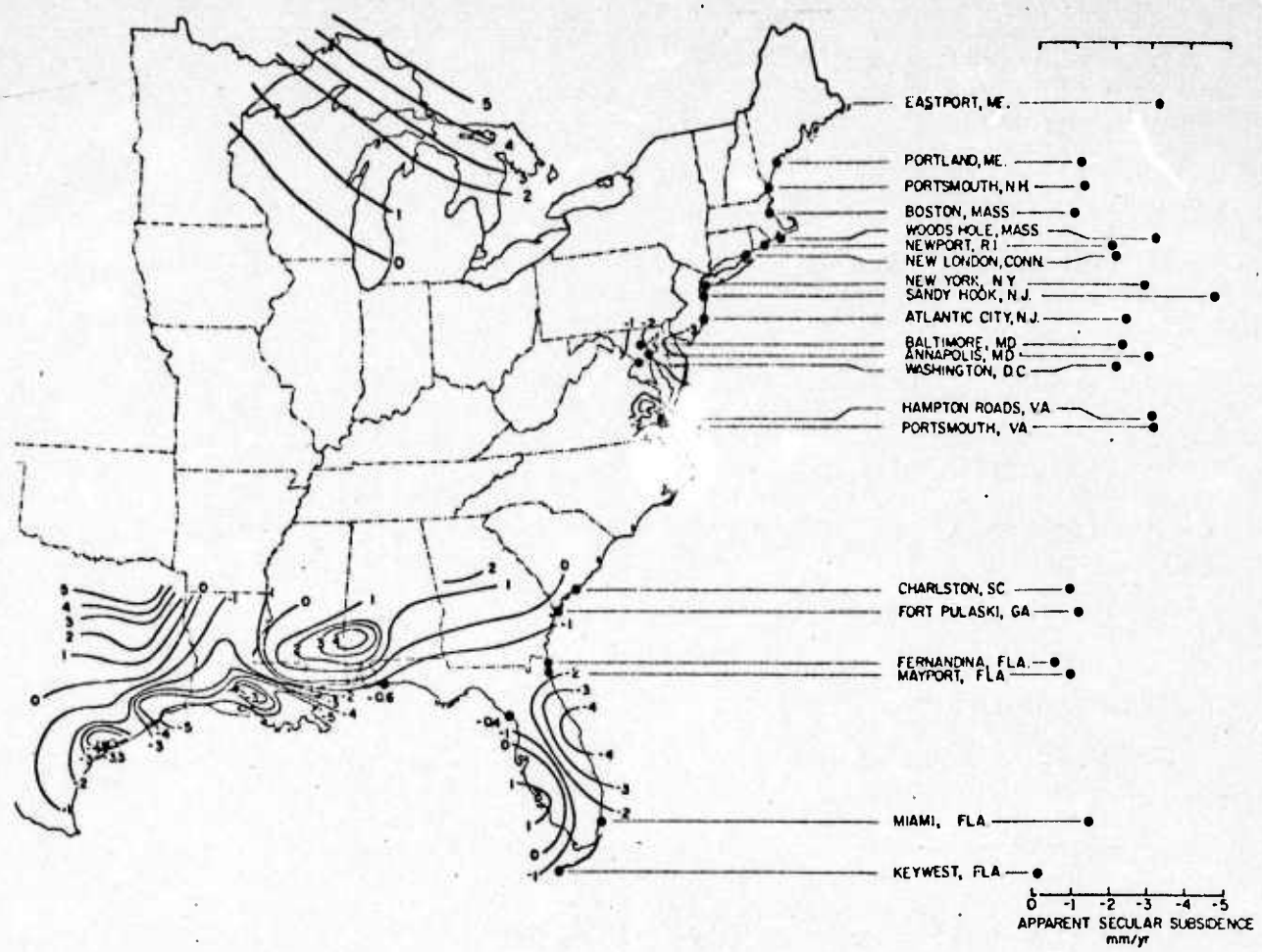


Fig. 15. Summary map of vertical crustal movements mapped in previous work by others. Great Lakes' isobases (relative) by *Walcott* [1972*b*] from water level gages. Chesapeake Bay and Gulf Coast maps by *Holdahl and Morrison* [1973] from adjustment of leveling and tide gage data. Apparent secular land subsidence rates derived by *Hicks* [1972*b*] from tide gage records are plotted along the Atlantic Coast, with tide gage locations indicated by solid circles on the left. Individual measurements by *Hicks* [1972*b*] for the Gulf Coast are also shown. All values in mm/yr.

Georgia, seen in Figure 12 may be attributed to such effects [*Davis et al.*, 1963]. It seems unlikely, therefore, that groundwater variation due to pumping is a serious problem in interpreting long-wavelength data. On the other hand, long-term natural water level variations may be a factor, since they characteristically have amplitudes of several decimeters to a few meters [*Wenzel*, 1936; *Fischel*, 1956]. These variations may be especially pronounced in karst regions. However, a number of considerations suggest that groundwater variations are not significant influences on the trends suggested by leveling data. Trends in the Atlantic Coastal Plain extend well into the Piedmont, and, in general, there is a poor correlation between aquifer patterns (e.g., the limestone sections responsible for karst topography) and vertical movement trends [*Meinzer*, 1959; *Domenico*, 1972]. Since the groundwater level is a function of a number of variables, including precipitation rates, surface runoff, and aquifer type, it is difficult to understand how coherent regional patterns of surface movement could result from its natural variation. However, until more is learned about the relationship between secular groundwater variations and resulting vertical motions of the surface, hydrologic factors cannot be completely dismissed. It is possible that these factors may be responsible for the apparent short-term variations in rates of vertical movements. For the purpose of investigating the correlations of vertical crustal motions with geological and geophysical parameters, the influence of hydrologic factors will be ignored in the remainder of this paper.

The Savannah 'uplift' occurs in the southeast Georgia basin, a structural low for most of the Cenozoic, with a possible Cretaceous basement ridge (Yamacraw) near Savannah [*Cramer*, 1969]. The absence of certain sequences in the stratigraphic record of the basin indicates intermittent uplift of the area relative to sea level [*Murray*, 1961]. Thus a short relative uplift of this area at the present time would not be inconsistent with the basin's Cenozoic history. The relative uplift of the continental side of the Coastal Plain as indicated by precise releveling agrees well, at least in sign, with the apparent uplift of Pleistocene terraces both on the Atlantic and Gulf Coast coastal plains [*Flint*, 1940; *Murray*, 1961; *Oaks and Dubar*, 1974]. Discriminating between terraces caused by uplift of the continent relative to a stationary sea level and those formed by eustatic changes in sea level is not a trivial problem [*Bloom et al.*, 1974]. The uncertainty in the ages of the U.S. coastal terraces makes it difficult to estimate the rates of uplift relative to sea level for these terraces. By using estimates of eustatic sea level fluctuations derived for the raised coral reef terraces in New Guinea, Barbados, and elsewhere, *Bloom* [1974] made estimates of the relative uplift of Atlantic coastal terraces which agree within an order of magnitude with rates of relative uplift indicated by releveling for the Coastal Plain. The general

horizontality of Atlantic coastal terraces, although recently questioned [*Oaks and Dubar*, 1974], argues against any long-term northward tilting of the Atlantic Coastal Plain [*Cooke*, 1930; *Flint*, 1940; *Murray*, 1961], such as that indicated in Figure 12. However, uncertainties in correlating the terraces and measuring their altitudes allow some latitude in placing an upper limit to how far back present rates might be extrapolated and still be undetected in terrace morphology [*Flint*, 1940; *Doering*, 1960; *Oaks and Dubar*, 1974].

The tilt of the Atlantic Coastal Plain down to the north, as indicated by leveling, does not agree in magnitude with that indicated by analysis of tide gage data [*Hicks and Shofnos*, 1965; *Hicks*, 1972*a*, *b*, 1973]. As can be seen in Figure 12, leveling indicates that Savannah, Georgia, is rising with respect to Norfolk, Virginia, at a rate of about 10 mm/yr, whereas tide gage records (Figure 15) show a difference of only about 1.5 mm/yr in the same direction. The large number of sources of contamination for tide gage measurements from factors other than secular sea level changes makes such information extremely suspect [*Higgins*, 1965; *Meade and Emery*, 1971; *Emery and Uchupi*, 1972; *Kaye and Stuckey*, 1973; *Balazs*, 1974]. Therefore, tidal trends are not used in this paper.

The Ocala uplift is one part of the Ocala arch, the other parts being the central Georgia uplift and the Peninsular arch, both subparallel to and east of the Ocala uplift [*Murray*, 1961]. The central Georgia uplift-Peninsular arch represents the late Paleozoic and Mesozoic axis of maximum uplift whereas the Ocala uplift is the center of Cenozoic uplift, i.e., there has been a westward migration of the axis of maximum relative uplift [*Murray*, 1961]. Releveling data suggest that the pattern of contemporary vertical movements in Florida represents a continuation of this trend. The present axis of maximum relative uplift has migrated parallel to and west of the Ocala uplift (compare Figures 5 and 15). This migration may be illusory, for it is difficult to understand why such a pattern should persist coherently for such a long time interval given the complex geologic history of the area. The broad uplift in southeast Mississippi and southwest Alabama corresponds to the Hatchetigbee anticline and Wiggins uplift (Figure 5). Active during the early Tertiary, these structures lie at the junction of the Ouachita and Appalachian foldbelts, the exact nature of which is as yet unknown [*King*, 1959, 1969*a*; *Murray*, 1961]. As will be shown later, relative uplift characterizes releveling results in the Appalachian Highlands, therefore relative uplift at this junction is not a complete surprise. However, the profile in Figure 9 indicates relative stability north of this junction, implying that extrapolation of relative velocity trends along the Appalachians is not valid for the entire length of the orogenic belt. Profile D (Figure 10) shows that the Black Warrior basin is presently being uplifted relative to the Central Lowlands, a pattern which will be shown to be characteristic of the Appalachian foreland basin to the north (Figures 7 and 8). It therefore seems plausible to attribute these anomalous vertical movements in the central Gulf Coastal Plain to the underlying extensions of the Paleozoic Appalachian-Ouachita fold system. However, the very fact that these extensions are buried whereas the portions of the foldbelt to the north are exposed indicates quite dissimilar movements in the past, thus making inference based on similarity of recent movements questionable. For example, the southeast Mississippi uplift may not be associated with movements in the Appalachian orogenic trend at all, but rather with sedimentation in the Mississippi delta. *Walcott* [1972*a*] proposed a sediment-loading model for the Mississippi delta region which calls for the formation of a peripheral bulge in southeastern Mississippi. Walcott pointed to the gravity high at this location as evidence of a forebulge. The uplift indicated by leveling in southeast Mississippi may, therefore, represent growth of the forebulge, modified perhaps by preexisting weaknesses represented by the Hatchetigbee anticline and Wiggins uplift.

Appalachian Highlands

For the purposes of this paper, the Appalachian Highlands will be considered as being comprised of four separate parts (Figure 5). From east to west these divisions are the Piedmont, the Blue Ridge, the Valley and Ridge, and the Appalachian Plateaus (or foreland basin). We will be concerned with the southern and central Appalachians in this paper, where the above classification is applicable [*Fenneman*, 1946; *Rodgers*, 1970].

Profiles A and B (Figures 7 and 8) traverse the Appalachian Highlands in the central and southern sections, respectively. Both profiles indicate that the Highlands region is presently being uplifted relative to the coast at rates of up to 6 mm/yr. In both traverses there appear to be smaller peaks of relative velocity superimposed on this broader uplift. In Pennsylvania, peaks can be seen near Harrisburg, Tyrone, and possibly Pittsburgh. The Harrisburg feature is located near the eastern boundary of the Valley and Ridge province along a northward extrapolation of the eastern limit of the Blue Ridge province, which pinches out to the south. Structurally this limit is the western boundary fault of a Triassic graben filled with sediments of the Newark group [*King*, 1969*a*]. The Tyrone feature, a more pronounced peak, is located at the western limit of the Valley and Ridge province, i.e., the Allegheny Front [*King*, 1969*a*]. The Pittsburgh feature appears upon close examination to be a relative velocity minimum east of Pittsburgh rather than a pronounced peak to the west of the city. There does not appear to be any prominent geological structure associated with this feature. Near the western limit of the Appalachian Plateaus there is a very pronounced minimum in the relative velocity curve.

In the southern Appalachians, similar secondary features in the releveling profile can be seen. Peaks in relative velocity near Greensboro, North Carolina, and Asheville, North Carolina (about 170 km east of Morristown, Tennessee) dominate profile B. Structurally, the Greensboro feature occurs at the western boundary of the Carolina slate belt [*King*, 1955]. The Asheville peak occurs at the boundary between the Piedmont and the Blue Ridge provinces, structurally corresponding to the Brevard fault zone [*King*, 1969*b*]. In contrast with profile A, there does not appear to be a prominent minimum marking the western boundary of the Appalachian Highlands province.

Profile E (Figure 11) crosses the Appalachian Highlands in a north-south direction. In general this profile shows a tilt down to the south for the Appalachian Plateaus and Valley and Ridge provinces. However, due to the meander of the leveling route between Portsmouth, Ohio, and Morristown, Tennessee, it is difficult to interpret secondary trends in this segment. There is a minimum in the curve at Portsmouth, Ohio, near the western limit of the Highlands. Pronounced minima also occur south of Morristown, Tennessee, and south of Atlanta, Georgia. Between these two minima is a region of broad relative uplift, corresponding to the traverse of the leveling route in the Valley and Ridge province around the southern limit of the Blue Ridge. The segment between Atlanta, Georgia, and Rockmart, Georgia, also suggests a minor peak. This peak can be correlated geographically with the Brevard fault zone, al-

though here the fault is located within the Piedmont and not at its boundary [*King*, 1969*b*]. Small peaks in relative velocity can also be recognized just south of Portsmouth, Ohio, and just north of Columbus, Georgia.

Before the correlation of these features with geological parameters can be assessed, one should note that many of the peaks in relative velocity show a striking correlation with absolute elevation (Figures 7 and 8). Elevation-correlated errors would appear to be a possible explanation for these movements. The nature of these errors and the problems associated with their interpretation were discussed above. In order to provide an estimate of the amount of correlation between elevation and elevation changes as a function of position along the leveling route, the ratio $c = d\Delta h/\Delta h$ was calculated for each bench mark interval and plotted versus distance along the profile route for the portion of profile B between Morristown, Tennessee, and New Bern, North Carolina (Figure 14). This segment has the lowest values of c and the most consistent time interval of any of the profiles. Figure 14 shows the results of this calculation. Values of c greater than 20 cm/100 m rise were plotted at this value for scaling convenience. The elevation curve is also shown for orientation. The majority of values for c are significantly larger than those one could attribute to an elevation-correlated error such as refraction. Although some of the values for c corresponding to the elevation peak near 170 km do lie within the error limits, most do not. Almost none of the values corresponding to the elevation peak at 410 km lie within error limits. However, for short distance intervals and small elevation differences, random error may easily exceed the systematic error and result in apparent values of c which bear no relation to actual elevation-correlated errors. In order to minimize the influence of random error, the profile was broken up into segments of considerable length. The net elevation difference (Δh) and relative elevation change ($d\Delta h$) for the entire segment were then used to calculate an 'effective' c. The resulting values are shown as horizontal bars over the segment interval. In all of the segments the effective values for c exceed the limits for refraction error and are positive in sign. The correlation between absolute elevation and relative velocity cannot, therefore, be attributed solely to known types of leveling error. *Karcz and Kafri* [1971, 1973] have reported similar correlations in the Negev of southern Israel, although the nature of the correlation there is negative, i.e., high elevation associated with relative subsidence. Although negative correlations may be present in certain segments of these profiles, by far the most prominent correlations are positive. The implication therefore is that the topography of the Appalachians is at least partially attributable to some dynamic mechanism which is currently active and not solely to differential erosion. *Hack* [1973] finds an erosional disequilibrium in the southeast Appalachians which corresponds spatially with the relative velocity maximum near Asheville, North Carolina. Relative uplift of this area such as that indicated by leveling could easily explain the anomalous stream gradients in the area. It should also be noted that the spatial pattern of high stream gradient parameters calculated by Hack for the Winston-Salem quadrangle suggests elongate zones trending northeast. As will be shown later, leveling results suggest a pattern of uplift remarkably similar to that indicated by the stream gradients.

The overall uplift of the Appalachian Highlands relative to the coast is consistent, at least in sign, with the post-Triassic vertical history of the area inferred from the clastic sediments of the Atlantic coastal margin. The rates of uplift determined from leveling are, in general, higher than those determined from geologic information. *Owens* [1970] suggested that the uniformity of Pliocene and Quaternary clastics implies a generally uniform uplift along the entire central and southern Appalachians. However, the sedimentary record reflects time averages of complex tectonic movements, erosion, and transport processes. As indicated by the present-day southward tilt of the Appalachian Highlands (Figure 11) and the northward tilt of the Atlantic Coastal Plain (Figure 12), simple extrapolations based on the sedimentary record may be misleading when trying to predict trends of recent crustal movements.

The rates of uplift of the Appalachians relative to the coast measured by releveling range up to 6 mm/yr. Such rates are at variance with those derived by analysis of coastal margin sediments as well as with estimates of the amount of sediments presently being transported from Appalachian drainage basins to the ocean. *Menard* [1961] calculated from the volume of Appalachian-derived sediments that the erosion rate over the past 125 m.y. has averaged 0.062 mm/yr. Based on the sediment load transported by rivers with drainage basins in the Appalachians, Menard estimated the present rate of erosion to be about 0.008 mm/yr, which agrees well with the earlier estimates of *Dole and Stabler* [1909] for the North Atlantic streams. *Gilluly* [1964] examined such calculations and concluded that the results would not be significantly changed by consideration of second-order effects. *Ahnert* [1970], assuming that rates of stream incision were equal to rates of uplift, obtained velocities of vertical movement on the order of 0.02–0.03 mm/yr. *Schumm* [1963] estimated that 1 mm/yr is a reasonable maximum denudation rate. The present rates of uplift of the Appalachians exceed these estimates by up to 2 orders of magnitude. This discrepancy, noted by *Mescherikov* [1959], *Schumm* [1963], and *Gilluly* [1964], clearly limits the time interval during which such movements can operate. Otherwise, an Appalachian mountain system 10 km high could be generated in a few million years. Although the exponential relationship between erosion rates and elevation [*Schumm and Hadley*, 1961] might limit the actual maximum elevation attainable, the volumes of sediments supplied in such a situation, given present rates of uplift as indicated by releveling, would be much greater than those observed. The movements indicated by releveling in the Appalachians must therefore be episodic or periodic, with periods of much less than 10^6 yr. The reversals in tilt directions discussed previously suggest that these periods might even be on the order of 10^2 yr. If these measurements represent true tectonic movements with periods less than 10^2 yr, the odds are small that this century, when compared with post-Triassic time, should be one of rapid motion. It is difficult, therefore, to bridge the gap between recent movements and earlier geologic crustal motions on the basis of similar directions of movement alone.

The secondary movements in the Appalachian Highlands delineated by releveling are difficult to interpret. They might be attributed to very local mechanisms (e.g., mining, local diapirism, etc.). However, absence of reasonable local mechanisms in most cases coupled with the fact that most of these features are located at or near major geological and tectonic boundaries suggests that these movements are related to large scale movements of the earth's crust. In Figure 16*a* the relative velocity maxima and minima have been plotted, along with the major structural provinces of the eastern United States. The similar character of the relative velocity curves in profile A between Massillon, Ohio, and Atlantic City, New Jersey, and in profile B between Morristown, Tennessee, and New Bern,

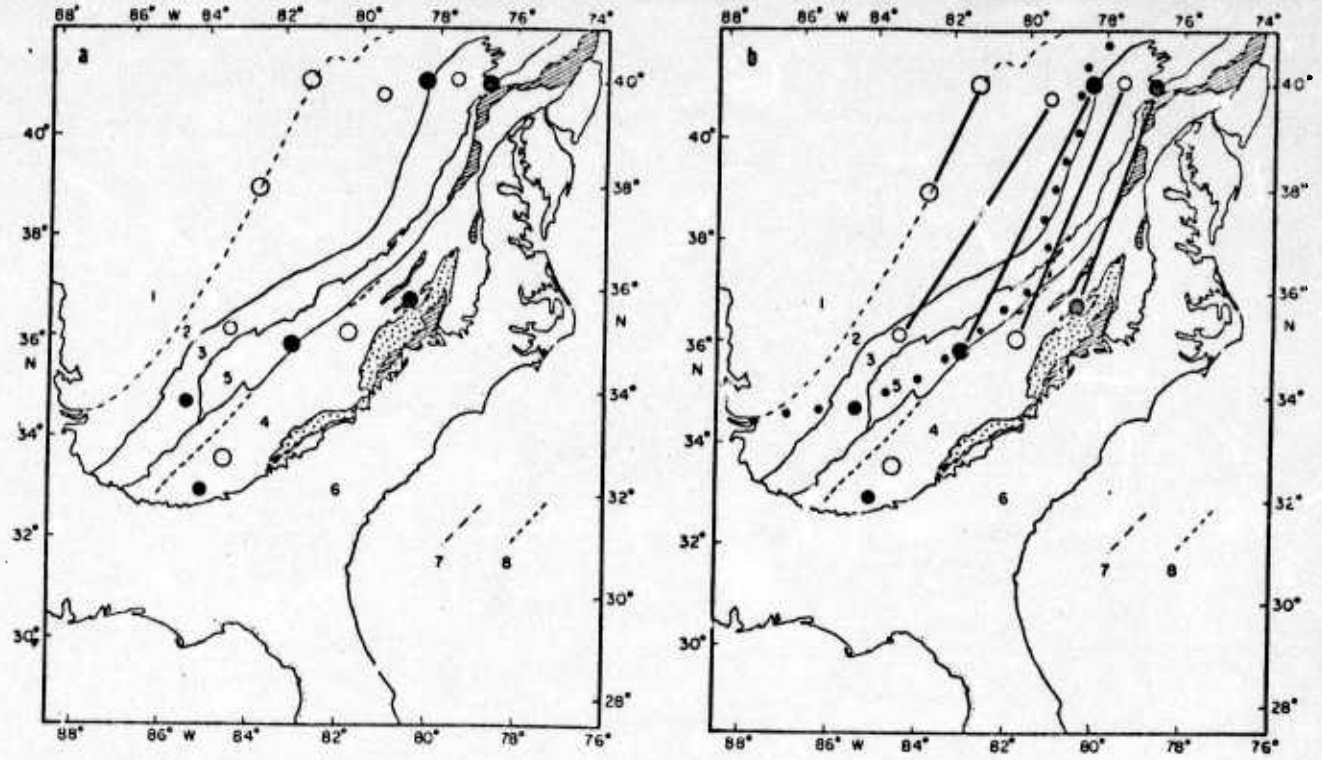


Fig. 16. Map of 'secondary' relative velocity features. Solid circles denote relative velocity maxima, open circles relative velocity minima. Larger circles represent better-defined features. (*a*.) These features are plotted on a generalized tectonic and geologic map [after *King*, 1969*b*; *Goddard et al.*, 1965]. (*b*) An interpretation of possible correlations between these features is shown. Also shown in (*b*) is the Appalachian drainage divide (heavy dotted line) [*Rodgers*, 1973]. (*c*) An alternative correlation. 1, Interior Plains; 2, Appalachian foreland basin; 3, Valley and Ridge; 4, Piedmont; 5, Blue Ridge; 6, Coastal Plain; 7, base of the Pennsylvanian; 8, extensions of the Brevard fault zone into the Piedmont. Striped areas are Triassic basins; area marked with carets represents the Carolina slate belt.

North Carolina, invites a correlation such as that shown in Figure 16*b*. The trends indicated by such a correlation cut across the structural grain of the Appalachians in a manner similar to that of the Appalachian drainage divide [*Thornbury*, 1965; *Meyerhoff*, 1972; *Hack*, 1973]. Such a correlation implies that present-day vertical movements in the Appalachians as indicated by releveling are independent of the near-surface structure of the region and are possibly related to the processes responsible for establishing the Atlantic drainage divide. Such an interpretation of the leveling data is not unique, however. If it is assumed that these movements are controlled by the near-surface structure of the Highlands, an alternative correlation can be made (Figure 16*c*). The trend of these lines matches that found by *Hack* [1973] from disequilibrium stream profiles at the Blue Ridge escarpment. Both of these interpretations differ significantly from that of *Meade* [1971], who postulated a broad domal uplift at the southern termination of exposed Appalachian structure. The lack of good quality leveling data in mountainous regions makes choosing between such alternatives difficult.

Although the similarities in the movements of the central and southern Appalachians have been stressed above, a significant difference is also revealed in the shape of the relative velocity profiles at the western boundary of the Highlands region. Profile A (Figure 7) shows a prominent minimum in the curve at Massillon, Ohio, near the western limit of the Appalachian Plateaus (Figure 5). Profile B (Figure 8) is relatively flat across this region, even considering the oblique angle at which the leveling route traverses the boundary. If the character of these movements is controlled by Appalachian structure, one would expect to see a corresponding difference in the tectonics of the central and southern Appalachians. Such a difference does exist. Possibly related to this difference is the change in the style of deformation in the Valley and Ridge as one progresses from north to south; the Valley and Ridge of Pennsylvania is characterized by folding while that of Tennessee is dominated by low-angle thrust faulting [*King*, 1959].

Interior Plains

Profiles A and D (Figures 7 and 10) cross parts of the Interior Lowlands in east-west and north-south directions, respectively. Profile B (Figure 8) crosses the Interior Low Plateaus region in an east-west direction. The most prominent characteristic of vertical crustal movement in the Interior Plains region east of the Mississippi River is an eastward tilt. From profile A, it is seen that Davis Junction, Illinois, is rising at a rate of 16 mm/yr with respect to Massillon, Ohio. The gradient of the velocity curve over the Lowlands in this profile appears to be constant from Massillon, Ohio, to about 50 km west of Deshler, Ohio, at about 3.4×10^{-8} rad/yr east. From 50 km west of Deshler to Davis Junction, the relative velocity curve oscillates about a gradient of 1.5×10^{-8} rad/yr east, in an en echelon manner. The segment of profile B from Somerset, Kentucky, to Wickcliffe, Kentucky, runs parallel to profile A and also shows a dominant eastward tilt. The magnitude of the tilt in the southern Interior Plains is about 1.0×10^{-8} rad/yr east, with an imbricate offset near Park City, Kentucky. The imbricate velocity patterns appear to have no counterparts in the geology along the leveling routes. The total velocity difference between Somerset and Wickcliffe is only 3.5 mm/yr. Scattered segments of east-west releveling located between profiles A and B tend to confirm a regional eastward tilt (Figure

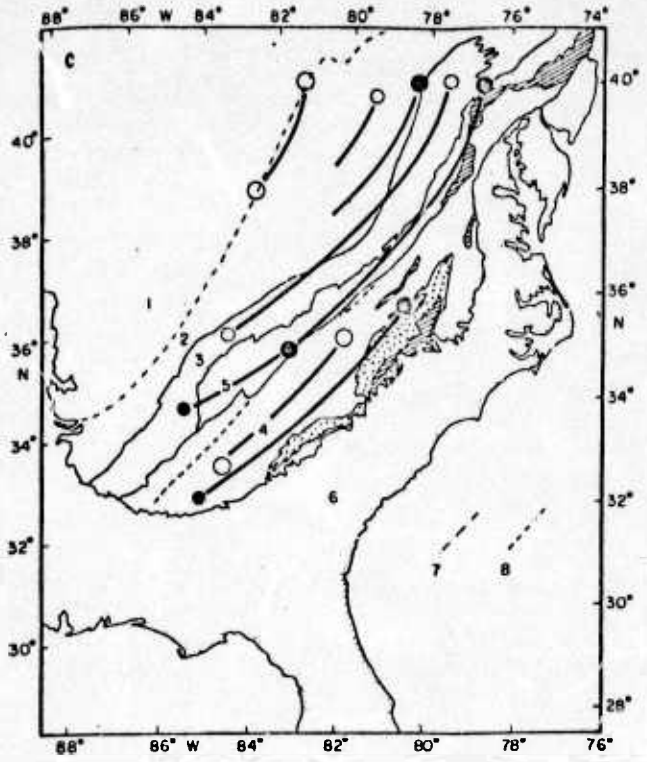


Fig. 16. continued.

13). An exception is the segment of releveling from Mitchell, Indiana, to Vincennes, Indiana (*d* in Figure 13) which shows a tilt rate of about 0.5×10^{-8} rad/yr west. This line terminates on the west near a region of relatively high seismicity [*Coffman and von Hake*, 1973]. Considerably more corroborative leveling data are needed, however, before the significance of this exception can be established.

Profile D, crossing the Interior Lowlands in a north-south direction, is of generally poorer quality than the other profiles. It shows a slight southward tilt in northern Illinois, a fairly broad relative velocity peak in southern Illinois, and a relative velocity minimum in western Tennessee where the line has passed into the Mississippi embayment, part of the Coastal Plain province.

Again, correlations can be found between these movements and geologic structure. Profile A is generally confined to crossing structural highs in the Interior Lowlands, traversing the Findlay arch in western Ohio, and then running along the strike of the Kankakee arch through northern Indiana and Illinois (Figure 5). The east-west segment of profile B crosses the Cincinnati arch between Somerset, Kentucky, and Park City, Kentucky, then passes along the edge of the Illinois basin into the Mississippi embayment. The offset in profile B occurs very close to the eastern boundary of the Illinois basin. The relative uplift in southern Illinois corresponds well spatially with the Rough Creek fault zone, an east-west trending region of disturbed Paleozoic strata unique in the Interior Lowlands [*Gardner*, 1915; *Clark and Royds*, 1948; *King*, 1969*a*].

The predominantly eastward tilt of the Interior Plains as indicated by leveling seems to be in conflict with the regional southwest tilting that *Walcott* [1972*b*] reports from analysis of water level measurements in the Great Lakes region (Figure 15). Profile A, an east-west line, should be free of tidal errors; moreover, due to the lack of significant topography along its route in the Interior Plains, it can be considered free from elevation-correlated error. To reconcile these two disparate trends, both based on data covering roughly the same time interval, one must postulate a 'hinge' line just south of the Great Lakes. Structurally, the Kankakee arch may serve this purpose, in a manner analogous to that of the Cape Fear arch in the Atlantic Coastal Plain. The fact that the preglacial drainage divide for the Central Lowlands was also located along this 'hinge' line [*Thornbury*, 1965], as well as its significance as the partition between the Illinois and Michigan basins, suggests that the hinge line exerts a fundamental control on the past and present evolution of the Central Lowlands. Unfortunately, very few good leveling data are available in the Illinois and Michigan basins. The nature of basins in 'stable' continental interiors (autogeosynclines; *Kay* [1951]) is little understood. Knowledge of their present behavior might shed significant light on their causes [*Joyner*, 1967].

Seismicity

Although great progress has been made in the last few years in understanding the distribution and causes of earthquakes in the major seismic belts around the world [*Isacks et al.*, 1968], very little is understood about the seismicity of normally aseismic regions. According to the principles of plate tectonics, these regions, which are located away from the boundaries of lithospheric plates, should be tectonically passive [*Morgan*, 1968]. Whereas plate boundary seismicity can be associated with horizontal movement, e.g., along a transform fault, or vertical movement, e.g., at the boundaries of a down-going lithospheric slab, the relationship between crustal movements and seismicity in intraplate regions, if such a relationship exists, is unknown. Although a large amount of documentation now exists on earthquakes in the eastern United States [*Dutton*, 1889; *Fuller*, 1912; *Heinrich*, 1941; *Woollard*, 1958; *Bradley et al.*, 1965; *Bollinger*, 1972], until quite recently almost nothing has been known about crustal movements in the area. Attempts have been made to correlate seismicity in the eastern United States with various factors, including geologic structure [*Woollard*, 1958; *Fox*, 1970], magnetic anomalies [*Straley*, 1966], postglacial rebound [*Fox*, 1970], water loading in rivers [*McGinnis*, 1963], and topographic elevations [*Oliver and Isacks*, 1971]. Following a suggestion by Oliver, *Bollinger* [1973] attempted to correlate seismicity with vertical crustal movement using Meade's preliminary isobase map [*Meade*, 1971]. Bollinger suggested that seismicity in the southern portion of the Appalachians is correlated with a relative minimum in the uplift pattern, bounded on the south by an uplift near Atlanta, Georgia. Meade's map, however, suffers from the sources of distortion inherent in adjustment procedures used on data from different time intervals. As proposed earlier, alternative patterns of vertical crustal movement are suggested by the releveling data.

In Figure 17, the trend lines of Figure 16 are superimposed on a seismicity map of eastern North America. In general, these trends are subparallel to the Appalachian seismic trend. However, the resolution of the leveling data along the extrapolated trend line cannot be considered very good. Where the resolution of the leveling data is good, correlations can be made. Near Harrisburg, Pennsylvania, and Asheville, North Carolina, where leveling indicates maxima in the velocity curve, there are concentrations of seismicity [*Coffman and von Hake*, 1973]. There appears to be no activity associated with the relative velocity peak at Greensboro, North Carolina, and very little with the peak west of Tyrone, Pennsylvania. There does appear to be a strong correlation of seismicity and vertical movements near the western boundary of the Appalachian

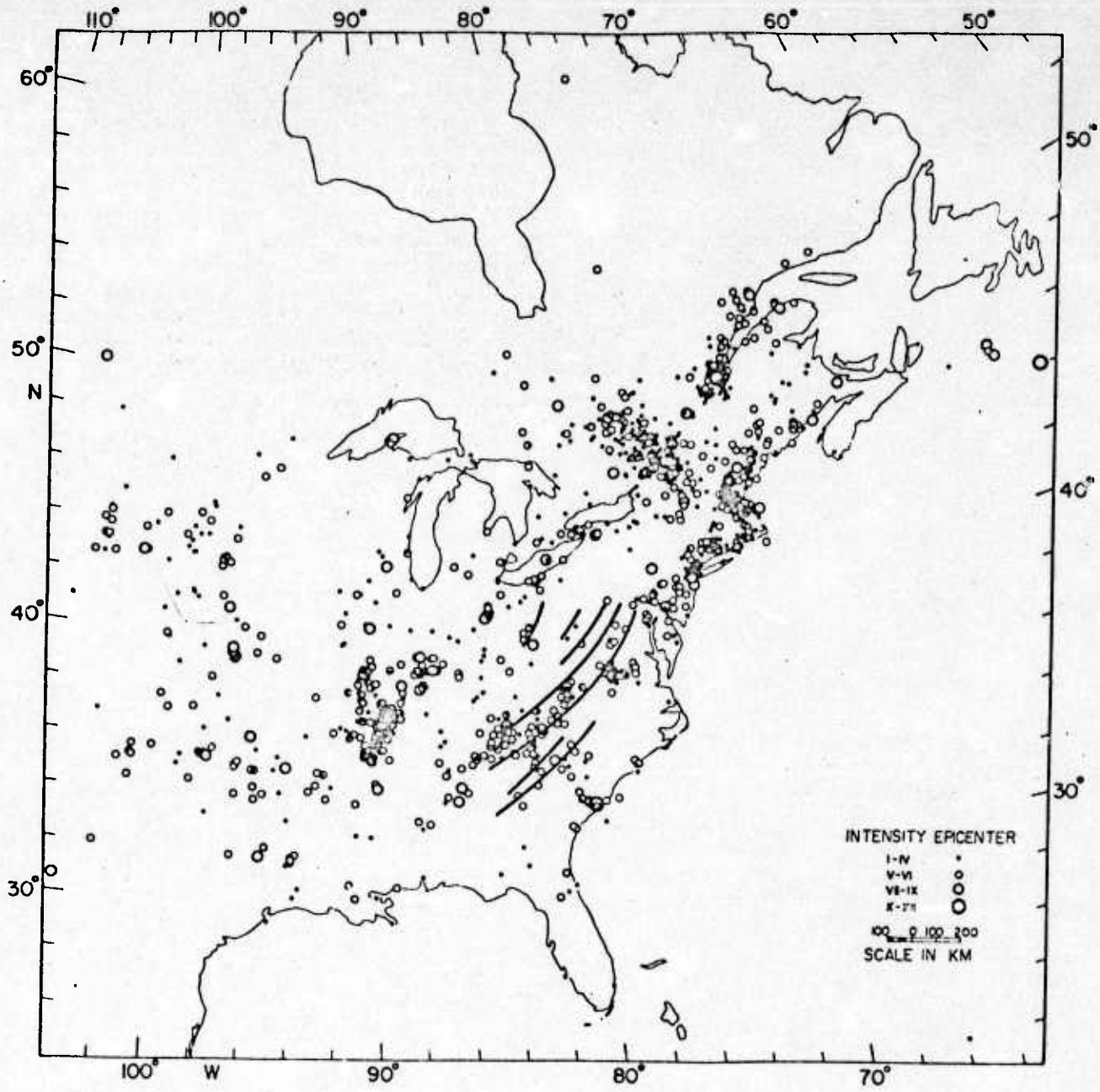


Fig. 17. Trend lines in Figure 16*c* superimposed on a seismicity map of eastern North America. Seismicity map compiled by J. York and J. Ni.

Plateaus province. Profiles A and E show minima in the relative velocity curves relatively close together. A line drawn between the geographic positions of these minima falls very close to a belt of minor seismicity trending northeast through eastern Ohio (Figure 17). The proximity of the two lines and their right angle intersection define this minimum more precisely than is usually possible for many of the other features. Given the uncertainty in the location of the seismic events [*Bradley et al.*, 1965], all fit well onto the trend defined by these minima. These relationships suggest that at least some extremes in the vertical movement curves are associated with seismicity; however, without further data it is impossible to demonstrate that the relationship is more than coincidental. It is intriguing to speculate about the relative velocity extremes which appear not to have associated seismicity. Are they regions where the strain accumulates via some creep mechanism, or are they regions where preseismic strain is accumulating in preparation for future shocks? Clearly the answer to this question is of more than academic interest. Without an understanding of the underlying mechanism or a sufficient number of leveling data, the question must remain unanswered.

A number of leveling profiles in the NGS data base show offsets in the velocity curves. At first glance the movement suggests vertical faulting with the characteristics of the classic elastic rebound model [*Reid*, 1911]. However, the large values of the offsets coupled with the lack of associated seismicity, field evidence, or continued movement in subsequent levelings for most of these features argue against their representing actual ground movements. Inquiry is presently continuing into the cause of these anomalous movements.

Conclusions

From the foregoing discussion it is apparent that the discrepancies between results of successive levelings cannot be

attributed to random processes. There are systematic correlations between patterns of vertical movement and geologic structure. The Atlantic Coastal Plain, as well as the Gulf Coastal Plain, is tilting down away from the continental interior. The Atlantic Coastal Plain between Pennsylvania and Georgia is also tilting down to the north with a hinge line at the Cape Fear arch. The Appalachian Highlands are being uplifted with respect to the Atlantic Coast at rates up to 6 mm/yr. The Interior Plains are tilting down to the east at rates up to 3×10^{-9} rad/yr. On a larger scale, relative velocity maxima tend to correspond with topographic highs in the Appalachian Highlands.

The vertical crustal movements in the Appalachians suggest long linear patterns of successive relative uplifts and subsidences. One interpretation of the movements is that the pattern cuts across Appalachian structures in a manner similar to the Atlantic drainage divide. This interpretation implies that the movements are independent of Appalachian structures. Perhaps the location of the drainage divide is controlled by the same mechanism responsible for the recent vertical movements. The wavelengths between successive maxima are about 300 km, which is characteristic of several lithospheric loading phenomena [*Walcott*, 1970*b*]. An alternative interpretation is that the movements are controlled by Appalachian structures and therefore the wavelengths are coincidental. Lack of data makes it difficult to choose between these alternatives. Clearly, however, the actual patterns of movement need to be resolved in order to isolate the mechanism responsible.

Releveling suggests that present-day vertical movements, in general, are a continuation of Phanerozoic trends as recorded in Mesozoic and Cenozoic sediments and terraces of the Coastal Plain and in major Paleozoic structural trends. However, the rates of present-day movements are up to 2 orders of magnitude larger than average rates over the past 135 m.y. and therefore appear to be relatively transient (or oscillatory) phenomena with time constants less than about 10^6 yr. Some recent geological studies suggest that rates averaged over long (geologic) time periods may be misleading in this respect [*Mescherikov*, 1967]. *Sloss and Speed* [1974] argue from analysis of the sedimentary record that the Phanerozoic history of continental cratons is marked by oscillatory, emergent, or submergent modes of vertical movement. They conclude that much of the Cenozoic, including the present, can be classified as oscillatory, characterized by areas 'generally elevated or oscillating with respect to sea level; marginal and submarginal areas subject to highly differentiated uplift and subsidence; periodicity of oscillations and uplifts 10^5–10^6 years; wavelengths of intercratonic tectonic elements 10^1–10^2 km; (and) duration of episodes 10^7–10^8 years' [*Sloss and Speed*, 1974]. The vertical crustal movements indicated by leveling fit this description well, with the possible exception of those in a few areas with extraordinarily high rates of movement. Even these exceptions may not be significant, given the relatively poor time resolution of most geologic information. With increased resolution of geological and geomorphological data, it should be possible to successfully bridge the gap between the long-period (e.g., geological) and short-period (e.g., leveling-derived) ends of the vertical crustal movement spectrum.

The rates of vertical crustal movement presented in this study, as well as those found by other investigators in the United States, compare very well with those found in other portions of the world. The most extensive studies of these movements have been made in Japan and Eastern Europe, most notably in the Soviet Union, where special observation nets are leveled frequently. Whereas the tectonic setting of Japan (i.e., an active island arc) contrasts markedly with that in the eastern United States, portions of Eastern Europe appear to be comparable in setting to the areas examined in this paper. A comparison of the patterns of movement in the eastern United States with those mapped by *Mescherikov* [1973] in Eastern Europe points up some interesting contrasts. Whereas the Appalachian mountain system is presently rising with respect to the interior United States platform and the East Coast, the Urals are subsiding relative to the Russian Platform. On the other hand, both the Russian Platform and the Central United States Platform are tilting toward the east. It is therefore very dangerous to extrapolate the results found in one region to other areas which are structurally similar. The mechanisms of the movements may be entirely different.

The large magnitudes of these movements cannot be explained by several mechanisms which have been proposed for the evolution of continental margins. *Sleep's* [1971] thermal model for the plate tectonic evolution of the Atlantic margin, the sediment compaction model of *Jacquin and Poulet* [1970], and the sediment-loading models of *Dietz* [1963] and *Walcott* [1970*a*, 1972*a*], while providing plausible mechanisms for supplying the observed volumes of sediments, do not provide explanations for the large magnitudes of present-day coastal tilting indicated by leveling data. *Kaitera* [1966], *Bloom* [1967, 1970], *Walcott* [1972*c*], *Chappell* [1974], and others have proposed loading of the ocean basins by melting glacial ice as a mechanism for inducing relative uplift of continental regions. Assuming equal areas of continental and oceanic crust, a eustatic rate of sea level rise of about 1.0 mm/yr, and a density contrast of 1.7 between the water load and displaced continental crust, it would seem difficult to account for rates of relative uplift of about 5 mm/yr. However, as *Bloom* [1967] pointed out, the difference in surface area between the continents and the oceans would cause a focusing of the loading response. In addition, the rate of eustatic sea level rise might have been larger in the past than it is at present [*Gutenberg*, 1954], and, given the high viscosity of the mantle [*Walcott*, 1972*b*], there could be a rather complex response delay. Further complications could arise from the interaction of strains induced by lithospheric and sublithospheric driving mechanisms with near-surface structure, which could account for the coincidence of relative velocity features with surface structure. Other possible mechanisms include isostatic and thermal responses to erosional unloading [*Haxby and Turcotte*, 1975], deviatoric stresses due to preexisting loads [*Artyushkov*, 1972], gravity convection [*Artyushkov and Mescherikov*, 1969], subcrustal erosion [*Gilluly*, 1955], phase transitions in the lithosphere and upper mantle [*Joyner*, 1967; *Magnitsky and Kalishnikova* 1970], redistribution of asthenospheric melts [*Sloss and Speed*, 1974], triple junction and hot spot evolution [*Morgan*, 1972; *Burke and Dewey*, 1973], and lithospheric interaction with asthenospheric 'bumps' [*Menard*, 1973; *Gilluly*, 1973]. In addition, certain nontectonic near-surface processes (e.g., groundwater variations) may be significant influences on some measured movements. A more detailed consideration of driving mechanisms is outside the scope of this study.

Although the rates of relative vertical movements determined from leveling seem large by comparison with rates deduced from some forms of geological evidence, e.g., the sedimentary record, these velocities do not seem unreasonable in terms of other types of geological information. Crustal rebound following the removal of the ice caps surely exceeded 1 cm/yr (which is about the present-day maximum rate in

Finland, see *Kaariainen* [1953]). Horizontal velocities at the surface associated with lithospheric plate movements are commonly 10 cm/yr, and therefore comparable velocities must occur in parts of the asthenosphere. It is difficult to conceive of an earth with such rapid horizontal motion and no manifestations of that motion in the form of vertical movements.

In a period when the paradigm of plate tectonics is providing increased understanding of earth processes, vertical movements of the continents remain a little known phenomenon. The importance of these movements for engineering planning and seismic risk estimation has not yet been fully evaluated [*Clark and Persoage*, 1970], although results here and elsewhere clearly suggest a close association of seismicity with vertical crustal movement. The wavelengths of the phenomenon which can be measured by precise leveling range from individual bench mark intervals (a few meters) up to several thousand kilometers (possibly). Leveling measurements therefore reflect both near-surface and mantle processes alike. It is therefore reasonable to expect several different mechanisms to be operating at the same time. Clearly, much more releveling needs to be done, not only to expand areal coverage and test models of crustal movement but to investigate the temporal variations in the rates of movement. Understanding such variations may be the crucial step in determining the driving forces behind recent vertical crustal movements. Organized programs of observation of vertical crustal movements by means of leveling in selected areas in the United States would provide systematic results and help to resolve many of the uncertainties suggested by this work. Such programs must be started as soon as possible in order to obtain results within a reasonable length of time.

Acknowledgments. The authors wish to thank S. R. Holdahl of the National Geodetic Survey for his valuable advice on the analysis and interpretation of leveling data. Most of the data used in this study were compiled by S. R. Holdahl and N. C. Morrison. Appreciation is also due C. F. Ellingwood and L. S. Baker of the NGS for generously providing working space and NGS materials for this study. A. L. Bloom, W. Haxby, G. B. Lyon, R. Reilinger, D. L. Turcotte, and J. York provided assistance and many useful suggestions during the course of this study. L. Brown, N. Fitzpatrick, J. Ni, and S. Schilt assisted in the processing of the data. N. Fitzpatrick and J. Ni prepared the figures used in this paper. M. Barazangi, A. L. Bloom, S. R. Holdahl, B. Isacks, D. L. Turcotte, and J. York critically reviewed the manuscript. This research was supported by the Advanced Research Projects Agency of the Department of Defense and was monitored by the Air Force Office of Scientific Research under contract AFOSR-73-2494. One of the authors (L.B.) was supported by a National Science Foundation Graduate Fellowship while engaged in the research herein reported. Cornell University Department of Geological Sciences Contribution 556.

References

Ahnert, F., Functional relationships between denudation, relief, and uplift in large mid-latitude drainage basins, *Amer. J. Sci., 268*, 243–263, 1970.

Artyushkov, E. V., The origin of large stresses in the earth's crust, *Izv. Acad. Sci. USSR Phys. Solid Earth, 8*, 3–25, 1972.

Artyushkov, E. V., and Y. A. Mescherikov, Recent movements of the earth's crust and isostatic compensation, in *The Earth's Crust and Upper Mantle, Geophys. Monogr. Ser.*, vol. 13, edited by P. J. Hart, pp. 379–390, AGU, Washington, D. C., 1969.

Balazs, E. I., Vertical crustal movements on the Middle Atlantic Coastal Plain as indicated by precise leveling, paper presented at the Northeastern Section Annual Meeting, Geol. Soc. of Amer., Boulder, Colo., 1974.

Beloussov, V. V., *Basic Problems in Geotectonics*, 809 pp., McGraw-Hill, New York, 1962.

Beloussov, V. V., G. I. Reismer, E. M. Rudich, and V. M. Sholpo, Vertical movements of the earth's crust on the continents, *Geophys. Surv., 1*, 245–273, 1974.

Bendefy, L., A method for the elimination of the reference point and of the two different network-adjustments in investigations of recent crustal movements, *Ann. Acad. Sci. Fenn., Ser. A3, 90*, 47–55, 1966.

Berry, E. W., North Carolina, Possible future petroleum provinces of North America, *Bull. Amer. Ass. Petrol. Geol., 35*, 412–415, 1951.

Bloom, A. L., Pleistocene shorelines: A new test of isostasy, *Geol. Soc. Amer. Bull., 78*, 1477–1494, 1967.

Bloom, A. L., Discussion—Isostatic response to loading of the crust in Canada, *Can. J. Earth Sci., 7*, 731–733, 1970.

Bloom, A. L., Late Pleistocene vertical crustal movements on the southeastern U.S. Atlantic Coastal Plain, paper presented at the Penrose Conference on Pleistocene Stratigraphy, Geol. Soc. of Amer., Boulder, Colo., 1974.

Bloom, A. L., W. S. Broecker, J. M. A. Chappell, R. K. Matthews, and K. J. Mesolella, Quaternary sea level fluctuations on a tectonic coast: New $^{230}Th/^{234}U$ dates from the Huon Peninsula, New Guinea, *Quaternary Res., 4*, 185–205, 1974.

Bollinger, G. A., Historical and recent seismic activity in South Carolina, *Bull. Seismol. Soc. Amer., 62*, 851–864, 1972.

Bollinger, G. A., Seismicity and crustal uplift in the southeastern United States, *Amer. J. Sci., 273A*, 396–408, 1973.

Bomford, G., *Geodesy*, 3rd ed., 732 pp., Clarendon Press, Oxford, 1971.

Bonini, W. E., Seismic-refraction studies of geologic structure in North Carolina and South Carolina (abstract), *Geol. Soc. Amer. Bull., 66*, 1532–1533, 1955.

Bowie, W., Comparison of old and new triangulation in California, *Spec. Publ. 151*, 50 pp., U.S. Coast and Geod. Surv., Washington, D. C., 1928.

Bradley, E. A., S. J. Bennett, and T. J. Bennett, Earthquake history of Ohio, *Bull. Seismol. Soc. Amer., 55*, 745–752, 1965.

Burke, K., and J. F. Dewey, Plume-generated triple junctions: Key indicators in applying plate tectonics to old rocks, *J. Geol., 181*, 406–433, 1973.

Carder, D. S., and J. B. Small, Level divergences, seismic activity and reservoir loading in the Lake Meade area, Nevada and Arizona, *Eos Trans. AGU, 29*, 767–771, 1948.

Castle, R. O., J. N. Alt, J. C. Savage, and E. I. Balazs, Elevation changes preceding the San Fernando earthquake of February 9, 1973, *Geology, 2*, 61–66, 1974.

Chappell, J., Late Quaternary glacio- and hydro-isostasy, on a layered earth, *Quaternary Res., 4*, 405–428, 1974.

Chugh, R. S., Study of recent crustal movements in India and future programme, paper presented at the International Symposium on Recent Crustal Movements, Comm. on Recent Crustal Movements, Zurich, Switzerland, 1974.

Clark, R. H., and N. P. Persoage, Some implications of crustal movement in engineering planning, *Can. J. Earth Sci., 7*, 628–633, 1970.

Clark, S. K., and J. S. Royds, Structural trends and fault systems in Eastern Interior basin, *Bull. Amer. Ass. Petrol. Geol., 32*, 1728–1749, 1948.

Coffman, J. L., and C. A. von Hake (Eds.), Earthquake history of the United States, *Publ. 41-1*, 208 pp., Environ. Data Serv., Washington, D. C., 1973.

Cooke, C. W., Correlation of coastal terraces, *J. Geol., 38*, 577–589, 1930.

Cramer, H. R., Structural features of the Coastal Plain of Georgia, *Southeast. Geol., 10*, 111–123, 1969.

CRCM (Commission on Recent Crustal Movements), *First International Symposium on Recent Crustal Movements*, 508 pp., Akademie Verlag, Berlin, 1962.

CRCM (Commission on Recent Crustal Movements), Second international symposium on recent crustal movements, *Ann. Acad. Sci. Fenn., Ser. A3, 90*, 1–498, 1966.

CRCM (Commission on Recent Crustal Movements), *Third International Symposium on Recent Crustal Movements*, 565 pp., Academy Nauk SSSR, Moscow, 1968.

Crittenden, M., Jr., New data on the isostatic deformation of Lake Bonneville, *U.S. Geol. Surv. Prof. Pap. 454-E*, 1–31, 1963.

Davis, G. H., J. B. Small, and H. B. Counts, Land subsidence related to decline of artesian pressure in the Ocala Limestone at Savannah, Georgia, in *Engineering Geology, Case Histories, Number 4*, edited by P. D. Trosk and G. A. Kiersch, pp. 1–8, Geological Society of America, Boulder, Colo., 1963.

Dietz, R. S., Collapsing continental rises: An actualistic concept of geosynclines and mountain building, *J. Geol., 71*, 314–333, 1963.

Doering, J. A., Quaternary surface formations of southern part of Atlantic Coastal plain, *J. Geol., 68*, 182–202, 1960.

Dole, R. B., and H. Stabler, Denudation, *U.S. Geol. Surv. Water Supply Pap. 234*, 78–93, 1909.

Domenico, P. A., *Concepts and Models in Groundwater Hydrology*, 405 pp., McGraw-Hill, New York, 1972.

Drake, C. L., M. Ewing, and G. H. Sutton, Continental margins and geosynclines: The east coast of North America north of Cape Hatteras, in *Physics and Chemistry of the Earth*, vol. 3, edited by L. H. Ahrens, F. Press, K. Rankama, S. K. Runkorn, pp. 110–198, Pergamon, New York, 1959.

Dutton, C. E., The Charleston earthquake of August 31, 1886, *U.S. Geol. Surv. Ann. Rep. 1887–88*, 203–508, 1889.

Ellingwood, C. F., and S. R. Holdahl, The precise leveling test network of the National Geodetic Survey, paper presented at the Annual Meeting, Amer. Congr. of Surv. and Mapping, Washington, D. C., 1972.

Emery, K. O., and E. Uchupi, *Western North Atlantic Ocean: Topography, Rocks, Structure, Water, Life, and Sediments*, 532 pp., American Association of Petroleum Geologists, Tulsa, Okla., 1972.

Fenneman, N. M., Physical divisions of the United States, map, U.S. Geol. Surv., Washington, D. C., 1946.

Ferenczi, I., Structural control of the North Carolina Coastal Plain, *Southeast. Geol., 1*, 105–116, 1959.

Fischel, V. C., Long term trends of ground-water levels in the United States, *Eos Trans. AGU, 37*, 429–435, 1956.

Flint, R. F., Pleistocene features of the Atlantic coastal plain, *Amer. J. Sci., 23*, 757–787, 1940.

Fox, F. L., Seismic geology of the eastern United States, *Ass. Eng. Geol. Bull., 7*, 21–43, 1970.

Fuller, M. L., The New Madrid earthquake, *U.S. Geol. Surv. Bull. 494*, 1–119, 1912.

Gabrysch, R. K., Land-surface subsidence in the Houston-Galveston region, Texas, in *Subsidence: Proceedings of the Tokyo Symposium, 1969*, pp. 43–54, IASH/AIHS-UNESCO, Paris, 1969.

Gale, L. A., Geodetic observations for the detection of vertical movement, *Can. J. Earth Sci., 7*, 602–606, 1970.

Gardner, J. H., A stratigraphic disturbance through the Ohio valley, running from the Appalachian Plateau in Pennsylvania to the Ozark Mountains in Missouri, *Geol. Soc. Amer. Bull., 26*, 477–483, 1915.

Gerasimov, I. P. (Ed.), *Recent Crustal Movements*, translated from Russian by Z. Garfunkel, 410 pp., Israel Program for Scientific Translations, Jerusalem, 1967.

Gilluly, J., Geologic contrasts between continents and ocean basins, Crust of the Earth, a Symposium, *Geol. Soc. Amer. Spec. Pap. 62*, 7–18, 1955.

Gilluly, J., Atlantic sediments, erosion rates, and the evolution of the continental shelf: Some speculations, *Geol. Soc. Amer. Bull., 75*, 483–492, 1964.

Gilluly, J., Steady plate motion and episodic orogeny and magmatism, *Geol. Soc. Amer. Bull., 84*, 499–514, 1973.

Goddard, E. N., et al., Geologic map of the United States, U.S. Geol. Surv., Washington, D. C., 1965.

Gordon, F. R., Faulting during the earthquake at Meckering, Western Australia: 14 October 1968, Recent Crustal Movements, *Roy. Soc. N. Zealand Bull. 9*, 85–93, 1971.

Gutenberg, B., Changes in sea level, postglacial uplift, and mobility of the earth's interior, *Geol. Soc. Amer. Bull., 52*, 721–772, 1941.

Gutenberg, B., Postglacial uplift in the Great Lakes region, *Archiv. Meteorol. Geophys. Bioklimatol. A, 7*, 243–251, 1954.

Hack, J., Drainage adjustment in the Appalachians, in *Fluvial Geomorphology*, edited by M. Morisawa, pp. 51–69, State University of New York at Binghamton Publications in Geomorphology, Binghamton, N.Y., 1973.

Hagiwara, T., Example of land deformations witnessed by the people before a great earthquake and of those detected by the leveling just before strong earthquakes, Proceedings of the United States-Japan Conference on Research on Earthquake Prediction Problems, pp. 24–25, Earthquake Res. Inst. of the Univ. of Tokyo, Tokyo, 1964.

Haxby, W., and D. L. Turcotte, Stresses induced by the addition or removal of overburden, including associated thermal effects, submitted to *Geology*, 1975.

Heinrich, R. R., A contribution to the seismic history of Missouri, *Bull. Seismol. Soc. Amer., 31*, 187–224, 1941.

Hicks, S. D., On the classification and trends of long period sea level series, *Shore Beach, 40*, 20–23, 1972*a*.

Hicks, S. D., Vertical crustal movements from sea level measurements along the east coast of the United States, *J. Geophys. Res., 77*, 5930–5934, 1972*b*.

Hicks, S. D., Trends and variability of yearly mean sea level, 1893–1971, *Tech. Mem. NOS 12*, 13 pp., Nat. Ocean. and Atmos. Admin., Boulder, Colo., 1973.

Hicks, S. D., and W. Shofnos, Yearly sea level variations for the United States, *J. Hydraul. Div. Proc. Amer. Soc. Civil Eng., 91*, 23–32, 1965.

Higgins, C. G., Causes of relative sea-level changes, *Amer. Sci., 53*, 464–476, 1965.

Holdahl, S. R., Geodetic evaluation of land subsidence in the central San Joaquin Valley of California, paper presented at the Fall Meeting, Amer. Geophys. Union, Washington, D. C., 1969.

Holdahl, S. R., Vertical crustal movements—Status of NGS investigations, paper presented at Geop-3 Research Conference: Vertical Crustal Movements and their Causes, AGU, Washington, D. C., 1973*a*.

Holdahl, S. R., Elevation change along the Gulf coast as indicated by precise leveling and marcograph data, paper presented at the National Fall Meeting, Amer. Congr. Surv. and Mapping, Washington, D. C., 1973*b*.

Holdahl, S. R., Times and heights, paper presented at the International Symposium on Problems Related to the Redefinition of North American Geodetic Networks, Int. Assoc. of Geod., Paris, 1974.

Holdahl, S. R., and N. C. Morrison, Regional investigations of vertical crustal movements in the U.S. using precise relevelings and mareograph data, paper presented at the Symposium on Recent Crustal Movements and Associated Seismic and Volcanic Activity, Comm. on Recent Crustal Movements, Prague, 1973.

Hytonen, E., Measuring of the refraction in the second levelling of Finland, *Suom. Geodeettisen Laitoksen Julka., 63*, 1–22, 1967.

Isacks, B., J. Oliver, and L. R. Sykes, Seismology and the new global tectonics, *J. Geophys. Res., 73*, 5855–5899, 1968.

Isacks, B., I. I. Mueller, R. I. Walcott, and M. Talwani, Vertical crustal motions and their causes—Report on the third Geop research conference, *Eos Trans. AGU, 54*, 1257–1260, 1973.

Jacquin, C., and M. J. Poulet, Study of the hydrodynamic pattern in a sedimentary basin subject to subsidence, *Pap. SPE 2988*, 6 pp., Soc. of Petrol. Eng., Dallas, Tex., 1970.

Johnson, D. W., *Shore Processes and Shoreline Development*, 584 pp., John Wiley, New York, 1919.

Joyner, W. B., Basalt-eclogite transition as a cause for subsidence and uplift, *J. Geophys. Res., 72*, 4977–4998, 1967.

Kaariainen, E., On the recent uplift of the earth's crust in Finland, *Suom. Geodeettisen Laitoksen Julka., 42*, 1–106, 1953.

Kaariainen, E., The second levelling of Finland in 1935–1955, *Suom. Geodeettisen Laitoksen Julka., 62*, 1–313, 1966.

Kaitera, P., Sea pressure as a cause of crustal movements, *Ann. Acad. Sci. Fenn., Ser. A3, 90*, 191–200, 1966.

Karcz, I., and U. Kafri, Geodetic evidence of possible recent crustal movements in the Negev, southern Israel, *J. Geophys. Res., 76*, 8056–8065, 1971.

Karcz, I., and U. Kafri, Recent vertical crustal movements between the Dead Sea rift and the Mediterranean, *Nature, 242*, 42–44, 1973.

Kasahara, K., Earthquake fault studies in Japan, *Phil. Trans. Roy. Soc. London, 274*, 287–296, 1973.

Kay, M., North American geosynclines, *Geol. Soc. Amer. Mem. 48*, 1–143, 1951.

Kaye, C. A., and G. W. Stuckey, Nodal tidal curves of the east coast of the United States and its value in explaining long-term sea level changes, *Geology, 1*, 141–144, 1973.

King, P. B., A geologic section across the southern Appalachians: An outline of the geology in the segment in Tennessee, North Carolina, and South Carolina, in *Guides to Southeastern Geology*, pp. 332–373, Geological Society of America, Boulder, Colo., 1955.

King, P. B., *The Evolution of North America*, 189 pp., Princeton University Press, Princeton, N. J., 1959.

King, P. B., *The Tectonics of Middle North America: Middle North America East of the Cordilleran System*, 203 pp., Hafner, New York, 1969*a*.

King, P. B., Tectonic map of North America, U.S. Geol. Surv., Washington, D. C., 1969*b*.

Kulkamaki, T. J., Über die nivellistischen Refraktion, *Suom. Geodeettisen Laitoksen Julka., 25*, 1–48, 1938.

Kukkamaki, T. J., Formeln und Tahellen zur Berechnung der nivellistischen Refraktion, *Suom. Geodeettisen Laitoksen Julka., 27*, 1–18, 1939.

Kukkamaki, T. J., The land uplift in Finland determined with two levelings as well as with water level observations, *Bull. Geod. 36*, 18–20, 1955.

Lensen, G. J., Phases, nature and rates of earth deformation, Recent Crustal Movements, *Roy. Soc. N. Zealand Bull. 9*, 97–105, 1971.

Lensen, G. J., and P. M. Otway, Earthshift and post-earthshift deformation associated with the May 1968 Inangahua earthquake, New Zealand, Recent Crustal Movements, *Roy. Soc. N. Zealand Bull. 9*, 107–116, 1971.

Leont'ev, G. I., Temporary atmospheric and aquatic loads on the earth's surface and their influence on high-precision levelling in the lower Volga region, in *Recent Crustal Movements*, edited by I. P. Gerasimov, translated from Russian by Z. Garfunkel, pp. 114–120, Israel Program for Scientific Translations, Jerusalem, 1967.

Levallois, J. J., Sur la mise en evidence d'un mouvement de surrection des massifs cristallins alpins, *Bull. Geod., 105*, 229–318, 1972.

Lilienberg, D. A., and L. E. Setunskaya, Methods and some results of geological-geomorphological inspections of signs of repeated levelling, in *Problems of Recent Crustal Movements—3rd International Symposium*, pp. 116–125, Academy Nauk SSSR, Moscow, 1969.

Longwell, C. R., Interpretation of the levelling data, *U.S. Geal. Suro. Prof. Pap. 295*, 33–38, 1960.

Louisiana Geological Survey, Oil and gas map of Louisiana, La. Geol. Surv., Baton Rouge, La., 1973.

Lutsar, R. V., L. A. Saapar, and R. J. Arbeiter, Investigation of the crustal movements within the precincts of towns of the Estonian SSR, in *Recent Movements of the Earth's Crust-No. 5*, edited by L. Y. Riives, pp. 139–143, ESSR Academy of Science, Tartu, ESSR, 1973.

Magnitsky, V. A., and I. K. Kalishnikova, Problem of phase transitions in the upper mantle and its connection with the earth's crustal structure, *J. Geophys. Res., 75*, 877–885, 1970.

Maher, J. C., Correlations of subsurface Mesozoic and Cenozoic rocks along the Atlantic coast, Cross Section Publication, *Bull. Amer. Ass. Petrol. Geol., 6*, 1–29, 1968.

McGinnis, L. D., Earthquakes and crustal movement as related to the water load in the Mississippi Valley region, *344*, 20 pp., Ill. State Geol. Surv., Urbana, Ill., 1963.

Meade, B. K., Earthquake investigation in the vicinity of El Centro, California—Horizontal movement, *Eos Trans. AGU, 29*, 27–31, 1948.

Meade, B. K., Horizontal crustal movements in the United States, *Ann. Acad. Sci. Fenn., Ser. A3, 90*, 256–266, 1966.

Meade, B. K., Report of the sub-commission on recent crustal movements in North America, paper presented to 15 General Assembly of International Union of Geodesy and Geophysics, Int. Assoc. of Geod., Brussels, 1971.

Meade, R. H., and K. O. Emery, Sea level as affected by river runoff, eastern United States, *Science, 173*, 425–428, 1971.

Meinzer, O. E., The occurrence of groundwater in the United States with a discussion of principles, *U.S. Geol. Surv. Water Supply Pap. 489*, 1–321, 1959.

Menard, H. W., Some rates of regional erosion, *J. Geol., 69*, 154–161, 1961.

Menard, H. W., Epeirogeny and plate tectonics, *Eos Trons. AGU, 54*, 1244–1255, 1973.

Mescherikov, Y. A., Secular crustal movements of the East European plain and associated problems, *Bull. Geod., 52*, 69–75, 1959.

Mescherikov, Y. A., Secular movements of the earth's crust: Some results and problems, in *Recent Crustal Movements*, edited by I. P. Gerasimov, translated from Russian by Z. Garfunkel, pp. 1–21, Israel Program for Scientific Translations, Jerusalem, 1967.

Mescherikov, Y. A., Recent crustal movements in seismic regions-Geodetic and geomorphic data, *Tectonophysics, 6*, 29–39, 1968.

Mescherikov, Y. A. (Ed.), Map of recent vertical crustal movements of Eastern Europe, in *Recent Movements of the Earth's Crust*, p. 8, ESSR Academy of Science, Tartu, ESSR, 1973.

Meyerhoff, H. A., Post-orogenic development of the Appalachians, *Geal. Soc. Amer. Bull., 83*, 1709–1728, 1972.

Miyabe, N., Vertical earth movements as deduced froni the results of rerunning the precise levels, *Bull. Earthquake Res. Inst. Univ. Tokyo, 30*, 127–161, 1952.

Miyabe, N., Vertical earth deformation in Nankai district, *Geogr. Surv. Inst., 4*, 1–4, 1955.

Miyabe, N., S. Miyamura, and M. Mizoue, A map of secular vertical movements of the earth's crust in Japan, *Ann. Acad. Sci. Fenn., Ser. A3, 90*, 287–289, 1966.

Mizoue, M., Modes of secular vertical movements of the earth's crust, I, *Bull. Earthquake Res. Inst. Univ. Tokyo, 45*, 1019–1090, 1967.

Morgan, W. J., Rises, trenches, great faults, and crustal blocks, *J. Geophys. Res., 73*, 1959–1982, 1968.

Morgan W. J., Plate motions and deep mantle convection, *Geol. Soc. Amer. Mem., 132* (Hess volume), 7–22, 1972.

Murray, G. E., *Geology of the Atlantic and Gulf Coastal Province of North America*, 692 pp., Harper and Brothers, New York, 1961.

Myers W. B., and W. Hamilton, Deformation accompanying the Hebgen Lake earthquake of August 17, 1959, *U.S. Geol. Surv. Prof. Pap. 435*, 55–98, 1964.

Oaks, R. Q., and J. R. Dubar, Tentative correlation of post-Miocene units, central and southern Atlantic coastal plain, in *Post-Miocene Stratigraphy: Central and Southern Atlantic Coastal Plain*, edited by R. Q. Oaks and J. R. Dubar, pp. 232–245, Utah State University Press, Logan, Utah, 1974.

Oliver, J., and B. Isacks, Seismicity and tectonics of the eastern United States, *Earthquake Notes, 43*, 30, 1971.

Owens, J. P., Post-Triassic movements in the central and southern Appalachians as recorded in the sediments of the Atlantic Coastal Plain, in *Studies af Appalachian Geology: Central and Southern*, edited by G. W. Fisher, F. J. Pettijohn, J. C. Reed, Jr., and K. N. Weaver, pp. 412–427, Interscience, New York, 1970.

Poland, J. F., and G. H. Davis, Subsidence of the land surface in the Tulare-Wasco (Delano) and Los Banos-Kettleman City area, San Joaquin Valley, California, *Eos Trans. AGU, 37*, 287–296, 1956.

Poland, J. F., and G. H. Davis, Land subsidence due to withdrawal of fluids, in *Reviews in Engineering Geology II*, pp. 187–269, Geological Society of America, Boulder, Colo., 1969.

Rappleye, H. S., Manual of geodetic leveling, *U.S. Coast Geod. Surv. Spec. Publ. 239*, 1–94, 1948.

Reid, H. F., The elastic rebound theory of earthquakes, *Bull. Dep. Geol. Univ. Calif., 6*, 413, 1911.

Rezanov, E. A., and N. N Zarudny, *History of Oscillatory Tectonic Movement in the Northeast USSR* (in Russian), Akademy Nauk SSSR, Moscow, 1962.

Ricke, H. H., III, and G. U. Chilingarian, *Compaction of Argilloceous Sediments*, 424 pp., Elsevier, New York, 1974.

Riives, L. Y. (Ed.), *Recent Movements of the Earth's Crust—No. 5*, 685 pp., ESSR Academy of Science, Tartu, ESSR, 1973.

Rikitake, T., Earthquake prediction studies in Japan, *Geophys. Surv., 1*, 4–26, 1972.

Rodgers, J., *The Tectonics of the Appalachians*, 271 pp., Interscience, New York, 1970.

Savage, J. C., and J. P. Church, Evidence for post-earthquake slip in the Fairview Peak, Dixie Valley, and Rainbow Mountain fault areas of Nevada, *Bull. Seismol. Soc. Amer., 64*, 687–698, 1974.

Schaer, J., and F. Jeanrichard, Mouvements verticaux anciens et actuels dans les Alpes Suisses, *Eclogae Geolag. Helvet., 67*, 101–119, 1974.

Schumm, S. A., The disparity between present rates of denudation and orogeny, *U.S. Geol. Surv. Prof. Pop. 454-H*, 1–13, 1963.

Schumm, S. A., and R. F. Hadley, Progress in the application of landform analysis in studies of semiarid erosion, *U.S. Geol. Surv. Circ. 437*, 1–14, 1961.

Simonsen, D., Is the levelling datum for a continental levelling network so stable that it would permit the determination of secular movements as accurate as modern precise levellings may be observed?, *Bull. Geod., 79*, 39–68, 1966.

Sleep, N. H., Thermal effects of the formation of Atlantic continental margins by continental breakup, *Geophys. J., 24*, 325–350, 1971.

Sleigh, R. W., C. C. Worrall, and G. H. L. Shaw, Crustal deformation resulting from the imposition of a large mass of water, *Bull. Geod., 93*, 245–254, 1969.

Sloss, L. L., and R. C. Speed, Relationships of cratonic and continental-margin tectonic episodes, Tectonics and Sedimentation, edited by W. R. Dickinson, *Spec. Publ. 22*, 98–119, Soc. Econ. Paleontol. and Mineral., Tulsa, Okla., 1974.

Small, J. B., Subsidence in the Texas Gulf Coast area, paper presented at the Joint Meeting of the Texas Surveyors Association and the Southwestern Regional Conference of the American Congress of Surveying and Mapping, Austin, Tex., Tex. Surv. Ass., Amer. Congr. Surv. and Mapping, Washington, D. C., 1960.

Small, J. B., Settlement studies by means of precision levelling: Report to International Association of Geodesy—IUGG, Helsinki, Finland, *Bull. Geod. 62*, 317–325, 1961.

Small, J. B., Interim report on vertical crustal movement in the United States, Report to Commission on Recent Crustal Movements, 14 pp., Int. Assoc. of Geod.—Int. Union of Geod. and Geophys., Paris, 1963.

Small, J. B., Vertical crustal movements in the United States, *Ann. Acad. Sci. Fenn., Ser. A3, 90*, 252–256, 1966.

Small, J. B., and C. C. Wharton, Vertical displacements determined by surveys after the Alaska earthquake of March 1964, The Prince William Sound, Alaska, Earthquake of 1964 and Aftershocks, vol. 3, part A, *U.S. Coast Geod. Surv. Publ. 10-3*, 21–33, 1969.

Spangler, W. B., Subsurface geology of the Atlantic coastal plain of North Carolina, *Bull. Amer. Ass. Petrol. Geol., 34*, 100–132, 1950.

Spangler, W. B., and J. J. Peterson, Geology of the Atlantic coastal plain in New Jersey, Delaware, Maryland, and Virginia, *Bull. Amer. Ass. Petrol. Geol., 34*, 1–99, 1950.

Straley, H. W., Magnetic anomalies and epicentral lines on the South Carolina coastal plain, *Tectonophysics, 3*, 375–381, 1966.

Thornbury, W. D., *Regional Geomorphology of the United States*, 609 pp., John Wiley, New York, 1965.

Thurm, H., Some systematic errors of precision levelling, *Jena Rev., 3*, 172–176, 1971.

Tsubokawa, J., and K. Nagasawa, Anomalous land deformation in the Niigata area before the Niigata earthquake and in the Matsushiro area revealed by precise levelling, *Proc. U.N. Reg. Cartogr. Conf. Asia, Far East, 5th, Canberra, 7*, 13–19, 1966.

Uchupi, E., Atlantic continental shelf and slope of the United States: Shallow structure, *U.S. Geol. Surv. Prof. Pap. 529. I*, 1–44, 1970.

USCGS (United States Coast and Geodetic Survey), Control levelling, *U.S. Dep. Comm. Spec. Publ. 226*, 1–20, 1961.

USGS (United States Geological Survey), Productive aquifers and withdrawals from wells, in *The National Atlas of the United States of America*, pp. 122–123, U.S. Department of the Interior, Washington, D. C., 1970.

Uspenskii, M. S., An investigation into the stability of marks, *Bull. Geod., 67*, 311–314, 1961.

Uspenskii, M. S., Vertical displacements of the earth's surface due to certain non-tectonic processes, in *Recent Crustal Movements*, edited by I. P. Gerasimov, translated from Russian by Z. Garfunkel, pp. 148–152, Israel Program for Scientific Translations, Jerusalem, 1967.

Vanicek, P., and D. Christodulidis, A method for the evaluation of vertical crustal movement from scattered geodetic relevellings, *Can. J. Earth Sci., 11*, 605–610, 1974.

Vanicek, P., and A. C. Hamilton, Further analysis of vertical crustal movement observations in the Lac St. Jean area, Quebec, *Can. J. Earth Sci., 9*, 1139–1147, 1972.

Walcott, R. I., An isostatic origin for basement uplifts, *Can. J. Earth Sci., 7*, 931–937, 1970*a*.

Walcott, R. I., Flexural rigidity, thickness, and viscosity of the lithosphere, *J. Geophys. Res., 75*, 3941–3954, 1970*b*.

Walcott, R. I., Gravity, flexure and the growth of sedimentary basins at a continental edge, *Bull. Geol. Soc. Amer., 83*, 1845–1848, 1972*a*.

Walcott, R. I., Late Quaternary vertical movements in eastern North America: Quantitative evidence of glacio-isostatic rebound, *Rev. Geophys. Space Phys., 10*, 849–884, 1972*b*.

Walcott, R. I., Past sea levels, eustasy, and deformation of the earth, *Quaternary Res., 2*, 1–14, 1972*c*.

Weller, J. M., Compaction of sediments, *Bull. Amer. Ass. Petrol. Geol., 43*, 273–310, 1959.

Wenzel, L. K., Several methods for studying fluctuations of groundwater levels, *Eos Trans. AGU, 17*, 400–405, 1936.

Werner, A. P. H., The measurement of settlement of structures by precise levelling, paper presented at the 4th South African National Survey Conference, Univ. of Natal, Durban, S. Africa, 1970.

Whitten, C. A., Horizontal earth movement, vicinity of San Francisco, California, *Eos Trans. AGU, 29*, 318–323, 1948.

Whitten, C. A., Horizontal earth movement in California, The Journal, *U.S. Coast Geod. Surv., 2*, 84–88, 1949.

Whitten, C. A., Crustal movement in California and Nevada, *Eos Trans. AGU, 37*, 393–398, 1956.

Whitten, C. A., Geodetic measurements in the Dixie Valley area, *Bull. Seismol. Soc. Amer., 47*, 321–325, 1957.

Whitten, C. A., and C. N. Claire, Analysis of geodetic measurements along the San Andreas Fault, *Bull. Seismol. Soc. Amer., 50*, 404–415, 1960.

Woollard, G. P., Areas of tectonic activity in the United States as indicated by earthquake epicenters, *Eos Trans. AGU, 39*, 1135–1150, 1958.

(Received April 7, 1975;
accepted June 2, 1975.)

RECENT VERTICAL CRUSTAL MOVEMENTS ALONG THE EAST COAST OF THE UNITED STATES

Larry D. Brown

Department of Geological Sciences

Cornell University

Ithaca, New York 14853

ABSTRACT

The first detailed profile of apparent vertical crustal movement along the east coast of the United States, extending from Calais, Maine to Key West, Florida, has been produced from the results of precise leveling carried out by the National Geodetic Survey. Comparison of this profile with that obtained from secular trends in sea level data reveals a serious systematic disagreement between the two methods, as large as 19 mm/yr. Estimates of normal measurement error account for some, but not all, of the misclosures indicated. Thus one of the methods must be seriously affected by some secular, non-tectonic influence. Although the actual source of this discrepancy is presently unknown, these results make it possible to estimate its magnitude, an important step toward identification of the source and elimination of its effect. In spite of the uncertainty raised by this discrepancy, leveling and sea level measurements can be used to construct profiles of crustal movement which correlate with geophysical parameters and geological structure. The two data sets have been adjusted using different assumptions as to the source of their disagreement to produce several possible versions of a crustal movement profile along the east coast. Comparison of these profiles with topography, depth to basement, gravity, and seismicity indicate some

correlations, though weak. However, there are several significant correlations between apparent movements and tectonic and geomorphic features; in particular, the Connecticut River Valley graben, the Chesapeake embayment, the Cape Fear arch, the Cape Canaveral prominence, and the Florida drainage divide all correspond to marked changes in the crustal movement profile. Analysis of 93 leveling profiles oriented transverse to the coastline indicate a general tilting down to the east-southeast, with significant variations of tilt direction in both time and space.

Introduction

Results of precise leveling surveys carried out over a number of years by the National Geodetic Survey (NGS) have been used to derive a profile of apparent vertical crustal movements extending from Calais, Maine along the Atlantic coast of the United States to Key West, Florida. Comparison of this profile with one derived from sea level measurements (Hicks, 1972, 1974) reveals a serious discrepancy between the results of the two techniques. The implications of this discrepancy for the measurement of vertical crustal movement by leveling and sea level measurements are considered in this paper. Apparent crustal movement profiles are constructed based on extreme assumptions as to the source of this discrepancy, and are then correlated with geological and geophysical parameters. It is found that significant correlations can be discerned which are common to all the derived profiles.

The recent tectonics of the eastern United States is very poorly understood. To a first approximation, plate tectonics theory suggests that the area should be passive. However, the 1811-1812 New Madrid earthquakes (Fuller, 1912) and the 1886 Charleston earthquake (Dutton, 1889), as well as the extent of recent seismicity (Coffman and von Hake, 1973), clearly point out the fact that tectonic forces of some kind are

presently active in this intra-plate region. Glacial rebound (Oliver and Isacks, 1971), epeirogenic uplift (Woollard, 1958), localization of regional stress by pre-existing weaknesses (Fox, 1970), and pervasive regional compressive stresses (Sbar and Sykes, 1972) are some of the mechanisms put forward to explain the contemporary tectonics of the eastern United States. None of them is completely satisfying. The importance of understanding the present day tectonic regime cannot be overestimated in view of its relevance to seismic risk in heavily populated areas and near nuclear power generation sites.

The poor understanding of what is actually going on stems to a large extent from the lack of field measurements of relevant tectonic parameters. The seismic record is too short and too sporadic to be properly exploited. Systematic measurement of the existing regional stress field is only beginning and the results are fraught with ambiguity (Sbar and Engelder, 1976). On the other hand, the data base of leveling measurements collected by the National Geodetic Survey represents a substantial amount of presently available information relevant to this subject. Proper analysis and interpretation of these data could provide important clues to unraveling the nature of crustal stability in the eastern United States.

The first attempt to analyze leveling data in the United States to determine crustal movements on a regional scale was made by Small (1963). Outside of areas known to be undergoing subsidence due to groundwater withdrawal (Small, 1961; Poland and Davis, 1969) or reservoir loading (Longwell, 1960), little was known of movements in the United States until Meade (1971) published a preliminary map of crustal movement rates in the East. Using more appropriate adjustment procedures, Holdahl and Morrison (1974) presented relatively detailed maps of rates of crustal movements in the Chesapeake Bay and Gulf Coast areas, incorporating

results from sea level measurements. Balazs (1974) extended the Chesapeake Bay results north to New York City and south to Charleston, South Carolina. Using a different approach, Brown and Oliver (1976) examined long profiles of apparent vertical crustal movement in the eastern United States and found correlations between the patterns of movement and geologic structure and seismicity. Similarly, Isachsen (1975) found evidence from leveling data for contemporary uparching in the Adirondacks. Hicks (1972) used tide gauge measurements to deduce the broad pattern of crustal movement along the east coast of the United States. Similarly, Dohler and Ku (1970) and Walcott (1972) used lake level measurements in the Great Lakes to infer vertical crustal movements in those regions.

The study of recent vertical crustal movements utilizing leveling and tide gauge data has been much more extensive outside the United States, most notably in Finland (Kaariainen, 1966), Japan (Miyabe et al., 1966), and the Soviet Union (Meshcherikov, 1967, 1968). Miyabe (1952) and Beloussov et al. (1974) have attempted to synthesize some of the results on a global basis, finding that much of the earth is characterized by movements with contemporary rates that are large compared with average rates over the past few million years. In spite of this large body of data, very little is known about the mechanism responsible for these movements. Furthermore, the relationship, if any, between these recent movements and longer term trends as evidenced by the geologic and geomorphic record is poorly defined. The relationship between secular crustal movements and earthquakes is another important problem which is as yet unresolved, at least in nominally "aseismic" regions.

In this paper new information relevant to these general problems is

presented. The results of this study include: (1) the compilation of a profile of apparent recent vertical crustal movement; (2) evaluation of the internal consistency of leveling and tide gauge data; and (3) the identification of presently active tectonic elements along the east coast of the United States.

The Tide Gauge Data

The tide gauge information used in this study was taken directly from Hicks and Crosby (1974). It consists of the computed slopes (and their associated error limits) of least-squares regression lines fit to time series of yearly mean sea level for stations along the east coast of the United States. The location of these stations is shown in Figure 1. The rate of secular sea level change for the Wilmington, North Carolina station was determined from data generously supplied by Mr. Hicks, inasmuch as it is not included in his published compilation. The sea level series for Wilmington is shown in Figure 2. These rates reflect all of the available measurements through 1972 (1973 for Wilmington). The precise rate one obtains depends on what portion of the available record is used, as can be seen by comparing the rates calculated by Hicks and Shofnos (1965), Hicks (1972), Hicks (1973), and Hicks and Crosby (1974). The rates were independently re-computed for observations through 1973 from data provided by Hicks, and found to be in general agreement with those calculated by Hicks for the interval up to and including 1972. The uncertainty raised by the selection of the time interval used for calculation of secular trends will be discussed later, but it appears to be negligible.

The number of variables which are reflected in sea level measurements are numerous, and their contribution to the secular trend is generally

poorly known. Lisitzin (1974) and Emery and Uchupi (1972) give reviews of many of these factors, which include tectonic movements, river run-off, density, salinity, temperature, atmospheric pressure, and wind velocity. Of these, only river run-off has been examined for its contribution to secular trend, which was found to be nil (Meade and Emery, 1971). Kaye and Stuckey (1973) found evidence of the 18.6-year lunar nodal tide cycle, which might be a serious factor for analysis of data series covering shorter intervals, although that is not the case here. Emery and Uchupi (1972, p. 238) find strong evidence linking density, salinity, and river discharge to secular sea level trends for some, but not all, eastern United States stations. Sea slope changes due to dynamic oceanic circulation changes might also contribute to secular sea level changes (Sverdrup et al., 1942). However, given the ongoing controversy over measuring the present sea slope (Fisher, 1957; Braaten and McCombs, 1963; Sturges, 1967, 1968; Chew and Chew, 1976), it is unlikely that changes in the slope will be well determined by oceanographic methods for some time.

The eustatic sea level changes generally attributed to addition to the world ocean of melted glacial ice (Gutenberg, 1941) would be easy to take into account if it were easy to determine. However, the response of the continental margins (and therefore sea level measuring sites) to the added water load could be very complex (Bloom, 1967; Walcott, 1972). In this paper the eustatic, or constant, sea level effect is ignored, since only relative changes of sea level are considered. The eustatic correction, generally estimated at 1.0 to 1.5 mm/yr additional sea level rise, is not applied to the sea level trends used in this paper. The loading effects are an interpretational problem and will be discussed in a later section.

From the above discussion it is clear that extracting rates of true

land uplift relative to a fixed datum using sea level measurements is not without its ambiguities. The rates used in this study are not corrected for any of the above effects. Further consideration will be given to these effects later.

The Leveling Data

By comparing the elevations determined for a given reference point (benchmark or BM) with respect to some datum by precise leveling at two different times, an estimate of the rate of apparent vertical crustal movement of that benchmark relative to the rate of movement of the datum can be made as follows:

$$\Delta V = \frac{\Delta h_1 - \Delta h_o}{\Delta t}$$

where Δh_1 = elevation difference at time t_1

Δh_o = elevation difference at time t_o

$\Delta t = t_1 - t_o$

Note that rates determined in this manner are relative, i.e., the rate at some reference benchmark must be specified from another method in order to consider absolute movements. These rates can only be considered as average rates over the time interval concerned, and contain no information as to changes of rate during the time interval.

The error limits associated with the leveling-determined rates are calculated according to the relation:

$$m_v^2 = \frac{(m_o^2 + m_1^2) \cdot L}{\Delta t^2}$$

where m_v = one standard deviation for the velocity measurement relative to a given reference point (mm/yr)

m_o = standard deviation for leveling of unit length at time t_o ($mm/km^{\frac{1}{2}}$)

m_1 = standard deviation for leveling of unit length at time t_1 ($mm/km^{\frac{1}{2}}$)

L = distance between reference point and benchmark at which velocity is determined (km)

$\Delta t = t_1 - t_o$, the time interval between levelings

Estimates of m_o and m_1 were taken from Holdahl (1973). The above relation is relevant to random error only, and does not take into account any systematic error in the leveling.

Leveling, like tide gauge measurements, has inherent sources of uncertainty. One of these relates to the question of the stability of the benchmarks used. Although Karcz et al. (1975) find that certain types of benchmarks appear less stable than others, it is difficult to see how such variations can be systematic from benchmark to benchmark, especially over considerable distances. Therefore, in this study reliance is placed on the trends defined by sets of benchmarks rather than upon the stability of an individual mark. This limitation tends to restrict the lower dimension of apparent movement which might be considered significant. On the scale with which this paper is concerned, individual benchmark eccentricities do not appear significant. Furthermore, restricting attention to trends of movement over distances on the order of 25 km or more tends to minimize the risk of misinterpreting localized phenomena such as mine collapse or fluid withdrawal as tectonic movement. Although tectonic disturbances on a localized scale may be occurring, they will not be considered in this study.

A more serious problem for the interpretation of leveling results is

due to the fact that the method is subject to a number of possible systematic influences. Unequal refraction, tidal attraction, ocean loading, and unequal lighting are some of the systematic effects which might be encountered. Since there is no significant topography along the level route with which this paper is concerned, refraction effects should be insignificant. The direct effect of the tidal attraction of the sun and the moon on a north-south line should be less than 0.1 mm/km (Holdahl, 1974). The effect of ocean loading and earth tides on leveling is not well known, but is probably on the same order as the direct tide (Lennon, 1961). Differences in the lighting of the fore and back level rods have been found to give rise to a systematic error of as much as 0.4 to 0.9 mm/km (Edge, 1959; Bomford, 1971) when using certain types of rods. It has not been conclusively shown, however, that the equipment used by the NGS is susceptible to this error to a significant degree, although Balazs (1975) found an apparent systematic effect, possibly due to lighting, on some east-west lines with a magnitude of about 0.4 mm/km.

Even if the individual leveling measurements contain some systematic error, their differences, which are used to calculated apparent crustal movements, probably have less error, since most of these systematic effects have the same sign. Assuming similar working conditions for the two levelings, it might be expected that any systematic effects would cancel out, or nearly so. Since working conditions can vary even over a day, it should be expected that the net effect of these "systematic" errors has a more random nature. Over large distances, possibly on the order of 50-100 km, "systematic" influences could appear as random influences (Bomford, 1971). One type of systematic error not subject to such a randomization process is that due to instrumental or observer eccentricity, if one instrument or observer is used over a considerable distance

on one of the surveys and another is used on the subsequent survey. There is no evidence that such is the case with the data examined in this paper.

East Coast Profile

Using data supplied by the NGS, a more or less continuous profile of apparent recent vertical crustal movement has been constructed along the east coast of the United States from Calais, Maine to Key West, Florida (Figure 1). Figure 3 shows the profile thus obtained, assuming a rate of movement at Portland, Maine of -2.3 mm/yr relative to sea level as indicated by the secular trend of the tide gauge at Portland. Also shown in Figure 3 is the topography along the profile route and the standard deviation of leveling as a function of distance. From an historical vantage point, Portland seems particularly appropriate as a reference since it was the starting point for the United States precise leveling system and may become a standard for all measurements which require knowledge of mean sea level (Lisitzin, 1974).

In Figure 4, the apparent recent vertical crustal movement profile derived from leveling is compared with a similar profile derived from the sea level trends computed by Hicks and Crosby (1974). Hicks (1972) was the first to use sea level measurements to make a profile of apparent recent vertical crustal movement in this manner. Many of the tide gauges are located at some distance from the profile route and their effect should be downgraded. Those stations located less than about 5 km from the route are plotted as triangles in Figure 4, those at greater distances as squares. The vertical dimensions of the symbols represent twice the standard error of the measured trends.

Inspection of Figure 4 immediately reveals a large discrepancy between the two types of measurements. For example, leveling indicates that

Key West, Florida is moving up with respect to Portland, Maine at a rate of 18.9 mm/yr, whereas the tide gauges at these respective points suggest a difference of only 0.2 mm/yr. The respective error limits of the two differences are only 3.5 mm/yr and 0.3 mm/yr, thus the discrepancy is over five times as large as that one could expect from random measurement error. One or both of the methods must be seriously affected by some systematic non-tectonic influence. Since each method has its own possible sources of error and since our understanding of the role of these effects is insufficient to ascribe the discrepancy to any one effect, a deterministic solution is not possible.

Although the exact nature of the discrepancy cannot be isolated, these data can be used to estimate the magnitudes that a systematic error must have to account for the observed differences. If the error is attributable to meteorological effects on the tide gauges, it would amount to as much as 270% of the actual sea level trend estimate. If, on the other hand, the discrepancy is attributed to the leveling measurements, it is necessary to postulate a systematic error of about 0.35 mm/km. The largest systematic error acceptable for leveling of high precision is 0.2 mm/km. Tidal error could only account for 0.1 mm/km, although including earth tides and ocean loading it might be as large as 0.2 mm/km. Unequal lighting might be responsible, since it can be as large as 0.4 mm/km. However, it is by no means apparent that such an effect is present in the data used in this study, especially since such errors should tend to cancel when velocities are calculated from the leveling data.

In view of the lack of a deterministic solution, the approach used here is to generate a set of recent vertical crustal movement profiles according to different hypotheses as to the origin of the discrepancy between the two methods. Profile I (Figure 4) represents one extreme,

i.e., the leveling is assumed to be correct and the tide gauge data incorrect. Profile II (Figure 5) represents the other extreme, that the tide gauge data are correct and that the leveling results are in error. In this and subsequent adjustments, only the tide gauges closer than 5 km to the profile route are used. For Profile III, the tide gauges at Portland, Maine and Key West, Florida were arbitrarily assumed accurate and a constant systematic correction was applied to all the data to yield the proper rates at these two points. In spite of the arbitrariness of this adjustment, the fit between the adjusted leveling data and the original sea level trends is quite good from the Chesapeake Bay northward. In Profile IV (Figure 7) a probabilistic model was used, in which the sea level and leveling results were adjusted by a least squares technique (Veress, 1974). For comparison, the tide gauge data shown on all of the profiles are the original, unadjusted values.

Correlation of Profile with Geophysical and Geological Parameters

Since it is not known which of the profiles is most correct, it seems reasonable to restrict attention to those features which persist in all of the adjustments. For example, the minimum in the profiles at about 3300 km is pronounced in all four adjustments and does not, therefore, appear to be attributable to error in either the tide gauge or leveling data. On the other hand, the minimum at about 1300 km on Profiles II and IV corresponds to the Sandy Hook tide gauge, whose sea level trend is very suspect as a measure of regional movement due to the effects of local non-tectonic subsidence at the gauge (Hicks, 1972). Savannah, Georgia is another area where a pronounced local subsidence is evident, here due to water withdrawal (Poland and Davis, 1969). This effect appears as a pronounced vertical scatter of benchmark values near 2800 km and is easily recognized.

Whether or not the tide gauge at Fort Pulaski is affected by this withdrawal is not known for certain, although close inspection of leveling in this area indicates that it is not. The tide gauge trend at Eastport, Maine is also suspect (Hicks, 1972), although it seems to agree quite well with the leveling between Bangor and Calais, Maine. At any rate, it is not used in the adjustments. When interpreting results such as these, it should be remembered that localized non-tectonic movements could be present, although focussing on the longer wavelength trends helps to minimize their effects.

Examination of these profiles reveals several features of interest. First, there is a marked change in the slope of the curves at approximately 1050 km, very near to the junction of the Connecticut River Valley and the coast. The Connecticut River Valley occupies a north-south trending Triassic graben, and the correspondence of a change in the pattern of crustal movement at this large scale weakness in the crust seems to be too close for coincidence. Another prominent change in slope occurs around New York, which stands at the junction of the north-south trending structures of the northern Appalachians and the northeast-southwest trending structures of the central Appalachians (King, 1969). Furthermore, the eastern boundary of the Newark Valley, another Triassic graben, runs near the profile line at this point. As mentioned above, the minimum at 1300 km on some of the profiles would appear to have no tectonic significance. The sharp change in slope of the recent vertical crustal movement curve at Philadelphia (about 1500 km) seems to correspond to a sharp change in the direction of the profile route rather than any structural element. The minimum at 1700 km corresponds nicely to the Chesapeake-Delaware embayment, a pronounced structural low. The marked peak in the profiles

near 1900 km is something of a mystery. There are no pronounced structural features near this part of the profile route (Murray, 1961), which lies along the southern tip of the Delaware-Maryland peninsula. The proximity of this segment of the profile to the ocean on two sides as well as an abnormally short time interval between the levelings indicates that leveling error induced by ocean loading could be responsible, although it is by no means certain. Moving south from Norfolk, Virginia, the leveling and tide gauge data diverge strongly. Therefore, the reality of the broad uplift from Norfolk, Virginia to Savannah, Georgia is in some doubt. However, all of the profiles show a marked change near Wilmington, North Carolina (2300 km) as the line crosses the Cape Fear arch (Murray, 1961). South of Charleston, South Carolina, the slope of the recent vertical crustal movement profile increases drastically, decreasing again at Savannah, Georgia. Little structure is known in this area, although it is one of the zones of highest seismic risk in the eastern United States. Near Melbourne, Florida (3350 km) is a very pronounced minimum in the curve, corresponding to the junction of the east-west trending Florida drainage divide and the coast. Cape Canaveral, the only Atlantic Coast cape not associated with a river mouth, is located here. Again, the relationship is too good to be coincidence. Finally, the profile shows subsidence of Key West with respect to the Florida mainland, which seems to correlate with no structural feature and, like the peak near 1900 km, may be reflecting ocean loading effects.

In Figure 8, Profile IV is shown along with corresponding profiles of the depth to basement and Bouguer gravity anomalies along the profile route, as adapted from Flawn (1974) and the American Geophysical Union (1964). Inspection of this figure shows some correlation between recent

vertical crustal movement and depth of basement between Atlantic City, New Jersey and Philadelphia, Pennsylvania, in the Chesapeake Bay region, and at the Cape Fear arch. Interestingly, there is some correlation between a minor basement high and the peak in recent vertical crustal movement near 1900 km. On the other hand, the correlation between the recent vertical crustal movement profile and gravity is ambiguous at best.

A relationship, if any, between these movements and seismicity is not clear. Although some of the changes in the profile noted above occur in areas of higher than average seismicity for the east, some do not. Knowledge of a relationship between recent vertical crustal movement and seismicity is important, not only for seismic hazard estimation, but for understanding the mechanisms for these movements. For example, do these movements represent strain buildup precursory to earthquakes or strain release by aseismic creep? These questions cannot be answered as yet.

Recent Vertical Crustal Movement Near the Profile

A cursory examination was made of a large number of short profiles of recent vertical crustal movement oriented transverse to the coast. These profiles exhibit large variations in both time and space. However, 65% of these profiles indicate a strong regional component of tilt down to the east-southeast. This regional tilt is more pronounced in some areas, for example in the North Carolina-South Carolina area (Figure 9). This trend agrees at least in sign with the post-Jurassic trend indicated by the oceanward increase in the thickness of coastal sediments.

Summary

A profile of recent vertical crustal movement along the east coast of the United States has been constructed from leveling data. Comparison of this profile with sea level trends suggests that one of the methods contains serious sources of error. In spite of the uncertainties in these data, it is found that the recent vertical crustal movements they indicate do show some correlations with geologic structure and long-term trends. These results suggest that present-day vertical crustal movements may reflect deformation localized by pre-existing weaknesses in the crust.

Acknowledgments

This research was supported by the Advanced Research Projects Agency of the Department of Defense and was monitored by the Air Force Office of Scientific Research under Contract No. AFOSR-73-2494.

American Geophysical Union, . .guer Gravity Anomaly Map of the United States, 1964.

Balazs, E.I., Vertical crustal movements on the Middle Atlantic Coastal Plain as indicated by precise leveling, paper presented at the Northeastern Section Annual Meeting, Geological Society of America, Boulder, Colorado, 1974.

Balazs, E.I., Report on a preliminary experiment to detect a possible systematic type error in precise leveling, paper presented to Subcommittee of Marine Geodesy on the Discrepancy in the Geoids, AGU, 1975.

Beloussov, U.V., G.I. Reismer, E.M. Rudich, and V.M. Sholpo, Vertical movements of the earth's crust on the continents, Geophys. Surv., 1, 245-273, 1974.

Bloom, A.L., Pleistocene shorelines: A new test of isostasy, Geol. Soc. Am. Bull., 78, 1477-1494, 1967.

Bomford, G., Geodesy, 3rd edition, 732 pp., Clarendon Press, Oxford, 1971.

Braaten, N.F., and C.E. McCombs, Mean sea levels as indicated by a 1963 adjustment of first-order leveling in the United States, U.S. Coast and Geodetic Survey, 22 pp., 1963.

Brown, L.D., and J.E. Oliver, Vertical crustal movements from leveling data and their relation to geologic structure in the eastern United States, Rev. Geophys. Space Physics, 14, 13-35, 1976.

Chew, F., and F.S. Chew, On sea level slope along continental boundaries, preprint, 1975.

Coffman, J.L., and C.A. von Hake (Eds.), Earthquake History of the United States, Publ. 41-1, 208 pp., Environmental Data Service, Washington, D.C., 1973.

Dohler, G.G., and L.F. Ku, Presentation and assessment of tides and water level records for geophysical investigations, Can. J. of Earth Sci., 7, 607, 1970.

Dutton, C.E., The Charleston earthquake of August 31, 1886, U.S. Geol. Surv. Ann. Rep. 1887-88, 203-508, 1889.

Edge, R.C.A., Some considerations arising from the results of the second and third geodetic levelings of England and Wales, Bull. Geodesique, 52, 28-36, 1957.

Emery, K.O., and E. Uchupi, Western North Atlantic Ocean: Topography, Rocks, Structure, Water, Life, and Sediments, 532 pp., Amer. Assoc. Petrol. Geol., Tulsa, Oklahoma, 1972.

Fisher, I., Does mean sea level slope up or down towards North?, Bull. Geodesique, 115, 17-26, 1957.

Flawn, P.T., Basement Map of North America, AAPG and U.S. Geol. Surv., 1974.

Fox, F.L., Seismic geology of the eastern United States, Assoc. Engr. Geol. Bull., 7, 21-43, 1970.

Fuller, M.L., The New Madrid earthquake, U.S. Geol. Surv. Bull. 494, 1-119, 1912.

Gutenberg, B., Changes in sea level, postglacial uplift, and mobility of the earth's interior, Geol. Soc. Am. Bull., 52, 721-772, 1941.

Hicks, S.D., Vertical crustal movements from sea level measurements along the east coast of the United States, J. Geophys. Res., 77, 5930-5934, 1972.

Hicks, S.D., Trends and variability of yearly mean sea level, 1893-1971, Tech. Mem. NOS 12, 13 pp., National Oceanic and Atmospheric Administration, Boulder, Colorado, 1973.

Hicks, S.D., and J.E. Crosby, Trends and variability of yearly mean sea level, 1893-1972, Tech. Mem. NOS 13, 1-14, National Oceanic and Atmospheric Administration, Boulder, Colorado, 1974.

Hicks, S.D., and W. Shofnos, Yearly sea level variations for the United States, J. Hydraul Div. Proc. Amer. Soc. Civil Engr., 91, 23-37, 1965.

Holdahl, S.R., Vertical crustal movements - Status of NGS investigations, paper presented at Geop-3 Research Conference, Vertical Crustal Movements and Their Causes, AGU, Washington, D.C., 1973.

Holdahl, S.R., Times and heights, paper presented at the International Symposium on Problems Related to the Redefinition of North American Geodetic Networks, Int. Assoc. of Geod., Paris, 1974.

Holdahl, S.R., and N.L. Morrison, Regional investigations of vertical crustal movements in the U.S. using precise relevelings and mareograph data, paper presented at the Symposium on Recent Crustal Movements and Associated Seismic and Volcanic Activity, Comm. on Recent Crustal Movements, Prague, 1973.

Isachsen, Y.W., Evidence for contemporary doming of the Adirondack Mountains, New York, and possible implications for regional tectonics and seismicity, preprint, 1975.

Kaariainen, E., The second leveling of Finland in 1935-1955, Suom. Geodeettisen Laitoksen Julka., 62, 1-313, 1966.

Karcz, I., J. Morreale, and F. Porebski, Vertical crustal movements in New York and Pennsylvania - Neotectonics or benchmark instability, Geol. Soc. Am. Abstr. with Programs, Ann. Meeting, Salt Lake City, p. 1138, 1975.

Kaye, C.A., and G.W. Stuckey, Nodal tidal cycle of 18.6 yr: Its importance in sea-level curves of the east coast of the United States and its value in explaining long-term sea level changes, Geology, 11, 141-144, 1973.

King, P.B., Tectonic Map of North America, U.S. Geol. Surv., Washington, D.C., 1969.

attraction of ocean tides, Geophys. J. R. Astr. Soc., 6, 64-84, 1961.

Lisitzin, E., Sea-Level Changes, Elsevier Oceanography Series, 8, 286 pp., Amsterdam, Elsevier, 1974.

Longwell, C.R., Interpretation of the leveling data, U.S. Geol. Surv. Prof. Pap. 295, 33-38, 1960.

Meade, B.K., Report of the sub-commission on recent crustal movements in North America, paper presented to 15th General Assembly of International Union of Geodesy and Geophysics, Int. Assoc. of Geod., Brassek, 1971.

Meade, R.H., and K.O. Emery, Sea level as affected by river runoff, eastern United States, Science, 173, 425-428, 1971.

Mescherikov, Y.A., Secular movements of the earth's crust: Some results and problems, in Recent Crustal Movements, I.P. Gerasimov (Ed.), 1-21, Israel Program for Scientific Translations, Jerusalem, 1967.

Mescherikov, Y.A., Recent crustal movements in seismic regions - Geodetic and geomorphic data, Tectonophysics, 6, 29-39, 1968.

Miyabe, N., Vertical earth movements as deduced from the results of rerunning the precise levels, Bull. Earthquake Res. Inst. Univ. Tokyo, 30, 127-616, 1952.

Miyabe, N.S., S. Miyamura, and M. Mizoue, A map of secular vertical movements of the earth's crust in Japan, Ann. Acad. Sci. Fenn., Ser. A3, 90, 287-289, 1966.

Murray, G.E., Geology of the Atlantic and Gulf Coastal Province of North America, 629 pp., Harper and Brothers, New York, 1961.

Oliver, J.E., and B. Isacks, Seismicity and tectonics of the eastern United States, Earthquake Notes, 43, 30, 1971.

Poland, J.F., and G.H. Davis, Land subsidence due to withdrawal of fluids, in Reviews in Engineering Geology II, 187-269, Geological Society of America, Boulder, Colorado, 1969.

significance for nuclear power plant siting, Geol. Soc. Am. Abstracts with Programs, Northeast and Southeast Sections, 8, p. 260, 1976.

Sbar, M.L., and L.R. Sykes, Contemporary compressive stress and seismicity in eastern North America: An example of intra-plate tectonics, Bull. Geol. Soc. Am., 84, 1861-1882, 1973.

Small, J.B., Settlement studies by means of precision leveling: Report to the International Association of Geodesy, IUGG, Helsinki, Finland, Bull. Geod., 62, 317-325, 1961.

Small, J.B., Interim report on vertical crustal movement in the United States, Report to Commission on Recent Crustal Movements, 14 pp., Int. Assoc. of Geod., IUGG, Paris, 1963.

Sturges, W., Slope of sea level along the Pacific coast of the United States, J. Geophys. Res., 72, 3627-3637, 1967.

Sturges, W., Sea-surface topography near the Gulf Stream, Deep Sea Res., 15, 149-156, 1968.

Sverdrup, H.U., M.W. Johnson, and R.H. Fleming, The Oceans: Their Physics, Chemistry and General Biology, 1087 pp., Prentice Hall, New York, 1942.

Veress, S.A., Adjustment by Least-Squares, 217 pp., Amer. Cong. Surv. Mapping, Washington, D.C., 1974.

Walcott, R.I., Late Quaternary vertical movements in eastern North America: Quantitative evidence of glacio-isostatic rebound, Rev. Geophys. Space Physics, 10, 849-884, 1972.

Woollard, G.P., Areas of tectonic activity in the United States as indicated by earthquake epicenters, EOS, Trans. AGU, 39, 1135-1150, 1958.

FIGURE CAPTIONS

Figure 1: Index map showing location of leveling route (dashed line) and tide gauges (solid circles) used in this study.

Figure 2: Sea level trend at Wilmington, North Carolina. The straight line represents the least-squares regression fit to the data and has a slope of 1.85 ± 0.61 mm/yr. Arbitrary datum.

Figure 3: Unadjusted profile of recent vertical crustal movement derived from leveling. Velocity of -2.30 mm/yr assumed at Portland, Maine. Also shown are the topography along the profile route and the magnitude of the standard deviation for the leveling relative to Calais, Maine.

Figure 4: Profile I: Leveling profile compared to tide gauge results. Portland, Maine sea level trend assumed correct. Letters at the top (outside) represent cities along leveling route while those at the top (inside) represent tide gauge locations. Data for tide gauges more than 5 km from leveling route shown as squares; those closer than 5 km as triangles. Vertical dimension of tide gauge symbols represents two standard errors for sea level trend.

Figure 5: Profile II: Leveling profile adjusted assuming tide gauge data (triangles) correct. Same conventions as in Figure 4.

Figure 6: Profile III: Leveling data adjusted to fit tide gauge results at Portland, Maine and Key West Florida. Same conventions as in Figure 4.

Figure 7: Profile IV: Leveling and tide gauge results adjusted by least-squares (unadjusted tide gauge results plotted). Same conventions as in Figure 4.

Figure 8: Profile IV shown with depth to basement and Bouguer gravity profiles along leveling route.

Figure 9: Recent vertical crustal movements on selected profiles trending northwest to southeast in North and South Carolina. Note predominance of tilt down to the southeast (right). Arbitrary datums.

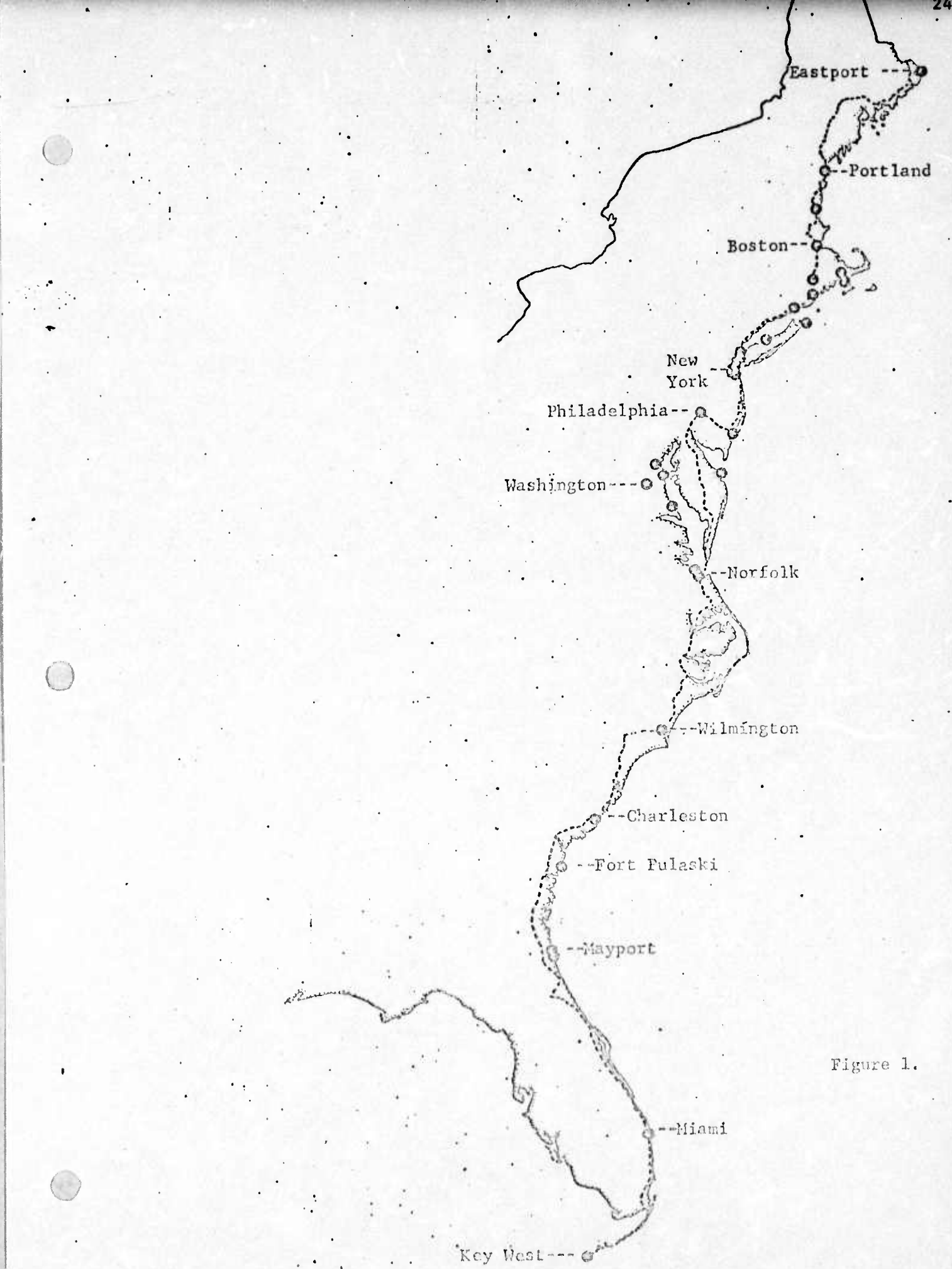

Eastport
Portland
Boston
New York
Philadelphia
Washington
Norfolk
Wilmington
Charleston
Fort Pulaski
Mayport
Miami
Key West

Figure 1.

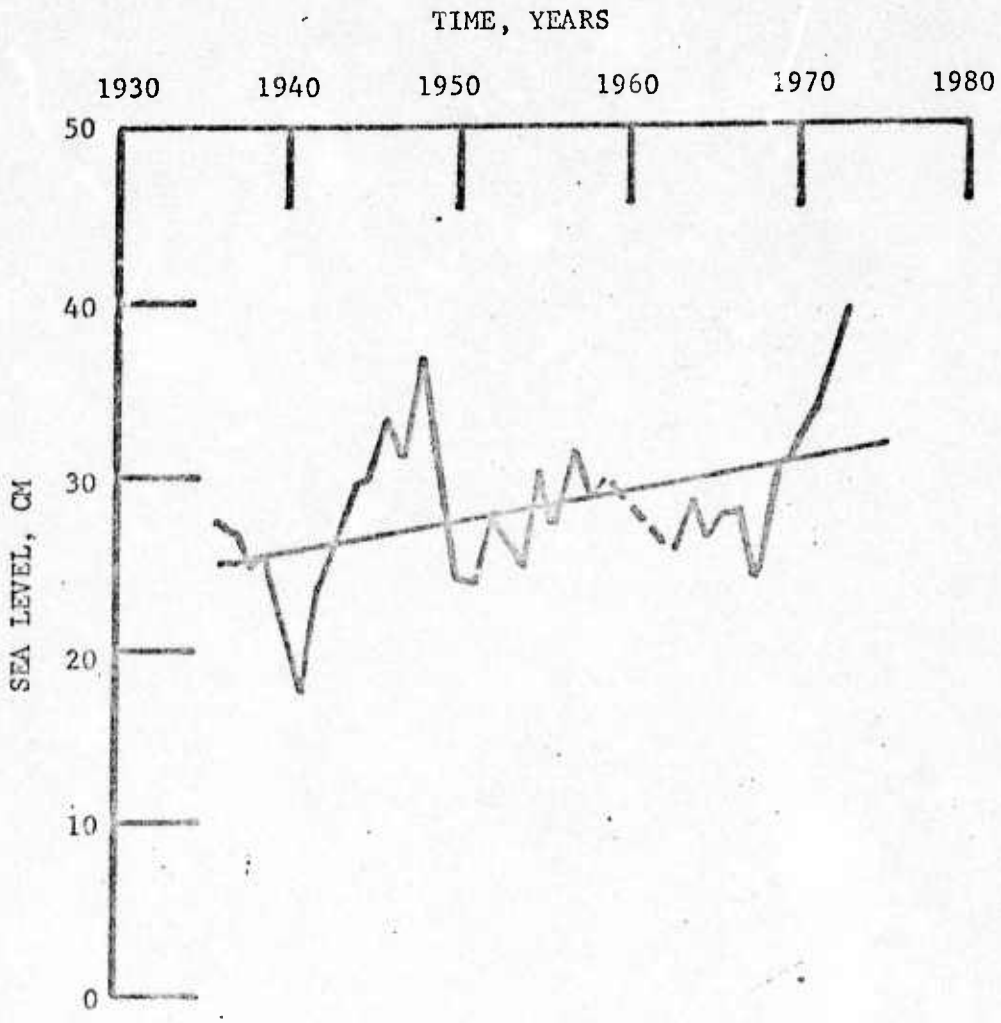

TIME, YEARS
1930
1940
1950
1960
1970
1980
50
40
30
20
10
0
SEA LEVEL, CM

Figure 2.

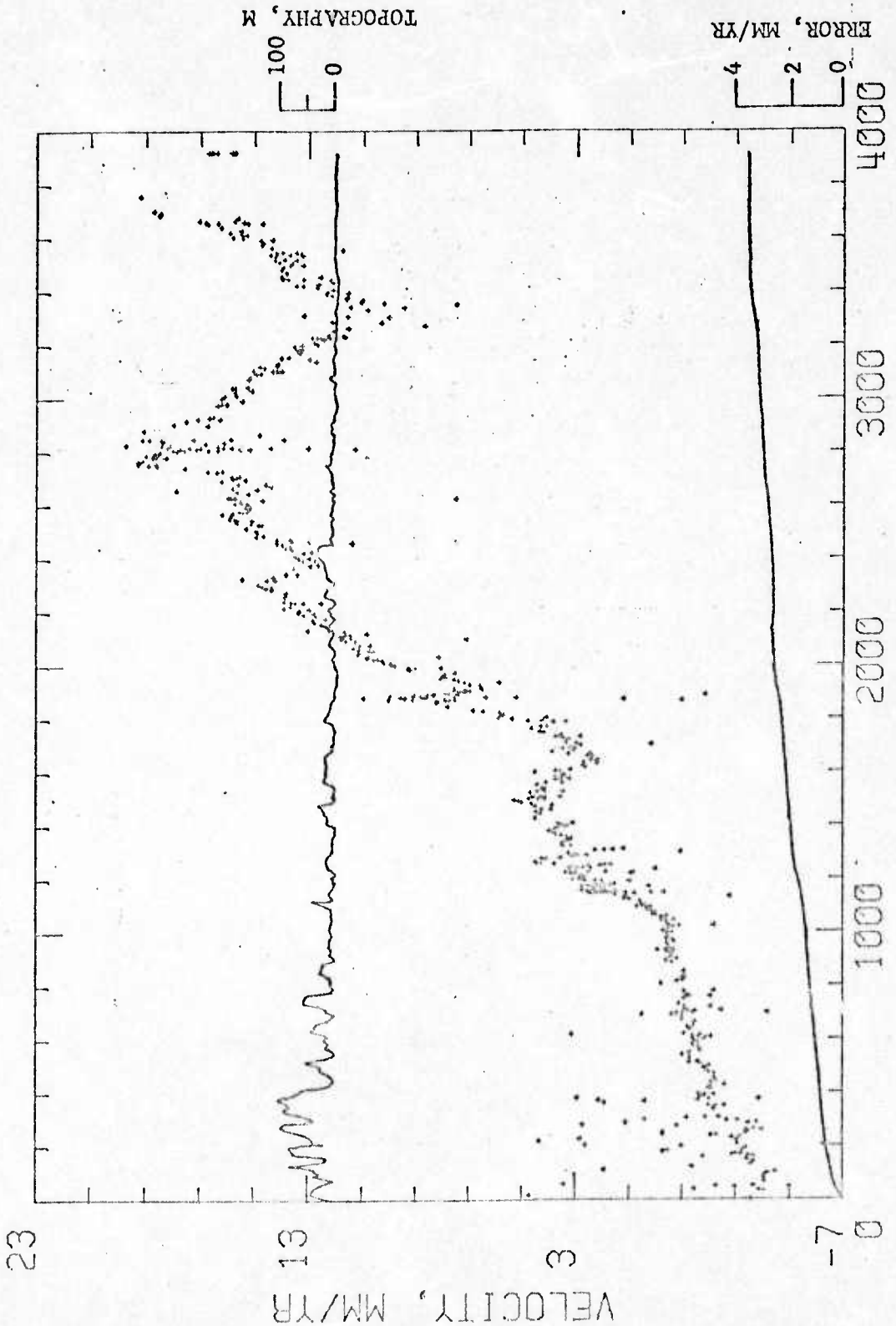

TOPOGRAPHY, M
100
0
ERROR, MM/YR
4
2
0
4000
3000
2000
1000
DISTANCE, KM
23
13
3
-7
0
VELOCITY, MM/YR

Figure 3.

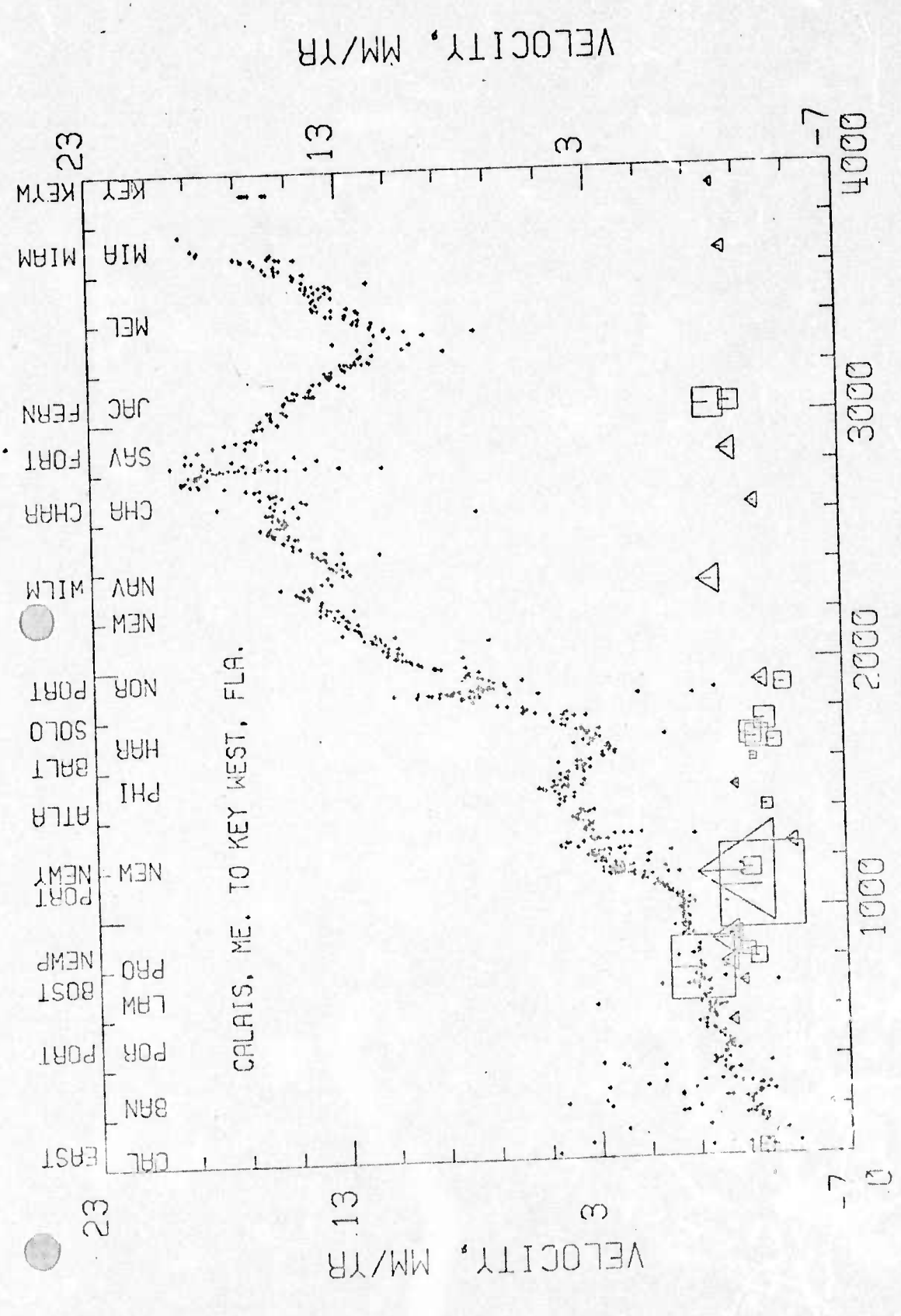

VELOCITY, MM/YR
23
13
3
-7
KEYW
MIAM
FERN
FORT
CHAR
WILM
PORT
SOLO
BALT
ATLA
PORT
NEWY
BOST
NEWP
PORT
EAST
KEY
MIA
MEL
JAC
SAV
CHA
NAV
NEW
NOR
HAR
PHI
NEW
LAW
POR
BAN
CAL
CALAIS, ME. TO KEY WEST, FLA.
4000
3000
2000
1000
0
DISTANCE, KM
VELOCITY, MM/YR

Figure 4.

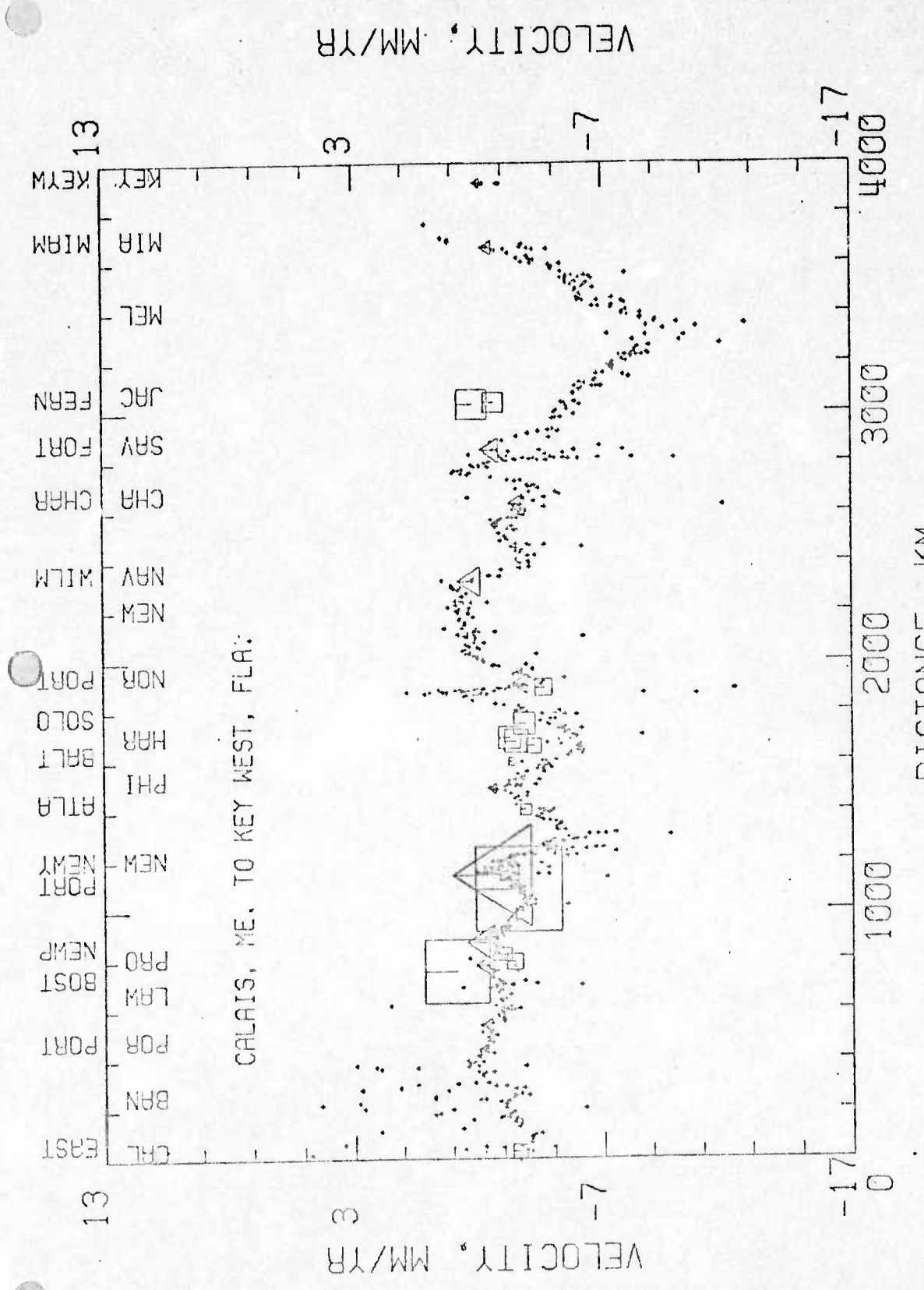

VELOCITY, MM/YR
13
3
-7
-17
KEYW
MIAM
MIA
MEL
FERN
JAC
FORT
SAV
CHAR
CHA
WILM
NAV
NEW
PORT
NOR
SOLO
HAR
BALT
PHI
ATLA
PORT
NEW
NEW
NEWP
PRO
BOST
LAW
PORT
POR
BAN
EAST
CAL
CALAIS, ME. TO KEY WEST, FLA.
4000
3000
2000
1000
0
DISTANCE, KM
VELOCITY, MM/YR

Figure 5.

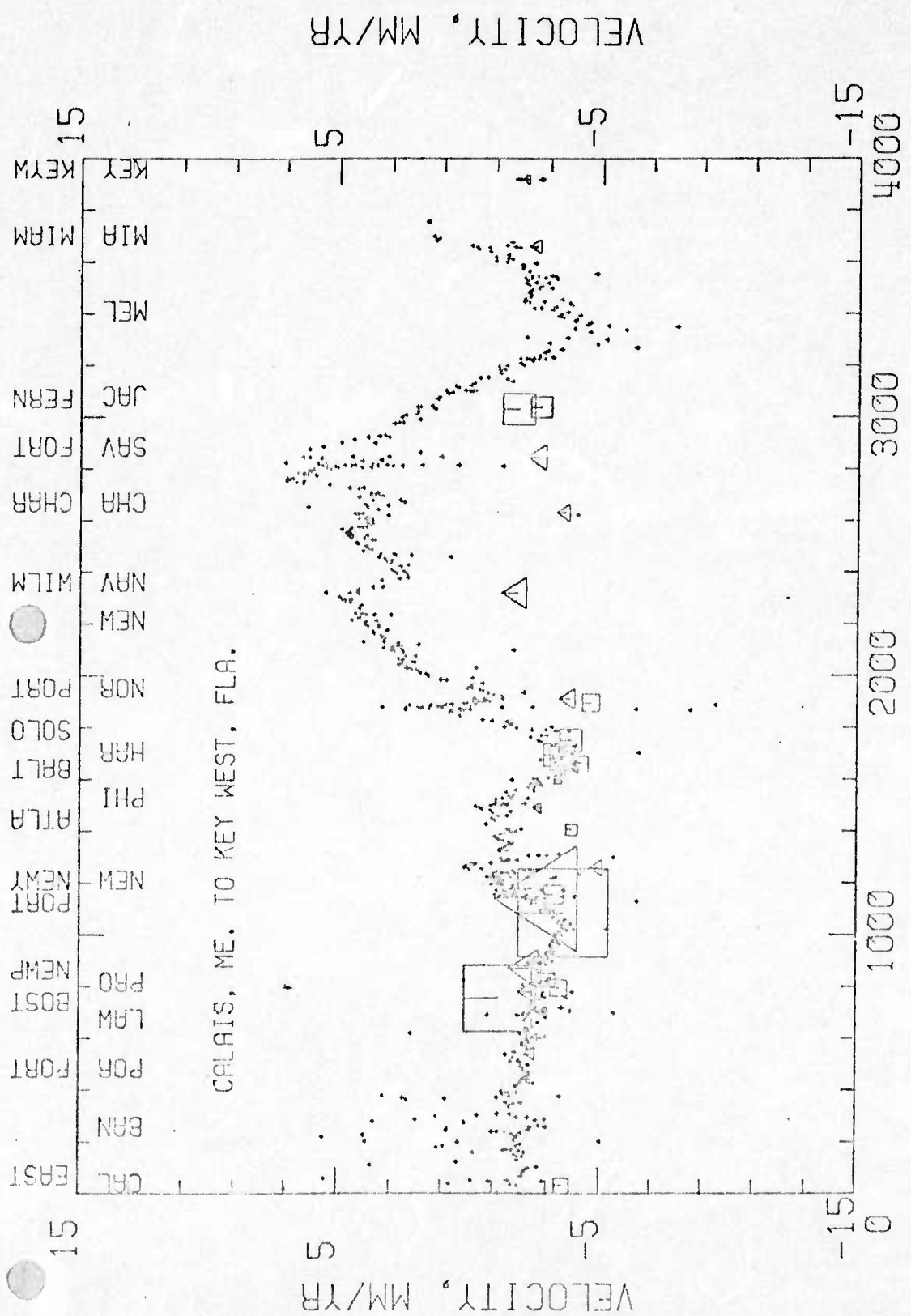

VELOCITY, MM/YR
15
5
-5
-15
KEYW
MIAM
MEL
FERN
FORT
CHAR
WILM
NEW
PORT
SOLO
BALT
ATLA
PORT
NEWY
NEWP
BOST
FORT
EAST
KEY
MIA
JAC
SAV
CHA
NRV
NEW
NOR
HAR
PHI
NEW
PRO
LAW
POR
BAN
CAL
CALAIS, ME. TO KEY WEST, FLA.
4000
3000
2000
1000
0
DISTANCE, KM
VELOCITY, MM/YR

Figure 6.

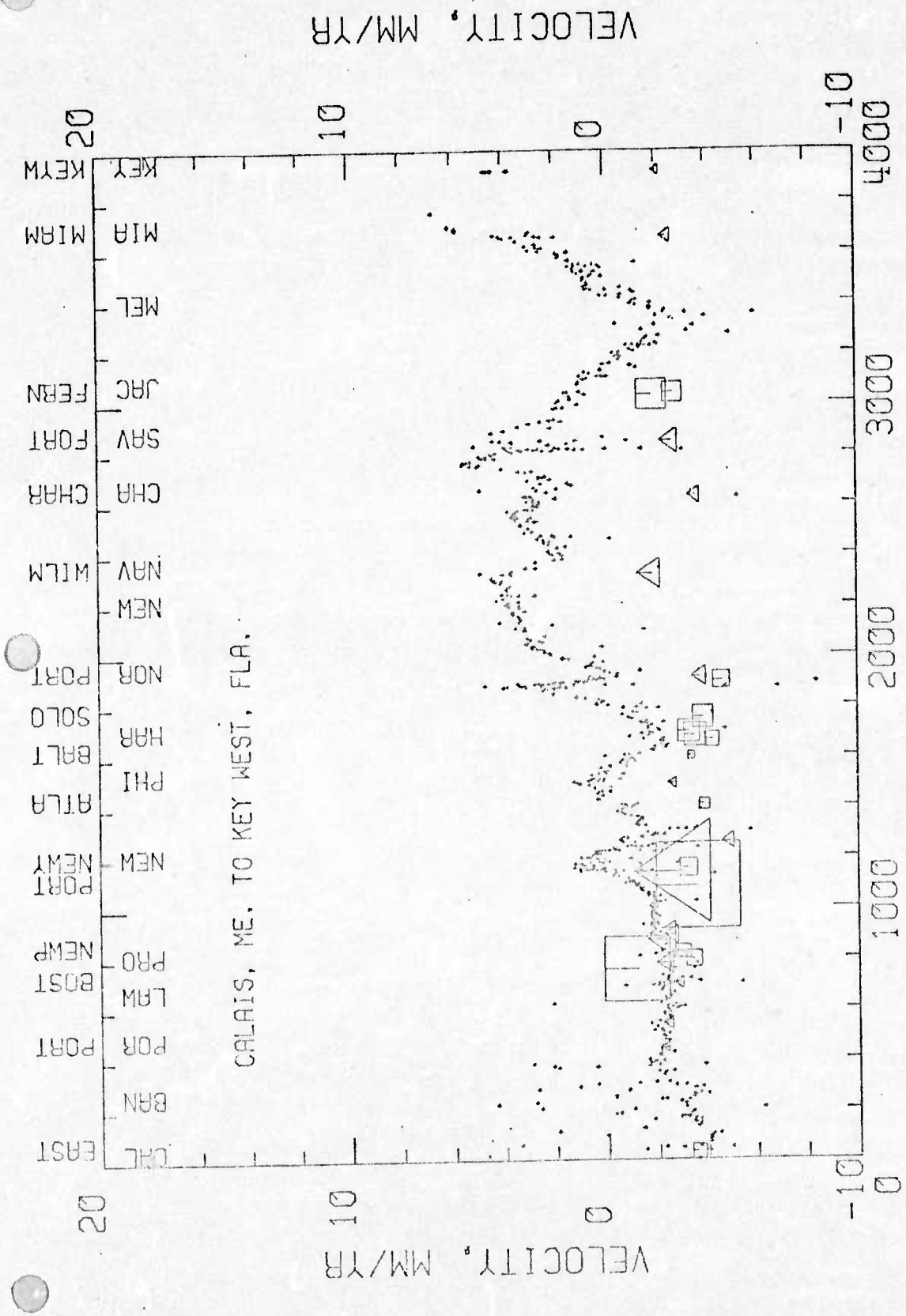

VELOCITY, MM/YR
20
10
0
-10
4000
3000
2000
1000
0
DISTANCE, KM
CALAIS, ME. TO KEY WEST, FLA.
KEYW
MIAM
MEL
FERN
FORT
CHAR
WILM
NEW
PORT
SOLO
BALT
ATLA
NEWY
NEWP
BOST
PORT
EAST
KEY
MIA
JAC
SAV
CHA
NAV
NOR
HAR
PHI
NEW
PRO
LAW
POR
BAN
CAL

Figure 7.

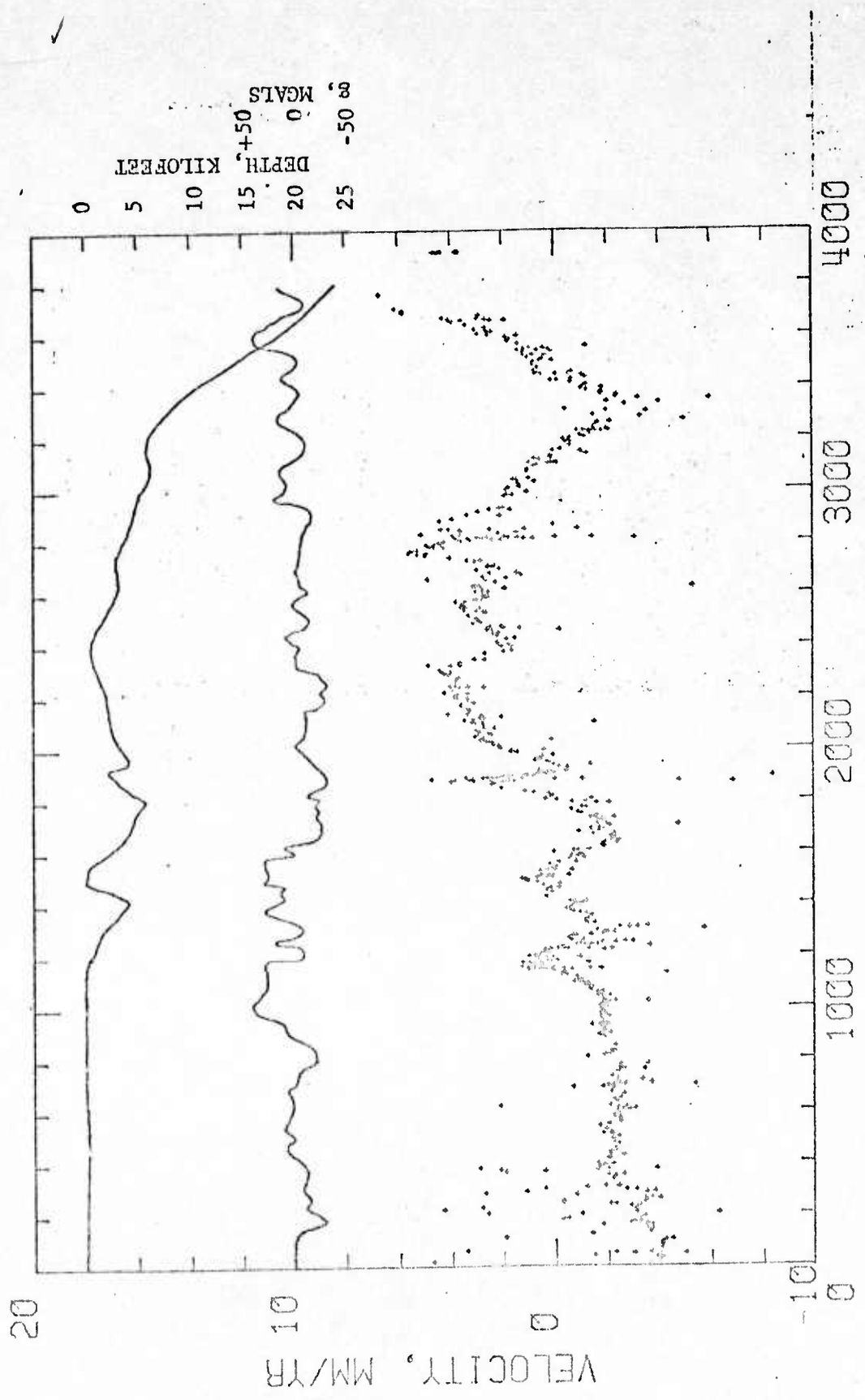

VELOCITY, MM/YR
20
10
0
-10
0
1000
2000
3000
4000
DISTANCE, KM
DEPTH, KILOFEET
0
5
10
15
20
25
g, MGALS
+50
0
-50

Figure 8.

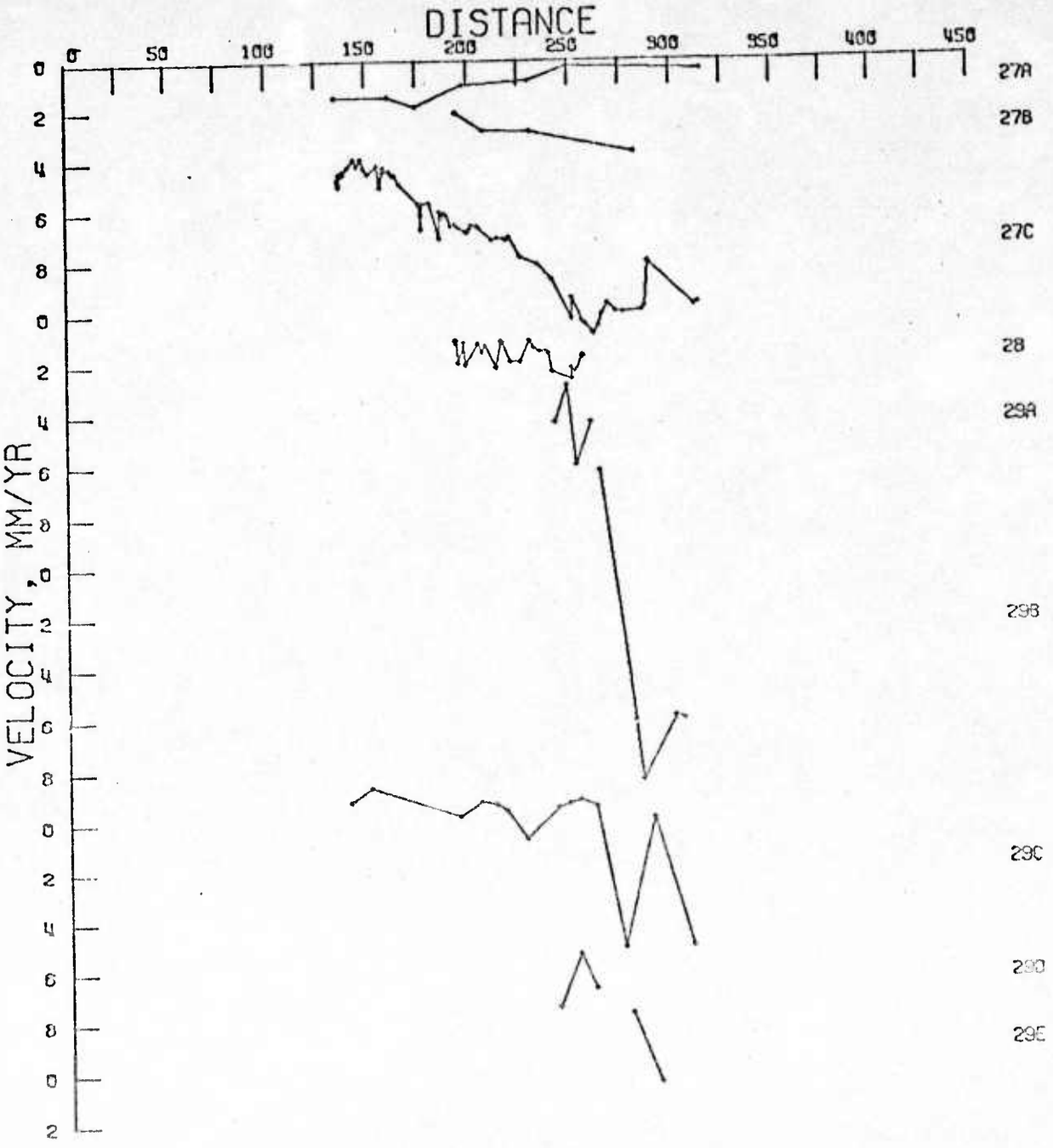

DISTANCE
0
50
100
150
200
250
300
350
400
450
VELOCITY, MM/YR
27A
27B
27C
28
29A
29B
29C
29D
29E

Figure 9.

APPENDIX D

SUBSURFACE FAULT MOVEMENT AND PRECISE RELEVELING: A CASE STUDY IN WESTERN KENTUCKY

F. Steve Schilt

Department of Geological Sciences

Cornell University

Ithaca, New York 14853

ABSTRACT

Both geological and geophysical data are consistent with the existence of a concealed, high angle, dip-slip fault (possibly a normal fault) in extreme western Kentucky, located within the northern boundary of the Mississippi Embayment and the New Madrid seismic zone. Inferred faults have previously been proposed in this region (Stearns and Wilson, 1972), but recent analysis of first order leveling data lends strong support to the existence of a potentially active fault or fault zone which has experienced approximately 31 mm of relative displacement in a 21 year interval.

The location is defined to within 10 km by an abrupt steep gradient in the relative vertical movement profile, which is derived from leveling measurements by dividing the change in elevation by the time interval. A trend of NNE is obtained for the fault from other geological and geophysical evidence. A focal mechanism for a nearby earthquake which occurred between the times of leveling suggests a normal fault, although it is not certain this mechanism correlates with the alleged fault.

In Nevada, aromalies in elevation changes similar to that reported here have been correlated with known surface faults and

interpreted as post-earthquake slip (Savage and Church, 1974). Workers in Hungary and Japan have postulated faults at depth to explain relative vertical surface movements monitored by leveling and accompanying earthquake (Bendefy, 1966; Mizoue, 1969). The results presented here may constitute a similar phenomenon, as the region studied is a zone of known seismicity. They further demonstrate the utility of precise leveling as a tool to measure crustal movements and evaluate earthquake hazard. It is recommended that the appropriate bench marks be resurveyed in five to ten years to monitor any additional movements, and after any earthquakes that occur in the vicinity.

INTRODUCTION

The purpose of this study is to examine the possibility that apparent deformation of the surface, as measured by repeated precise leveling surveys, can indicate vertical displacements across a fault situated at some depth below the surface. If such a fault is not mappable at the surface, and insufficient drill holes exist to allow subsurface mapping, leveling measurements could conceivably be the most direct evidence for such fault movement.

Specifically, such faults may exist in the Mississippi Embayment at the New Madrid seismic zone. The area studied here is near Wickliffe and Paducah, Kentucky, and the leveling data suggest dip-slip displacement along an unmapped, concealed fault when supplemented with other geological and geophysical information.

In a recent paper by Brown and Oliver (1976), regional structural features of the eastern United States are compared with relative vertical crustal velocities (time-averaged) as determined from multiple first-order leveling surveys. They find a significant correlation between

the velocity patterns and large scale (hundreds of kilometers) geological structure. The same data they have used is here examined on a more local scale, with interest in shorter wavelength behavior.

Regional Structure and Geology

The dominant structural feature in this region (see Figure 1) is the Mississippi Embayment, which began to form in Late Cretaceous when the Pascola Arch (then connecting the Ozark and Nashville domes) was downwarped. The cause of this subsidence is not well understood, but it has been viewed as an isostatic adjustment subsequent to Precambrian rifting, which extended into the continent as the so-called failed arm of a triple-junction (Burke and Dewey, 1973; McGinnis and Ervin, 1975). Depression continued as a linear trough until late Eocene, accumulating about 3000 feet of sediment in the central portion of the embayment. A cover of alluvial deposits is Late Tertiary in age, and is locally overlain by Pleistocene loess.

Nearly all of the observed surface faults lie in the Paleozoic rocks surrounding the Cretaceous and younger fill of the Mississippi Embayment. The major displacements on these Paleozoic faults probably occurred in Pennsylvanian and Mississippian time (King, 1969). Far fewer faults are mapped within the Cretaceous and younger rocks of the embayment, yet the major pattern of historical seismicity is a northeast linear trend approximately coincident with the embayment axis (Figure 2a). This may be largely due to a masking effect of the unconsolidated alluvial cover, and Fisk (1944) inferred an orthogonal fault pattern within the embayment from a detailed study of lineations. More recently, Stearns (1975, manuscript in preparation) has made a similar study, and his inferred faults based on well data and lineations show some correlation to seismic focal plane solutions. York (1976, in press) has collected

from the literature and sought in the field the few known examples of Cretaceous and Cenozoic faults (considering only those for which there is direct evidence) for this region, and suggests that pre-Cretaceous faults are being reactivated with some consequent faulting in the younger embayment sediments.

Local Structure

The locality of this study is the northern tip of the Mississippi Embayment, where southern Illinois meets western Kentucky. Here the dense Paleozoic faulting of the western Kentucky faulted area disappears at the northeastern edge of the embayment. The western Kentucky faulted area has been mapped in detail and shown to be a northeast trending horst and graben fault complex with vertical displacements commonly 500-1500 ft, associated with a northwest-southeast lateral extension of approximately 1 mile (Hook, 1974). Normal faulting (with dips averaging 70^{o}-75^{o}) is predominant, although minor strike-slip motion is evident. This fault zone is apparently now quiescent, as almost no seismic activity is situated there.

Considerable evidence, however, suggests the continuation of basement faulting beneath and/or into the embayment. In southernmost Illinois, subsurface mapping has revealed a complex of buried grabens and faults just within the northern boundary of the embayment. At least a part of these displacements occurred after the formation of the sub-Cretaceous erosional surface, with episodic activity dating Late Cretaceous, post-Eocene, Pliocene, and Pleistocene (Ross, 1963a, b).

Seismotectonics

The pattern of historical seismicity since 1928, mostly instrumentally determined, is shown in Figure 2 (Hadley and Devine, 1974). The major

characteristics are the moderately well-defined northeast trend within the embayment and a more diffuse pattern outside it. The existence of smaller scale northeast trending lineaments in the seismic pattern has recently been confirmed by results from a microearthquake study (Stauder, 1975). The inset rectangle seen in Figures 1 and 2 indicates the locality for which leveling data will be presented, and Figure 3 shows this locality at large scale. The center of Figure 3 is approximately 75 km northeast of New Madrid, Missouri, the site of the very large earthquakes of 1811-12.

Figure 3 shows the seismicity near the leveling route for two different time intervals. Solid circles represent events between 1947.5 and 1968.7 (listed in Table 1), the times of first-order leveling surveys. Open circles represent events for all other time since 1928 (listed in Table 2). If all historical seismicity were shown in Figure 3, the greatest activity would appear at Cairo, Illinois. Since 1855, 29 events have been located at Cairo, including one damaging event (intensity VI-VIII) in 1883. The sharp clustering at Cairo, however, may reflect to some extent population bias, in absence of instrumental locations before 1928.

The published depths of hypocenters for earthquakes of the New Madrid seismic zone range from 5 to 38 km. Only five published depth determinations exist for the area shown in Figure 3, as noted in Table 2. The precision of these depths is limited by inadequate station distribution, but better depth information should be forthcoming from the recently installed microearthquake network.

Although all three types of mechanisms are evident in Figure 3, three important points should be noted:

(1) Six of the eight nodal planes of the four mechanisms in

Figure 3 strike north-northeast between 356° and 031°, a span of 35°.

(2) A large majority of nearby focal mechanisms (within about 1° of Figure 3) are thrust mechanisms, as noted by Street et al. (1974).

(3) If the strike-slip event in southern Illinois can be associated with movement along the trend of the New Madrid fault zone, the sense of diaplacement is consistent with east-west compression.

If pre-Cretaceous faults are being reactivated, it is interesting to note that reactivation is apparently largely ESE-WNW compression, in contrast to the Paleozoic southeast-northwest extension seen in the adjacent western Kentucky faulted area.

Leveling Data

The bold line in Figure 3 is a path twice surveyed by first order leveling, once in 1947 and again in 1968. By arbitrarily choosing one bench mark as a fixed reference point (in this case the bench mark at Wickliffe, Kentucky), one can measure the change in elevation of all other bench marks relative to the reference. The relative displacements describe the deformation of the surface, to the extent that the bench marks are stable, i.e. do not move with respect to the surface. If these displacements are divided by the time interval, an average relative velocity of the surface at discrete points is obtained. (The main purpose of this division operation would often be to normalize profiles with different time intervals -- a problem which does not concern us here.)

Topography along the route is shown by the curve labelled "elevation". The "error" curve shows the accumulation of random error relative to the reference bench mark, and grows as the square root of the distance multiplied by a precision factor (Bomford, 1962; Brown and Oliver, 1976). With regard to random error, th local slope of the velocity profile may

be significant if it exceeds the local slope of the error curve. Both surveys were first-order, and therefore double-run, with differences between forward and backward measurements not allowed to exceed $4L^{\frac{1}{2}}$ mm, where L is the distance surveyed in kilometers. In practice, this difference is usually closer to $2L^{\frac{1}{2}}$ mm.

Figure 4 shows the relative vertical velocity profile along the bold line path in Figure 3. A striking anomaly in the velocity gradient (or equivalently, the displacement gradient) is apparent between bench marks A and B, which represents a tilt rate of

$$\frac{1.5 \text{ mm/yr}}{9.0 \text{ km}} = 1.6 \times 10^{-7} \text{ rad/yr}$$

It should be noted that this is a minimal tilt rate, since there is a hiatus of 5 km from B to the first bench mark towards A. A reasonable upper limit to the tilt is obtained by using bench mark A and the first bench mark towards B, given by

$$\frac{.76 \text{ mm/yr}}{2.3 \text{ km}} = 3.3 \times 10^{-7} \text{ rad/yr}$$

which suggests that the tilt rate is in the range of $1.0\text{-}4.0 \times 10^{-7}$ rad/yr.

Figure 5 (from Brown and Oliver, 1976) shows the regional velocity profile from Wickliffe, Kentucky to New Bern, North Carolina, with the data of Figure 4 visible in the first 60 kilometers. In Figure 5, the steep tilt of segment AB can be seen superimposed on an opposite regional tilt of 1.0×10^{-8} rad/yr. The tilt rate of segment AB is about an order of magnitude larger than most regional tilts in the eastern United States, and is definitely larger than random error could account for. In general, larger tilts are seen only in areas of intense fluid withdrawal such as near Galveston, Texas. Although there are some

apparently similar irregularities along other parts of Figure 5, most have lesser tilt rates than segment AB. More importantly, the slope discontinuity AB is more distinct and isolated, and lies admid noticeably less bench mark scatter than much of the long profile in Figure 5.

DISCUSSION AND INTERPRETATION

The location of segment AB lies between and along the trends of the Big Creek fault zone (as defined by Fisk in 1944) and the western Kentucky faulted area (Hook, 1974), as shown in Figure 1. It seems possible and not unreasonable, in light of the evidence previously presented, that the movement indicated by Figure 4 is fault related. Before immediately invoking a fault, however, possible errors and various alternative explanation of the leveling data should be considered.

Neglecting blunders (which the double-run procedure renders highly improbable), leveling errors may be classified as random or systematic. Random error has already been examined ans shown to be of insufficnet magnitude to explain the apparent movements.

The known sources of systematic error include:

(1) rod miscalibration or other instrumental misalignment

(2) refraction of the line-of-sight due to temperature gradients (typically 5 mm/100 m rise)

(3) tidal forces (important only on north-south lines)

(4) gravity anomalies due to mass redistribution (which may distort the equipotential reference)

(5) atmospheric pressure changes

Except for gravity anomalies, these kinds of systematic error are most important for long wavelength features, and less so for the short wavelength phenomenon reported here. The reader is referred to Brown

and Oliver (1976) for a more detailed discussion of leveling errors, which concludes that observed regional tilts (generally of magnitude 10^{-8} rad/yr) cannot be completely accounted for by known systematic errors.

If, as the author believes, the tilting of segment AB is not entirely due to systematic error, there remain many non-tectonic geologic explanations. Fluid withdrawal with consequent sediment compaction is a known cause of vertical movement (subsidence). However, there are no oil or gas wells in this part of Kentucky, nor are there any large municipalities that consume sufficient amounts of water to depress the water table. In fact, the State of Kentucky regards the largely untapped ground water of this area as a natural resource for stimulating economic development. Although karstlands occur in west-central Kentucky, the region studied here is not karstland (National Atlas of the United States, 1970).

Local bench mark instability due to frost heaving, soil/sediment compaction, mineral dissolution, or slumping can show large movements, but the resulting movements are too localized and irregular to explain the pattern here extending over several kilometers. Such local perturbations could be expected to contribute to scatter over wavelengths like the bench mark spacing, but would be unlikely to account for the systematic variation observed. Furthermore, there is little correlation between relative movements and type of monumentation along this line. Table 3 lists bench mark monumentation, with bench marks divided about equally into two major categories, bench mark post and concrete construction (a distinction defined in Table 3). If these two groups of bench marks are viewed independently, the curves of Figure 4b are obtained. If each curve in Figure 4b were smoothed to suppress apparent noise of wavelength $\leq$ 5 km, the resulting smoothed curves would

coincide quite closely. This implies that the tendency for a bench mark to rise or sink unstably is the same for both types of monumentation. In general, one would expect different responses to instability processes from different types of monumentation. It is therefore suggested that both types of bench marks are approximately stable in an absolute sense.

Crustal loading (e.g. reservoirs) has been shown to cause appreciable downwarps, but the author discovered no such large artificial loads near segment AB. McGinnis (1963) found evidence that water loading due to fluctuation of the water level of the Mississippi River is correlated with seismicity, and may act as a trigger for earthquakes. He subsequently reasoned that the crust must be regionally subsiding, which is logically unclear.

Whether or not river level is related to crustal movements, the evidence supports the hypothesis that the anomalous tilt in Figure 4 is in fact due to fault movement. The four open circles in Figure 3 from 88.9° to 89.0°W are a series of four events that occurred in 1930-31 and may have been associated with the same fault zone postulated on the basis of the leveling data. The sense of surface deformation (downward to the west) would be consistent with a westward dipping normal fault or an eastward dipping thrust fault, assuming the motion is predominantly dip-slip (a reasonable assumption on the basis of regional focal plane solutions, very few of which are strike-slip). The closest focal mechanism is a thrust type (about 10 km southwest), which occurred four years after the second leveling survey. A mechanism farther to the south (about 20 km away) and within the time interval between surveys is a normal type, which makes it difficult to associate the inferred fault with one or the other type.

Various ways to reconcile the existence of both kinds of mechanisms

so near each other are illustrated by Figure 6. In all these cases, a regional compressional stress system in the basement is postulated. This compressive stress results in tensional stresses in a less competent, less consolidated upper strata, which are represented by the Cretaceous coastal plain sediments that overly Paleozoic basement. Any of these models could explain the rather singular normal fault mechanism in the midst of mostly reverse ones, and it would be reasonable to ascribe the measured movements to the normal event since it occurred within the specified time interval. However, the movement need not be associated directly with earthquakes at all, since it could alternatively be aseismic creep.

After the suspicion of a hidden fault in this region, a search for lineations was undertaken. Although aerial photography (scale 1:13,000) gave no definite indication of lineaments near the segment AB, the local stream pattern (Figure 7, taken from U.S.G.S. topographic quadrangle maps) does exhibit a noticeable lineation pattern trending approximately 11°–14° north-northeast. This trend closely parallels the trends of the nodal planes of the normal event, the trend of the structural trough formed by the top of the Paleozoic, and the trend of the Mississippi River as it bounds western Kentucky. While the presumed faulting probably does not break the surface here, it may have influenced the drainage pattern.

Previous Fault-Movement Interpretations Based on Precise Leveling

One of the first (and few) studies of deformation of the earth's surface as measured by precise leveling in connection with earthquakes was that of Bendefy (1966) in Hungary. The leveling surveys were done in 1955-56, before and after the 12 January 1956 earthquake at Dunahavaszti, near Budapest, Hungary. Although I.S.C. lists no magnitude or depth for

this event, it was reported by over 90 stations as far as 144° away, and the village of Dunaharaszti was completely destroyed. Thus a magnitude of 6.0 or greater is likely.

Bendefy reported dynamic undulations of the crust within 100 km of the epicenter, clearly associated with the stress accumulation and release of the earthquake. Permanent relative displacement was a maximum of 40 mm near the epicenter (Dunaharaszti) and was observed between bench marks separated by 1.5 km, although no surface faults or fractures were reported. The relative velocity profile (in units of 10^{-3} mm/day) for a time interval containing the earthquake is shown in Figure 8a as the curve labelled G_2. The steepest gradients occur directly over the epicenter, and indicate an uplift of the region west of the epicenter with respect to the east, suggesting a fault at some depth with a component of dip-slip motion.

In an attempt to determine the degree of dip-slip motion associated with this 1956 earthquake, a preliminary focal mechanism was constructed by the author from 16 first motion data presented in I.S.S. (January, 1956). These data (plotted in Figure 9) are consistent with a thrust mechanism with some strike-slip component, although some of the data is not internally consistent and the mechanism is not strongly constrained. However, the better defined nodal plane dips northwest and trends northeast and, as the fault plane, would be consistent with the sense of displacement (uplift to the west) seen in the east-west leveling line crossing the epicenter. From an examination of other leveling lines as well, Bendefy postulated a regional northwest-southeast compressional strain pattern.

The Japanese have studied surface deformations associated with several earthquakes by repeated precise leveling surveys (Mizoue, 1969). Perhaps the best example of apparent fault movement reflected in surface

leveling measurements was noted after the 19 October 1955 Futatsui earthquake (M = 5.7). An antisymmetric relative displacement pattern (Figure 8b) shows a maximum offset of 140 mm between adjacent bench marks approximately 2 km apart. Mizoue suggested the existence of a "hidden seismic fault" at a depth of a few kilometers in absence of surface faulting.

More confidence can be placed in these fault-at-depth interpretations by examining leveling displacement patterns near recently active fault breaks. Such a case exists in the study of Savage and Church (1974), who looked at first order surveys of 1955 and 1967 which passed over numerous fault scarps (Slemmons, 1957) mapped after a sequence of earthquakes (magnitudes 6.6-7.1) in 1954. They found a clear correlation between several distinct waveforms (amplitudes of 10^1-10^2 mm) in the relative displacement profile and the fault scarps, and therefore concluded that post-earthquake slip was occurring along normal faults to a depth of several kilometers.

Leveling Data and Regional Vertical Crustal Movements

Figure 10 shows a free air gravity profile from northern to southern Illinois, with a large positive gradient as southern Illinois reaches the Mississippi Embayment (from McGinnis, 1974). McGinnis (1970, 1974) considers the high positive anomalies near southernmost Illinois to be a reflection of rift-intrusive igneous bodies which are uncompensated and thus causing isostatic subsidence. If the intrusive activity stopped in the Cretaceous (the youngest dated igneous rocks), the crust should have been mechanically compensated by now, with only small thermal/erosional effects remaining. From a study of the geology of the area, Stearns and Wilson (1972) state: "since Eocene time the region (Mississippi Embayment)

appears to have been relatively stable but perhaps subjected to regional uplift." There were probably adjustments following the deposition of extensive Plio-Pleistocene gravels also.

The lack of compensation seen in the free air anomaly, however, may not be due solely to mass-excessive intrusives. If regional uplift is occurring as the leveling data imply, the anomaly may be a reflection of non-isostatic movements. The evidence for relative uplift is seen in two leveling profiles previously examined by Brown and Oliver (1976). Figure 5 shows the eastward tilting of western Kentucky, at the rate of 1.0×10^{-8} rad/yr from 0-100 km on the abscissa, and decreasing to 1.0×10^{-9} rad/yr from 100-300 km. Figure 11 shows a northward tilting of 1.1×10^{-8} rad/yr which appears to begin approximately where the large positive gravity gradient of Figure 10 becomes prominent. Taken together, these two lines suggest a possible doming centered near the border of Illinois and Kentucky. That uplift should be occurring there subsequent to Eocene subsidence is not completely unreasonable, as the geologic record shows that northwestern Louisiana was domically uplifted to form the Sabine Uplift in Miocene time, which had been part of a basin through the Jurassic (King, 1969). Other similar uplifts are known in Louisiana.

If the crust near the head of the embayment were being uplifted, it would provide a qualitative explanation for the regional compressional stress pattern apparent there. The Paleozoic basement structure there is a regional downwarp, and if a downwarp is uplifted near its center, the crust would be subjected to crustal shortening.

CONCLUSION

Evidence presented here suggests that precise leveling can indicate subsurface fault movement not apparent from other observations. In particular, a leveling profile of relative movement in western Kentucky resembles previous leveling measurements which have been interpreted as subsurface faulting. Furthermore, a fault interpretation is consistent with other geophysical and geological evidence, and seems more plausible than other alternative explanations. Additional leveling in this region would certainly seem warranted after an appropriate time interval has elapsed, or after any earthquakes occur.

In view of the above, precise leveling should be considered a valuable tool (especially in the long term) in site decision for large construction projects whose vulnerability to damage by earth movements must be minimized.

Although inconclusive, leveling data is not consistent with regional subsidence of the northern tip of the Mississippi Embayment, as has been previously suggested. Whether or not subsidence is occurring (with some unknown long-range systematic error in the leveling) or the area is indeed uplifting should be a subject for further study.

References

Bendefy, L., Elastic, plastic, and permanent deformations of the earth's crust in connection with earthquakes, Proc. 2nd Intern. Symp. on Recent Crustal Movements, Helsinki, 57-65, 1966.

Bomford, G., Geodesy, Clarendon Press, Oxford, 1962.

Brown, L.D., and J.E. Oliver, Vertical crustal movements from leveling data and their relation to geologic structure in the eastern United States, submitted to Reviews of Geophysics and Space Physics, 1976.

Burke, K., and J.F. Dewey, Plume-generated triple juctions: key indicators in applying plate tectonics to old rocks, J. Geol., 81, 406-433, 1973.

Docekal, J., Earthquakes of the stable interior, with emphasis on the mid-continent, Ph.D. dissertation, Univ. of Nebraska, 1970.

Ervin, C.P., and McGinnis, L.D., Reelfoot Rift: reactivated precursor to the Mississippi Embayment, Bull. Geol. Soc. Amer., 86, 1287-1295, 1975.

Fisk, H.N., Geological investigation of the alluvial valley of the lower Mississippi River, U.S. Army Corps of Engineers, Mississippi River Commission, Vicksburg, Mississippi, 1944.

Gerlach, A.C., ed., The National Atlas of the United States of America, U.S. Department of Interior, Geological Survey, p. 77, 1970.

Hadly, J.B., and J.F. Devine, Seismotectonic Map of the Eastern United States, U.S. Geol. Surv., 1974.

Heyl, A.V., and others, Regional structure of the southeast Missouri and Illinois-Kentucky mineral districts, U.S. Geol. Surv. Bull. 1202-B, 1965.

Hook, J.W., Structure of the fault systems in the Illinois-Kentucky fluorspar district, Kentucky Geol. Surv. Spec. Publ. 22, Series X, 1974.

International Seismological Summary, January 1956, p. 32.

King, P.B., The Tectonics of Middle North America: Middle North America East of the Cordilleran System, Hafner Publishing Co., New York, 203 pp., 1969.

Lammlein, D.R., Spar, M.L., and J. Dorman, A microearthquake reconnaissance of southeastern Missouri and western Tennessee, Bull. Seism. Soc. Amer., 61, 1705-1716, 1971.

McGinnis, L.D., Earthquakes and crustal movement as related to water load in the Mississippi Valley region, Illinois Geol. Surv. Circ. 344, 1963.

McGinnis, L.D., Tectonics and the gravity field in the continental interior, J. Geophys. Res., 75, 317-331, 1970.

McGinnis, L.D., and C.P. Ervin, Earthquakes and block tectonics in the Illinois basin, Geology, 2, 517-519,

Mizoue, M., Types of crustal movements accompanied with earthquakes in inner northeastern Japan, Problems of Recent Crustal Movements: Third Intern. Symp., 357-370, 1968.

Nuttli, O.W., Magnitude recurrence relation for central Mississippi Valley earthquakes, Bull. Seism. Soc. Amer., 64, 1189-1207, 1974.

Ross, C.A., Structural framework of southernmost Illinois, Illinois Geol. Surv. Circ. 351, 1963a.

Ross, C.A., Faulting in southernmost Illinois, Geol. Soc. Amer. Spec. Publ. 73, 229, 1963b.

Ross, C.A., Geology of the Paducah and Smithland quadrangles in Illinois, Illinois Geol. Surv. Circ. 360, 1964.

Savage, J.C., and J.P. Church, Evidence for post-earthquake slip in the Fairview Peak, Dixie Valley, and Rainbow Mountain fault areas of Nevada, Bull. Seism. Soc. Amer., 64, 687-698, 1974.

Slemmons, D.B., Geological effects of the Dixie Valley-Fairview Peak, Nevada, earthquakes of December 16, 1954, Bull. Seism. Soc. Amer., 47, 353-375, 1957.

Stauder, W., and others, Relation of microearthquakes in southeastern Missouri to structural features, Trans. Amer. Geophys. Union, 56, no. 6, 398, 1975.

Stearns, R.G., and C.W. Wilson, Jr., Relationships of earthquakes and geology in west Tennessee and adjacent areas, Report for TVA, Nashville, Tenn., Vanderbilt Univ., 344 pp., 1972.

Stearns, R.G., and A. Zurawski, Post-Cretaceous faulting in the head of the Mississippi Embayment, manuscript in preparation, 1975.

Street, R.L., R.B. Hermann, and O.W. Nuttli, Earthquake mechanics in the central United States, Science, 184, 1285-1287, 1974.

U.S. Dept. of Commerce Coast and Geodetic Survey, Bench Mark Descriptions, Wickliffe to Paducah, Kentucky, 1972.

York, J.E., and J.E. Oliver, Cretaceous and Cenozoic faulting in eastern North America, submitted to Bull. Geol. Soc. Amer., 1976.

Table I

Earthquakes near Cairo, Illinois from 1947 to 1968.7

Date (yr.mo.day)	Lat (N)	Lon. (W)	Depth (km)	Intensity	Magnitude	Ref used
1947.1.16	36°59'	89°11'	---	II-III	(3.2)*	a,b
1953.5.06	36°59'	89°11'	---	III	(3.4)	a,b
1953.5.15	36°59'	89°11'	---	III	(3.4)	a,b.
1957.3.26	37°05'	88°36'	___	IV	(3.8)	a,b
1958.1.27	37°03'	89°12'	___	VV	(4.2)	a,b
1962.2.16	37.0°	87.7°	25	III-IV	(3.6)	b,d
1963.3.31 M	36.9°	89.0°	___	___	3.0	b,c
1963.5.02	36.7°	89.4°	___	___	3.1	a,b
1963.8.02 M	37.0°	88.7°	18	V	4.0	b,c,d
1965.8.13	37°19'	89°28'	33	IV	3.2	a,b,d
1965.8.14 M	37°2°	89.3	38	VII	3.8	b,c,d
1965.8.15	37°22'	89°28'	16	V	3.5	a,b,d
1965.8.15	37°24'	89°28'	___	V	3.4	a,b

a, Docekal (1970)

b, Nuttli (1974)

c, Street et al. (1974)

d, Stearns and Wilson (1972)

*( ) indicates estimation of Nuttli (1974)

M indicates focal mechanism of Street (1974)

Table 2
Earthquakes near Cairo, Illinois from 1928-1947 and 1968.7-1972

Date (yr.mo.day)	Lat (N)	Lon (W)	Intensity	Mag.	Ref. Used
1928.4.15	37° 17'	89° 32'	IV	(3.8)	a,b
1930.8.29	37.9°	89.0°	V	---	d
1930.9.03	36° 58'	88° 54'	III	(3.4)	a,b
1930.9.03	36° 58'	88° 54'	III	(3.4)	a,b
1931.4.06	36° 51'	89° 01'	IV	(3.8)	a,b
1933.10.24	37° 17'	89° 32'	III	(3.4)	a,b
1934.8.19	36° 56'	89° 12'	VI	(4.7)	a,b
1934.8.19	36° 59'	89° 09'	II-III	(3.2)	a,b
1936.8.02	36.7	89.0	III	(4.1)	a,b
1936.12.20	37°17°	89° 32'	II	(3.0)	a,b
1939.4.15	36° 48'	89° 24'	III	(3.4)	a,b
1940.2.04	37° 13'	89° 29'	III	(3.4)	a,b
1940.5.31	37° 05'	88° 36'	V	(4.2)	a,b
1940.10.10	36.8°	89.2°	II-III	(3.2)	a,b
1941.10.21	36° 58'	89° 08'	IV	(3.8)	a,b
1941.11.22	37° 17'	89° 32'	II-III	(3.2)	a,b
1942.8.31	36° 59'	89° 11'	IV	(3.8)	a,b.
1942.11.13	36° 59'	89° 11'	IV	(3.8)	a,b
1970.12.24	36.7°	89.5°	IV	3.6	b
1972.6.18 M	37.0	89.1	III	3.2	c

Table 3

Bench Mark Tabulation

No.	Name	BM Design[1]	Monumentation[2]	Distance (km)	Relative Movement (mm)
1	Wickliffe	RMD	P	0.00	0.0
	RM No. 1				
2	Wickliffe	RMD	P	0.14	-0.4
	RM No. 2				
3	M128	D	P	2.18	-1.0
4	Z130	D	(B)	3.92	-2.7
5	Y130	D	P	5.56	-5.8
6	X130	D	P	7.01	-2.5
7	W130	D	(B)	8.49	-5.4
8	Barlow	RMD	P	9.98	-11.5
	RM No. 2				
9	Barlow ≡ "A"	TSD	P	10.01	-6.0
10	U130	D	P	12.29	9.6
11	T130	D	(C)	13.86	4.5
12	R130 ≡ "B"	D	(B)	19.08	24.9
13	Q130	D	P	21.15	27.8
14	P130	D	P	22.77	30.0
15	N130	D	(C)	24.51	30.5
16	M130	D	(C)	25.91	24.2
17	Kevil				
	RM No. 2	RMD	P	27.37	24.8
18	Kevil	TSD	P	27.66	27.0
19	Kevil	RMD	P	27.69	-17.4
	RM No. 1				
20	L130	D	(C)	29.14	27.3
21	G130	D	(B)	35.65	22.4
22	E130	D	(W)	36.21	7.1
23	F130	D	(W)	36.29	12.7
24	C130	D	(U)	38.50	20.3
25	64M	D (USGS)	P	40.44	19.2
26	B130	D	(U)	42.12	26.6
27	63M	D (USGS)	P	45.50	14.2

Table 3 (cont.)

No.	Name	BM Design[1]	Monumentation[2]	Distance (km)	Relative Movement (mm)
28	L129	D	(F)	47.83	18.4
29	N129	D	P	50.87	16.7
30	P129	D	(B)	52.10	10.9
31[3]	R129	D	(FT)	55.01	11.3
32	G18	D	P	57.45	-4.2
33	F18	D	P	58.06	11.9
34	H129	D	P	59.02	6.9
35	E18	D	P	60.10	5.3

[1] RMD = a C & GS Reference Mark Disk
D = a C & GS Bench Mark Disk
TSD = a C & GS Triangulation Station Disk
D (USGS) = a USGS Bench Mark Disk

[2] P = Concrete Bench Mark Post
B = Highway Bridge
C = Highway Calvert
W = Concrete Wall
U = Railroad Underpass
FT = Concrete Footing

( ) designates a concrete construction type of monumentation, i.e. a pre-existing construction which accomodated a bench mark without requiring new installation of a standard bench mark support (usually a concrete post).

[3] Paducah is between 31 and 32.

Figure Captions

Figure 1: Central United States portion of Hadley and Devine's tectonic map of the eastern United States (1974), with the addition of the Big Creek fault zone defined by Fisk (1944). The bold rectangle shows the locality of the leveling data analyzed, and is the area covered in Figure 3.

Figure 2a: Central United States portion of Hadley and Devine's epicenter map of the eastern United States (1974). The rectangular inset is the same as in Figure 1.

Figure 2b: Explanation for Figure 2a.

Figure 3: Seismotectonic map of the rectangular inset seen in Figures 1 and 2, showing the path of two leveling surveys (1947 and 1968.7). See text for further explanation. The basemap with faulting is adapted from Stearns and Wilson (1972).

Figure 4a: Plot of the relative vertical bench mark velocity (as described in text) versus distance from Wickliffe (WIC) to Paducah, Kentucky (PAD). Also shown are curves representing elevation and random error. Two bench marks have been labelled "A" and "B" for purposes of discussion.

Figure 4b: Same data as in Figure 4a divided according to type of bench mark monumentation. The solid line connects bench marks that are in concrete posts specially designed as stable supports for bench marks, and the dotted line connects bench marks that are in other concrete constructions, as listed and defined in Table 3.

Figure 5: Relative velocity curve from Wickliffe, Kentucky to New Bern, North Carolina (from Brown and Oliver, 1976). The small rectangle shows the fault-like offset seen in Figure 4.

Figure 6: Possible crustal models for which shallow normal faulting could accompany deeper, regional thrusting. Both 6a and 6b are schematics of gravitationally induced normal-faulting in relatively incompetent sediments over thrust-faulting in stronger basement rocks.

(6a) Differential elevation of upper strata caused by thrusting acts to induce shearing in upper incompetent sediments.

(6b) Curvature of steeply thrusting acts to produce normal bending stresses in upper strata with continued movement.

Figure 7: Stream-defined, north-northeast trending lineaments based on USGS 7½' topographic quadrangle maps. Bench marks A and B are shown by squares, and others by "x".

Figure 8: Examples from the literature of anomalously steep relative velocity (or displacement) gradients as measured by precise leveling, near earthquake epicenters (8a and 8b) and near surface faulting (8c).

(8a) 40 mm relative displacement associated with the 12 January 1956 earthquake near Dunaharaszti, Hungary (Bendefy, 1966).

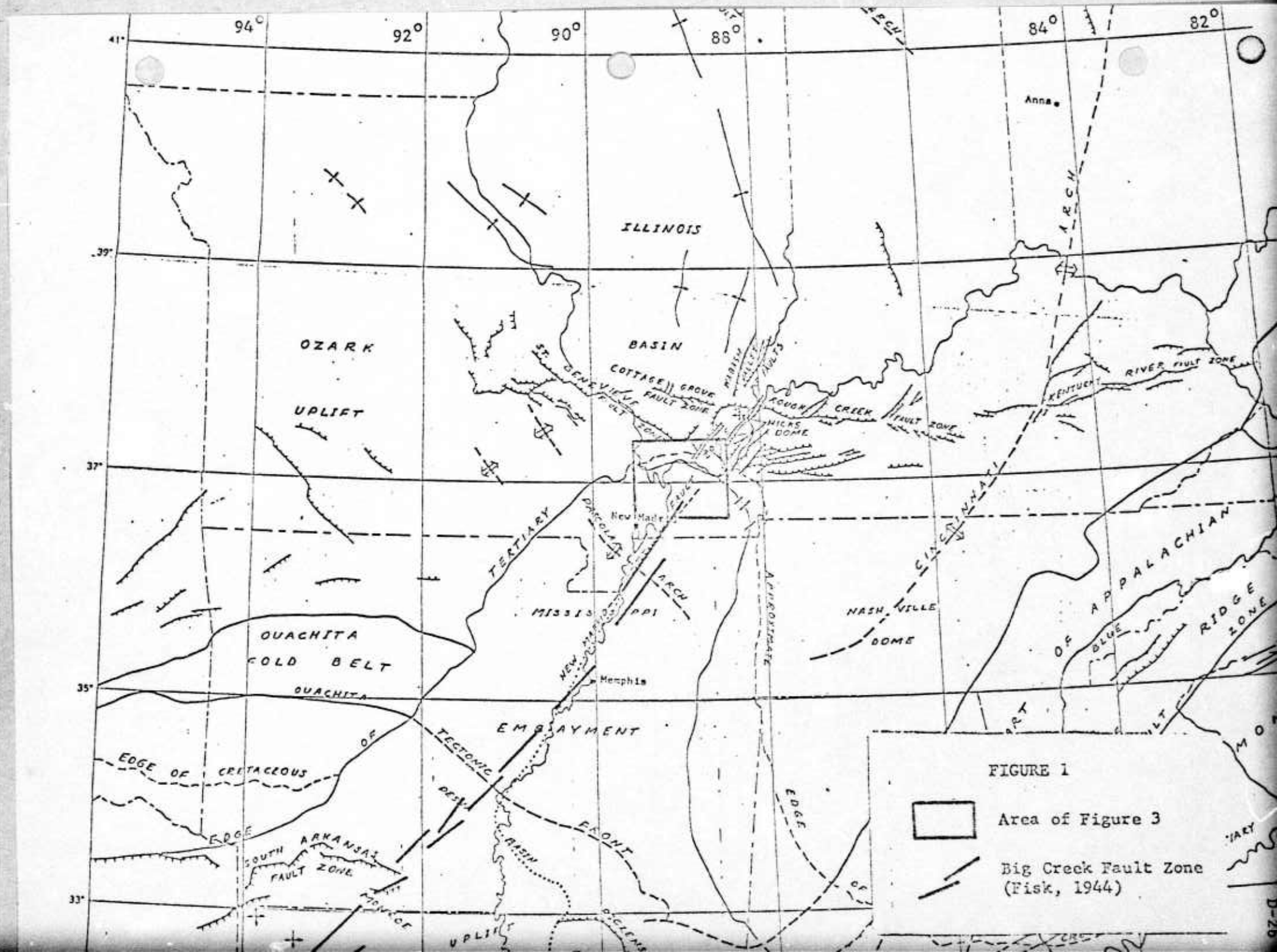
(8b) 140 mm relative displacement associated with the 19 October 1955 earthquake near Futatsui, Japan (Mizoue, 1969).

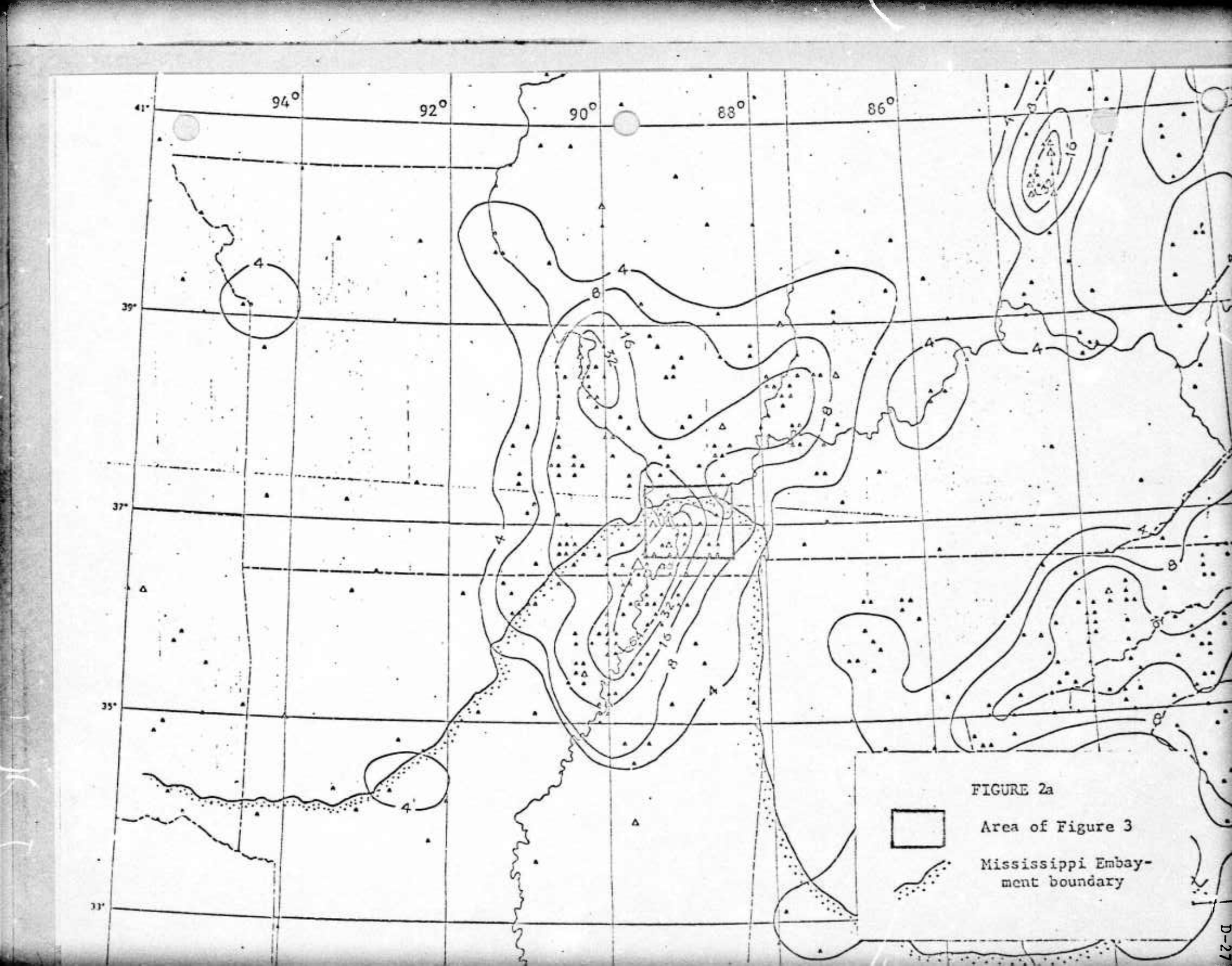
(8c) 20-70 mm relative displacement associated with surface faults in Nevada (Savage and Church, 1974).

Figure 9: Tentative focal plane solution fo the 12 January 1956 earthquake (Dunaharaszti, Hungary) from 16 first motion data given in I.S.S.

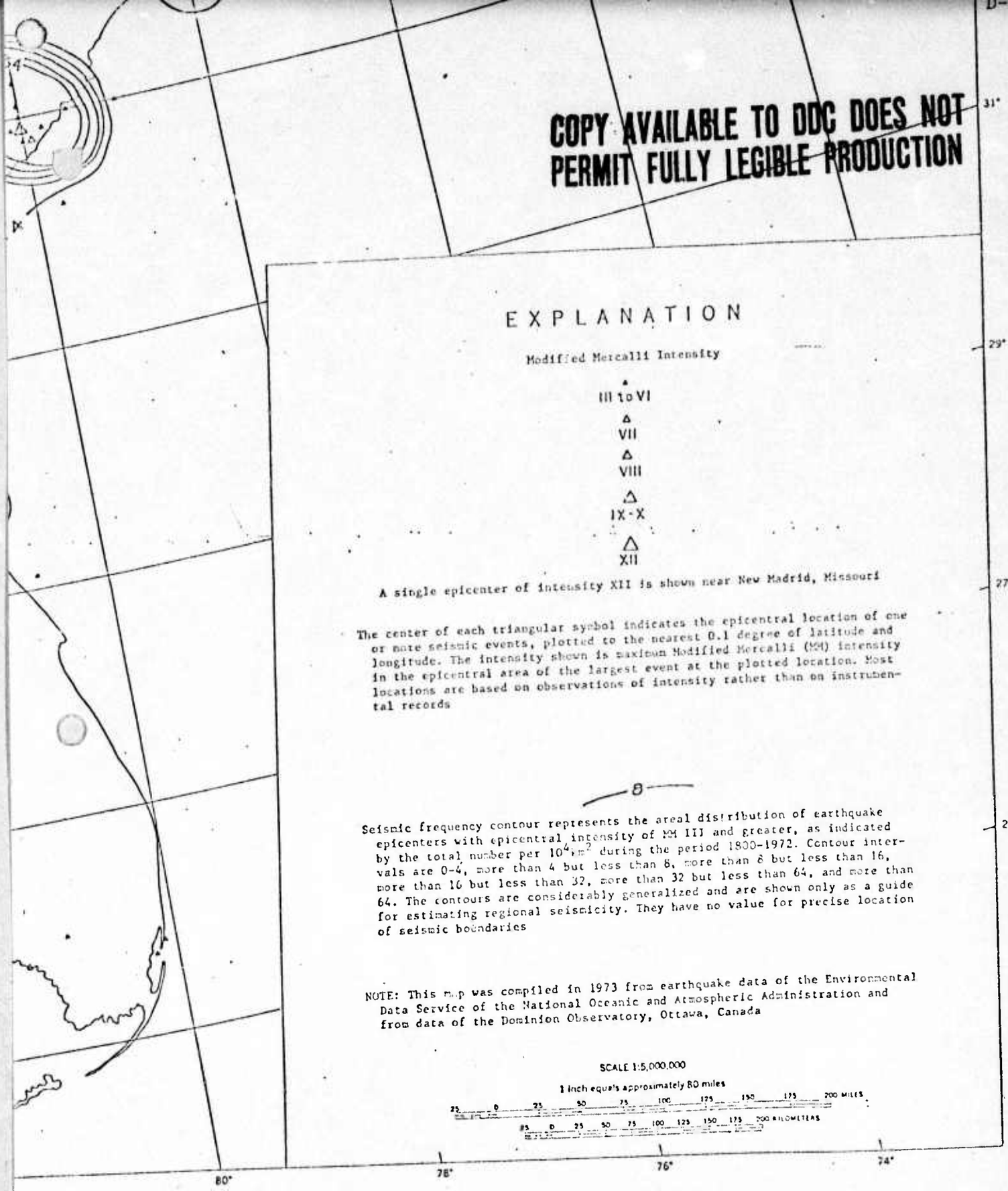
Figure 10: Mean free air anomaly along latitude 89°W. Computation technique described by McGinnis (1970). Figure from McGinnis, (1974).

Figure 11: Regional relative velocity profile determined by precise leveling, from Davis Junction, Illinois, to Cairo, Illinois, to Meridian, Mississippi (figure from Brown and Oliver, 1976). The time spans over which particular segments were leveled is given in the lower portion of the figure.


94°
92°
90°
88°
84°
82°
41°
39°
37°
35°
33°
ILLINOIS
BASIN
OZARK
UPLIFT
Anna
ARCH
COTTAGE GROVE FAULT ZONE
ST. GENEVIEVE FAULT ZONE
WICKS DOME
KENTUCKY RIVER FAULT ZONE
TERTIARY
EMBAYMENT
MISSISSIPPI
ARCH
New Madrid
Memphis
NASHVILLE DOME
OUACHITA
FOLD BELT
EDGE OF CRETACEOUS
SOUTH ARKANSAS FAULT ZONE
TECTONIC
FRONT
EDGE
OF
APPALACHIAN
BLUE RIDGE
FIGURE 1
Area of Figure 3
Big Creek Fault Zone
(Fisk, 1944)


94°
92°
90°
88°
86°
41°
39°
37°
35°
33°
4
8
16
32
64
FIGURE 2a
Area of Figure 3
Mississippi Embay-
ment boundary

COPY AVAILABLE TO DDC DOES NOT PERMIT FULLY LEGIBLE PRODUCTION



72

NITED STATES

FIGURE 2b

Copy available to DDC does not permit fully legible reproduction

For sale by U.S. Geological Survey, price $1.50 per set

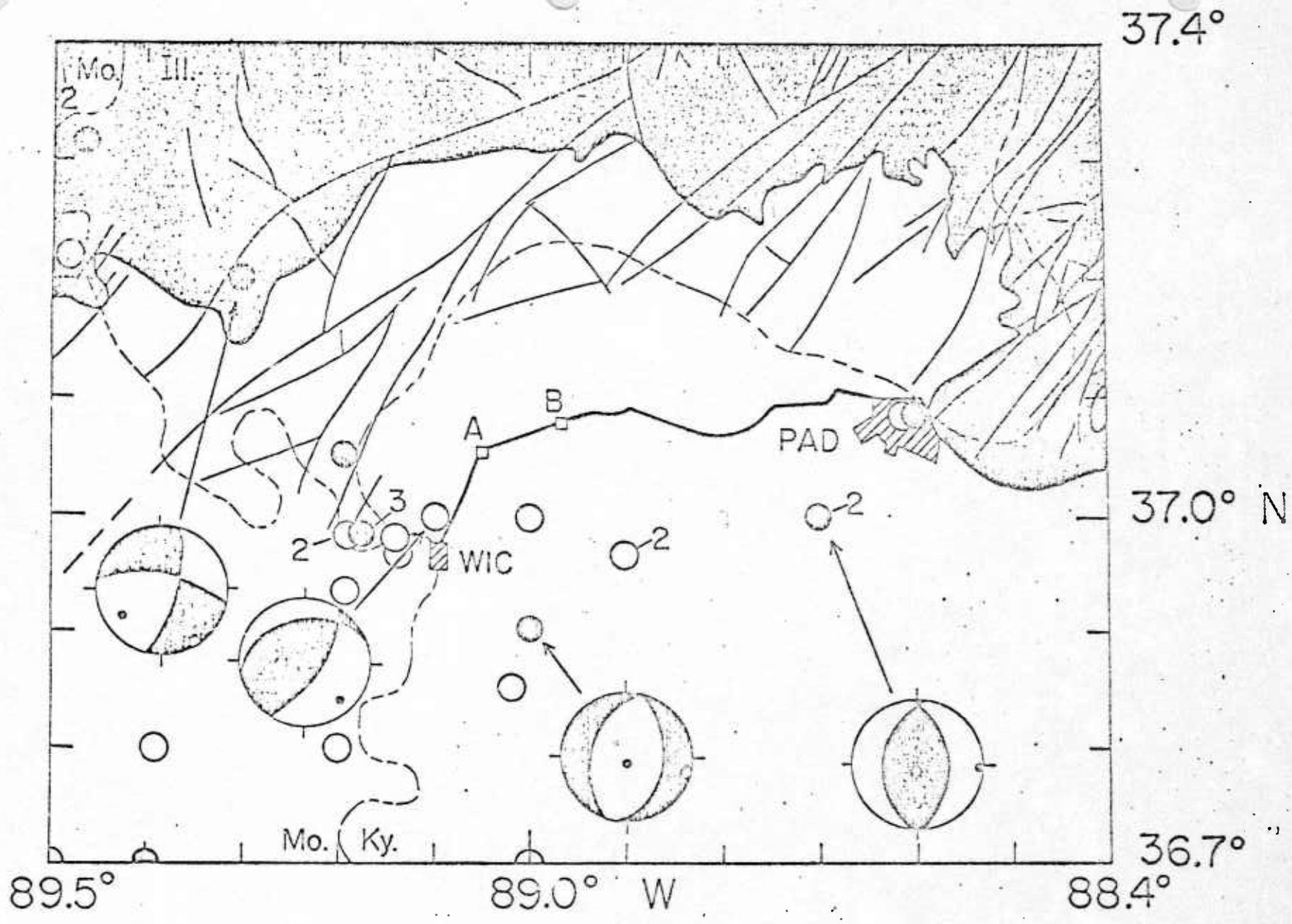


FIGURE 3

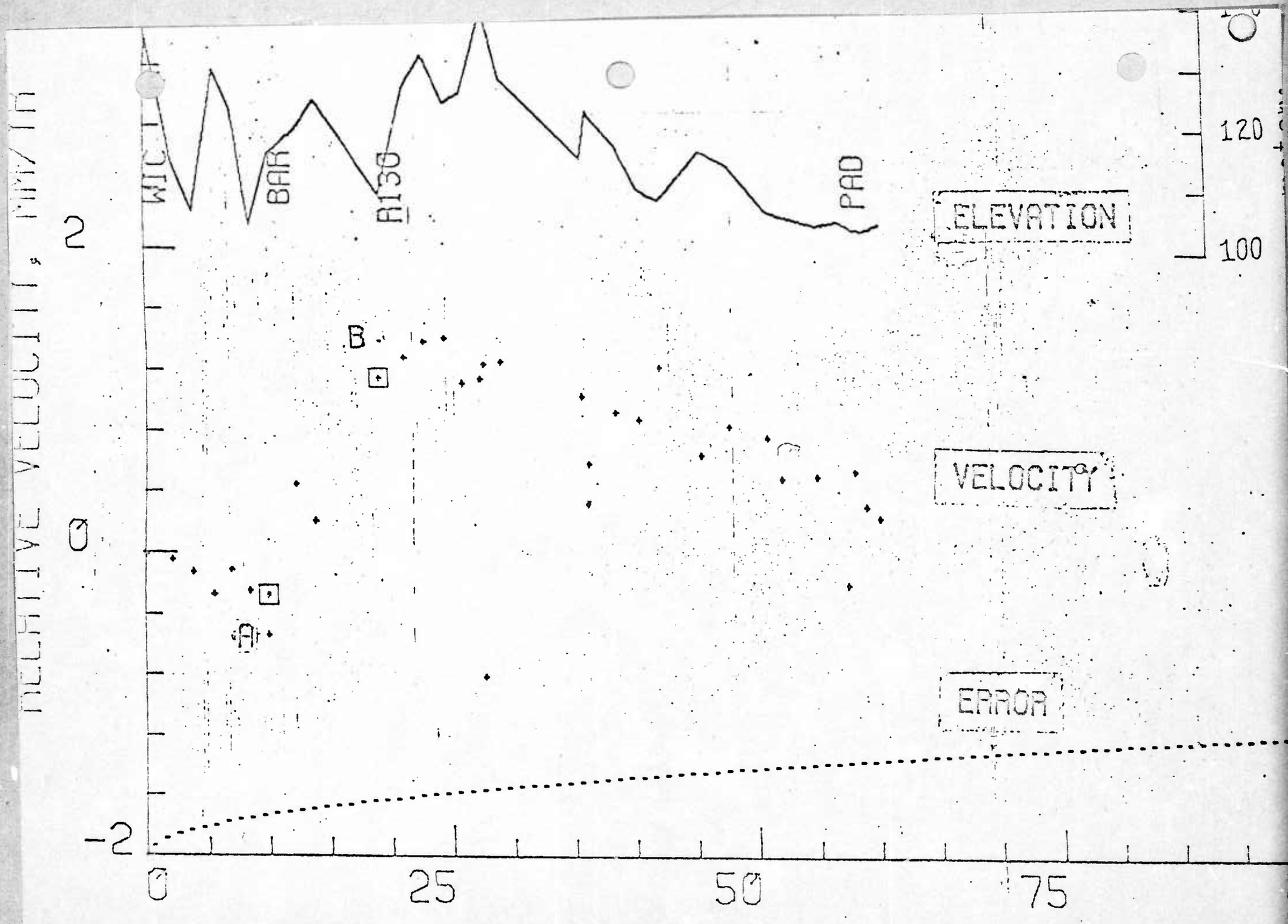

WIC
BAR
R130
PAD
ELEVATION
120
100
VELOCITY
ERROR
A
B
2
0
-2
0
25
50
75
RELATIVE VELOCITY, KM/HR
DISTANCE, KM

FIGURE 4a

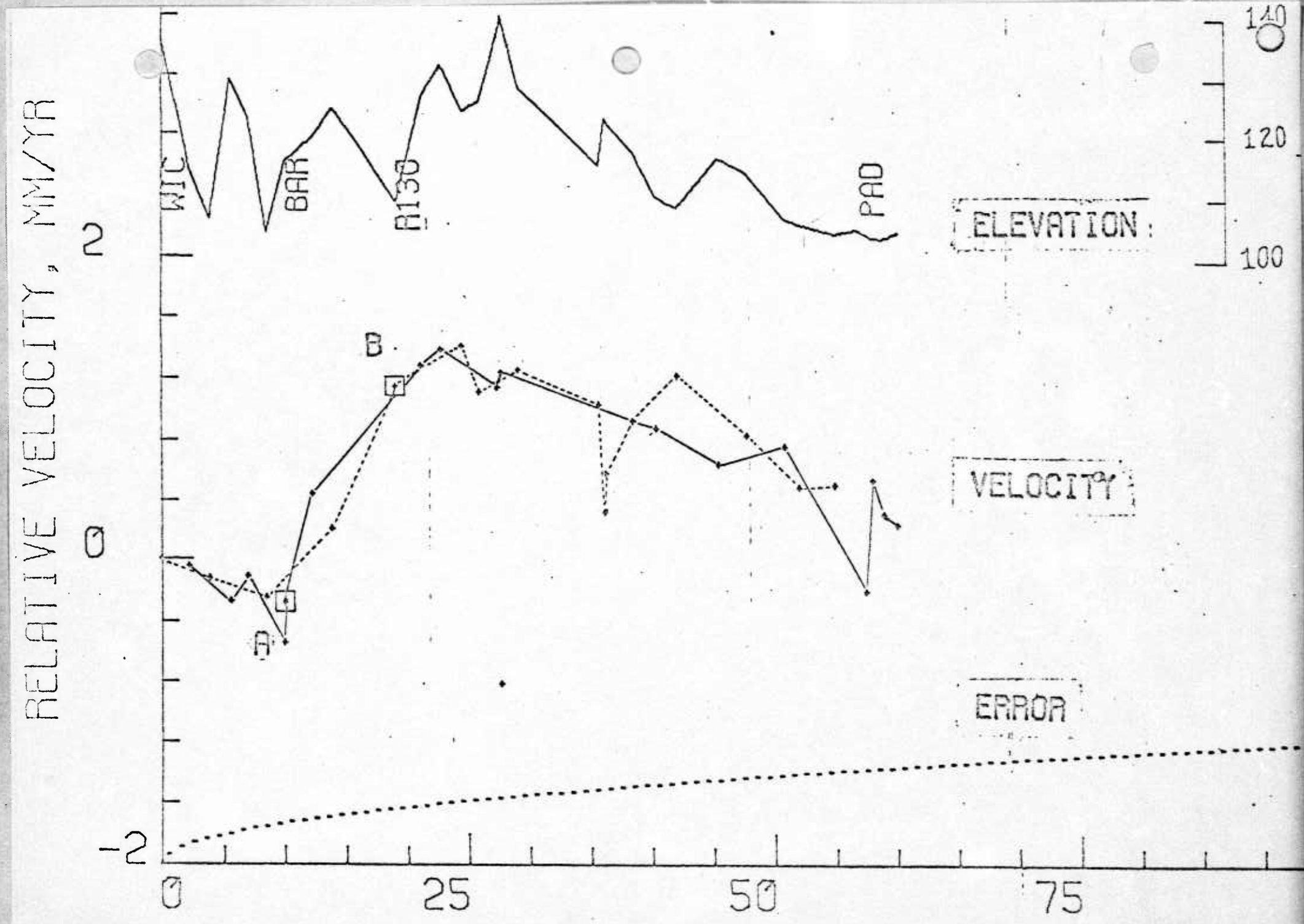

RELATIVE VELOCITY, MM/YR
2
0
-2
WIC
BAR
R130
PAD
ELEVATION
140
120
100
B
A
VELOCITY
ERROR
0
25
50
75
DISTANCE, KM

FIGURE 4b

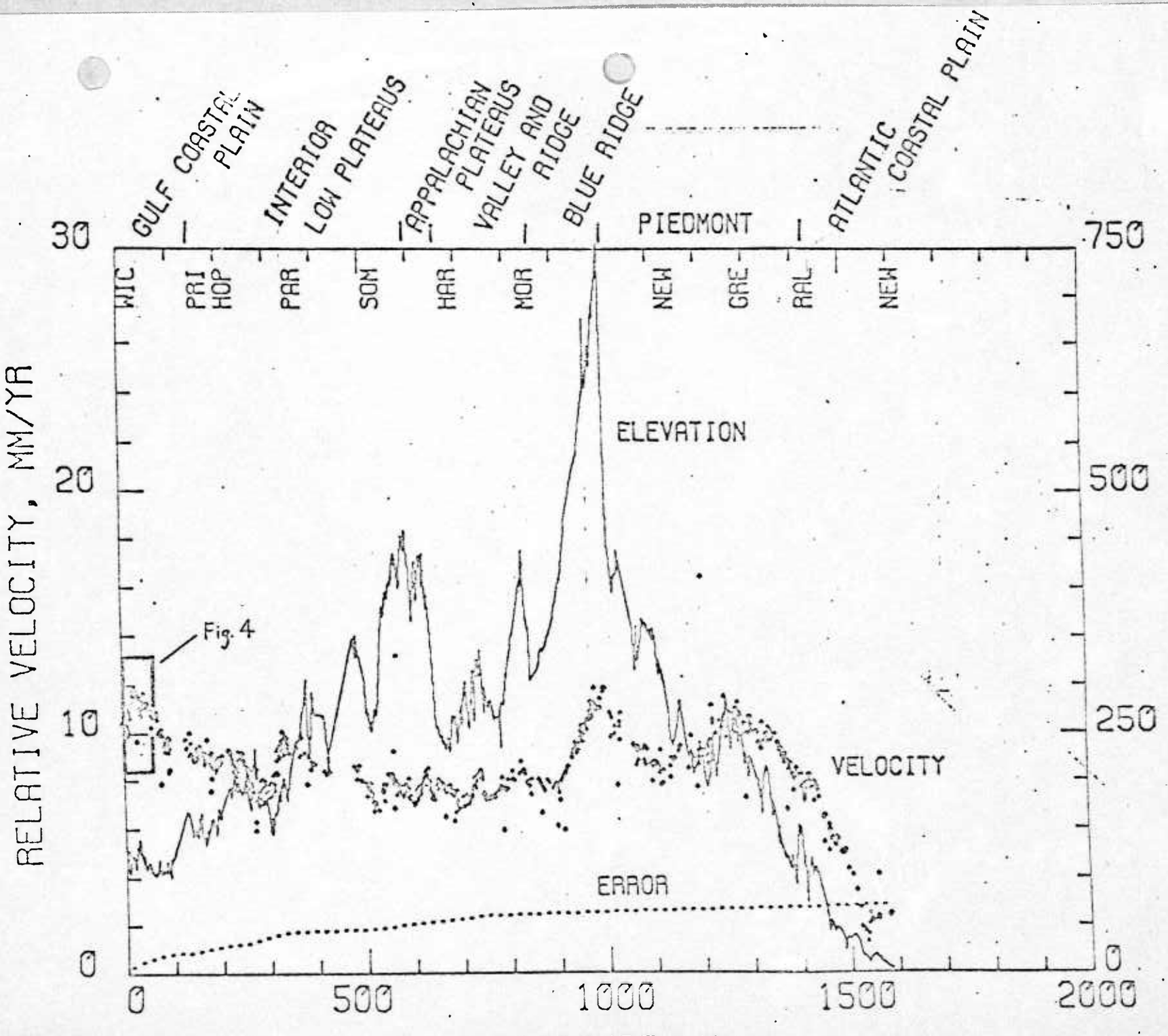
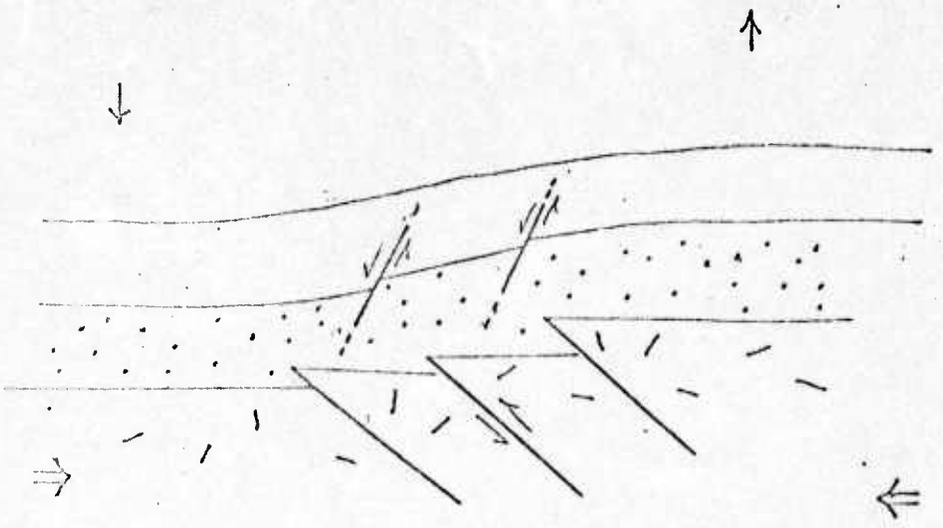
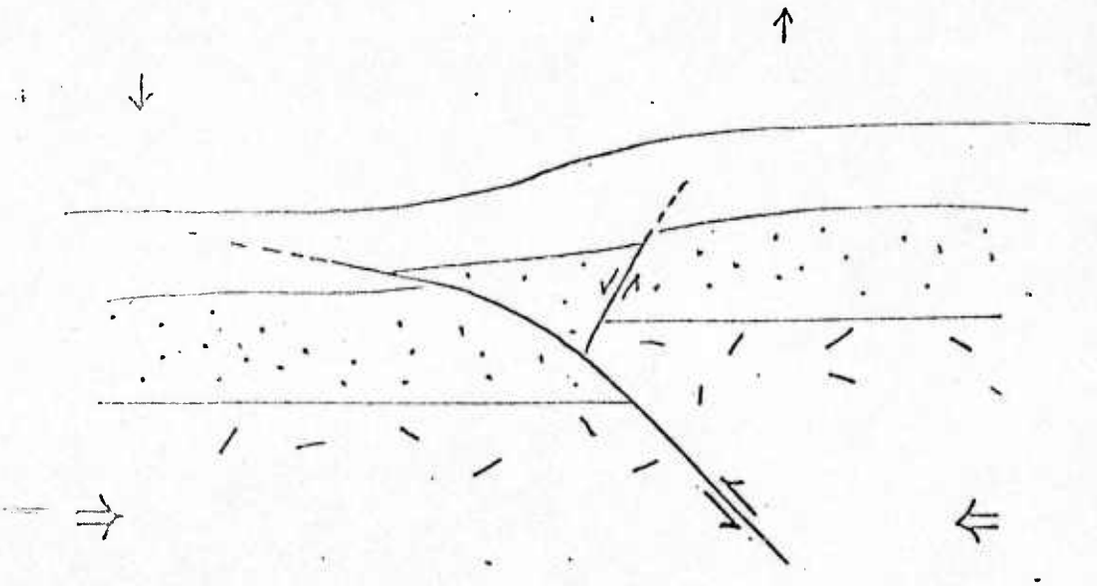

GULF COASTAL PLAIN
INTERIOR LOW PLATEAUS
APPALACHIAN PLATEAUS
VALLEY AND RIDGE
BLUE RIDGE
PIEDMONT
ATLANTIC COASTAL PLAIN
WIC
PRI HOP
PAR
SON
HAR
MOR
NEW
GRE
RAL
NEW
ELEVATION
VELOCITY
ERROR
Fig. 4
RELATIVE VELOCITY, MM/YR
ELEVATION, M
DISTANCE, KM
0
10
20
30
0
250
500
750
0
500
1000
1500
2000

FIGURE 5



6a



6b

FIGURE 6

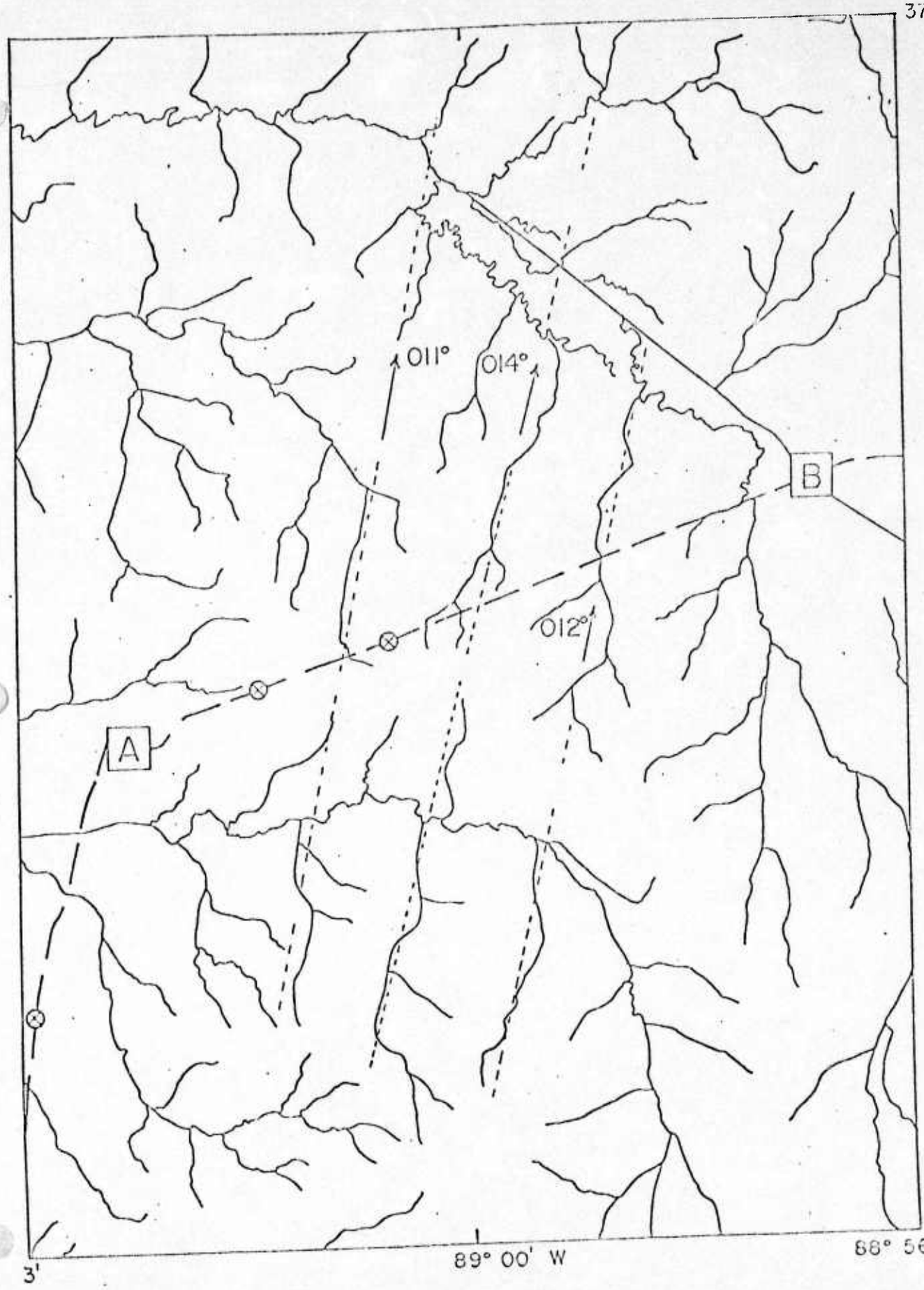


FIGURE 7

Copy available to DDC does not permit fully legible reproduction

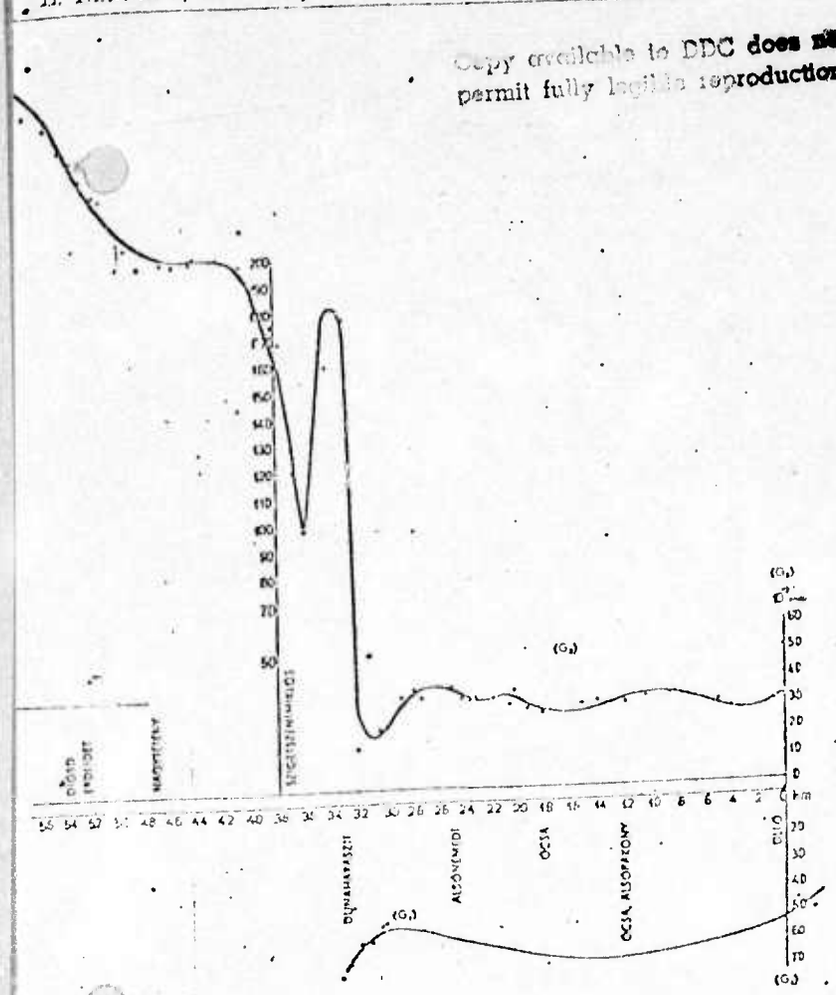


Fig. 4. Crustal deformations near the epicenter. Unit = 10^{-3} mm/day.

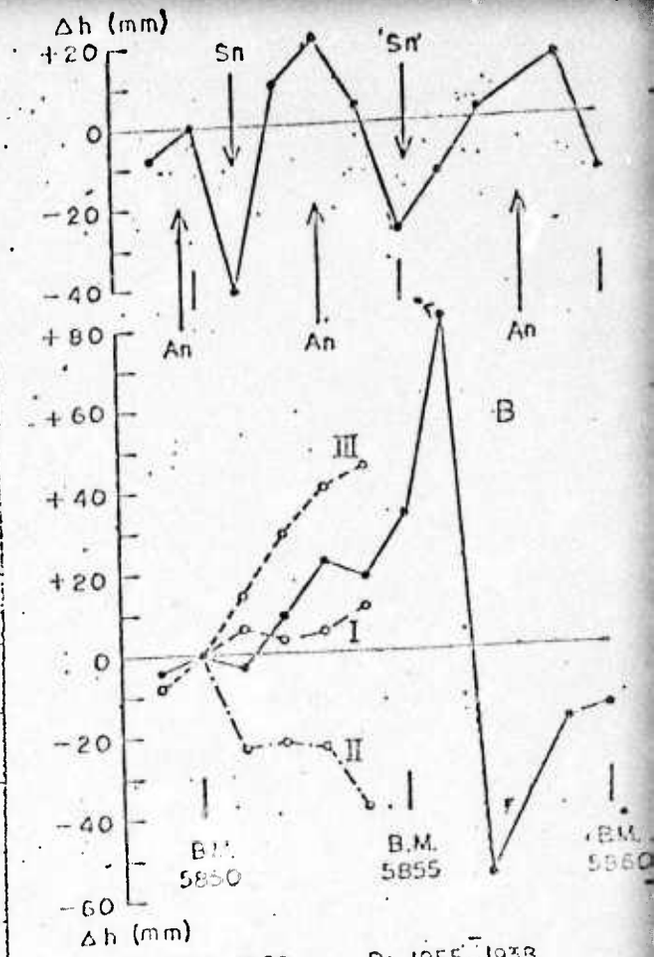
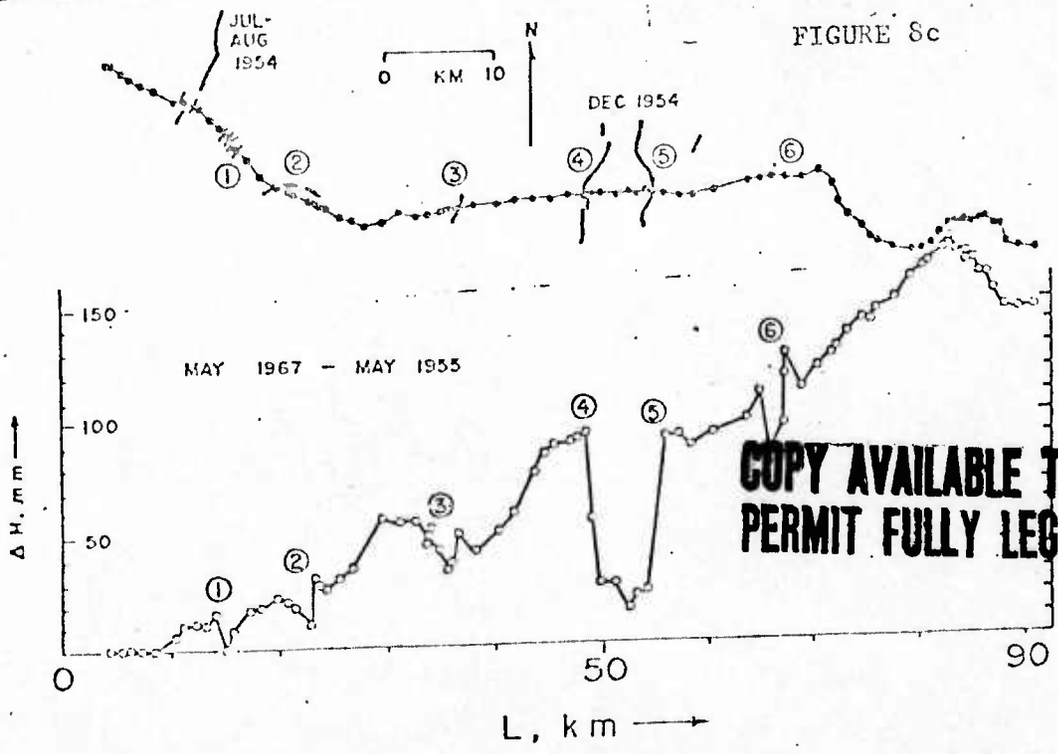


Fig. 3-a. Vertical crustal movements accompanied wi
the Fulafsui Earthquake of 1955. An: Anticline, Sn
Syncline. (after S. Miyamura, und A. Okada, 1955

FIGURE 8c



COPY AVAILABLE TO DDC DOES NO
PERMIT FULLY LEGIBLE PRODUCTIO

FIG. 2. Elevation changes indicated by the differences between adjusted elevations determined in the 1955 and 1967 surveys (*lower line*) as a function of distance measured west to east across the fault zone. The *upper line* is a plan view of the location of bench marks from BM B353 to Carroll Summit. The earthquake ground breakage along Highways 50 is also shown. Local anomalies in the lower curve are identi-

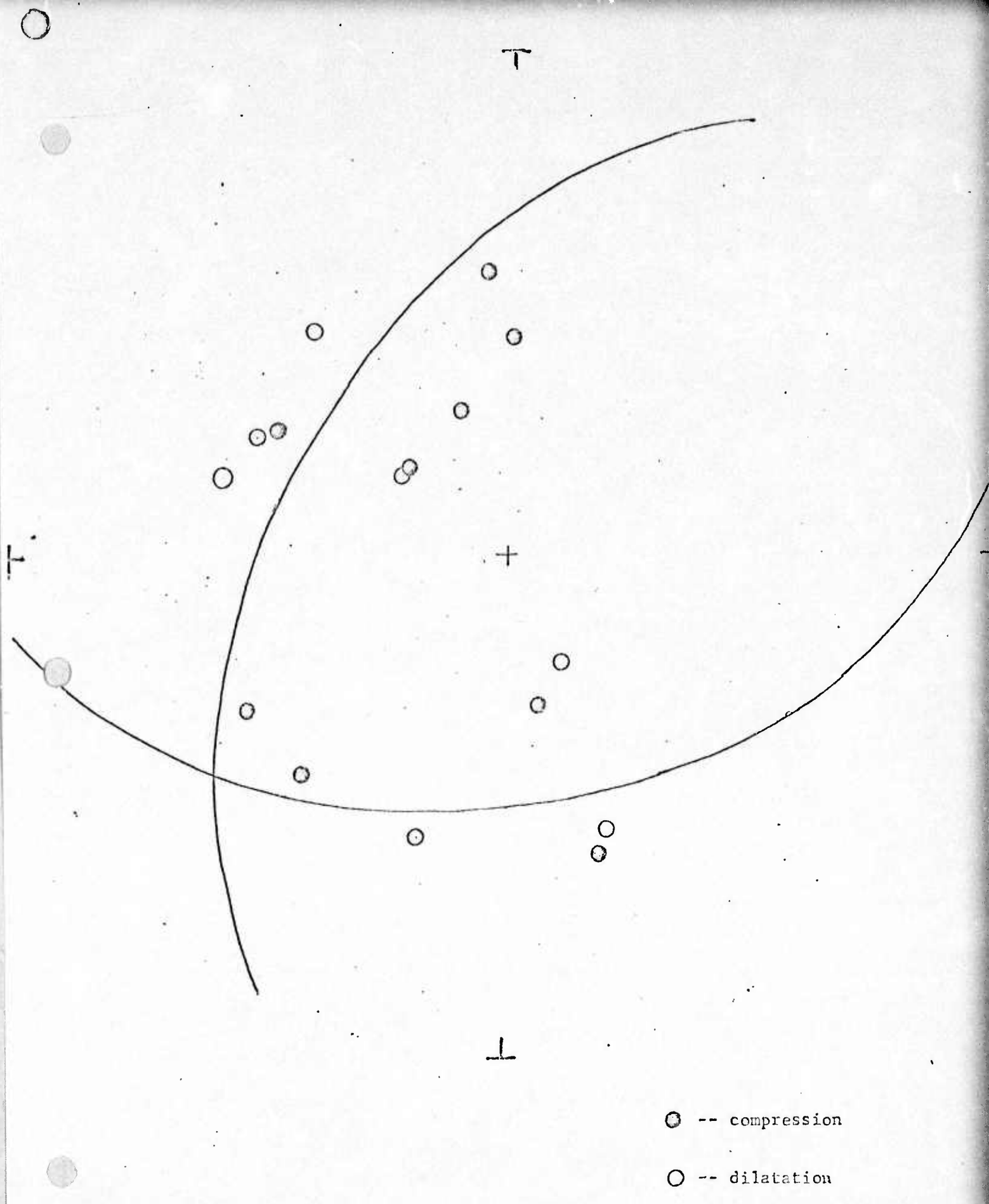


FIGURE 9

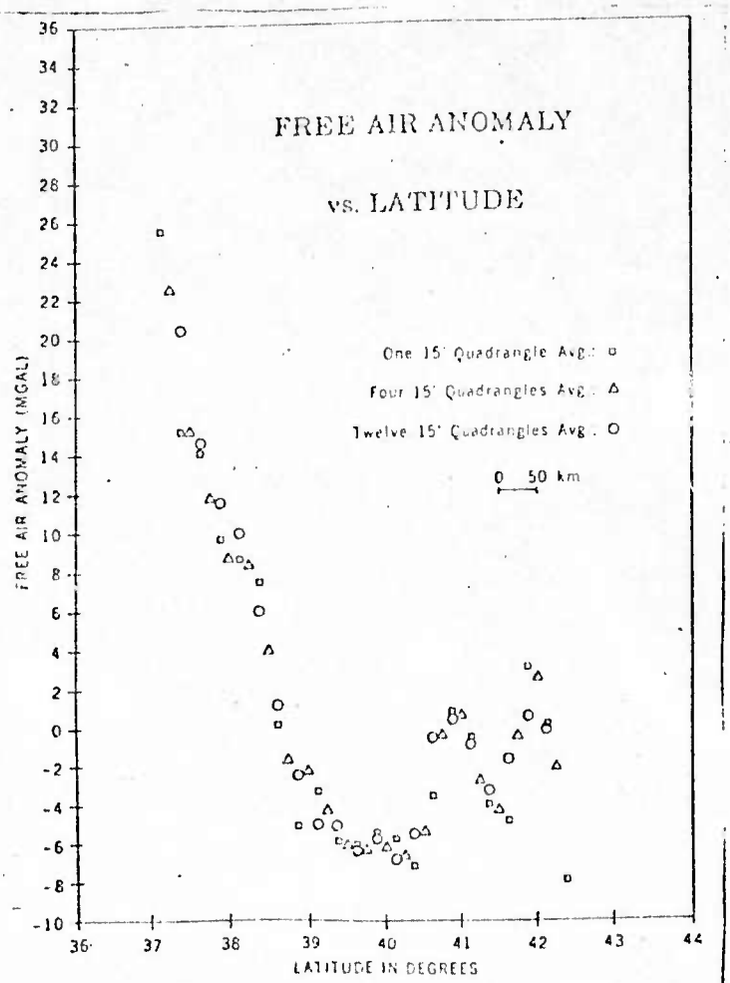


Figure 2. Mean free-air anomaly profile along long 89° W. Computation technique described by McGinnis (1970).

FIGURE 10

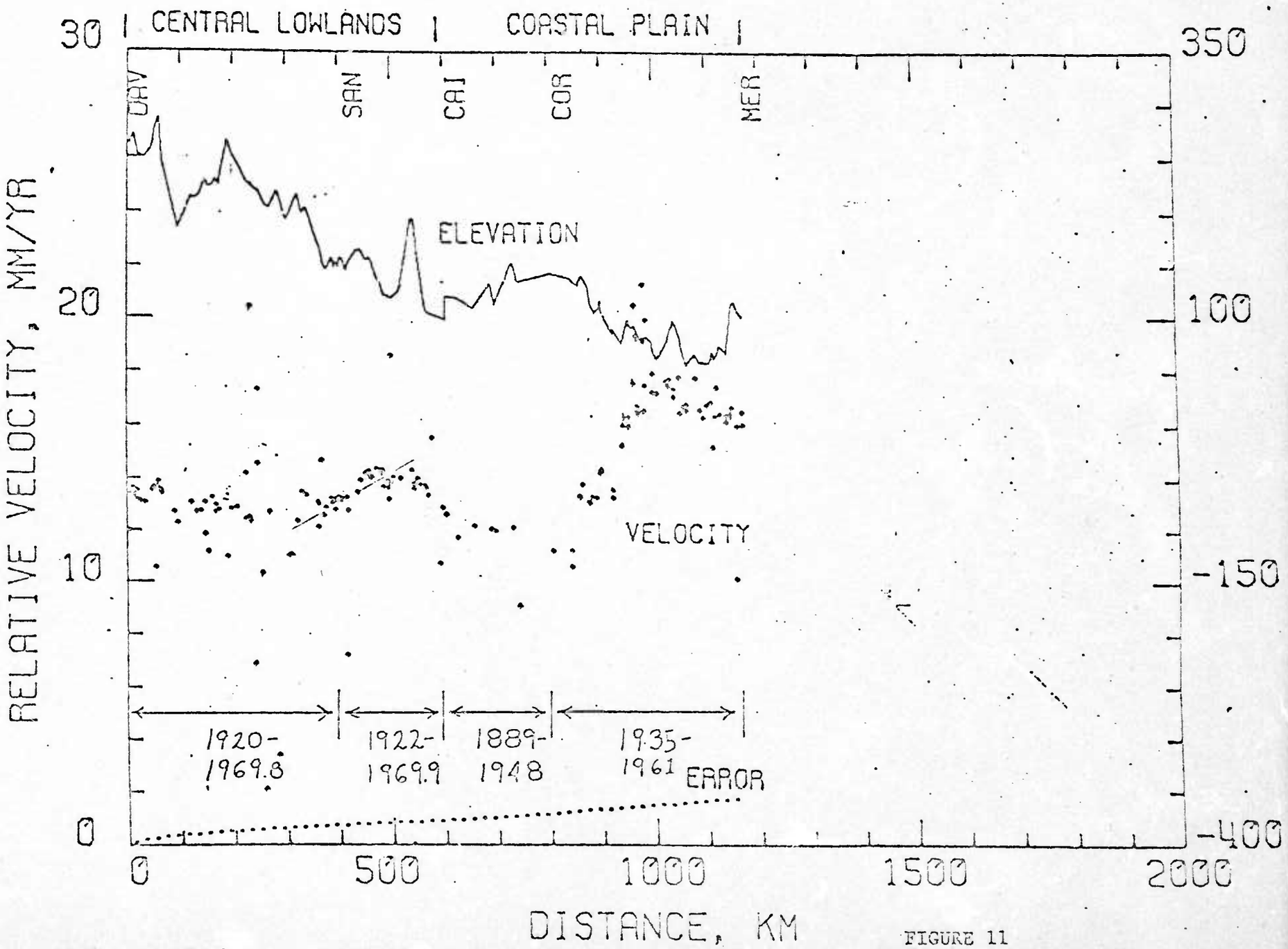

CENTRAL LOWLANDS
COASTAL PLAIN
DAV
SAN
CAI
COR
MER
ELEVATION
VELOCITY
1920-1969.8
1922-1969.9
1889-1948
1935-1961
ERROR
RELATIVE VELOCITY, MM/YR
30
20
10
0
350
100
-150
-400
0
500
1000
1500
2000
DISTANCE, KM

FIGURE 11

REFRACTION ERROR IN LEVELING

James E. York
Department of Geological Sciences
Cornell University
Ithaca, New York 14853

ABSTRACT

Previous estimates of the refraction error in leveling reached up to several tens of mm per 100 m change in elevation. Errors are found in these estimates. For a linear temperature gradient, the error is usually less than 1 mm per 100 m change in elevation. The refraction error is probably less than the standard deviation in leveling for a linear temperature gradient. However, non-linear temperature gradients may be important

INTRODUCTION

Systematic errors in precise leveling which accumulate with elevation are difficult to detect. Two sources of such errors are incorrect calibration of the leveling rods and bending of light rays caused by changes in the index of refraction of light. In leveling a closed loop, these errors may give systematically high or low elevations without contributing to the error in loop closure. In addition, if two levelings of the same route are compared, and if the magnitude of the systematic error was different in the two surveys, then measurements of apparent, but unreal, vertical crustal movements would result.

If the apparent vertical movements were to correlate (either negatively or positively) with elevation, then such systematic errors might be suspected. In their studies of vertical movements from releveling data in the United States, Brown and Oliver (1975) have observed such correlations

(Figure 5). Therefore an investigation of the magnitude of possible refraction errors was made.

Changes in the index of refraction are caused by variations in temperature, pressure, and composition of the atmosphere. Kukkamäki (1938) has shown that the most important variations are those of temperature. Hence only temperature variations will be considered here.

A typical set-up used in leveling measurements, along with conventions and symbols for this paper, is shown in Figure 1. Mathematical symbols to be used in this paper are as follows:

α acute angle between horizontal and ground surface

a temperature at instrument (^{o}K)

b temperature gradient ($^{o}C/m$)

c a constant (^{o}K) relating n and T (equation 5)

e net refraction error between foresight and backsight (mm/100 m change in elevation)

h refraction error between instrument and rod (m)

n index of refraction

s horizontal sighting length (m)

T temperature (^{o}K)

x distance measured parallel to ground surface with origin at instrument

z distance measured perpendicular to ground surface with origin at instrument

subscripts: 0 values at instrument

1 values where light ray intersects rod_1

2 values where light ray intersects rod_2

PREVIOUS WORK

The calculation of the refraction correction is complicated by the uncertainty in the form of the temperature distribution. Even if a vertical temperature profile is known at one locality on a leveling route, the profile may change along the route and with time. A further complication is the difficulty in integrating many forms of the temperature distribution.

Based on some early temperature observations, Lallemand (1896) used

$$T = c_1 + c_2 \log (z+c_3) \tag{1}$$

where the c_i are constants. From more recent observations, Kukkamäki (1938) obtained the formula

$$T = c_4 + c_5 z^{c_6} \tag{2}$$

A third formula,

$$T = c_7 + c_8 z + c_9 z^2 \tag{3}$$

was used by Bomford (1928), because it simplified the mathematics.

All three of the above authors used Snell's law and a simple dependence of the index of refraction on temperature (see equation 5) to calculate the refraction error. The difficulty in integrating the resulting equations led each of these authors to make approximations. Because the refraction error is small, approximations must be made carefully or else they may greatly affect the obtained magnitude of the refraction error. Unfortunately, the approximations of these authors do have such effects. For example, they each give a net refraction error of zero for a linear temperature gradient (equation 4) with equal backsight

and foresight. As the present study shows, this net error is not zero. Therefore, further calculations were deemed necessary to determine possible magnitudes of the refraction error.

REFRACTION ERROR

Temperatures

A temperature distribution of the form

$$T = a + bz \tag{4}$$

will be assumed. This linear temperature gradient may be a fair approximation over vertical distances such as are encountered between instrument and rod (a few meters or less), but clearly this gradient cannot be extrapolated to much larger vertical distances. This advantage of this formula is its simplification of computations of the refraction error. Should a more complicated temperature distribution be found necessary, it could be approximated as a number of discrete linear sections and the formulas presented in this paper could still be used.

This simple formula also ignores any x-dependence of the temperature. Before refraction corrections based on equation 4 are made, temperature measurements should be made while leveling.

In the calculations that follow, the value of a used is 288°K. The sign of b is taken to be positive. If b is negative, only the sign, not the absolute value, of the net error is changed.

Index of Refraction

For a pure substance, the index of refraction for a given wavelength depends only on the density. Using an ideal gas law approximation

$$n = 1 + \frac{c}{T} \tag{5}$$

where c is a constant dependent on pressure, wavelength, and composition of the gas. Empirical evidence supports an equation of this form (Meggers and Peters, 1918). For the purposes of this paper, c is constant and equal to 0.0801 ^{o}K.

Fermat's Principle

Fermat's principle is used to determine the path of the ray which travels between rod 1 and rod 2 and is tangent to the instrument. This principle states that the ray path is such that the value of the travel time is stationary. Thus the problem is one of the calculus of variations.

The integral

$$\int n \left[(dx)^2 + (dz)^2\right]^{\frac{1}{2}} = \int n \left[1 + \left(\frac{dz}{dx}\right)^2\right]^{\frac{1}{2}} dx \tag{6}$$

must be extremized. Because n is independent of x, the Euler-Langrange equation becomes

$$\frac{dz}{dx} = \pm\sqrt{\left(\frac{n}{n^2}\right)^2 - 1} \tag{7}$$

where n^2 is a constant. Because the slope $\frac{dz}{dx}$ is $-\tan\alpha$ at the origin, equation 7 becomes

$$\frac{dz}{dx} = \pm\sqrt{\left(\frac{n}{n_c}\right)^2 (1 + \tan^2\alpha) - 1} \tag{8}$$

Calculation of Error

Using equations 4 and 5, the square root expression may be written in terms of z. Then equation 8 may be integrated from the origin to each rod. This procedure (see Appendix A) gives transcendental equations for the refraction errors h_1 and h_2.

The transcendental equations can be solved iteratively by Newton's method (see Appendix B). In order to facilitate comparisons with apparent vertical movements indicated by leveling and releveling data, the net refraction error (in mm) per 100 m change in elevation is calculated for a given angle α, temperature gradient b, and sighting length s.

$$e = (h_2 - h_1)\ (1000)\ (\text{number of instrument set-ups necessary to change 100 m in elevation}) \qquad (9)$$

Figures 2, 3, and 4 give e as a function of α, b, and s, respectively. The net refraction error is seen to vary as the square of both the temperature gradient and the sighting length. Therefore, temperature gradients must be well known before applying corrections. Also, the refraction error may be greatly reduced by shortening sighting lengths.

CONCLUSIONS

Because observed temperature gradients in the air are usually less than $1^{\circ}C/m$ (see tables of Best in Kukkamäki, 1938), and because sighting lengths are usually less than 100 m in practice, the refraction error is usually less than 1 mm/100 m change in elevation for linear temperature gradients. This figure is approximately equal to the systematic error caused by inaccuracies in correcting for thermal changes affecting rod length (Thurm, 1971). It is also usually less thar the estimated standard deviation in precise

leveling, which includes only random errors.

Some of the releveling profiles studied by Brown and Oliver (1975) show correlations of elevation with movement. If caused by systematic errors, these correlations would indicate errors ranging from 20 to 100 mm/100 m change in elevation (Figure 5). These hypothetical errors appear much too large to be explained by refraction caused by simple linear temperature gradients. Therefore, the apparent movements may reflect actual crustal movements, as Brown and Oliver (1975) suggest. Alternatively, non-linear temperature gradients may be important.

Thurm (1971) and Hytonen (1967) have made refraction corrections to leveling data based on Kukkamäki's (1938, 1939) formulas and tables. Because of errors in Kukkamäki's work, these corrections may not be valid. Before any refraction corrections are made, average temperature distributions must be known accurately. Because air movements cause rapid variations in temperature, only approximate, average corrections can be made. On long lines of near constant slope, where refraction errors could be larger than the standard deviation, using short sighting lengths will keep the error small.

ACKNOWLEDGMENTS

Beneficial discussions have been held with L. Brown, R. Reilinger, and S. Schilt. This research was supported by the Advanced Research Projects Agency of the Department of Defense and was monitored by the Air Force Office of Scientific Research under Contract Number AFOSR-73-2494. Cornell University Department of Geological Sciences Contribution Number:

REFERENCES CITED

Bomford, G., Three sources of error in precise leveling, Survey of India Professional Paper No. 22, 40 p., 1928.

Brown, L.D. and Oliver, J.E., Vertical crustal movements from leveling data and their relation to geologic structure in the eastern United States, Rev. Geophys. Space Phys., 13, , 1975.

Hytönen, E., Measuring of the refraction in the second leveling of Finland, Suomen Geodeettisen Laitiksen Julkaisuja Veröffentliehunger des Finnischen Geodätischen Institutes No. 63, 41 p., 1967.

Kukkamäki, T.J., Uber die nivellitische Refraktion, Suomen Geodeettisen Laitoksen Julkaisuja Veröffentliehunger des Finnischen Geodätischen Institutes No. 25, 48 p., 1938.

Kukkamäki, T.J., Formeln und Tabellen zur Berechnung der nivellitischen Refraktion, Suomen Geodeettisen Laitoksen Julkaisuja Veröffentliehunger des Finnischen Geodätischen Institute No. 27, 18 p., 1939.

Lallemand, C., L'erreur de réfraction dans le nivellement geometrique, Verhandlunger Conferenz der Permanenten Commission der Internationalen Erdmessung, 247-276, 1897.

Meggers, W.F., and Peters, C.G., Measurement of the index of refraction of air for wavelengths from 2218 A to 9000 A, National Bureau of Standards Bulletin, 14, 697-740, 1918.

Thurm, H., Some systematic errors of precision leveling, Jena Review, 16, 172-176, 1971.

Appendix A

Derivation of Transcendental Equation for Refraction Error

Upon substitution of equations 4 and 5 into equation 8 and integration:

$$(A1) \quad \pm\int dx = \int (a+c)(a+bz)\Big[(a^2\tan^2\alpha - 2ac - c^2)(bz)^2 + (2a)(a+c)(a\tan^2\alpha - c)(bz) + (a)^2(a+c)^2\tan^2\alpha\Big]^{-\frac{1}{2}} dz$$

$$= F + \text{constant}$$

From geometry of Figure 1:

$$(A2) \quad h_1\cos\alpha = s\sin\alpha - z_1$$

$$(A3) \quad h_2\cos\alpha = -s\sin\alpha - z_2$$

$$(A4) \quad h_1\sin\alpha = -x_1 - s\cos\alpha$$

$$(A5) \quad h_2\sin\alpha = -x_2 + s\cos\alpha$$

Integrating equation A1 from the origin to the rods:

(A6) $$x_2 = -F(z_2) + F(0)$$

If the light ray is never tangent to a line parallel to the x-axis:

(A7a) $$x_1 = -F(z_1) + F(0)$$

If the tangent to the light ray does become parallel to the x-axis:

(A7b) $$x_1 = -F(z_p) + F(0) + F(z_1) - F(z_p)$$

where z_p is the value of z when the tangent is parallel to the x-axis. On either side of z_p the sign of the slope is different, and thus two integrations of equation A1 are necessary.

Substituting equations A2-A5 into equations A6 and A7:

(A8) $$h_2 \sin\alpha = s\cos\alpha + F(-s\sin\alpha - h_2\cos\alpha) - F(0)$$

If tangent to the light ray is never parallel to the x-axis:

(A9a) $$h_1 \sin\alpha = -s\cos\alpha + F(s\sin\alpha - h_1\cos\alpha) - F(0)$$

If tangent to the light ray does become parallel to the x-axis:

(A9b) $$h_1 \sin\alpha = -s\cos\alpha - F(s\sin\alpha - h_1\cos\alpha) - F(0) + 2F(z_p)$$

Equations A8 and A9 are the transcendental equations in h to be solved numerically.

The formulas for F are:

if $a^2\tan^2\alpha - 2ac - c^2 > 0$,

(A10a) $$F(z) = (b)^{-1}(a+c)(a^2\tan^2\alpha - 2ac - c^2)^{-1}\left[(a^2\tan^2\alpha - 2ac - c^2)(bz)^2 + (2a)(a+c)(a\tan^2\alpha - c)(bz) + (a)^2(a+c)^2\tan^2\alpha\right]^{\frac{1}{2}} + (a+c)(a^2\tan^2\alpha - 2ac - c^2)^{-\frac{1}{2}}(b)^{-1}(a)\left\{1 - \left[(a+c)(a\tan^2\alpha - c)(a^2\tan^2\alpha - 2ac - c^2)^{-\frac{1}{2}}\right]\right\} \ln\left\{\left[(a^2\tan^2\alpha - 2ac - c^2)(bz)^2 + (2a)(a+c)(a\tan^2\alpha - c)(bz) + (a)^2(a+c)^2\tan^2\alpha\right]^{\frac{1}{2}} + (a^2\tan^2\alpha - 2ac - c^2)^{\frac{1}{2}}(bz) + a(a+c)(a\tan^2\alpha - c)(a^2\tan^2\alpha - 2ac - c^2)^{-\frac{1}{2}}\right\}$$

if $a^2\tan^2\alpha - 2ac - c^2 < 0$,

(A10b) $$F(z) = (b)^{-1}(a+c)(a^2\tan^2\alpha - 2ac - c^2)^{-1}\left[(a^2\tan^2\alpha - 2ac - c^2)(bz)^2 + (2a)(a+c)(a\tan^2\alpha - c)(bz) + (a)^2(a+c)^2\tan^2\alpha\right]^{\frac{1}{2}} + (a+c)(-a^2\tan^2\alpha + 2ac + c^2)^{-\frac{1}{2}}(b)^{-1}(a)\left\{1 - \left[(a+c)(a\tan^2\alpha - c)(a^2\tan^2\alpha - 2ac - c^2)^{-1}\right]\right\}\operatorname{Arcsin}\left\{\left[(-2)(b)^2(a^2\tan^2\alpha - 2ac - c^2)(z) - (2ab)(a+c)(a\tan^2\alpha - c)\right]\left[(2ab)^2(a+c)^2(a\tan^2\alpha - c)^2 - 4(a)^2(b)^2(a+c)^2(a^2\tan^2\alpha - 2ac - c^2)\tan^2\alpha\right]^{-\frac{1}{2}}\right\}$$

The formula for z_p is:

(A11) $$z_p = \left\{-(2ab)(a+c)(a\tan^2\alpha - c) - \left[(2ab)^2(a+c)^2(a\tan^2\alpha - c)^2 - 4(a)^2(b)^2(a+c)^2(a^2\tan^2\alpha - 2ac - c^2)\tan^2\alpha\right]^{\frac{1}{2}}\right\}\left[2(b)^2(a^2\tan^2\alpha - 2ac - c^2)\right]^{-1}$$

Appendix B

Numerical Calculation of Refraction Error

Rewrite equations A8 and A9 in the form

(B1) $$G(h) = 0.$$

Then, if $G'(h)$ and $G''(h)$ do not change sign in the interval (h', h^2) and $G(h') \cdot G''(h') > 0$, $h^n \to h$ as $n \to \infty$, where

(B2) $$h^{n+1} = h^n - \frac{G(h^n)}{G'(h^n)}$$ (Newton's method)

and $h', h^2, h^3, \ldots$ represent successive approximations of h. This method was found to compute h to sufficient accuracy after a few iterations.

To show that $G'(h)$ and $G''(h)$ do not change sign in the interval (h', h^2), let equations A8 and A9 be rewritten as:

(B3)
$$\begin{aligned} &A8: && G_2(h_2) = 0 \\ &A9a: && G_{1a}(h_1) = 0 \\ &A9b: && G_{1b}(h_1) = 0 \end{aligned}$$

Then,

(B4) $$G_2'(h_2) = -\cos\alpha\left[(a^2\tan^2\alpha - 2ac - c^2)(bz_2)^2 + (2a)(a+c)(a\tan^2\alpha - c)(bz_2) + (a)^2(a+c)^2\tan^2\alpha\right]^{-\frac{1}{2}} - \sin\alpha$$

$$\leq 0$$

By substituting z_1 for z_2 in the above formula, one obtains $G_{1a}'(h_1)$. Thus

$$G_{1a}'(h_1) \leq 0$$

By also substituting $(+\sin\alpha)$ for $(-\sin\alpha)$ in B4, one obtains $-G_{1b}'(h_1)$. Then

$$G_{1b}'(h_1) \geq 0$$ for reasonable values of n and for α less than about 30°.

(B5) $$G_2''(h_2) = a^2bc(1+\tan^2\alpha)\cos^2\alpha(a+c)(a+c+bz_2)\left[(a^2\tan^2\alpha - 2ac - c^2)(bz_2)^2 + (2a)(a+c)(a\tan^2\alpha - c)(bz_2) + (a)^2(\ )^2\tan^2\alpha\right]^{-}$$

$$\geq 0$$

By substituting z_1 for z_2 in equation B5 one obtains $G_{1a}''(h_1)$. Thus

$$G_{1a}''(h_1) \geq 0$$

Finally, $$G_{1b}''(h_1) = -G_{1a}''(h_1) \leq 0$$

Therefore $G'(h)$ and $G''(h)$ do not change sign in the interval (h', h^2).

To insure that Newton's method will work, h' must be picked such that

$$G(h') \cdot G''(h') > 0 .$$

For equations A8 and A9a, this condition is met if $h' = 0$.

For equation A9b, this condition is met if $h' \cos\alpha = s \sin\alpha - z_p$.

FIGURE CAPTIONS

Figure 1: Mathematical conventions and symbols used in this paper. The net refraction error is $h_2 - h_1$.

Figure 2: Dependence of net refraction error e (mm/100 m change in elevation) on slope α, using sighting length s = minimum of 50 m or a sighting length such that difference in elevation between the bases of the two rods is 4 m. a = 288°K, c = .0801°K.

Figure 3: Graph showing b^2 dependence of net refraction error e, where b is temperature gradient. a = 288°K, c = .0801°K.

Figure 4: Graph showing s^2 dependence of net refraction error e, where s is sighting length. a = 288°K, c = .0801°K.

Figure 5: Apparent vertical velocities between Morristown, Tennessee and New Bern, North Carolina, derived by comparing two levelings separated by 33 years. Each dot represents one bench mark. From Brown and Oliver (1975).

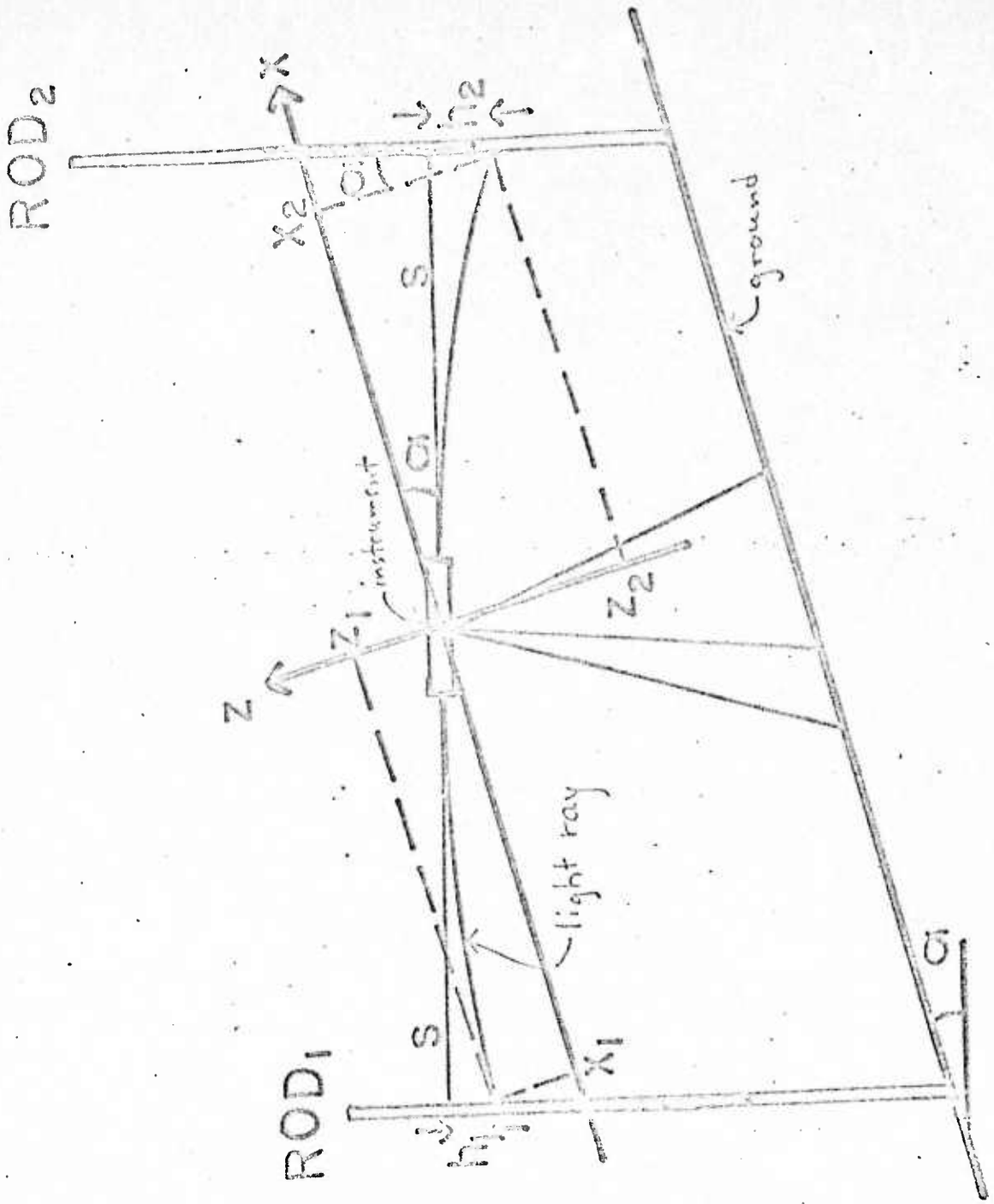


FIGURE 1.

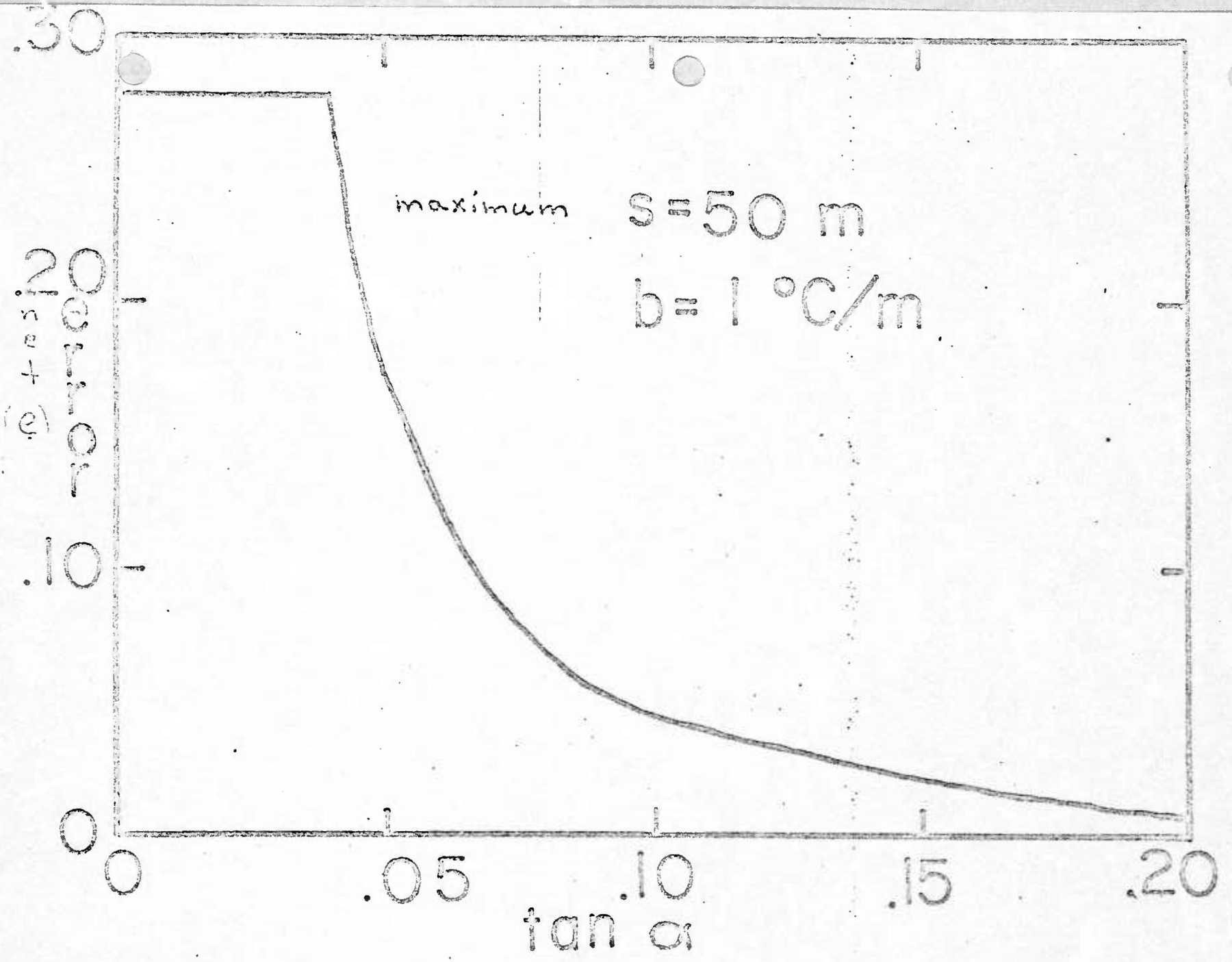


FIGURE 2.

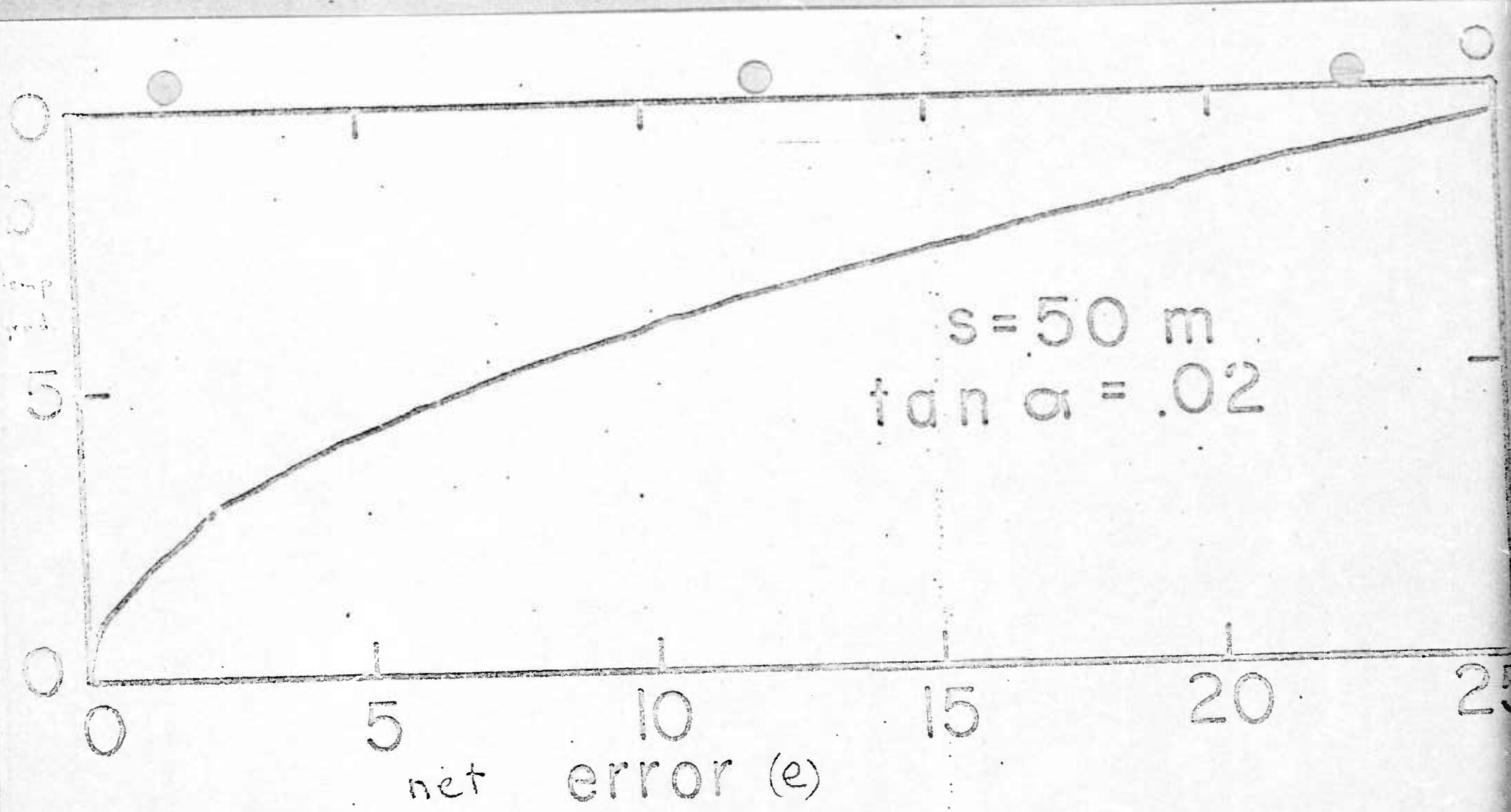


FIGURE 3.

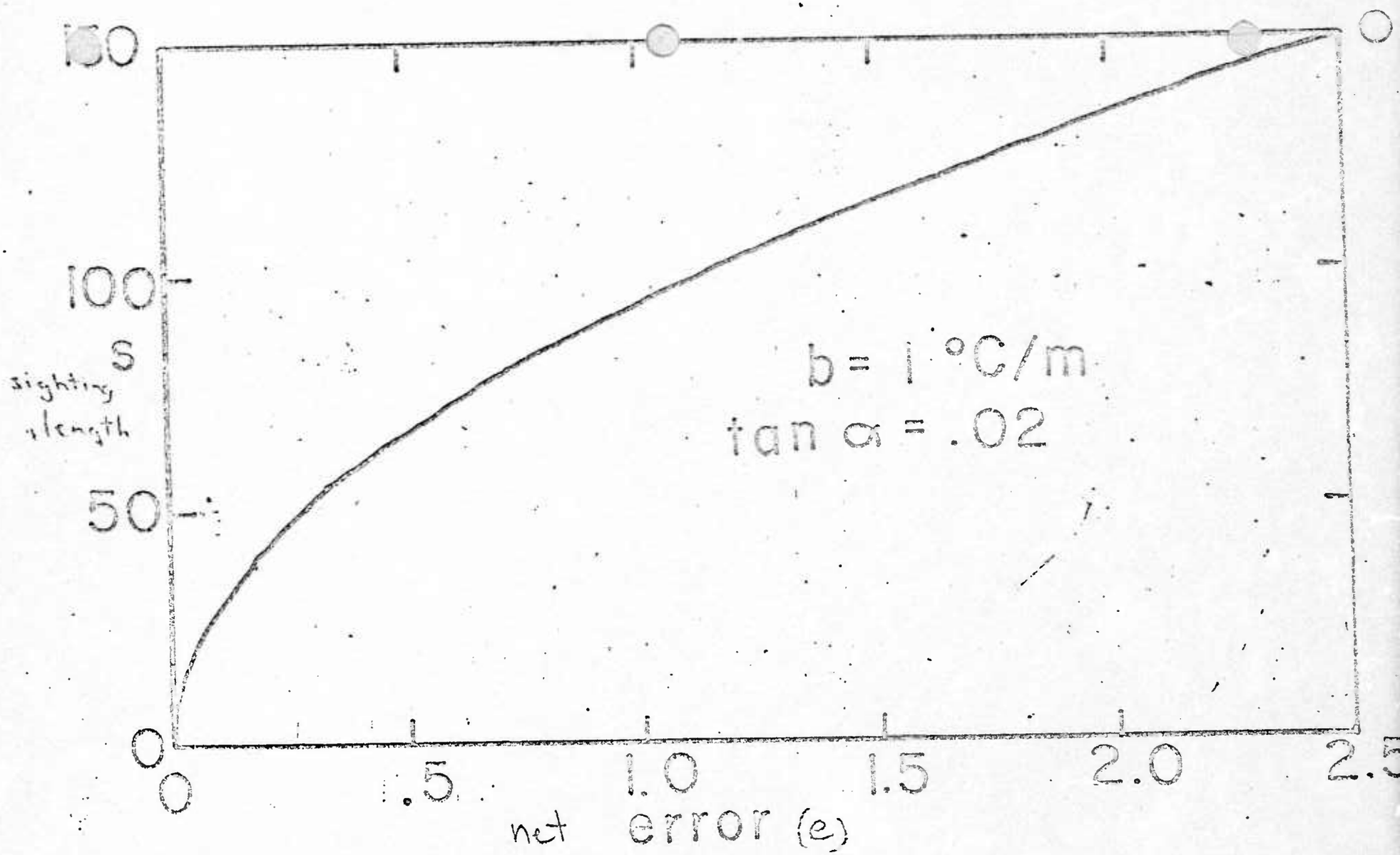

150
100
50
0
sighting length s
b = 1°C/m
tan α = .02
0
.5
1.0
1.5
2.0
2.5
net error (e)

FIGURE 4.

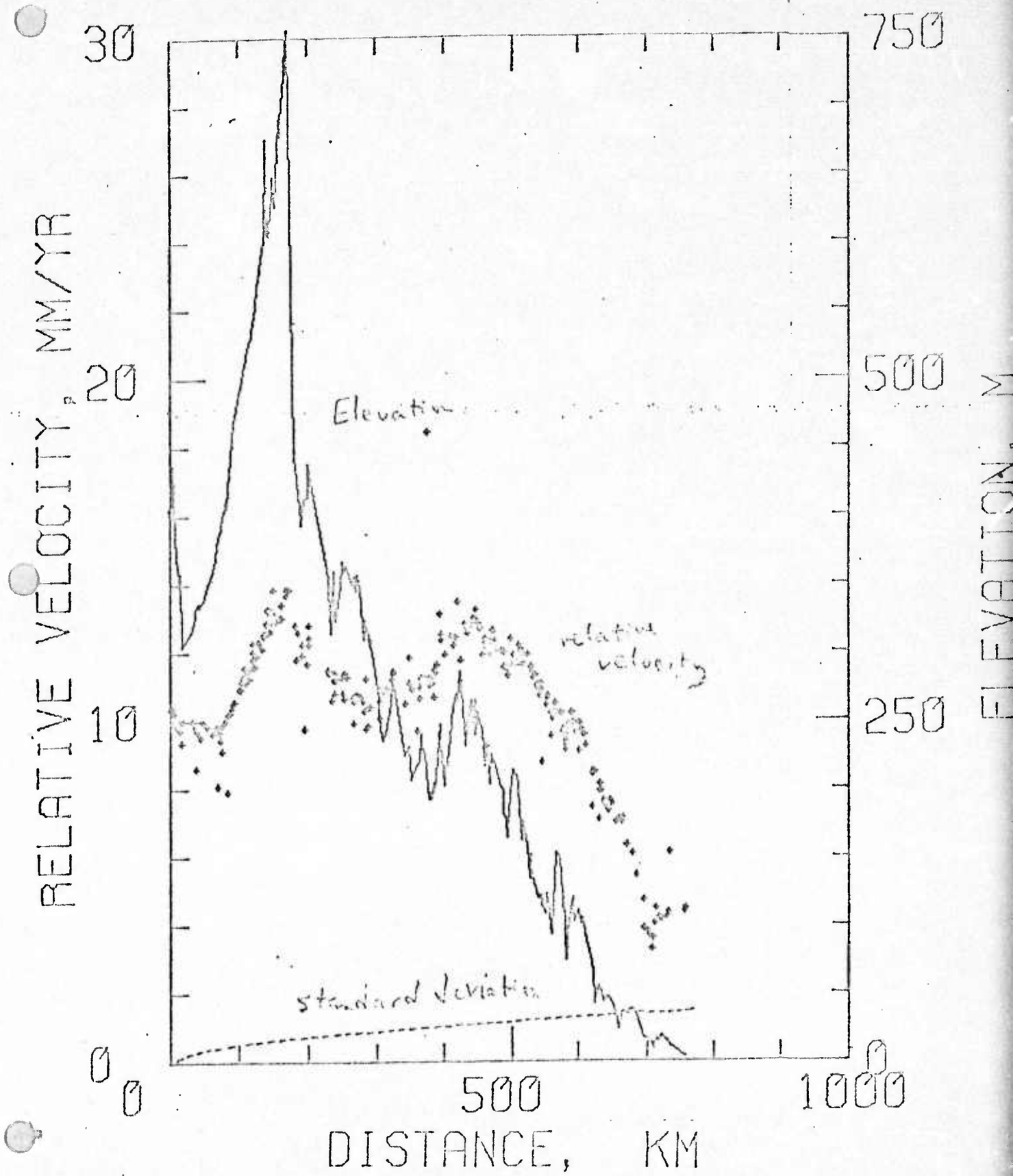

30
20
10
0
0
500
1000
750
500
250
0
RELATIVE VELOCITY, MM/YR
DISTANCE, KM
ELEVATION, M
Elevation
relative velocity
standard deviation

FIGURE 5.

Appendix F

SEISMICITY AND QUATERNARY FAULTING IN CHINA

James E. York, Richard Cardwell, and James Ni

Department of Geological Sciences

Cornell University

Ithaca, New York 14853

ABSTRACT

Both Quaternary faulting, based on an interpretation of a new mosaic of LANDSAT-1 imagery, and seismicity, based on maps of all reported earthquakes in historical records for 1177 B.C.-1903 A.D., of all instrumental data for 1904-February 1975, and of all earthquakes with $M \geq 6$ for 1177 B.C.-February 1975, demonstrate a distinct difference in Quaternary tectonics between western and eastern China. East-west trending reactivated Paleozoic mountain belts and subparallel large left-lateral strike-slip faults predominate in western China. The northeasterly trending Cenozoic Shansi graben and subparallel right-lateral strike-slip faults characterize eastern China. Nearly aseismic blocks occur in both east and west, but a satisfactory model of small plates that explains all of the observed phenomena is not apparent. The tectonic activity may be controlled by stresses from nearby plate margins, with the collision of India and Eurasia predominating, or by asthenospheric processes beneath China.

Large earthquakes and surface faulting have occurred on some of the faults observed in the satellite images. Because the Chinese historic record suggests the alternation of seismically active and quiet periods

of the order of a few hundred years in intraplate areas, data on Quaternary faulting may be especially valuable in supplementing seismicity data for areas with short seismic records.

INTRODUCTION

While most of the global seismic energy release occurs near major plate boundaries, occasional large earthquakes also occur in intraplate areas. Despite the success of the concepts of plate tectonics in explaining most seismicity, these intraplate earthquakes remain anomalous and not well understood. One of the largest and most active of the intraplate seismic regions is China. Although the parts of China in the Himalayas and in Taiwan are clearly along major plate boundaries, most of China can be classified as intraplate. Seismicity and Quaternary faulting occur throughout large parts of intraplate China. The long historical record of seismicity in China makes this area especially valuable for studying intraplate tectonics. In addition, LANDSAT imagery of most of China is now available. Thus a good comparison between intraplate seismicity and lineaments seen on the satellite imagery can be made for this region.

Our objectives are to locate lineaments that represent Quaternary faulting, to compare the faulting with historical and instrumental seismic data, to relate the faults and earthquakes to regional tectonics, and to compare China with other intraplate areas. For these purposes we have made a mosiac of LANDSAT-I imagery and seismicity maps covering several time periods and magnitude ranges. Satellite imagery was chosen instead

of ground-based geologic data because such data are sparse or unavailable for much of China and because the imagery provides a uniform and accurate base. We find that changes in intraplate tectonics from western to eastern China correlate both with the Quaternary faults and with the seismicity. In the dry climate of western China, where fault features are well-preserved, there is a short historic record of seismicity, and faulting is the primary data concerning Quaternary tectonics. The wet climate of eastern China does not preserve fault features as well, but a long history of seismicity is available.

This study is intended to complement previous papers based mainly on seismicity and fault plane solutions (Molnar et al., 1973; Shi et al., 1973) and overlaps somewhat with that of Molnar and Tapponnier (1975) and Allen (1975) and Bonilla and Allen (1975).

LANDSAT-I IMAGERY

Construction of Mosaic

The Landsat images of China used are 18 cm square and at a scale of 1:1,000,000, being enlarged from the original scale of 1:3,369,000. The resolution is 70m (ERTS Data Users Handbook, 1972). Approximately 780 images, mostly of band 7 (near infrared, 0.8-1.1μm wavelength) and some of band 5 (lower red, 0.6-0.7μm wavelength), were used to construct the mosaic. Because a low sun angle often accentuates topographic lineaments, fall and winter images were used where available. The images are close to a Lambert conic conformal projection or an Albers equal area projection (Short and Lowman, 1973, p. 5). The mosaic was partially controlled with the Operational Navigation Chart (O.N.C.) maps (1:1,000,000 scale, Lambert conic conformal

projection), which are also used to fill gaps where there was no LANDSAT coverage, where the LANDSAT images were too cloudy, and in several areas near the margin of the mosaic where imagery was not obtained by us.

The region of China and vicinity was divided into 24 areas. A mosaic of each region was made on boards 1.2 m square. Each board was photographed, and these photographs were mosaicked, this version being at a scale of approximately 1:6,000,000. In this version matching edges of images are usually less than 10 km off, although the mismatch may reach 50 km in the northern part of the mosaic. Where ice partially obscured the boundaries of some large lakes, the lakes were inked in black using the O.N.C. maps as a reference. The ocean was also inked in black where O.N.C. maps were used. The political boundaries are taken from the CIA Atlas (1971). Parts of the Philippine, Ryukyu and Japanese Islands are geographically within the bounds of the mosaic, but they are not included.

The physiographic map (Figure 2) shows the large-scale features which are visible in the mosaic (Figure 1).

Interpretation of Lineaments

Two important distinctions between different studies of lineaments using topographic maps, aerial photographs, side-looking airborne radar, or satellite images are the scale of lineaments and their ages of formation. In this study we consider lineaments which range in length from a few tens of kilometers to a few thousand kilometers. For a detailed study at this scale, only satellite images both provide consistent quality and are readily available.

Because our object is to relate the lineaments to Quaternary tectonics, we tried to choose lineaments that appeared to represent Quaternary faulting. Our criteria include linearity, sharpness, continuity, presence of a topographic, tonal, or textural difference across the lineament, and the presence of alluvial deposits along one or both sides of part of the lineament. The last criterium is intended to eliminate faults which have not had Quaternary movement. The previous criteria are meant to distinguish lineaments that represent faults and to eliminate cultural features such as railroads. Linearity, in our criteria, means that the lineament deviates from a straight line by less than about 10 percent of its length. Some sections of long lineaments may show greater curvature than this. The criterium of sharpness implies that a narrow feature such as a scarp is present along at least part of the lineament. Lineaments based entirely on straight stretches of river valleys are omitted, because of lack of evidence of Quaternary activity. Continuity implies that the lineament is distinguishable along at least 75 percent of its length. Lineaments that marginally meet the criteria are indicated by dashes in Figure 4. Examples of the various criteria are shown in Figure 3.

The map of Quaternary faulting (Figure 4) is based entirely on analysis of LANDSAT images at the scale of 1:1,000,000. Despite some attempt at quantification in our criteria, some of the interpretations remain somewhat subjective. Some probable omissions on this map are Quaternary faults that do not reach the surface, that do not define a linear trace along the ground (for example, faults with low dips), that

do not displace alluvial deposits, or that are too short to be clearly distinguishable on LANDSAT images. The shortest lengths for which our criteria were clearly met were 10 to 20 km. Also, some faults without Quaternary movement may have fault line scarps which are included in the map. However, these inclusions are probably not numerous and do not affect the regional picture greatly. Another important factor is climate, because fault features are usually better in a drier climate. Partly for this reason, the large faults in western China, with its desert climate, appear especially spectacular. An important omission in the faulting map is the Himalayan thrust belt. These thrust faults do not satisfy our criteria, probably because of the heavy cover of vegetation and the low angle of fault dip. Thus the faulting map is mainly an indication of the extent of large scale Quaternary high-angle faulting in China.

The component of strike-slip motion shown on some faults in Figure 4 is obtained either from surface faulting during historic earthquakes or from offset geologic features interpreted from the LANDSAT images. Accurate ground mapping of the historic surface faulting (Table 1) leave little doubt when correlating the surface faulting with lineaments on the LANDSAT images, even though the epicenter determination may be a few tens of kilometers off the fault. Few clear indicators of sense of strike-slip motions in LANDSAT images were found. The best indicators appear to be offset rock units (Figure 3) or folds. Because the faults may be reactivated from tectonic regimes with different stress orientations it is possible that the apparent offset seen in the image may not represent the Quaternary

sense of movement of the fault. Consistent sense of offset along streams is often a valuable method in ground and air studies, but such offsets (usually a few tens to a few hundreds of meters) are not as clear on satellite images. Because larger apparent offsets (a few kilometers or more) may be caused more by erosion along the fault zone than tectonic displacement, we have not used apparent stream offsets as indicators of the sense of strike-slip movement.

SEISMICITY: DATA

One purpose of this study is to give a complete and consistent evaluation of the seismicity of China from both the historical and instrumental records. Previously, the distribution of seismicity in Asia has been described by Li and Gorshkov (1957), Min (1957), Mei (1960), Land and Sun (1966), Shi et al. (1973), Molnar et al. (1973), Academia Sinica (1956), Academia Sinica (1970), and Lee (1957). A history of early compilations of Chinese earthquake data is given by Drake (1912). The first maps of large earthquake epicenters in China were published by Li and Gorshkev in 1957. For the most part, the previous studies investigated the large events ($m \geq 6.0$) for varying intervals of time from historic records and instrumentally recorded data. For example, Shi et al. (1973) studied the seismicity pattern for events with magnitude ≥ 6.0 from 1500 A.D. until 1971. Molnar and Tapponier (1975) included a map of historical and instrumentally located events for magnitudes greater than 7.0 plus other well located events between 1961 and 1970. The most extensive historical compilation is by

Academia Sinica (1956). This is a collection from different sources of varying quality. Only Mei (1960) has attempted to look at the detailed historical and instrumental seismicity for magnitudes less than 6.0. Mei used data from various sources and made no attempt to discuss the compatibility of the different data sets. In addition, there was little attempt to relate the overall seismicity pattern to the tectonics of Asia. It is clear that with the increasing interest in Asian tectonics it is necessary to have an accurate representation of Asian seismicity to correlate with other geological and geophysical data.

The most important earthquake parameters for the study are the epicenter, depth, and magnitude. By carefully defining the data sets of earthquakes used, one can attempt useful correlation of seismicity with other data such as Quaternary faulting and the major observable geologic features for this intraplate area. This study includes approximately 5,000 earthquakes and attempts to select the best data available on hypocenter and magnitude for any given period of time. Note that no relocations of individual hypocenters have been attempted. The five sources of data used in this paper and the years covered are:

1177 B.C.-1903 A.D. Chinese Earthquake Catalog, Academia Sinica, Institute of Geophysics (1970)

1904-1952 Seismicity of the Earth, Gutenberg and Richter (1954)

1953-1965 Seismicity of the Earth, Rothe (1969)

1966-1970 Bulletin of the International Seismological Centre (I.S.C.)

1971-Feb. 1975 Preliminary Determination of Epicenters (P.D.E.), U.S. Geological Survey

Each of these sources will be discussed below.

In 1956 the Academic Sinica published (in Chinese) a 2-volume set entitled Chronological Tables of Earthquake Data of China containing over 3000 years of earthquake data. This is the most extensive compilation of earthquake data of China available. It was compiled by the Third Institute of History, Academic Sinica, from dynastic histories, local annals, memoirs, newspapers, and seismic station reports for the later years. These data were later compiled in 1970 into the Chinese Earthquake Catalog by the Academic Sinica, Institute of Geophysics (in Chinese). The period of time covered was from 1177 B.C. to 1949 A.D. In this work intensities were assigned to all areas that reported a given earthquake. The epicenter was assigned to the region of greatest destruction. Lee (1958) determined an empirical relationship between intensity at the epicenter and the surface wave magnitude (M) based on a study of instrumentally located earthquakes with well determined magnitudes and intensities. This magnitude (corresponding to M of Gutenberg and Richter) was assigned to historical earthquakes and ranges from 4.75 to 8.5. Lee estimated that this magnitude determination is accurate to half a scale of magnitude. This empirical formula between magnitude and intensity has been updated by Savarensky and Mei (1960), Mei (1960), and most recently by Chen and Liu (1975). More modern relationships include the effect of the focal depth, but the data of Chen and Liu (1975) indicate that the relationship determined by Lee is still good to ±0.5 magnitude units.

Although the first reported event was in 1177 B.C., coverage since then is not complete. The historical seismicity data depend crucially on the population density. For example, the historical seismicity data

for western China, which is still sparsely populated, are incomplete. Several provinces in eastern China have a continuous record starting in 206 B.C., the beginning of the Han dynasty. The description of smaller tremors on mainland eastern China is more complete and detailed after about 1500 (Mei, 1960). The seismicity data for Taiwan are incomplete before 1900 because of the lack of recorded chronicles.

Because this paper is primarily interested in the seismicity of China, historical data for areas outside this region have not been incorporated. An exception is the large Assam earthquake of 1897, which the Chinese did not include in their compilation because it occurred outside of China. This earthquake is included on our map of large earthquakes (Figure 4).

After 1900 the Chinese Earthquake Catalog data are from all available instrumental locations, revised in some cases from macroseismic data. Because Gutenberg and Richter (1954) report only the reliably determined instrumental epicenters, we have used their book as a source in order to map more accurate locations rather than simply to plot a greater number of epicenters. In the table of magnitude 7.8 and greater earthquakes (Table 2), only 5 events are located differently in the Chinese catalog. The difference is usually a few tens of kilometers.

For the instrumentally recorded earthquakes, several kinds of magnitude determination are used. The body wave magnitude (m) is used for the events reported by Gutenberg and Richter (1954), except in the map of larger events (Figure 4),for which the revised magnitudes (M) as given by Richter (1958) are used. The data from Rothe (1969) also use the surface wave magnitude (M). The data from the I.S.C. and P.D.E. use

the surface wave magnitude (M). The data from the I.S.C. and P.D.E. use the unified body wave magnitude (m_b) defined by Gutenberg and Richter (1956). For the map of large magnitude seismicity ($M \geq 6.0$) the average of the surface wave magnitudes (M) as reported in "Seismological Notes" from the Bulletin of the Seismological Society of America was used for all events after 1965 having more than 100 stations reporting. This average value of the surface wave magnitudes was almost always equal to that reported by station PAS (Pasadena). Thus the map of large earthquakes (Figure 4) shows surface wave magnitude (M) for nearly all events, and the map of instrumentally determined epicenters (Figure 6) shows body wave magnitudes, except for the period covered by Rothe. For earthquakes with magnitude less than 6, the different magnitude determinations are usually nearly equal, while the surface wave magnitude is usually greater for larger events. The difference is not sufficient to affect our conclusions regarding patterns of seismicity.

For the I.S.C. and P.D.E. earthquake data, those events located with less than 10 stations were rejected. Although 10 is an arbitrary number, we found that the earthquakes with less than 10 reporting stations were often poorly located. Many events with less than 10 reporting stations were preliminary determinations given by the Large Aperture Seismic Array (LASA) in Montana along with a few other stations. A plot was made of the events with less than 10 reporting stations and compared to the other instrumentally located events. Because the poorly located events did neither enhance the instrumental

seismicity pattern nor add any new trends, these events were rejected. The single deep earthquake in the East China Sea and a few isolated intermediate depth earthquakes elsewhere are probably also poor locations. In addition, various explosions were rejected if identified as such in the listings.

In order to compare accurately the large quantity of seismic data with features on the LANDSAT mosaic, computer plotting of the epicenters for different time periods and magnitude ranges was done at nearly the same scale and projection as the mosaic, and transparencies of these plots were made to overlay the mosiac. The map projection that provides the best overall fit for the entire mosiac is the Lambert conic conformal projection with standard parallels at 33°N and 45°N. The scale factor, or scale distortion, at the latitude extremes is only 1.01 and at the middle latitude is only 0.99. Redrafted computer plots covering the historical seismicity (1177 B.C.-1903 A.D., Figure 5), instrumentally located seismicity (1904-February 1975, Figure 6), and all large earthquakes ($M \geq 6.0$, Figure 4) are presented here. On each map only the largest event for a given location is plotted. Such locations where several events have occurred are not indicated on the maps. The hactured regions in the Hindu Kush and northeast of Taiwan represent areas of concentrated seismicity where individual events cannot be distinguished at this scale. Locations of the largest earthquakes ($M \geq 7.8$) are given in Table 2. Of the 37 earthquakes in this table, 8 occur in the Taiwan-Ryuky region and 29 on the Asian mainland.

SEISMICITY AND QUATERNARY FAULTING

The historical (Figure 5) and instrumentally located (Figure 6) seismicity and the faults (Figure 4) show apparent differences between eastern and western China. The most striking changes between the two seismicity maps are the reversal in density of epicenters between eastern and western China and the addition of many earthquakes along the boundary between the Eurasian and Philippine plates in the instrumental seismicity map. Both changes are probably caused by the lack of adequate historical records from western China and the Taiwan-Ryukyu Islands region. Historical records from Taiwan are not complete until about 1900 (Hsu, 1971). The sparse population of western China has prevented the making of an adequate record there. Thus the instrumental seismicity map is a better representation of relative tectonic activity between different regions, because the data coverage for it is fairly uniform. The historical seismicity map is important for showing longer term variations in activity in eastern China. These variations will be discussed later.

Differences between eastern and western China are seen in the map of large earthquakes with the interpretation of Quaternary faults (Figure 4). Plotting only large earthquakes ($M \geq 6$) eliminates much of the diffuse seismicity and enables trends to be seen more clearly. In addition, these earthquakes usually have more accurate locations and are more important in tectonic interpretations. This map shows that the tectonics of western China is dominated by reactivated Paleozoic mountain belts: the Altai, Tien Shan, A-erh-chin Shan, Nan Shan, and Kunlun mountains, in addition to the active plate margin seismicity at the Himalayas and to the seismicity within Tibet. These active belts

contrast with the nearly aseismic Tarim, Dzungarian, and Tsaidam basins. The large strike-slip faults within and along these belts may have been important in accomodating some of the relative motion between India and Eurasia after the beginning of their collision (Molnar and Tapponnier, 1975). For most of their length, these faults are not well-defined seismically, probably because the time period of existing data is too short. A similar argument may apply to some other major strike-slip faults such as the Alpine fault in New Zealand and the Garlock fault in California. However, some fault displacements along the strike-slip faults have been observed (Figure 4). In addition, thrusting in 1932 (Table 1) along the eastern extension of the major fault through the A-erh-chin Shan mountains suggests that this fault is connected to the fault northeast of the Nan Shan. This connection, being a thrust fault, is not distinct on the satellite images and is not shown in Figure 4. Although the total displacement on these faults is probably large, the determination of the amount of Quaternary and Cenozoic displacements must await field investigations.

The Quaternary tectonics of eastern China appears to be dominated by the Shansi graben and right-lateral strike-slip faulting (Figure 4). In contrast to the reactivated Paleozoic mountain belts in western China, the Shansi graben in a Cenozoic feature (Li and Li, 1973). Southeastern China, the site of much Mesozoic tectonic activity is relatively aseismic. As in western China, there are basins, here the Ordos and Swechwan basins, virtually without seismicity and Quaternary faulting.

Another important difference between western and eastern China is the

generally east-west trend of mountain ranges and basins in western China compared to the generally northeasterly trend in eastern China. This difference is reflected in the seismicity by the occurrence of more earthquakes in western China (Figure 6) and by a roughly north-south trend of seismicity along the border (approximately 100-105°E) between the two regions. This difference of trend from western to eastern China is also seen in the map of Quaternary faults (Figure 4). In part, the difference may reflect the change from west to east in Paleozoic and Mesozoic orogenic trends (Li and Li, 1973) In western China these orogenic trends may have been reactivated by the collision of India with Eurasia during the Cenozoic (Molnar and Tapponnier, 1975). Subsequent crustal shortening and isostatic uplift could be responsible for the higher average elevation in western China compared to eastern China.

In addition to the difference in trend, the Quaternary faults show a difference in the type of tectonics between western and eastern China. In western China, the long, linear nature of some of the faults and the juxtaposition of often contrasting rock types (Figure 3) suggests that these may be major strike-slip faults. Where observed or inferred (Figure 4), the sense of motion is left-lateral. Important thrust faults in western China may not be shown in Figure 4, because of the problems in interpretation discussed earlier. In contrast to this, the most spectacular feature seen in the LANDSAT images for eastern China is the Shansi graben with its normal faults. The LANDSAT images and fault plane solutions (Molnar and others, 1973) also indicate the presence of northeasterly trending right-lateral strike-slip faults in eastern China. Thus either the deformation in eastern and western China are caused by different forces or the two regions are responding differently to the same forces.

CYCLES OF SEISMICITY

Although instrumental data provide the most objective map of seismicity, the historic record shows that the 70-year instrumental period is too short to give an accurate representation of seismic activity. A good example comes from the Shansi graben area. Quaternary faulting in the graben is readily apparent in the LANDSAT images (Figure 1). Also the historical seismicity map (Figure 5) and the large earthquake map (Figure 4) show significant activity in this area. However, instrumentally located seismicity (Figure 6) here is virtually absent. Thus this area supports the thesis that faults with Quaternary activity should be considered as potential sites for future earthquakes, even though the instrumental record or a short historical record shows very little seismicity.

The relatively few instrumentally located epicenters in southeastern China compared to the historical record appears to reflect only the smaller time interval used for the instrumentally located epicenters. That is, for the area bounded by longitudes 105°E and 120°E and latitudes 20°N and 30°N, the instrumentally recorded earthquakes, if recorded at the same rate for 600-800 years, would produce approximately the number recorded historically. The historical record includes more than this 600-800 years, but much of the record is incomplete. One important aspect of the historical record for southeastern China is that it demonstrates that small earthquakes, usually less than magnitude 6, occur throughout this region. Other intra-plate areas may have similar diffuse seismicity over a period of a few thousand years.

Shih et al. (1974b) have attempted to quantify the length of record needed by studying cycles of seismicity. They divided China into 23 seismic zones and determined active and quite periods for each zone (for example, see Figure 7). They found that the average length of a cycle decreases from 700-1000 years for nearly aseismic regions such as southeastern China to 15-18 years for highly seismic regions such as Taiwan, although notable exceptions to this decrease in period with increase in seismicity do exist (Allen, 1975). The cycle could sometimes be divided into several stages, the final stage culminating with a large earthquake. If such cycles are applicable to other intraplate areas, which often have historic records of only a few hundred years at most, then clearly other studies, such as of Quaternary faulting, are needed to realistically evaluate seismic risk.

CONCLUSIONS

Because most of the instrumentally located intraplate seismicity in China is north of the Himalayas, this seismicity may be caused by the continuing collision of India and Eurasia. The resulting high relief of the Himalayas and Tibet and the clusters of intermediate depth earthquakes beneath the Hindu Kush and Burma distinguish this area from other active collision zones around the world. Using fault plane solutions and LANDSAT imagery, Molnar and Tapponnier (1975) have concluded that the intraplate deformation is caused by high stresses transmitted from the collision zone. In our more detailed study of the imagery the inferred senses of motion on the strike-slip faults in western China (Figure 4) are broadly consistent with their hypothesis. Our inferred left-lateral motion on the fault

immediately northeast of the Tarim Basin (see Figure 3D) is opposite to theirs, but this location is in an area of transition between left- and right-lateral faulting, and hence the change does not appear to affect their conclusion. Based on fault plane solutions, they choose right-lateral motion on the northwest trending faults in Russia north of the Tarim Basin, but we have found no evidence in the imagery for either sense of motion. Because this change from left- to right-lateral faulting is critical to their model our data do not unambiguously support their model. However, other fault plane solutions (Das and Filson, 1975) show east-west trending thrust faults near the same area, which have a direction of maximum compressive stress consistent with right-lateral motion on northwest trending faults and hence can be interpreted as supportive of Molnar and Tapponnier's model for this area.

A particularly difficult fault zone to model in terms of stress guided from major plate boundaries is between Tibet and the Swechwan Basin at approximately 100°E. Its north to northwest strike would indicate right-lateral faulting if its motion were to be similar to the plate boundary nearby in Burma. However, historic breaks (Table 1) and fault plane solutions demonstrate that this fault, which is clearly visible on LANDSAT imagery, is left-lateral. Thus this area is either moving independently of the Himalaya collision zone processes or responding to the collision by "squeezing" out material, as Molnar and Tapponnier (1975) suggested.

East of 105-110°E the style of deformation changes rapidly. The left-lateral faults of western China decrease in number and the normal faults of the Shansi graben predominant. Fault plane solutions indicate

that the north-northeast trending faults to the east and northeast of the graben are right-lateral. Das and Filson (1975) point out that north-south compression southwest of Lake Baikal quickly changes to northwest trending extension within the Baikal rift zone. Molnar and Tapponnier (1975) relate the Cenozoic Shansi and Baikal grabens to the large strike-slip faults and not to upper mantle diapirism beneath the grabens. Both of these gabrens are bounded on the south by strike-slip faults that appear to end near the grabens (Figure 4). The Cenozoic displacements near the end of the faults may have been taken up by the opening of the grabens. This is best seen in the Shansi graben, where left-lateral displacements have been observed on the strike-slip fault system and the graben is clearly widest at the southern end. We note that the termination of a strike-slip fault near one end of an intraplate graben may distinguish this mechanism of formation from other ones.

To explain the change in tectonics from western to eastern China, Shi et al. (1973) postulated that India-Eurasia plate boundary causes deformation in the west and that stresses from the Pacific-Eurasia boundary predominate in the east. The smaller Phillippine plate would not

be as important. While this model does account for the change in strike-slip faulting from west to east, the mechanism by which stresses are transmitted from the Japanese arc subduction zone with its complications of back-arc spreading is less apparent than for stress transmission from the Himalayas (discussed by Molnar and Tapponnier, 1975).

The models discussed thus far involve internal deformation within the Eurasian plate. The existence of nearly aseismic blocks, the basins disucssed earlier, separated by areas with seismicity and Quaternary faults lends support to the concept of a mosiac of small plates instead of internal deformation. The boundaries between these plates would not be single, discrete faults but broad zones of faults. While this concept is useful in pointing out that deformation is not uniform across China but is often concentrated in certain zones, a satisfactory division of all of the region in Figure 4 into small plates is not apparent. The main problem is that the zones of deformation do not form a continuous network. Das and Filson (1975) attempted to divide the region in Figure 4 into six plates. However, their attempt is not highly satisfying because much deformation occurs far from their boundaries and large segments of their boundaries are not associated with seismicity or Quaternary faulting. Therefore we would classify the deformation away from the major plate boundaries as intraplate tectonics.

Although the sources of high stress in intraplate regions of the world may well vary from area to area, there are certain similarities in the responses of the crust to these stresses. One characteristic is reactivation of Phanerozoic orogenic belts. In addition to the reactivated Paleo-

zoic belts in China mentioned earlier, others belts, usually with minor seismicity, are the Appalachians in eastern North America and the Tasman and Adelaide Geosynclines in Australia. While it is usually difficult to prove that the seismicity is associated with pre-existing faults, the observation that earthquakes often occur within the orogenic belt but rarely on adjacent platform areas is suggestive of such an association. There is field evidence for Quaternary movement on pre-existing faults in the Tien Shan (Dergunev, 1972), Altai (Adamenko, 1971) and Nan Shan (Shih et al., 1974a, Yu, 1963) ranges. Other Paleozoic ranges, such as the Khingans in northeast China and the Urals in Russia, appear to have only very minor seismicity. Thus reactivation of Phanerozoic orogenic belts in intraplate regions is common but not universal.

This effect of pre-existing zones of weakness may explain why India has very few earthquakes compared to the region north of the Himalayas. Other than the Cretaceous to Early Tertiary flood basalts, India consists predominantly of Precambrian shield rocks, many of whose fault zones may have been healed through metamorphism. Occasional earthquakes such as the 1967 Koyna earthquake (M-6.4) and the 1969 Bhadrachulam earthquake (M-5.7) indicate that India is under high north-south compressive stress, but the lack of Phanerozoic orogenic belts in India may dictate a different response to high stresses than for China.

In China and other intraplate regions there are also large earthquakes that do not occur within Phanerozoic orogenic belts. Earthquakes within and to the east and northeast of the Shansi graben, in the Rhinegraben, in the central Mississippi River valley, and in the St. Lawrence valley

are examples. The locations of such earthquakes are still usually sites of pre-existing weaknesses. Because these earthquakes are usually infrequent, geological and geophysical investigations, such as of Quaternary faulting, are especially valuable in these regions.

REFERENCES

Academia Sinica, Seismological Committee (1956). Chronological Tables of Earthquake Data of China (in Chinese), Science Press, Peking, 2 vol., 1653 pp.

Academia Sinica, Institute of Geophysics (1970). Chinese Earthquake Catalog (in Chinese), Academia Sinica, Peking, 361 pp.

Adamenko, O.M. (1971). Thrusts in marginal zones of neotectonic uplifts in the Altai, Geotectonics, No. 4, 260-261.

Allen, C.R. (1975). Historic records of Chinese earthquakes, in Earthquake research in China, Transactions, Am. Geophys. Union 56, 856-858.

Bonilla, M.G. and C.R. Allen (1975). Seismotectonics in China, in Earthquake research in China, Transactions, Am. Geophys. Union 56, 853-856.

Central Intelligence Agency (1971). Peoples Republic of China, Atlas, U.S. Government Printing Office, Washington, D.C. 82 pp.

Chen, P. and J. Liu (1975). A study of relation between seismic magnitude and intensity by using the dislocation model (in Chinese), Acta Geophysica Sinica 18, 183-195.

Das, S. and J. R. Filson (1975). On the tectonics of Asia, Earth and Planetary Science Letters 28, 241-253.

Dergunov, A.B. (1972). Compression and extension structures in the eastern Altai in the Quaternary, Geotectonics, No. 3, 187-192.

Drake, N.F. (1912). Destructive earthquakes in China, Bull. Seism. Soc. Am. 2, 40-133.

Earth Resources Technology Satellite Data Users Handbook (1972). General Electric Document No. 71504242, revised.

Florensov, N.A. and V.P. Solonenko, eds. (1965). The Gobi-Altai Earthquake, U.S. Dept. Commerce TT 65-50012, 424 pp.

Gutenberg, B. and C.B. Richter (1954). Seismicity of the Earth and Associated Phenomena, Princeton University Press, 310 pp.

Gutenberg, B. and C.F. Richter (1956). Magnitude and energy of earthquakes, Annals. Geofis., 9, 1 ff.

Heim, A. (1934). Earthquake Region of Taofu, Bull. Geol. Soc. Am. 45, 1035-1050.

Hsu, M.T. (1971). Seismicity of Taiwan and some related problems, Bull. Internat. Inst. of Seism. and Earthquake Eng. 8, 41-160.

Lang, W.J. and R.J. Sun (1966). Seismicity, in Atlas of Asia and Eastern Europe to Support Detection of Underground Nuclear Testing, Vol. 3, U.S. Geol. Surv., Washington, D.C.

Lee, S.P. (1957). The map of seismicity of China (in Chinese), Acta Geophysica Sinica, 6, 127-158.

Lee, S.P. (1958). A practical magnitude scale (in Chinese), Acta Geophysica Sinica, 7, 98-102.

Li, G.P. and Y.S. Li (1973). The features of Mesozoic and Cenozoic tectonic developments in eastern China and their relationship to seismicity (in Chinese), Sci. Geol. Sinica, No. 3, 238-244.

Li, S.P. and G.P. Gorshkov (1957). A map of the seismic regions of China, Acta Geophysica Sinica, 6.

Liu, Y.M., H. Yao, and H. N. Chou (1975). Analysis of the characteristics and trends of seismic activities in the Keping rupture zone in Sinkiang, China, Acta Geophysica Sinica 18, No. 1.

Mei, S.Y. (1960). The seismic activity of China, Akad. Nauk. SSR Izv. Ser. Geofiz. 254-264.

Min, T.C. (1957). Study of strong earthquakes from historical records, Acta Geophysica Sinica 6, 49-58.

Molnar, P. and P. Tapponnier (1975). Cenozoic tectonics of Asia: effects of a continental collision, Science 189, 419-426.

Molnar, P., T.J. Fitch, and F.T. Wu (1973). Fault plane solutions of shallow earthquakes and contemporary tectonics in Asia, Earth Planet. Sci. Letters 19, 101-112.

National Seismological Bureau (1975). The Geodetic Survey Brigade for Earthquake Research, Acta Geophysica Sinica 18, No. 4.

Richter, C.B. (1958). Elementary Seismology, W.H. Freeman and Company, Inc., San Francisco, 768 pp.

Rothe, (1969). The Seismicity of the Earth, UNESCO, Belgium, 336 pp.

Savarensky, E.F., and S.Y. Mei (1960). On the evaluation of the intensity of earthquakes in the territory of China, Akad. Nauk. SSR Izv. Ser. Geofiz., 86-88.

Shi, Z.L., W.L. Huan, H.R. Wu, and X.L. Cao (1973). On the intensive seismic activity in China and its relation to plate tectonics (in Chinese), Sci. Geol. Sinica, No. 4, 281-293.

Shih, C.L., W.L. Huan, K.K. Yao and Y.T. Hsie (1974a). On the fracture zones of Changna earthquake of 1932 and their causes (in Chinese), Acta. Geophysica Sinica 10, 272-287.

Shih, C.L., W. L. Huan, H. L. Tsao, H.Y. Wu, Y.P. Liu, and W. K. Huang (1974b). Some characteristics of seismic activity in China (in Chinese), Acta Geophysica Sinca 17, 1-13.

Short, N.M. and P.D. Lowman, Jr. (1973). Earth observations from space: Outlook for the geological sciences, Goddard Space Flight Center, Greenbelt, Maryland, 115 pp.

Shu, S. (1974). The characteristics of the Lahu earthquake (M-7.9) and the seismicity of this region (in Chinese), Acta Geophysica Sinica 17, no. 2.

Yu, P.L. (1963). Certain ideas on the particular features of young tectonic movements in the Kansu corridor, in Pavlinov, V.N., ed., Works of the first conference on neotectonics in China, U.S. Dept. Commerce, Joint Publications Research Service 19815, 183-197.

TABLE 1

SURFACE FAULTING IN CHINA AND SURROUNDING REGIONS

Date (D.M.Y.)	Latitude (°N)	Longitude (°E)	Magnitude	Fault Strike	Sense of Motion	Reference
09.07.1905	49	99	8.2	∽EW	not reported	A.V. Voznesenskii in Florensov and Solonenko (1965)
16.12.1920	36.5	105.7	8.5	not reported	left-lateral	M.C. Li, in Bonilla and Allen (1975)
24.03.1923	31.3	100.8	7.3	N55W	not reported	Heim (1934)
25.05.1927	37.5	102.8	8	not reported	not reported	Ambraseys in Bonilla and Allen 1975)
25.12.1932	39.7	97.0	7.6	∽EW	reverse, right-lateral	Shih et al. (1974a)
04.12.1957	45.2	99.2	8.3	∽EW	left-lateral	Florensov and Solonenko (1965)
05.01.1970	24.0	102.7	7.7	N70W	right-lateral	National Seismological Bureau (1975)
16.01.1972	40.3	79.0	6.2	N52E	reverse, left-lateral	Liu et al. (1975)
06.02.1973	31.5	100.7	7.9	N55W	left-lateral	Shu (1974)

TABLE 2

EARTHQUAKES OF CHINA AND SURROUNDING REGIONS ($M \geq 7.8$)

Date (D.M.Y.)	Origin Time (U.T.)	Latitude (°N)	Longitude (°E)	Magnitude	Depth (km)
17.09.1303	--	36.3	111.7	8.0	--
23.01.1556	--	34.5	109.7	8.0	--
29.12.1604	--	25.0	119.5	8.0	--
25.07.1668	--	35.3	118.6	8.5	--
02.09.1679	--	40.0	117.0	8.0	--
18.05.1695	--	36.0	115.0	8.0	--
03.01.1739	--	38.9	106.5	8.0	--
06.09.1883	--	25.2	103.0	8.0	--
22.08.1902	--	39.5	76.0	8.25	--
07.06.1904	08:17:54	40.0	134.0	7.9	350
24.08.1904	20:59:54	30.0	130.0	7.9	0
04.04.1905	00:50:00	33.0	76.0	8.6	0
02.06.1905	05:39:42	34.0	132.0	7.9	100
09.07.1905	09:40:24	49.0	99.0	8.4	0
23.07.1905	02:46:12	49.0	98.0	8.7	0
22.12.1906	18:21:00	43.5	85.0	8.3	0
07.07.1909	21:37:50	36.5	70.5	8.1	230
10.11.1909	06:13:30	32.0	131.0	7.9	190
12.04.1910	00:22:13	25.5	122.5	8.3	200
03.01.1911	23:25:45	43.5	77.5	8.7	0
18.02.1911	18:41:03	40.0	73.0	7.8	0
15.06.1911	14:26:00	29.0	129.0	8.7	160
23.05.1912	02:24:06	21.0	97.0	7.9	0
05.06.1920	04:21:28	23.5	122.0	8.3	0

TABLE 2

EARTHQUAKES OF CHINA AND SURROUNDING REGIONS (continued)

Date (D.M.Y.)	Origin Time (U.T.)	Latitude (°N)	Longitude (°E)	Magnitude	Depth (km)
16.12.1920	12:05:48	36.0	105.0	8.6	0
15.11.1921	20:36:38	36.5	70.5	8.1	215
22.05.1927	22:32:42	36.75	102.0	8.3	0
10.08.1931	21:18:40	47.0	90.0	7.9	0
15.01.1934	08:43:18	26.5	86.5	8.4	0
14.02.1934	03:59:34	17.5	119.0	7.9	0
12.09.1946	15:20:20	23.5	96.0	7.8	0
20.12.1946	19:19:05	32.5	134.5	8.4	0
29.07.1947	13:43:22	28.5	94.0	7.9	0
15.08.1950	14:09:30	28.5	96.5	8.7	0
18.11.1951	09:35:47	30.5	91.0	7.9	0
27.06.1957	00:09:28	56.4	116.5	7.9	33
04.12.1957	03:37:48	45.2	99.2	8.3	33

FIGURE CAPTIONS

Figure 1. Mosiac of LANDSAT imagery of China and surrounding regions. Approximately Lambert conic conformal projection.

Figure 2. Physical features of China and surrounding regions.

Figure 3. A. Lower fault is part of the major fault indicated in Figure 4 by a solid line immediately southeast of the Tarim Basin. Upper faults are smaller subsidary faults. Center of image is approximately 40°N, 95 1/2°E.

B. An apparently naturally dammed lake along the same major fault as in Figure 3A. Lake is approximately at 38 1/2° N, 90°E.

C. Portion of the left-lateral Bogdo fault, which moved in 1957 (Table 1). Fault is in Mongolia at approximately 45°N.

D. Apparent left-lateral offset of dark rock unit along fault immediately northeast of the Tarim Basin (Figure 4). Center of image is approximately 41°N, 91 1/2°E.

Figure 4. Map of large earthquakes ($M \geq 6$) and of Quaternary faulting interpreted from LANDSAT imagery. Sense of fault movement inferred from imagery is indicated by arrows with open heads and determined from known surface faulting is indicated by arrows with solid heads.

Figure 5. Seismicity of China and surrounding regions from historical records.

Figure 6. Instrumentally located seismicity of China and surrounding regions.

Figure 7. Examples of active and quiet periods of seismicity in two regions of China. From Shih et al. (1974b).

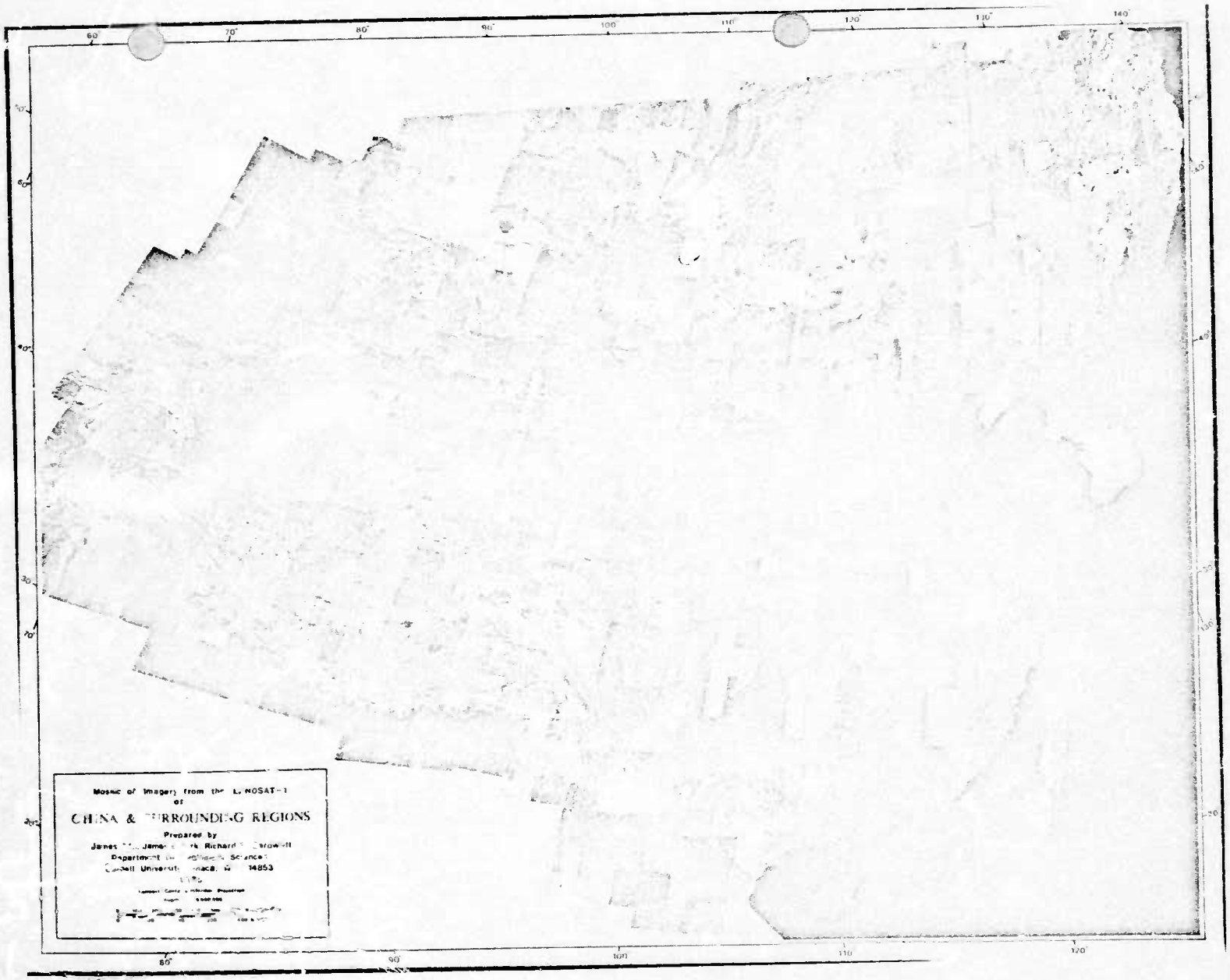
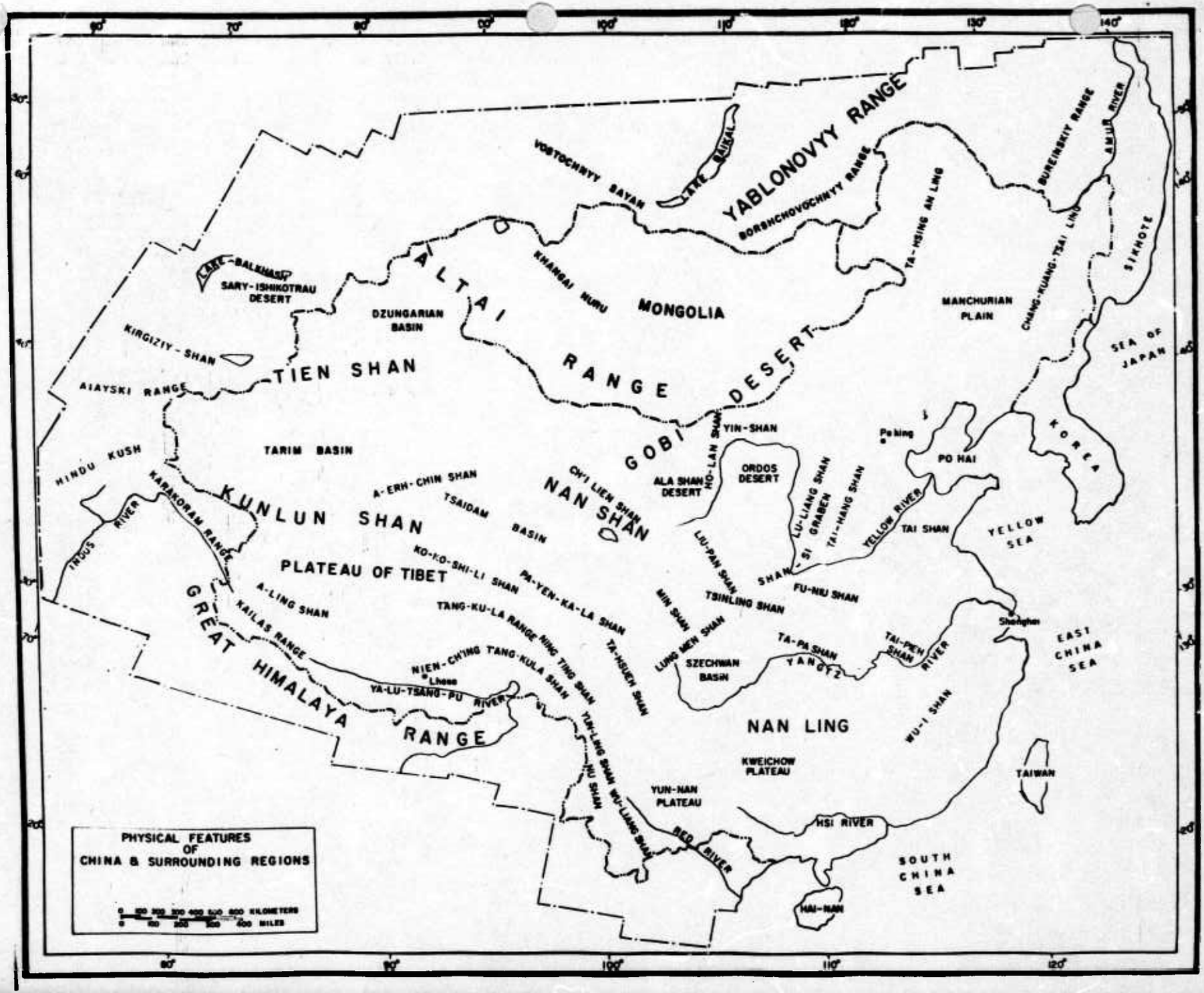
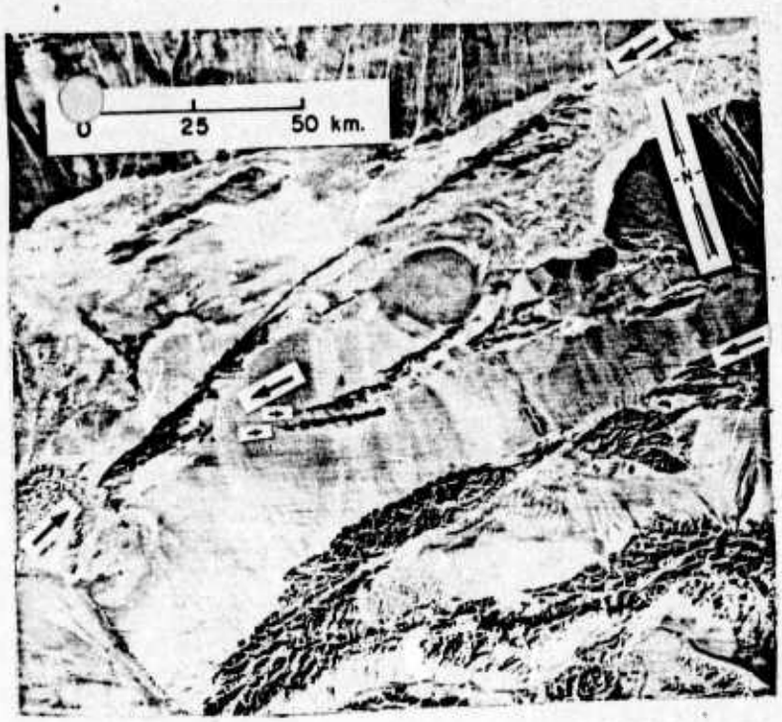
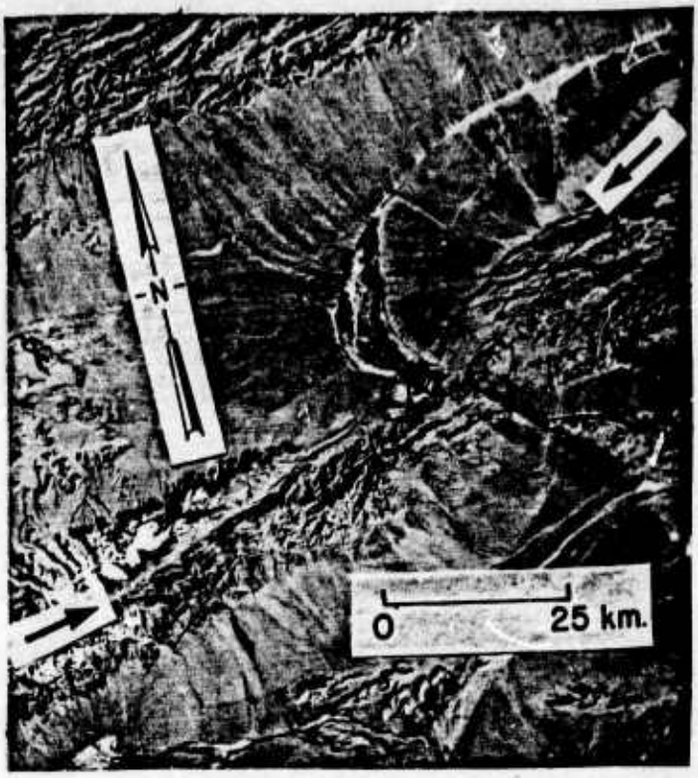

Mosaic of Imagery from the LANDSAT-1
of
CHINA & SURROUNDING REGIONS
Prepared by
Department of Agricultural Science
Cornell University, Ithaca, N.Y. 14853

Fig. 1

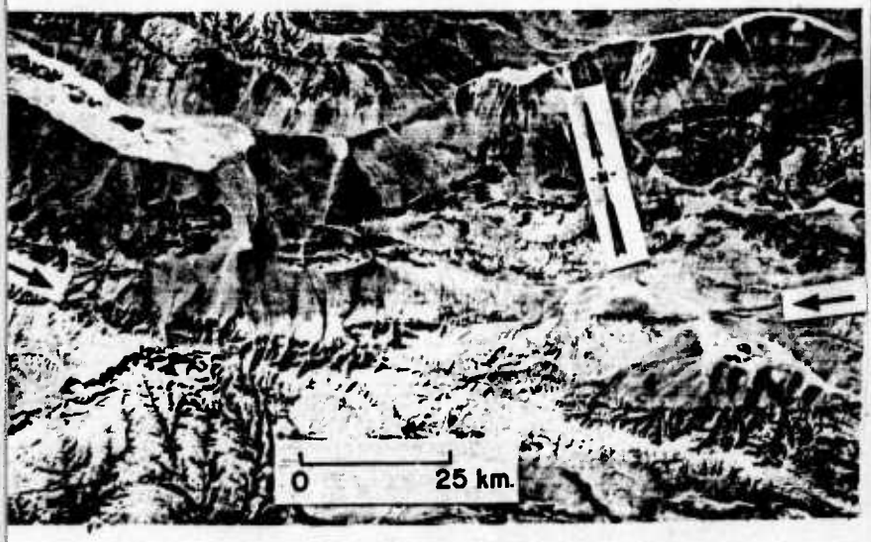

YABLONOVYY RANGE
VOSTOCHNYY SAYAN
BORSHCHOVOCHNYY RANGE
BUREINSKIY RANGE
AMUR RIVER
SIKHOTE
TA-HSING AN LING
CHANG-KUANG-TSAI LING
LAKE BAIKAL
LAKE BALKHASH
SARY-ISHIKOTRAU DESERT
DZUNGARIAN BASIN
ALTAI
KHANGAI NURU
MONGOLIA
MANCHURIAN PLAIN
SEA OF JAPAN
KIRGIZIY-SHAN
TIEN SHAN
AIAYSKI RANGE
RANGE
GOBI DESERT
YIN-SHAN
Peking
KOREA
HINDU KUSH
TARIM BASIN
HO-LAN SHAN
ORDOS DESERT
PO HAI
ALA SHAN DESERT
A-ERH-CHIN SHAN
CH'I LIEN SHAN
NAN SHAN
LU-LIANG SHAN
TAI-HANG SHAN
YELLOW RIVER
TAI SHAN
YELLOW SEA
KUNLUN SHAN
TSAIDAM BASIN
KARAKORAM RANGE
INDUS RIVER
LIU-PAN SHAN
SHAN-SI GRABEN
KO-KO-SHI-LI SHAN
PA-YEN-KA-LA SHAN
PLATEAU OF TIBET
TSINLING SHAN
FU-NIU SHAN
MIN SHAN
LUNG MEN SHAN
A-LING SHAN
TANG-KU-LA RANGE
NING TING SHAN
TA-HSUEH SHAN
KAILAS RANGE
GREAT HIMALAYA RANGE
NIEN-CH'ING TANG-KULA SHAN
Lhasa
YA-LU-TSANG-PU RIVER
SZECHWAN BASIN
TA-PA SHAN
YANGTZ
TAI-PEH SHAN
RIVER
Shanghai
EAST CHINA SEA
NAN LING
WU-I SHAN
KWEICHOW PLATEAU
TAIWAN
YUN-NAN PLATEAU
YUN-LING SHAN
WU-LIANG SHAN
HSI RIVER
RED RIVER
SOUTH CHINA SEA
HAI-NAN
PHYSICAL FEATURES OF CHINA & SURROUNDING REGIONS
KILOMETERS
MILES



A



B



C



D

Figure 3

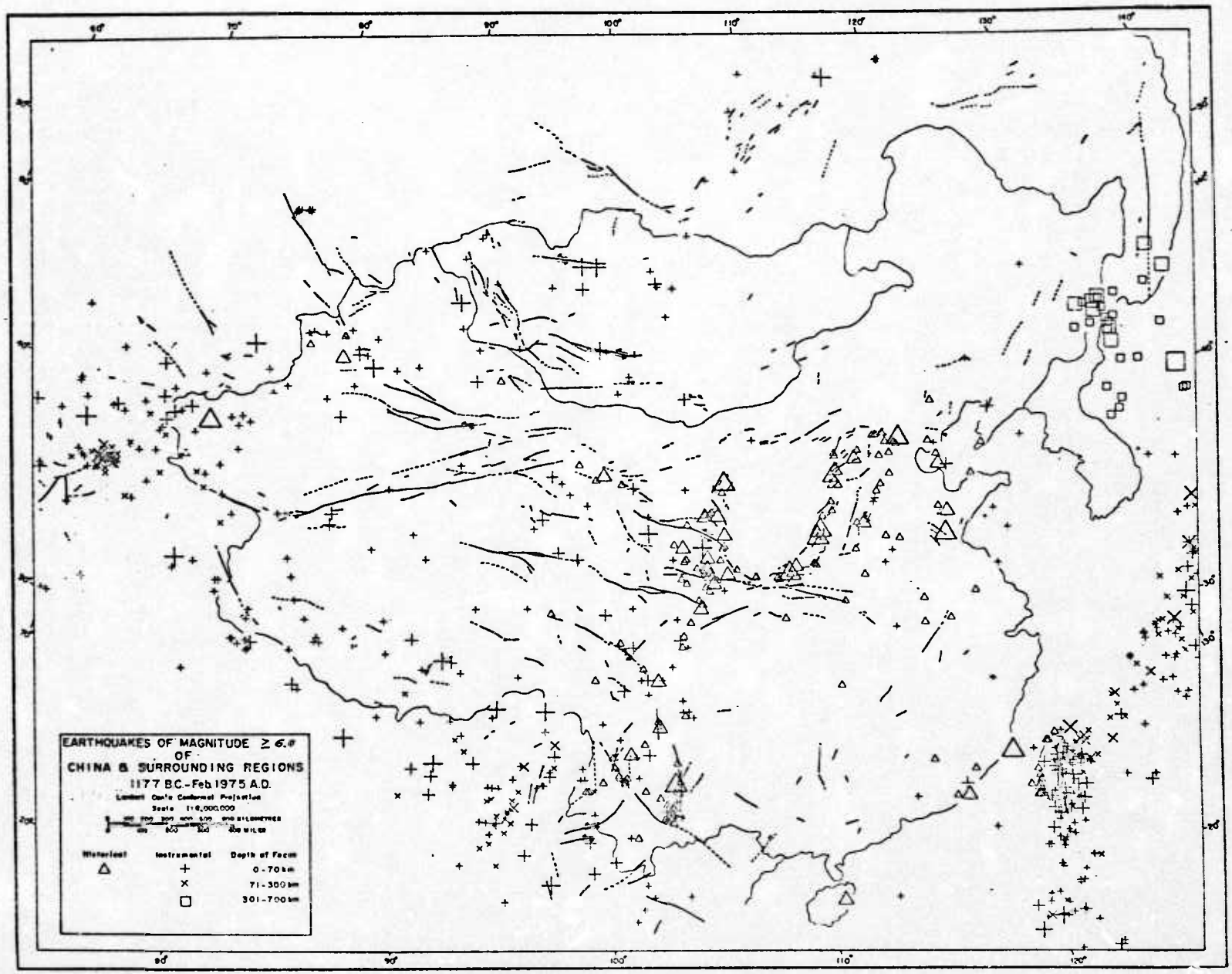

EARTHQUAKES OF MAGNITUDE ≥ 6.0
OF
CHINA & SURROUNDING REGIONS
1177 B.C.-Feb 1975 A.D.
Lambert Conic Conformal Projection
Scale 1:8,000,000
Historical
Instrumental
Depth of Focus
0-70 km
71-300 km
301-700 km

Fig 4.

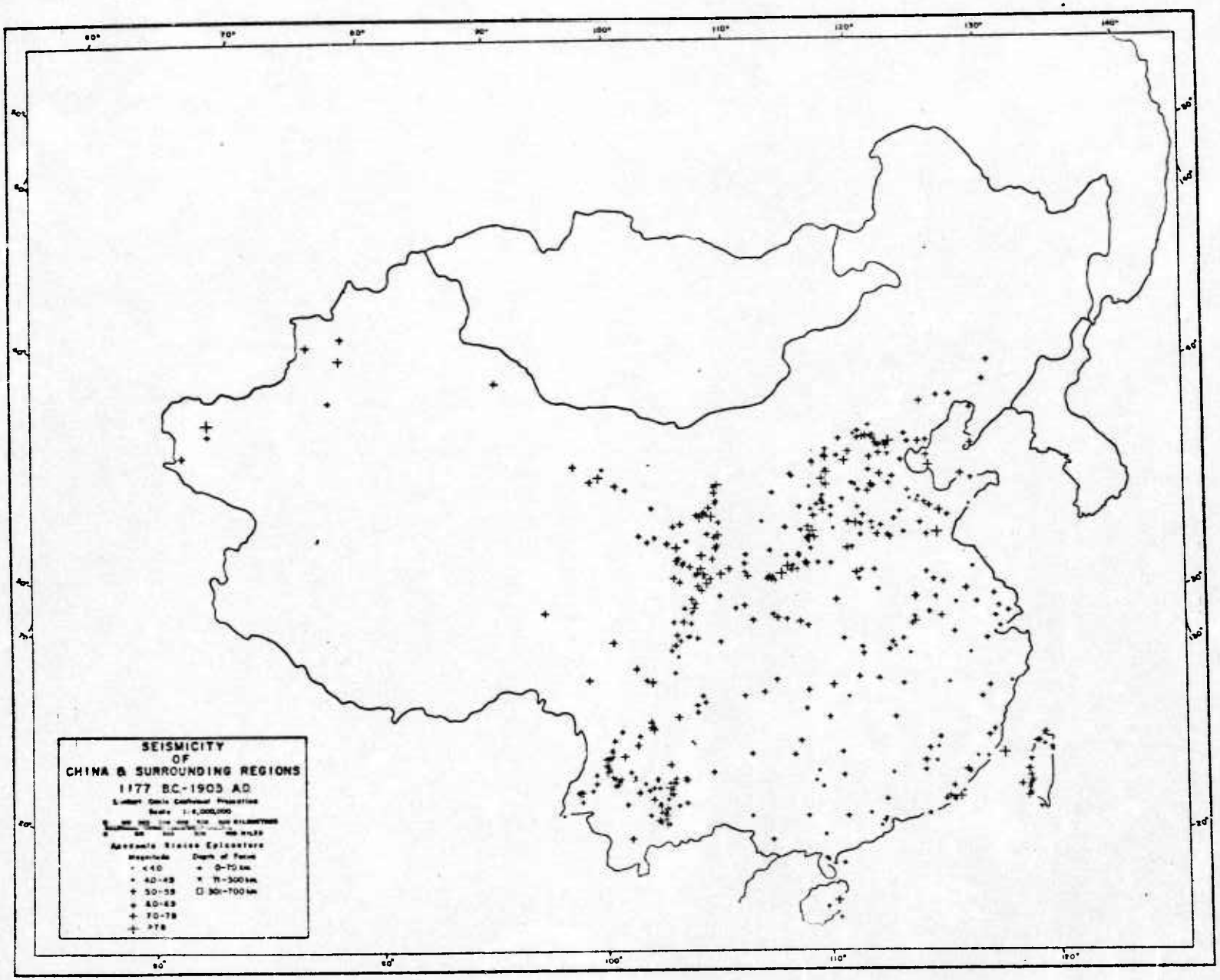


Fig. 5

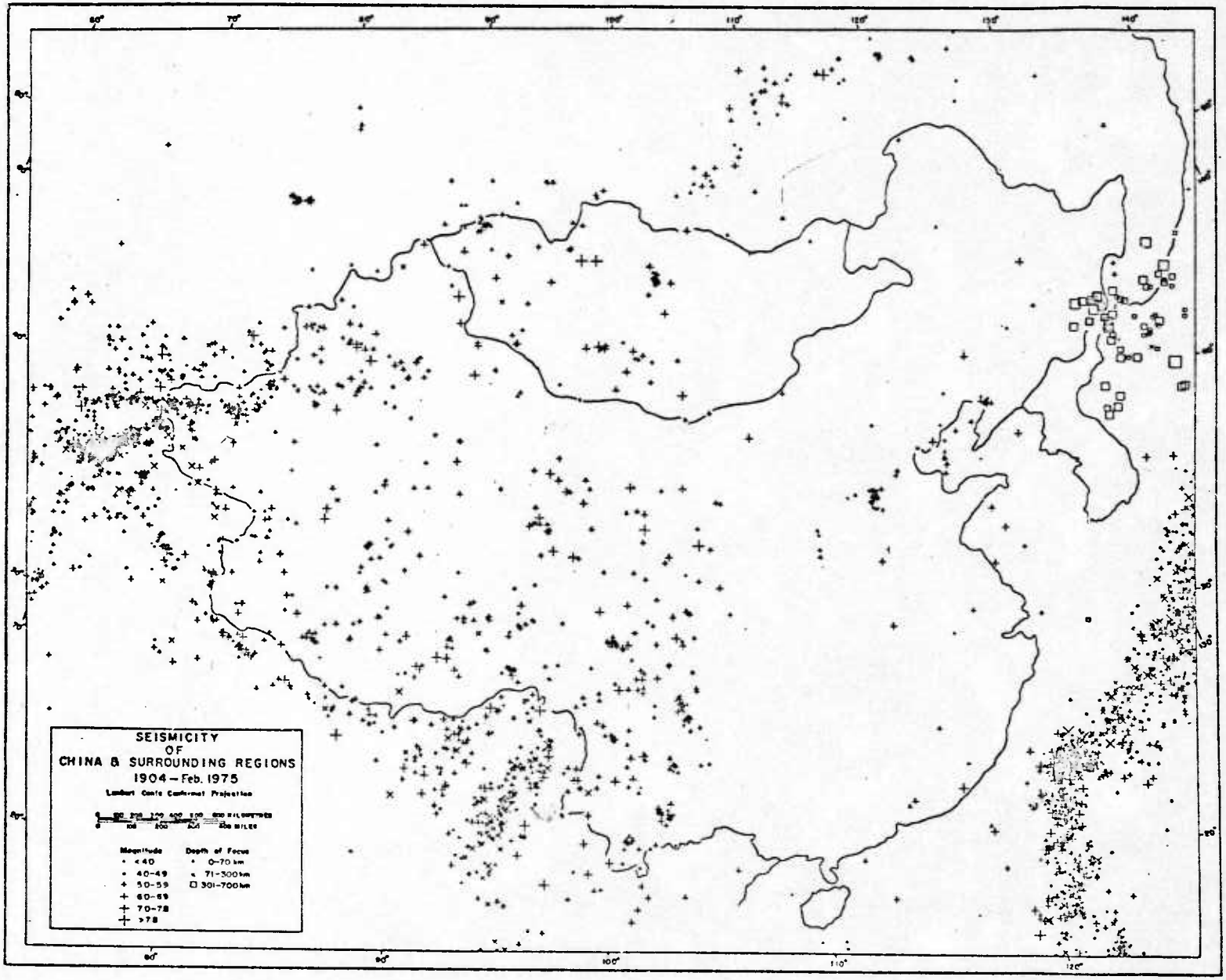
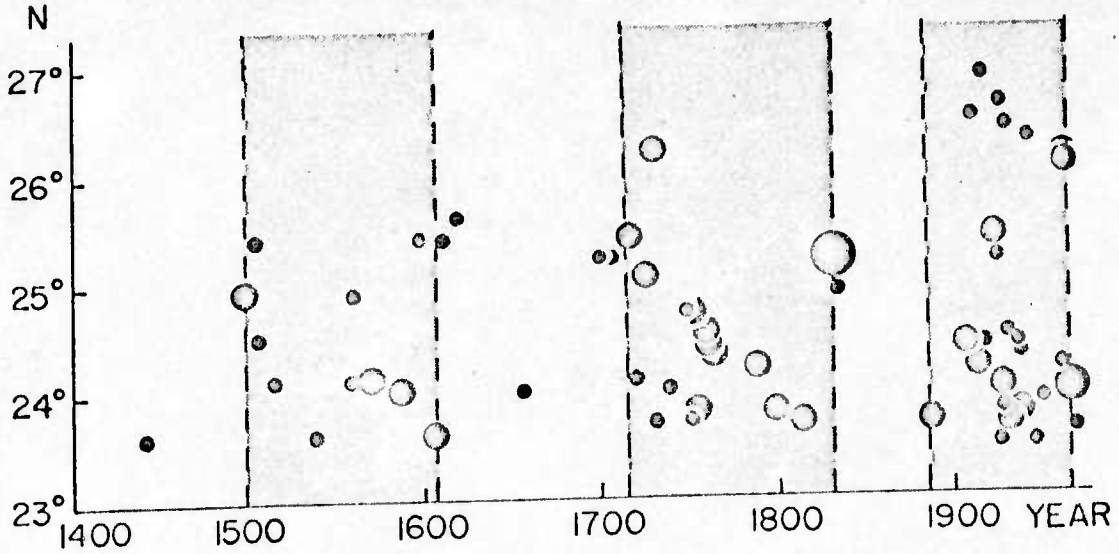
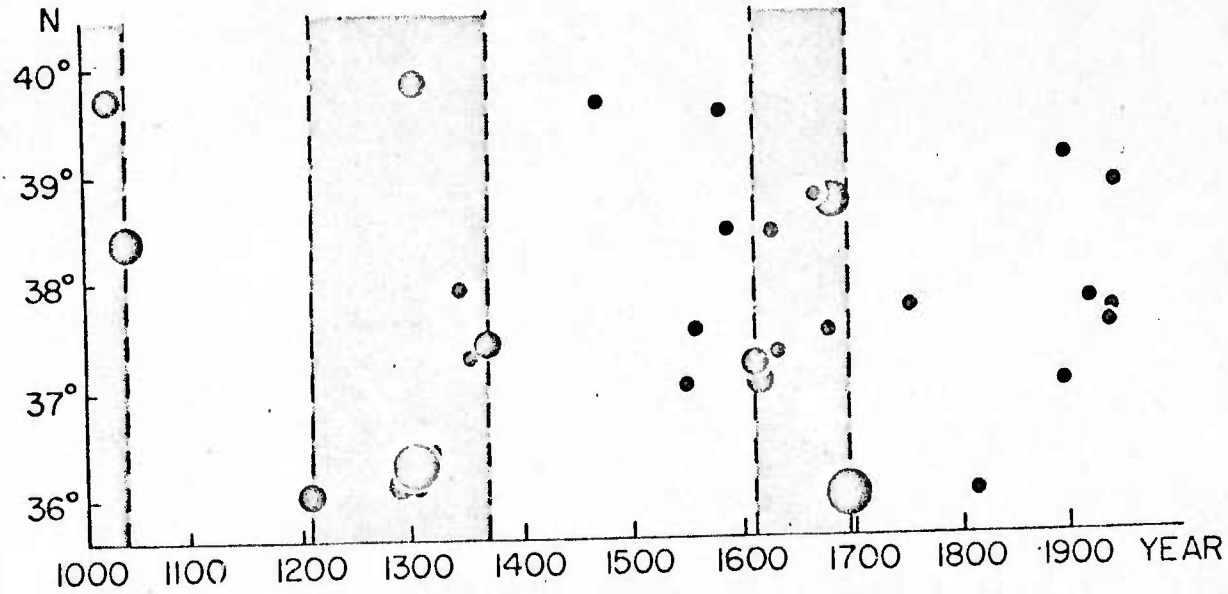

SEISMICITY
OF
CHINA & SURROUNDING REGIONS
1904 – Feb. 1975
Lambert Conic Conformal Projection
Magnitude
< 4.0
4.0–4.9
5.0–5.9
6.0–6.9
7.0–7.8
> 7.8
Depth of Focus
0–70 km
71–300 km
301–700 km

Fig. 6

EASTERN YUNNAN SEISMIC ZONE



SHANSI SEISMIC ZONE



• M=5.0-5.9 ◉ M=6.0-6.9 ○ M=7.0-7.8 ◯ M > 7.8

▭ QUIET PERIOD ▭ ACTIVE PERIOD

Figure 7

APPENDIX G

INVESTIGATION OF THE 1966 EARTHQUAKE SERIES IN NORTHERN CHINA USING THE METHOD OF JOINT EPICENTER DETERMINATION

Richard K. Cardwell and Bryan L. Isacks

Department of Geological Sciences

Cornell University

Ithaca, New York 14853

ABSTRACT

A series of destructive earthquakes occurred in northern China during March 1966 in an area with no previous instrumentally-located seismicity. The tectonics of this intraplate region are poorly understood. Examination of LANDSAT-1 imagery revealed evidence of recent surface faulting in this and other nearby regions of northern China. The method of "Joint Epicenter Determination" (JED) was used to relocate the epicenters of the earthquakes. The best relocations were obtained with the JED method using a station-corrected calibration event. These locations, along with published fault plane solutions, historical earthquake records, and LANDSAT-1 imagery are in very good agreement with the published field investigations that reported the earthquakes to have occurred along a large right-lateral strike-slip fault zone. The sense of motion on this strike-slip feature appears to be related to an extensional stress system oriented NNW-SSE in the region of the Shansi Graben and the North China Plain.

INTRODUCTION

The seismicity of intraplate areas is very poorly understood due to the sporadic occurrence and diffuse distribution of intraplate earthquakes. The problem is further complicated by the fact that detailed field studies of these intraplate areas are not always possible. It is thus desirable to develop reliable techniques using remote sensing data to study these areas. Seismograms recorded at teleseismic distances and satellite imagery are ideally suited for this type of investigation.

These data are used to examine a series of earthquakes that occurred in northern China -- an area well within the boundaries of the Eurasian Plate. The results of extensive field investigations are available for the earthquakes so that comparison can be made between these field investigations and the results from seismic and optical remote sensing. This paper compares various methods of location using teleseismic data in order to determine as accurately and precisely as possible the spatial distribution of the earthquakes. The best locations, fault plane solutions, and satellite imagery all agree with published field investigations and show that the earthquakes occurred along a large right-lateral strike-slip fault zone. It is concluded that careful relocation procedures and detailed analyses of satellite imagery make it possible to locate faults associated with shallow focus intraplate seismicity using remote sensing data.

REGIONAL GEOLOGY AND TECTONICS

Figure 1 is a map of the instrumentally located seismicity of China and surrounding regions from 1904 to February, 1975. There is a large

difference in the seismic activity between eastern and western China. Eastern China is presently characterized by a low level of activity, although historical records show that there have been periods of higher activity in the past. The large number of events shown in the center of the outlined area is investigated in this paper.

Figure 2 shows the shallow-focus seismicity and major tectonic features of the region outlined in Figure 1. The physiographic features and faults are mapped from LANDSAT-1 (formerly ERTS-A) imagery. The only lineations mapped are those that are greater than ten kilometers long, reasonably straight, and offset streams or cut alluvial deposits in a consistent direction. Other criteria considered are observable scarps and lineations separating different rock textures and tonal differences on either side. These criteria are used to define Quaternary faulting in Figure 2A. The fault types are unclassified except where both the imagery and the geologic literature support existence of normal faulting. The Quaternary or younger age of many of these faults is verified in the published Chinese literature.

Figure 2B is the same base map as in Figure 2A showing historically reported epicenters from the Chinese Earthquake Catalog by the Academia Sinica (1970). These epicenters cover the period from 1177 B.C. to 1903 A.D. and are the result of an intense study of pre-instrumental epicenter locations by the Academia Sinica.

In the region shown in Figure 2 the physiography and the various tectonic features such as faults have predominantly north-northeast and northeast trends. The region where the 1966 earthquake series occurred (outlined area) is on the western edge of the North China Plain. The North China Plain has an elevation of less than 100 meters and is a

sediment-filled basin surrounded by uplifted areas with elevations over one kilometer. In parts of the basin there are up to seven kilometers of sedimentary fill above the basement (Terman, 1974). The lowermost sedimentary strata are Cambrian silts and clays that lie above the crystalline basement. In the outlined area there is about one kilometer of sediment overlying the basement, and this sediment cover rapidly thins to the west (Yao et al., 1974). Chang (1959) cites evidence that this basin has been continuously subsiding since the middle to late Tertiary. More recently, Chen et al. (1975) determined a subsidence rate of 5 mm/yr in the outlined region. The crustal thickness is about 40 km (Yao et al., 1974).

Terman (1974) and various others have shown the western edge of the North China Plain to be faulted down against the northeast-trending T'ai-Hang Mountains. Here the T'ai-Hang Mountains are composed of metamorphosed schists and gneiss of Archean age. The basin was caused by the sinking of the eastern portion of the range (Chang, 1959). There is abundant geomorphologic evidence that the T'ai-Hang Mountains are still being uplifted (Huang, 1960). These mountains include north-northeast striking faults with apparent Quaternary movement.

The Shansi Graben system lies to the west of the T'ai-Hang Mountains. It is a system of grabens defined by north-northeast and northeast striking faults that lie between the T'ai-Hang Mountains and the Lü-Liang Mountains. This graben system is one of the largest in the world. The normal faults have evidence of Quaternary movement and some of China's most destructive earthquakes have occurred in this graben system. In addition to the T'ai-Hang Mountains, the Lü-Liang Mountains and the Ordos Platform (containing the Ordos Desert) are all undergoing recent uplift (Huang, 1960). There is a continuation of the graben system to the west of the

Ordos Platform. In summary, all the tectonic features west of the North China Plain are undergoing uplift except for the relative subsidence in the grabens.

To the north are the Yin Mountains and to the south are the Tsinling and Ta-Pieh Mountains. These ranges are being uplifted also and have many northeast trending faults in them in addition to faults with other strikes (Chang, 1960). The North China Plain is bounded on the east by the uplifted T'ai Mountains. This range was formerly connected to the Ch'ien Mountains across the Gulf of Chili. There is evidence of recent uplift here and the faults strike northeast and northwest. Pavlinov (1960) shows downfaulting of the North China Plain relative to the uplifted T'ai Mountains. Although it cannot be clearly seen on the LANDSAT-1 imagery, there is a large north-northeast trending fault zone crossing the T'ai Mountains, continuing across the Gulf of Chili, and then extending to the northeast at the western edge of the Ch'ien Mountains. This fault zone has been called the Tancheng-Lukiang fault zone by Wilson (1972), and the Chinese claimed to have predicted the large February 1975 earthquake ($M = 7.2$) along this fault.

By combining both instrumentally located events with the historically reported events it is possible to determine several seismic zones with northeast trends in this region. One zone is defined mainly by large historical earthquakes and trends north-northeast through the Shansi graben system. It then bends northeast towards Peking. The graben west of the Ordos Platform is also defined by a north-south trending seismic zone. There is some suggestion of a seismic zone which follows the boundary between the eastern edge of the uplifted T'ai-Hang Mountains and the western edge of the North China Plain. This zone is parallel to the Shansi

Graben zone and intersects it near Peking. The 1966 series of earthquakes would be part of this zone. Another diffuse north-northeast trending seismic region possibly occurs in the T'ai Mountains south of the Gulf of Chili and extends to the western edge of the Ch'ien Mountains. It is not, however, clear whether two distinct zones exist or whether the seismicity east of the Shansi Graben system is more complex.

Although the region of the North China Plain and Shansi Graben is considered an "intraplate" area, the historical record (Figure 2B) shows that a number of very large earthquakes have occurred there. For example, the Academia Sinica (1970) lists seven shocks with estimated magnitudes greater than or equal to 8.0 for the time period 1303 to 1739.

The directions of faulting determined from fault plane solutions shown in Figure 2A are from Molnar et al. (1974) and Banghar (1974). The fault plane solutions for the earthquakes in the North China Plain all show right-lateral strike-slip motion along northeast striking planes. The series of earthquakes investigated in this paper is shown in the outlined region of Figure 2A. Coe (1971), the American Seismology Delegation to China (1975), Chen et al. (1975), the Geodetic Survey Brigade for Earthquake Research (1975), and various others have visited this area since the earthquakes occurred and reported on a broad north-northeast striking fault zone.

LANDSAT-1 IMAGERY

Figure 3 shows a band 7 LANDSAT-1 image (photo number 1486-02285) of the region outlined in Figure 2. It is evident from the imagery that there is a fault scarp in the T'ai-Hang Mountains to the southwest of Hsing-t'ai. One can follow a linear from the fault scarp to the northeast

along a trend of N02°E. This linear is defined by offsets and kinks in stream channels. The linear is also defined by a contrast in shading on opposite sides of the lineament. Since near infrared imagery is used this shading contrast may indicate a slight difference in water content of the soil on opposite sides of the linear zone. The darker coloration lies to the east of the linear in an area of many irrigations ponds and channels. This linear may be a continuation of the fault scarp into the sediment-filled basin or perhaps a boundary of a fault zone. In the following figures the fault scarp in the mountain is shown as a solid line and the linear is shown as a dotted line. Although the linear may or may not represent the fault or the boundary of the fault zone, for this paper the lineation will be used as a fixed reference line with which to compare the epicenters relocated by different techniques.

SEISMICITY

Historical records of seismicity for northern China are complete for almost 3000 years. The small region of the North China Plain outlined in Figure 2 has been aseismic for much of this time. Only seven events were reported for this area prior to 1966 and none were instrumentally located. Five events were small and are probably not well located. The remaining two have estimated magnitudes of 6.0 and are probably reasonably well located. The dates for these two events are 777 and 1882. The locations are shown in Figure 2B and as crosses in Figure 4A. Since 1882, no other historically reported or instrumentally recorded events occurred until 1966. On March 7, 1966 at 2129 GMT, a devastating earthquake occurred in a rural area near Hsing-T'ai in the Hopei Province, China (about 300 km southwest of Peking). Although statistics on fatalities and

injuries are not available, the figures were probably high. Coe (1971) visited the village of Sha Wan, 30 km from the epicenter, and reported that 70 percent of the houses in that village had collapsed and that the rest were "unfit to live in." This event was the first of 30 earthquakes of magnitude 4.3 (m_b) or greater that occurred that month and continued with decreasing frequency and magnitude for the next few years. It was because of these destructive events that the Chinese began their intensive earthquake prediction program. These events illustrate the need for caution in basing seismic risk zoning on instrumental and even historical seismicity. Figure 4A shows the historical and instrumentally located earthquake epicenters in the region outlined in Figure 2.

Figure 5 shows the sequence of earthquakes for the first two months as reported by the PDE (Preliminary Determination of Epicenters). The March 7, 196 event (with a magnitude (M_s) of 6.8) initiated the series. Eight other events with magnitudes (m_b) greater than 4.2 quickly followed within the next four days. The next large event was the magnitude 5.6 (m_b) earthquake of March 22, 1966 at 0811 GMT followed eight minutes later by a magnitude 7.0 (M_s) earthquake. The damage from these two events was considerable. A series of eight additional events (located by the PDE) followed during that day. A total of thirty events occurred during the month of March. The activity decreased in frequency and magnitude the rest of that year for a total of 40 events. Eight other teleseismically recorded events occurred from 1967 to 1968. The largest had a magnitude of 5.8 (m_b) in January 1968. Since then only one small event (m = 4.8) occurred in June 1974.

In addition, there have been several reports of continuing micro-earthquake activity in the area (Coe, 1971; Li et al., 1973; Yao et al., 1974). These data will be examined later in this paper.

Although Figure 4A shows a definite clustering of events in space, the spatial pattern is ill defined. In order to better define the pattern, each earthquake was individually examined to determine the quality of the ISC (International Seismic Centre) location. Events were rejected if reported by too few stations, if the azimuthal distribution of the stations is poor, or if the residuals are anomalously large owing to emergent first arrivals and small amplitudes. Of the 49 teleseismic events, 14 were rejected, and the remaining 35 events are plotted in Figure 4B. Although this greatly reduces the scatter of epicenters and somewhat defines a linear grouping, the trend of the pattern of the epicenters is still uncertain. The ISC locations are subject to errors due to station and path effects. These errors affect the accuracy, and because of the variable network of stations, affect the precision of the locations. The method of Joint Epicenter Determination (JED; Douglas, 1967; Dewey, 1971, 1972) is ideally suited for precise relocation of events that are closely grouped in space as these events clearly are, and was chosen to improve the precision of the relative locations.

RELOCATION OF EVENTS WITH JOINT EPICENTER DETERMINATION

The JED method assumed that for a given set of closely grouped hypocenters the combined station and path correction is constant for each station. The input data to the program are initial earthquake hypocenters, a calibration event that is held fixed during the relocation, initial origin times and station arrival times of the events, all taken from the Bulletin of the International Seismic Centre. Given this information, one can simultaneously solve for a set of hypocenters, origin times, and path-station corrections for each of the stations used in the relocations by the method of least squares using the Herrin et al. (1968) travel-time

tables.

Thirty-five earthquakes were relocated by this method with a maximum of 17 possible stations per earthquake and a minimum of 7 stations per earthquake. The average number of stations used per earthquake was 11. Stations were chosen to give the best possible uniform azimuthal and epicentral coverage as well as reliability of readings. Epicentral distances were all between 20 and 90 degrees (with the exception of Seoul, Korea at 9.6 degrees) from the events. Table 1 gives the station locations and approximate azimuths and epicentral distances.

Since the critical factor in the relocations is the quality of the arrival time readings, the records were reread for many of the stations for which, in the original ISC locations, there was a time residual (observed arrival time minus calculated arrival time) of greater than one second.

The ISC reported depths for most of these events less than 30 km deep or else constrained depth to 33 km. These depth determinations are calculated from arrival times of P only. Thus, without pP data or arrival times at stations very close to the source, it is impossible to accurately determine focal depths. In order to check the ISC depth determinations a study was made of any second arrivals on the long and short period vertical components of the seismograms in an attempt to identify pP or sP phases. Depth phases such as pP are not clear on the seismograms of these events. However, some second arrivals were observed to follow the initial P phase by 4.5 to 8.0 seconds. From the Herrin et al. (1968) tables, this time difference would correspond to a depth range of 15 to 30 km if the second arrivals were pP phases. An example of a second arrival is shown in Figure 6 for the earthquake of March 7, 1966 at 2129 GMT for station ADE

($\Delta = 75.26^{o}$). The time separation between pP and P, 7.5 seconds, corresponds to a depth of 25 km. Depths for a given earthquake were consistent for different stations although the number of stations showing a second arrival was limited.

Thus, the range of depths calculated by the ISC and the times of the presumed pP phases are in agreement. This depth range also matches that determined by microearthquake studies in the region to be examined in detail later in this paper.

In the initial JED locations of the events the depths became negative because there were no local stations to provide depth control. Therefore for this paper all hypocenters are constrained to a surface focus. Since all events are shallow focus earthquakes there is little relative error in the location of the epicenter. The reason for this is that for any given event with good azimuthal station distribution there is a tradeoff between depth and origin time while the epicenter location is only slightly affected.

ACCURACY OF EPICENTER LOCATIONS

In any earthquake location, one must consider the effects of the following on the accuracy of the epicenter location: source effects, path effects, distant station corrections, accuracy of the travel-time tables, and effects due to non-uniform distribution of distant stations. These effects are individually considered below and summarized at the end.

Station distribution. A minimum of three stations in separate quadrants are needed to uniquely determine an epicenter using arrival times. It is desirable to have at least three other stations in these same quadrants in order to provide some measure of redundancy and prevent mislocations due to

reading errors. In this study a minimum of seven well-distributed stations were used for each earthquake. It is asserted that the station distribution shown in Table 1 is quite adequate for accurately determining the investigated epicenters. This assertion will be shown to be substantiated by the tight grouping of the epicenters with nearly circular 90% confidence ellipses.

Source effects. There is no obvious evidence in the tectonics, physiography, or crustal structure (Yao et al., 1974) to indicate the presence of a large velocity anomaly near or beneath the source which would cause a bias in a teleseismic location. In this study it will be assumed that there is no source effect. Comparison of the final results with local studies will be shown to justify this assumption.

Path effects, distant station corrections, and accuracy of travel-time tables. The method of JED assumes that for a closely grouped distribution of epicenters the combined effects of individual station corrections and travel path corrections are constant for all the earthquakes in the cluster. The method computes this correction for each of the rays from the epicenter cluster to each station using a least squares algorithm. The accuracy of an individual epicenter determined by the JED technique depends on two factors. First, the precision of an epicenter with respect to other epicenters is determined by the JED method of relocation using the computed path-station correction. Second, the accuracy of the location of the entire group of epicenters depends on the accuracy of the chosen calibration event location. These two factors will be discussed separately.

The precision of one epicenter with respect to the others is determined by the quality of arrival time readings and the station distribution.

Good arrival time readings obtained by re-reading seismograms and a good station distribution enabled the epicenters to be relocated quite precisely with respect to one another. It should be noted that one uncertainty in this study is the difficulty in precisely reading the arrival times of shallow focus emergent earthquakes. Of the 34 relocated epicenters (excluding the calibration event which is discussed below) 94% have epicenters whose 90% confidence ellipses have semi-major axes less than 13.3 km. In addition the confidence ellipses are nearly circular which indicates that there is little bias due to station distribution. The average ellipticity is 0.10. The semi-axes of the ellipses differ from each other by only 0.7 km on the average. Although the confidence ellipses are not as small as those determined for some deep earthquakes relocated by Joint Hypocenter Determination (Billington and Isacks, 1975), they are as good or better than published relocations using this method for shallow events (Dewey and Grantz, 1973; Dewey and Algermissan, 1974; Qamar, 1974).

The precision can also be checked by noting the stability of an epicenter located with respect to different groups of earthquakes with the same calibration event. Using the same calibration event a test group of five 1966 earthquakes was located with a group of all 1966 events and then located with a group of post 1966 events. After both relocations the epicenters were nearly identical and well within the confidence ellipses. For the two relocations the epicenter differences were less than 5 km and generally less than 1 km. Therefore, for a given calibration event the stability and precision of an epicenter with respect to other epicenters is quite good.

The position of the calibration event must be chosen with care because

an inaccurate calibration event can shift the entire group of epicenters, although the position of the epicenters with respect to each other remains essentially the same.

The calibration event used in this study is the event of March 22, 1966 at 0811 GMT. This is a well recorded event reported by 204 stations in the Bulletin of the ISC. The epicentral location of the event, taken from the Bulletin of the ISC, is $37.54^{\circ} \pm 0.024^{\circ}$N by $115.00^{\circ} \pm 0.026^{\circ}$E, and the depth is constrained to be at the surface. The accuracy of the calibration event location can be partly examined by using a standard single-event location method with different travel-time tables and published station corrections to see how much the resulting locations vary. Figure 7 and Table 2 show the results of this procedure.

It is expected that the "ISC" and "J-B" locations are essentially the same. The difference in travel-time tables results in a 5 km difference in location. Since the Jeffreys-Bullen tables are slow with respect to the Herrin et al. tables, this explains the slightly earlier origin time and shallower focus.

Various authors have considered the effects of using station corrections in relocating earthquakes. Bolt and Nuttli (1966) and Nuttli and Bolt (1969) considered the effects of azimuthal dependence of station corrections. Four published sets of station corrections are known to the authors. Lilwall and Douglas (1968) calculated azimuthally dependent station corrections determined from earthquakes and explosions using Herrin et al. (1961) travel-time tables. Cleary and Hales (1966) computed mean value station corrections determined from earthquakes using Jeffreys-Bullen travel-time tables. Jacob (1972) calculated mean value station corrections from the Longshot explosion using Herrin et al. (1968) travel-time tables. Herrin and Taggart (1968) computed azimuthally dependent

station corrections determined from earthquakes using Herrin et al. (1968) travel-time tables. Although for many stations the mean value residuals are somewhat similar, there is considerable scatter in the variation of the azimuthal dependence.

In Figure 7, "station-corrected" represents the location of the calibration event located using station corrections published by Herrin and Taggart (1968). This set of station corrections was chosen because of the inclusion of azimuthally dependent terms. In addition these station corrections are consistent with the use of Herrin et al. (1968) tables used in the JED location procedure. The largest station correction is 1.53 seconds and most corrections are considerably less. From Figure 7, one can see the "station-corrected" location differs by 7.45 km from the "J-B" location. "ISC", "J-B", and "Herrin" locations are close together while the "station-corrected" location is the most noticeably different.

The "ISC" and the "station-corrected" locations are chosen as calibration events in order to examine the effect of calibration event mislocation. The final locations after three iterations of the JED procedure using these two calibration events is shown in Figures 4C and 4D and listed in Table 3. Note how the use of a different calibration event shifts the group of epicenters compared to the lineation while the relative position of the epicenters remains unchanged. Also note how both JED relocations clearly provide a better epicenter clustering than the best ISC locations shown in Figure 4B. The JED relocations in this case form a linear epicenter trend that makes a tectonic interpretation less ambiguous than in Figure 4B.

This section has considered the following factors affecting the accuracy of the locations of shallow earthquakes: station distribution, source effects, path effects, distant station corrections, and travel-time

table accuracy. In this study network bias is eliminated by using an adequate station distribution including redundancy and this is further evidenced by the small average ellipticity of the confidence ellipses. There are no obvious anomalous velocity distributions in the crust of the epicentral region. Path and station corrections are determined by the JED method to account for any travel-time anomalies along the ray path. Since almost all of the stations except SEO (at 9.5°) are located at greater than 20° from the epicenters, the ray paths are through the lower mantle. This suggests that the corrections are mostly for crust and upper mantle at the stations since the lower mantle is thought to be relatively homogeneous (Carder, 1964; Jeffreys, 1968; Muirhead and Cleary, 1969). The effect of using different travel-time tables will only affect the location of the calibration event and not the relative locations of the epicenters. A check on the accuracy of slightly different epicenters for the calibration event is provided in the next section.

MICROEARTHQUAKE ACTIVITY

In Figures 4C and 4D both epicenter distributions form a linear zone trending N30°E (± 5°) which is parallel to the LANDSAT-1 lineation. Location of small earthquakes in the region provides independent data to determine which calibration event most accurately locates the epicenters. Seismologists from the Institute of Geophysics in Peking studied the epicentral area six months after the March 1966 events with data from seven district (permanent) stations, five temporary stations, and some portable instruments well distributed on and around the faults area (Yao et al., 1974). They recorded 78 microearthquakes in a three-month period from September to November, 1966. These epicenters are plotted in Figure 8B. The average

magnitude (M_s) was between 3.0 and 3.5 although events were reported as low as 2.4 and as high as 4.5. There is no obvious relationship between the magnitude or location of an event and the time the microearthquake occurred.

Another microearthquake survey was conducted by Li et al. (1973) using nearby stations. They recorded 231 small events from 1968 to 1972. These epicenters are plotted in Figure 8C. The range of magnitude (M_s) for these events is from 2.5 to 5.2. The trend of these epicenters is N35^{o}E which is the same as the trend of the 1966 microearthquakes shown in Figure 8B. In both cases the epicenters are slightly east of the LANDSAT-1 determined linear. The JED relocations using the station-corrected calibration event of Figure 4D best matches the distribution of microearthquakes determined by Chinese seismologists using local stations. This figure is shown again in Figure 8A.

The majority of the 231 small events recorded by Li et al. (1973) were between 15 and 25 km with extremes of 7 and 31 km. These depths are similar to the 78 recorded by Yao et al. (1974). Figure 9 shows two cross-sections parallel and perpendicular to the epicenter trend of the microearthquakes in Figure 8B. From both sections it is apparent that the majority of the microearthquakes occurred in a 15 km zone from 12 to 27 km in depht. This is in agreement with the depths determined from pP phases and ISC depth calculations for the teleseismically recorded events.

FAULT PLANE SOLUTIONS

An additional check on the epicenter distribution is provided by using the fault plane solutions of Molnar et al. (1974). They determined four fault plane solutions for the series for the events 1, 9, 10, and 17. Fault plane solutions for events 10 and 17 are not well constrained due to poor

azimuthal coverage. The azimuthal coverage for events 1 and 9 is better, but due to the difficulty in reading first motions from emergent phases of shallow focus earthquakes, as well as the small amplitudes near the nodal planes, the resulting fault planes are only approximately located. On each of the focal diagrams there are inconsistencies in the sense of motion around the nodal planes. The resulting fault planes they determined strike N24°E and N20°E for events 1 and 9 respectively as shown in Figure 4C. The faults are on a vertical plane and the sense of motion is right-lateral strike-slip. In addition, Li et al. (1973) determined two composite fault plane solutions for the 231 events they recorded between 1968 and 1972. There were again some inconsistencies, but the determined nodal plane strikes N18°E at a dip of 78° (Figure 8C).

DISCUSSION

The fault zone associated with the 1966 earthquakes is best defined by the relocated epicenters in Figure 4D using the method of Joint Epicenter Determination along with a station-corrected calibration event. The epicenter trend closely matches the linear determined from LANDSAT-1 imagery. The only surface manifestiation of the faulting were some sand volcanoes in the supra-basement sediments (Bolt, 1971). Chinese geophysicists have attempted to better define the fault zone in the basement rocks underlying the sediments by using leveling, seismic reflection and seismic refraction methods.

Teng, et al. (1975) used artificial explosions to determine the structure in the epicentral area. They reported results showing a complex fracture zone 10-20 km wide with deep faults extending through the Mohorovičić discontinuity. A report by the Geodetic Survey Brigade (1975)

correlated releveling measurements with the seismically determined faults. The faults were shown as northeast and north-northeast normal faults and are located in the region defined by the JED epicenters and microearthquakes of Figure 8. The results of the releveling measurements showed right-lateral horizontal offset accompanied by lesser movements of horizontal extension and vertical subsidence. Chen et al. (1975) modeled the ground deformation using dislocation theory and obtained a model of compound faulting in a zone 30 km wide. The faults had a strike of N35°E and were mostly right-lateral strike-slip faults with some normal faulting. This is in good agreement with the trend determined using the method of JED and the observed LANDSAT-1 linear. The linear determined from LANDSAT-1 imagery matches the western boundary of the geophysically determined fault zone of the Geodetic Survey Brigade. This explains why the majority of the relocated epicenters and the microearthquakes lie to the east of the linear.

Chen et al. (1975) also gives the locations of five earthquakes of the 1966 series. They did not report on the location method, number of reporting stations, station distribution, or accuracy of the given locations. The location of the station-corrected calibration event determined in this paper is only 1.6 km different from that reported by Chen et al. (1975). One of the largest differences in location is for the event on March 7, 1966. From the quality listed for this event in Table 8 one can see that this is the worst relocation. The poor location is because of the very emergent character of the P arrivals. This event was included in the relocations only because Molnar et al. (1974) published a fault plane solution for this event. This epicenter is 23 km different from the Chinese location.

The fault zone determined by the JED method of relocation, LANDSAT-1 imagery, and Chinese geophysical studies is parallel to many other northeast

striking faults in northern China. In addition to the faults shown in Figure 2A, Bolt (1971) reported that northeast striking faults have been extensively mapped on the northern part of the North China Plain near Peking. Locally, the faulting associated with the 1966 earthquakes is subparallel to the faulting in the eastern T'ai-Hang Mountains.

The four fault plane solutions determined for the 1966 events as well as the two others in the North China Plain all have nearly horizontal T-axes oriented north-northwest--south-southeast. The direction of horizontal extension determined by the Geodetic Survey Brigade (1975) from releveling data is also in this direction. In addition this orientation of the T-axes is consistent with the direction of extension of the Shansi Graben system. Both Bolt (1971) and Li et al. (1973) have suggested that the tectonics of northern China appears to be controlled by north-northwest--south-southeast extension. Molnar et al. (1975) suggest that these tectonics are end effects related to the large left-lateral strike-slip faults in central and western China that strike east-west.

Further studies are necessary to determine the origin of the stresses and complex tectonics of northern China.

CONCLUSION

This paper evaluates the use of the method of Joint Epicenter Determination along with LANDSAT-1 imagery for locating fault zones associated with shallow focus seismicity. The method of JED is a rational and statistical method of correcting for travel-time anomalies due to station and path effects. JED reduces the amount of scatter of epicenter

locations even when compared to the best ISC data. By carefully examining a series of earthquakes in northern China it is concluded that one can teleseismically locate well-determined fault planes by using the method of JED in conjunction with other remote sensing techniques such as fault plane solution studies and LANDSAT-1 imagery. These methods can provide valuable tectonic information for regions where detailed field studies are not possible.

ACKNOWLEDGMENTS

This research was supported by the Advanced Research Projects Agency of the Department of Defense and was monitored by the Air Force Office of Scientific Research under Contract No. AFOSR-73-2494.

REFERENCES

Academia Sinica (1970). Chinese Earthquake Catalog, Peking (in Chinese).

American Seismology Delegation (1975). Earthquake research in China, EOS, Trans. Am. Geophys. Union 56, 838-881.

Banghar, A.R. (1974). Mechanism of earthquakes in Albania, China, Mongolia, Afghanistan and Burma-India border, Earthquake Notes 45, 13-25.

Billington, S. and B.L. Isacks (1975). Identification of fault planes associated with deep earthquakes, Geophys. Res. Letters 2, 63-66.

Bolt, B.A. (1974). Earthquake studies in the People's Republic of China, EOS, Trans. Am. Geophys. Union 55, 108-117.

Bolt, B.A. and O.W. Nuttli (1966). P wave residuals as a function of azimuth, J. Geophys. Res. 71, 5977-5985.

Carder, D.A. (1964). Travel times from central Pacific nuclear explosions and inferred mantle structure, Bull. Seism. Soc. Am. 54, 2271-2294.

Chang, Ta (1959). The Geology of China, 1963 Translation, U.S. Department of Commerce, Washington, D.C.

Chang, Wen-yu (1960). The X-shaped fault systems in China and their relationship to the neotectonic movements, Works on the First Conference on Neotectonics in China, 1963 Translation, U.S. Department of Commerce, Washington, D.C. 134-141.

Chen, Y.T., B.H. Lin, Z.Y. Lin and Z.Y. Li (1975). The focal mechanism of the 1966 Hsingtai earthquake as inferred from the ground deformation observations, Acta Geophys. Sinica 18, 164-182 (in Chinese).

Cleary, J. and A.L. Hales (1966). An analysis of the travel times of P waves to North American stations, in the distance range 32° to 100°, Bull. Seism. Soc. Am. 56, 467-489.

Coe, R.S. (1971). Earthquake prediction program in the People's Republic of China, EOS, Trans. Am. Geophys. Union 53, 940-943.

Dewey, J.W. (1971). Seismicity Studies with the Method of Joint Hypocenter Determination, Ph.D. Dissertation, University of California, Berkeley, California.

Dewey, J.W. (1972). Seismicity and tectonics of western Venezuela, Bull. Seism. Soc. Am. 57, 9-26.

Dewey, J.S. and S.T. Algermissen (1974). Seismicity of the Middle America arc-trench system near Managua, Nicaragua, Bull. Seism. Soc. Am. 64, 1033-1048.

Dewey, J.S. and A. Grantz (1973). The Ghir earthquake of April 10, 1972 in the Zagros Mountains of southern Iran: seismotecton_ aspects and some results of a field reconnaissance, Bull. Seism. Soc. Am. 63, 2071-2090.

Douglas, A. (1967). Joint epicenter determination, Nature 215, 47-48.

Geodetic Survey Brigade for Earthquake Research, National Seismological Bureau (1975). Crustal deformation associated with the Hsingtai earthquake in March 1966, Acta Geophys. Sinica 18, 153-163 (in Chinese).

Gutenberg, B. and C.F. Richter (1954). Seismicity of the Earth and Associated Phenomena, Hafner Publishing Company, New York.

Herrin, E. (1961). Report Dallas Seis. Observatory, Dallas, Texas.

Herrin, E. (Chairman) (1968). Special number - 1968 seismological tables for P phases, Bull. Seism. Soc. Am. 58, 1193-1219.

Herrin, E. and J.N. Taggart (1968). Regional variations in P travel times, Bull. Seism. Soc. Am. 58, 1325-1338.

Jacob, K.H. (1972). Global tectonic implications of anomalous seismic P travel times from the nuclear explosion Longshot, J. Geophys. Res. 77, 2556-2573.

Jeffreys, H. (1962). Travel times from Pacific explosions, Geophys. J. 7, 212.

Jeffreys, H. and K.E. Bullen (1940). Seismological Tables, British Association for the Advancement of Science and Gray-Milne Trust, reprinted by Smith and Ritchie, Edinburgh, 1967.

Li, C.T., T.K. Wang, Y.N. Chia and Y.M. Chin (1973). Stress field obtained for two regions from weak earthquake data recorded at a single seismic station, Acta Geophys. Sinica 16, 59-61 (in Chinese).

Lilwall, R.C. and R. Doulgas (1968). Does epicenter source bias exist?, Nature 220, 469-470.

Molnar, P. T.J. Fitch and F.T. Wu (1974). Fault plane solutions of shallow earthquakes and contemporary tectonics in Asia, Earth Planet. Sci. Lett. 19, 101-112.

Molnar, P. and J.E. Oliver (1969). Lateral variation of attenuation in the upper mantle and discontinuities in the lithosphere, J. Geophys. Res. 74, 2648-2682.

Molnar, P. and P. Tapponnier (1975). Cenozoic tectonics of Asia: effects of a continental collision, Science 189, 419-421.

Muirhead, K.J. and J. Cleary (1969). Comparison of the 1968 P tables with times from nuclear explosions, 1, the Marshall Islands and Sahara series, Earth Planet. Sci. Lett. 7, 132-136.

Nuttli, O.W. and B.A. Bolt (1969). P wave residuals as a function of azimuth, J. Geophys. Res. 74, 6594-6602.

Qamar, A. (1974). Seismicity of the Baffin Bay region, Bull. Seism. Soc. Am. 64, 87-98.

Rothé, J.P. (1969). The Seismicity of the Earth, UNESCO, Belgium, 336 pp.

Terman, M.J. (1974). Tectonic Map of China and Mongolia, Geological Society of America, Boulder, Colorado.

Teng, J.W., G.C. Wang, D.H. Liu, J.R. Hsing, W... Liang and S.L. Xu (1975). Crustal structure of the central part of the North China Plain and the Hsingtai earthquake, Acta Geophys. Sinica 18, 196-207 (in Chinese).

Wilson, J.T. (1972). Mao's almanac: 3000 years of killer earthquakes, Saturday Rev. Sci. 60-64.

Yao, C.H., P.S. Chen, C.Y. Hsiao and K.M. Hsu (1974). On the intensity anomaly of the Hsingtai earthquake of March 22nd, 1966, Acta Geophys. Sinica 17, 106-121.

TABLE 1

STATIONS USED IN THE JED RELOCATIONS

Station Abbreviation	Latitude	Longitude	Epicentral Distance*	Azimuth*
SEO	37.57°N	126.97°E	9.5	86
BOD	57.85 N	114.18 E	20	358
BAG	16.41 N	120.58 E	22	165
SHL	25.57 N	91.88 E	23	245
CHG	18.79 N	98.93 E	23	221
QUE	30.19 N	66.95 E	40	274
KRV	40.65 N	46.33 E	52	296
BRW	71.30 N	156.75 W	54	23
KJN	64.09 N	27.71 E	56	328
COL	64.90 N	147.79 W	60	29
MBC	76.24 N	119.36 W	61	12
CTA	20.09 S	146.25 E	64	147
RES	74.69 N	94.90 W	66	8
YKC	62.48 N	114.48 W	73	22
BMO	44.85 N	117.31 W	85	34
EUR	39.48 N	115.97 W	90	37
UBO	40.32 N	109.57 W	92	33

* This is the epicentral distance (in degrees) and azimuth from the calibration event to the station.

TABLE 2

CALIBRATION EVENT LOCATIONS BY DIFFERENT TECHNIQUES

Technique*	Latitude (°N)	S.E.** (km)	Longitude (°E)	S.E.** (km)	Depth (km)	S.E.** (km)	Origin time (GMT)	S.E.** (seconds)
ISC	37.54	± 2.67	115.00	± 2.89	3.0	--	8:11:33.50	± 0.12
J-B	37.54	± 3.2	115.01	± 2.1	8.7	± 12.3	8:11:34.21	± 1.83
Herrin	37.52	± 3.0	115.04	± 2.0	39.4	± 7.1	8:11:40.74	± 0.74
Station-corrected	37.51	±3.2	115.07	± 2.2	22.4	± 13.7	8:11:38.36	± 1.94

* Technique is described in Figure 7

**S.E. = Standard Error

TABLE 3

RELOCATED EPICENTERS FOR THE EARTHQUAKE SERIES IN NORTHEASTERN CHINA

		I.S.C. CALIBRATION EVENT				STATION CORRECTED CALIBRATION EVENT					
EVENT	DATE	ORIGIN TIME	LATITUDE	LONGITUDE	QUALITY*	ORIGIN TIME	LATITUDE	LONGITUDE	QUALITY*	N**	MAGNITUDE***
1	7/3/66	21:29:12.25	37.47	115.08	D	21:29:17.19	37.41	115.12	D	16	5.8 (6.8 M_S)
2	8/3/66	00:04:48:22	37.77	115.03	A	00:04:53.07	37.75	115.08	A	9	4.3
3	8/3/66	02:04:17.45	37.41	114.91	A	02:04:22.30	37.38	114.96	A	13	4.7
4	8/3/66	03:46:34.13	37.63	115.04	A	03:46:38.99	37.60	115.10	A	14	4.8
5	8/3/66	07:36:41.89	37.58	114.86	B	07:36:46.71	37.54	114.93	B	13	4.7
6	11/3/66	06:20:45.73	37.38	114.90	A	06:20:50.60	37.37	114.95	A	10	4.4 (USCS)
7	19/3/66	16:59:38.53	37.46	114.85	A	16:59:43.40	37.43	114.91	A	15	4.8
8	22/3/66	05:57:41.49	37.60	115.08	B	05:57:46.38	37.57	115.15	B	10	4.5
9	22/3/66	08:11:33.50	37.54	115.00	-	08:11:38.36	37.51	115 07	-	--	5.6
10	22/3/66	08:19:30.03	37.59	115.20	A	08:19:34.91	37.57	115.26	A	12	5.9 (7.0 M_S)
11	22/3/66	11:08:34.39	37.68	115.02	A	11:08:39.29	37.66	115.08	A	15	5.1
12	22/3/66	11:37:26.01	37.68	115.11	A	11:37:30.89	37.65	115.19	B	11	4.7
13	22/3/66	12:08:00.82	37.71	115.09	A	12:08:05.80	37.70	115.15	A	12	4.8
14	23/3/66	17:27:58.15	37.54	114.98	A	17:28:03.03	37.51	115.04	A	14	4.8
15	25/3/66	06:33:19.23	37.77	115.18	B	06:33:24.09	37.74	115.24	B	11	4.5
16	26/3/66	15:14:29.03	37.78	115.16	A	15:14:33.96	37.76	115.22	A	12	4.7
17	26/3/66	15:18:59.55	37.78	115.27	A	15:19:04.43	37.75	115.33	A	12	5.2
18	26/3/66	18:14:18.25	37.78	115.15	A	18:14:23.06	37.75	115.21	A	14	4.9
19	27/3/66	20:57:15.63	37.74	115.14	B	20:57:20.44	37.72	115.20	B	12	4.8
20	28/3/66	03:26:26.59	37.32	114.82	A	03:26:31.45	37.29	114.88	A	13	4.9
21	28/3/66	14:03:00.58	37.90	115.18	A	14:03:05.41	37.87	115.25	A	9	4.5
22	29/3/66	06:11:56.57	37.53	115.00	A	06:12:01.44	37.51	115.06	A	14	5.3
23	29/3/66	15:44:54.72	37.80	115.18	A	15:44:59.59	37.78	115.23	A	14	4.7
24	5/4/66	16:29:38.13	37.89	115.29	A	16:29:42.99	37.86	115.34	A	14	4.8
25	6/4/66	03:12:12.21	37.46	114.91	B	03:12:16.98	37.43	114.95	B	7	4.9
26	19/4/66	06:53:04.79	37.66	115.22	A	06:53:09.64	37.63	115.28	A	13	4.9
27	20/4/66	14:31:20.98	37.28	114.87	B	14:31:25.80	37.24	114.94	B	13	4.7
28	25/8/66	23:42:50.75	37.60	115.20	B	23:42:55.50	37.57	115.28	B	7	4.8
29	10/10/67	01:07:46.86	37.43	114.78	B	01:07:51.95	37.38	114.93	B	12	4.7
30	28/11/67	18:21:45.56	37.87	115.21	B	18:21:50.44	37.84	115.34	B	9	4.6
31	2/12/67	20:05:52.13	37.80	115.25	B	20:05:57.06	37.78	115.37	A	15	5.3
32	7/1/68	04:05:34.32	37.54	115.30	B	04:05:39.45	37.55	115.42	B	9	4.8
33	15/1/68	19:33:55.00	37.82	115.52	B	19:33:59.88	37.79	115.62	A	15	5.0
34	14/5/68	19:47:00.50	37.35	114.93	B	19:47:05.44	37.36	115.01	B	11	4.8
35	15/5/68	00:27:20.47	37.44	114.85	B	00:27:25.31	37.42	114.95	A	10	4.7

All earthquakes relocated using the method of Joint Epicenter Determination.

*Quality A denotes semi-major axes of the 90% confidence ellipse less than 10 km;

**N is the number of stations used in the relocation procedure.

***Magnitude is the I.S.C. determination unless otherwise noted.

Event 9 is the calibration event.

FIGURE CAPTIONS

Figure 1: Instrumentally located seismicity of China and surrounding regions, 1904 to February 1975. The data are from the following sources:

1904-1952: Seismicity of the Earth, Gutenberg and Richter (1954)

1953-1965: Seismicity of the Earth, Rothé (1969)

1966-1970: Bulletin of the International Seismic Centre

1971-February 1975: Hypocenter Data File of the National Oceanic and Atmospheric Administration

Epicenters from the last two sources are plotted only for those events with more than ten reporting stations. The region in the dashed outline is shown in Figure 2.

Figure 2: A. Instrumentally located shallow focus seismicity and major tectonic features of northern China. Earthquakes cover the period from 1904 to February 1975 with the data sources listed in Figure 1. For two clusters of events only the largest events are shown and the total number of events is indicated. Earthquakes with published fault plane solutions are shown as darkened circles along with the sense of motion. Physiographic features and Quaternary faulting are mapped from LANDSAT-1 imagery. The boundary of the North China Plain is shown in light dashes.

B. Historically located earthquakes from the Chinese Earthquake Catalog (1970) covering the period 1177 B.C. to 1903 A.D.

Figure 3: LANDSAT-1 image (no. 1486-02285) of the region outlined in Figure 2 showing the fault scarp near the T'ai-Hang Mountains

southwest of Hsing-T'ai and its extension into the alluvium of the North China Plain.

Figure 4: A. Historically and instrumentally located epicenters in the region of the North China Plain outlined in Figure 2. The earthquake data cover the period from 777 to 1974 with the sources listed in Figure 1. Historically located epicenters ($M \geq 6.0$) are plotted as crosses (two events). The calibration event is shown as a darkened circle in all maps shown. The lineation is taken from LANDSAT-1 imagery.

B. Selected epicenters from Figure 4A with the best ISC locations.

C. JED epicenter locations using the calibration event location given by the ISC.

D. JED epicenter locations using the station-corrected calibration event. Published fault plane solutions are from Molnar et al. (1974).

Figure 5: ISC magnitudes (m_b) for the earthquakes during the first two months of the 1966 earthquake series. The calibration event is shown as a darkened circle.

Figure 6: WWNSS seismogram of the short period vertical component for the March 7, 1966 earthquake recorded at Adelaide, South Australia ($\Delta = 75^{\circ}$). The second arrival, a possible pP phase, occurs about 7.5 seconds after the first arrival.

Figure 7: Calibration event locations determined by different methods and the standard error of each solution. "ISC" represents the

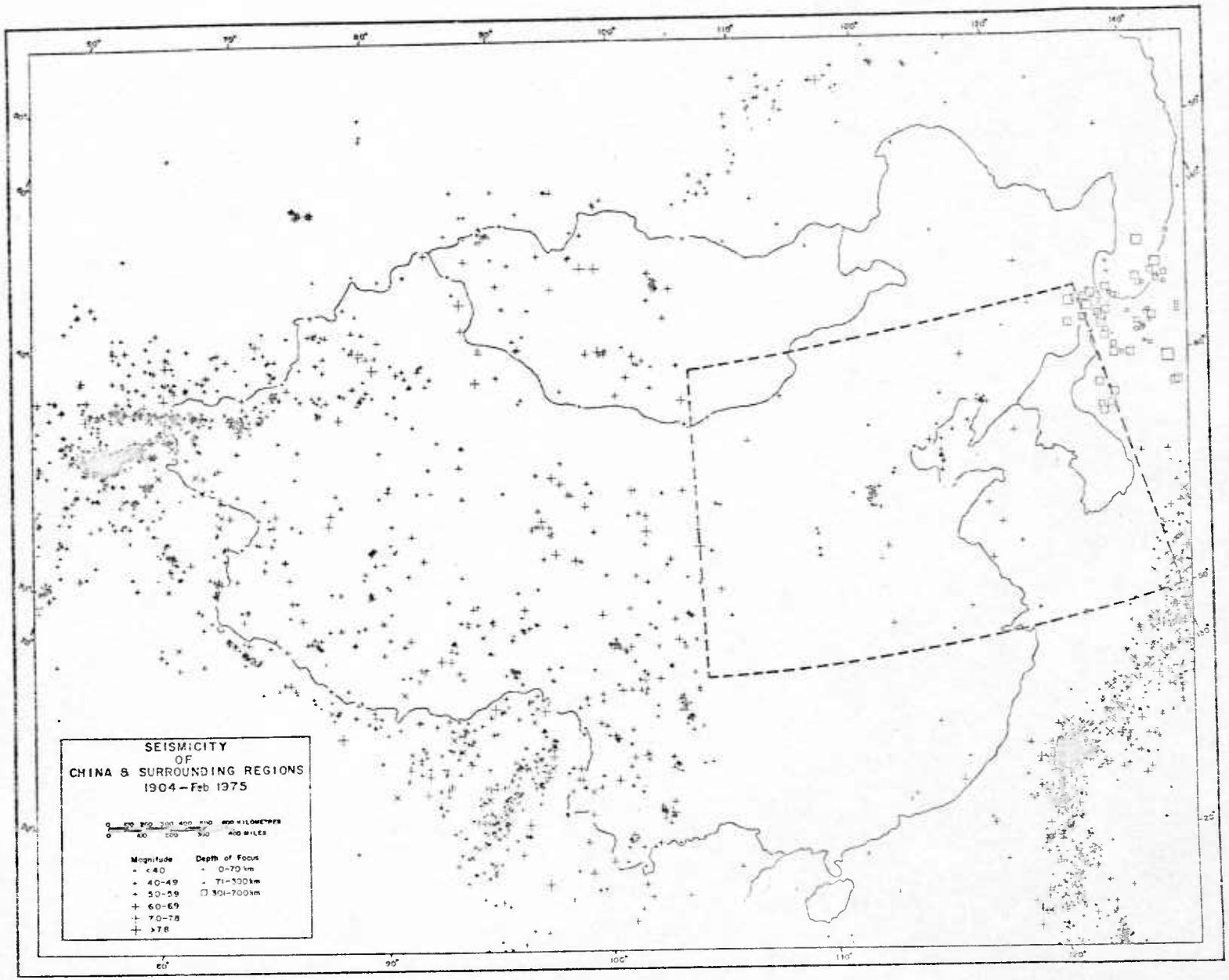
location taken from the Bulletin of the ISC. "J-B" and "HERRIN" represent the locations obtained by using the ISC arrival times and computed using Cornell's single-event location program with Jeffreys-Bullen (1940) tables and Herrin et al. (1968) tables, respectively. "STATION-CORRECTED" represents the location obtained by using the ISC arrival times and the station corrections published by Herrin and Taggart (1968).

Figure 8: A. JED epicenter locations using the station-corrected calibration event. Published fault plane solutions are from Molnar et al. (1974).

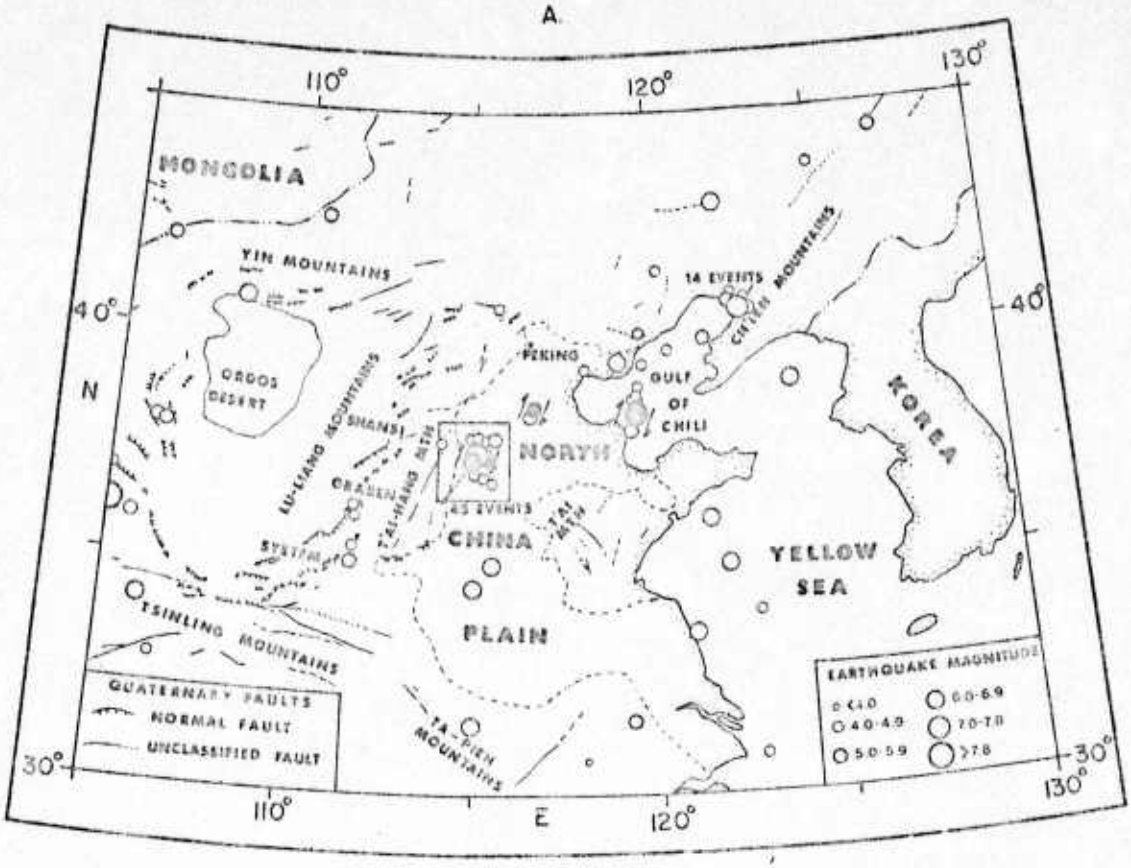
B. Microearthquakes located by Yao et al. (1974) during a two month period occurring six months after the main shocks in 1966.

C. Microearthquakes located by Li et al. (1973) occurring between 1968 and 1972 and their composite fault plane solution.

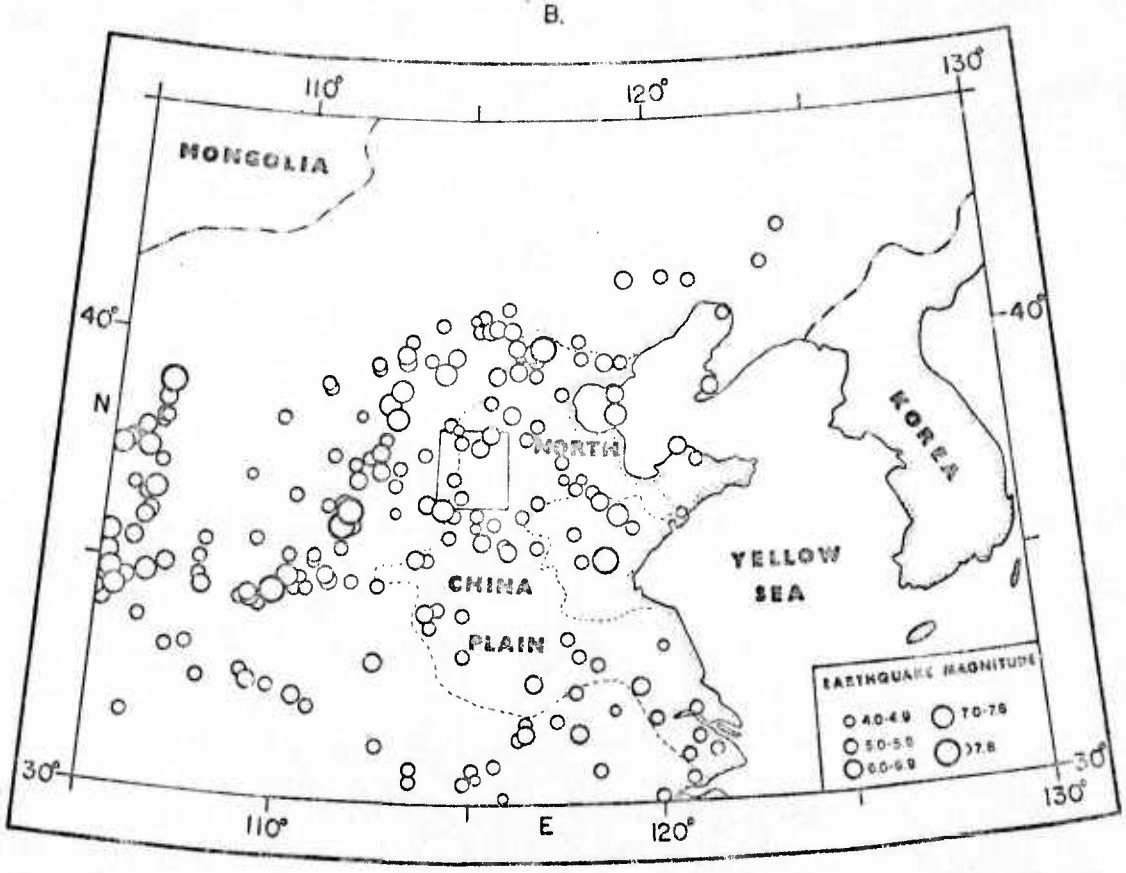
Figure 9: Cross-sections parallel (left) and perpendicular (right) to the trend of the 1966 microearthquake epicenters of Figure 8B.


SEISMICITY
OF
CHINA & SURROUNDING REGIONS
1904 – Feb 1975
0 200 400 600 800 1000 KILOMETRES
0 200 400 600 MILES
Magnitude
< 4.0
4.0-4.9
5.0-5.9
6.0-6.9
7.0-7.8
> 7.8
Depth of Focus
0-70 km
71-300 km
301-700 km

A.


110°
120°
130°
MONGOLIA
YIN MOUNTAINS
40°
N
ORDOS DESERT
LU-LIANG MOUNTAINS
SHANXI
GRABEN
FEN-HO GRABEN
SYSTEM
TSINLING MOUNTAINS
14 EVENTS
CHEKIANG MOUNTAINS
PEKING
GULF OF CHILI
NORTH
45 EVENTS
CHINA
PLAIN
TAI MTN
KOREA
YELLOW SEA
TA-PIEH MOUNTAINS
QUATERNARY FAULTS
NORMAL FAULT
UNCLASSIFIED FAULT
EARTHQUAKE MAGNITUDE
<4.0
4.0-4.9
5.0-5.9
6.0-6.9
7.0-7.8
>7.8
30°
E

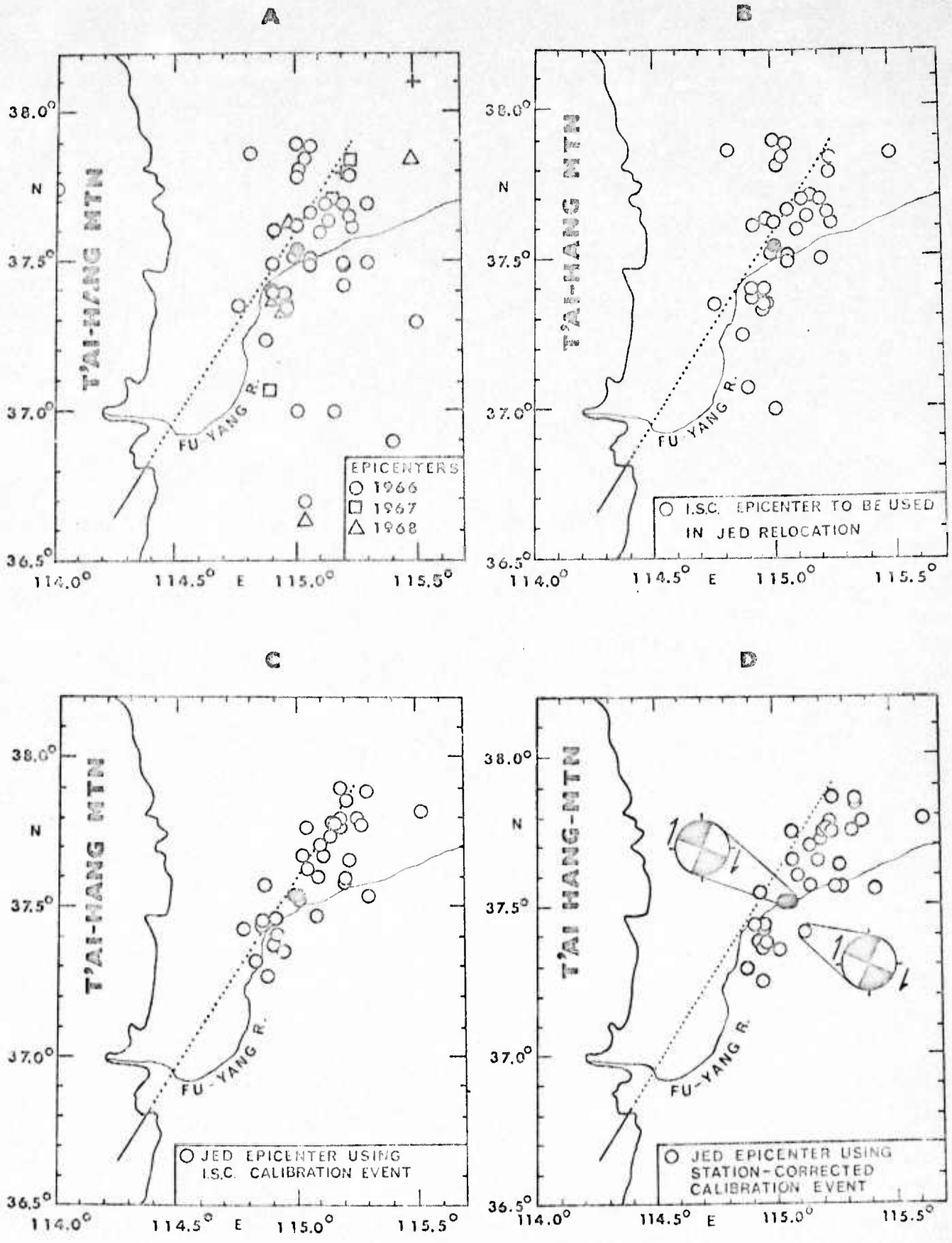
B.

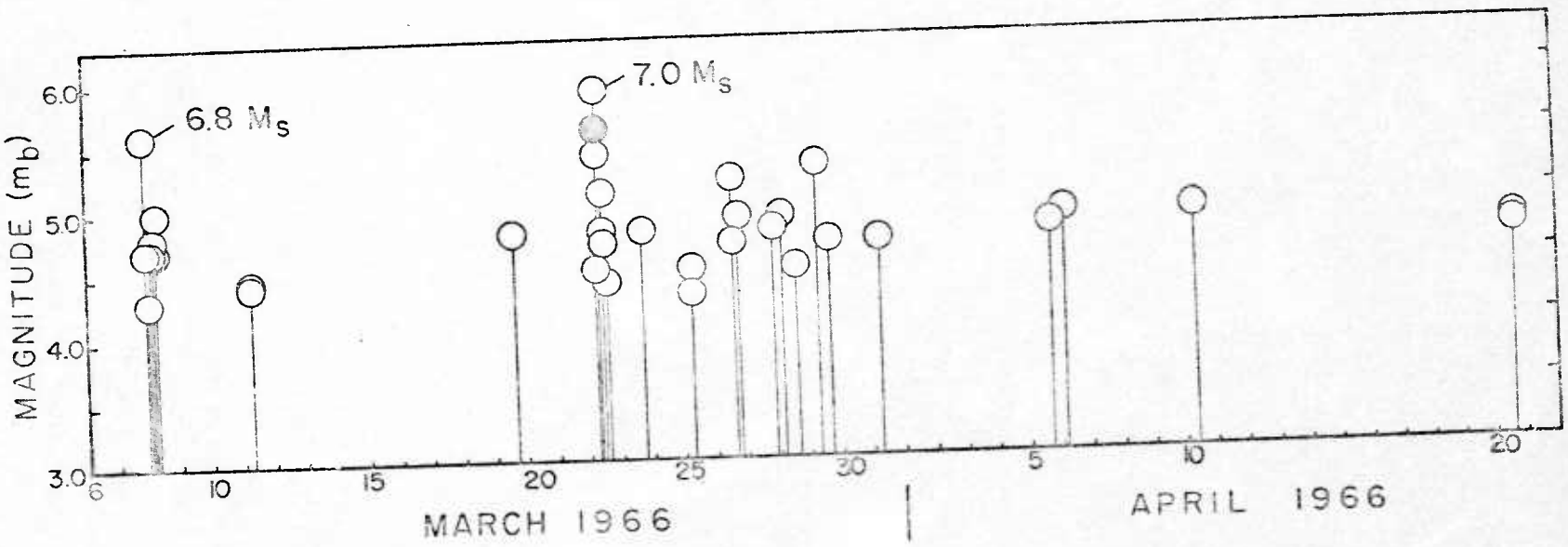

110°
120°
130°
MONGOLIA
40°
N
NORTH
CHINA
PLAIN
KOREA
YELLOW SEA
EARTHQUAKE MAGNITUDE
4.0-4.9
5.0-5.9
6.0-6.9
7.0-7.8
>7.8
30°
E

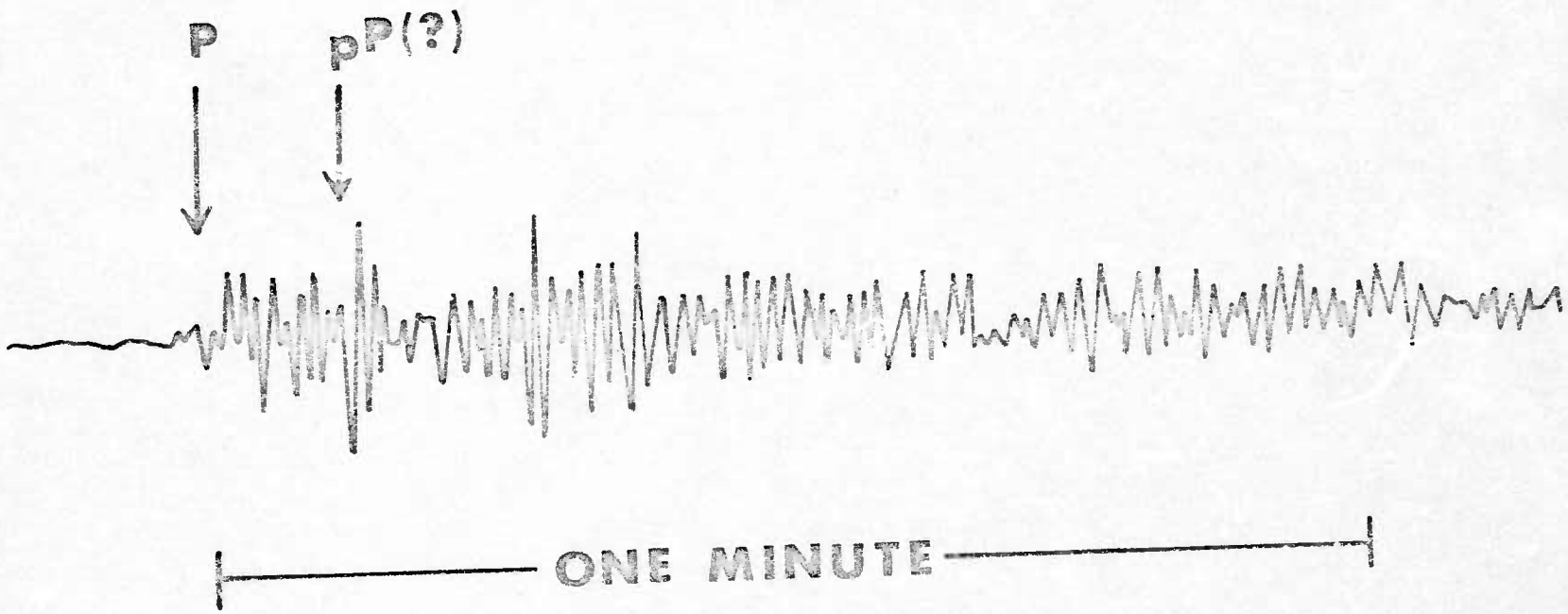
T'AI-HANG MOUNTAINS

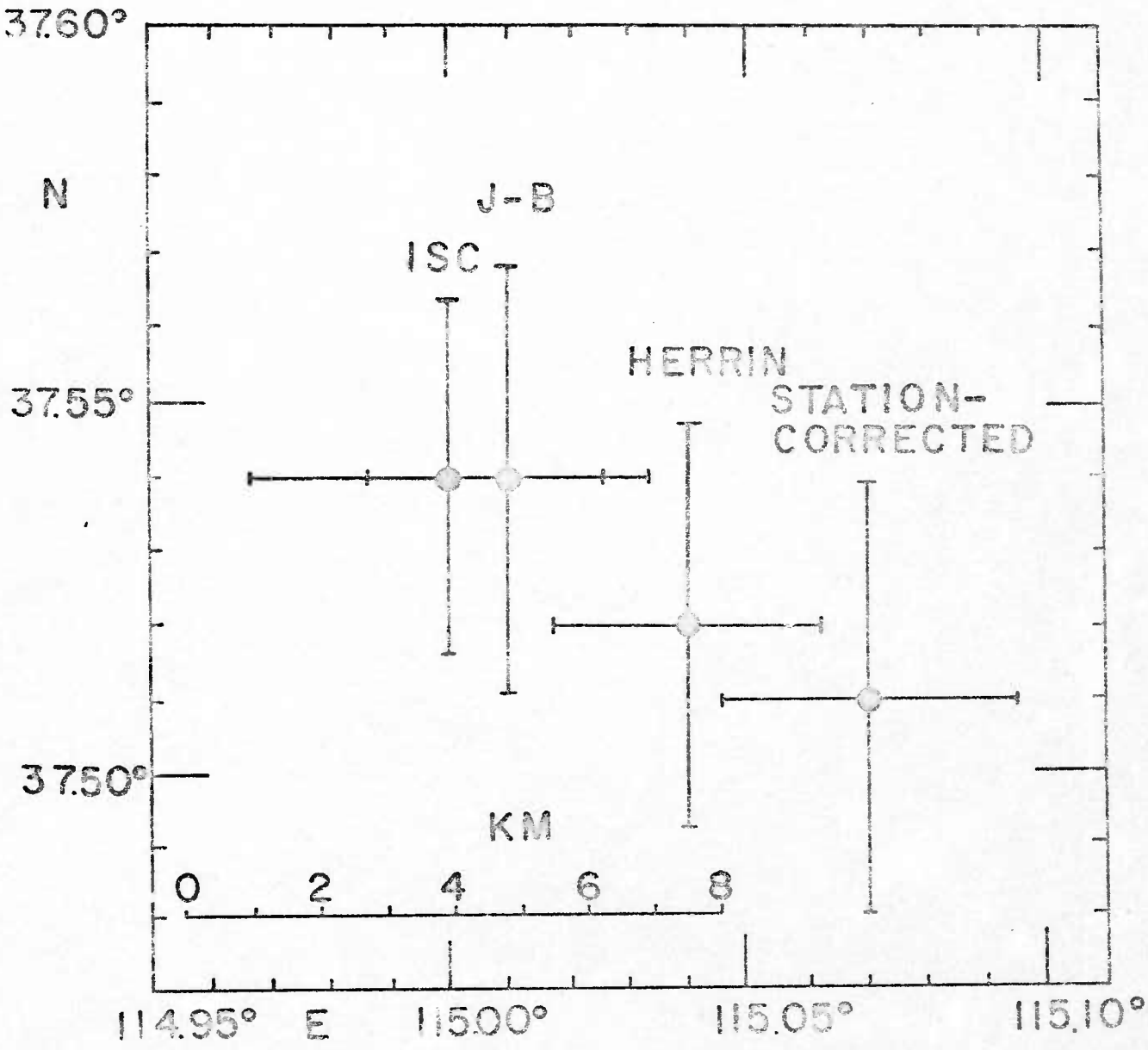
HSING-T'AI

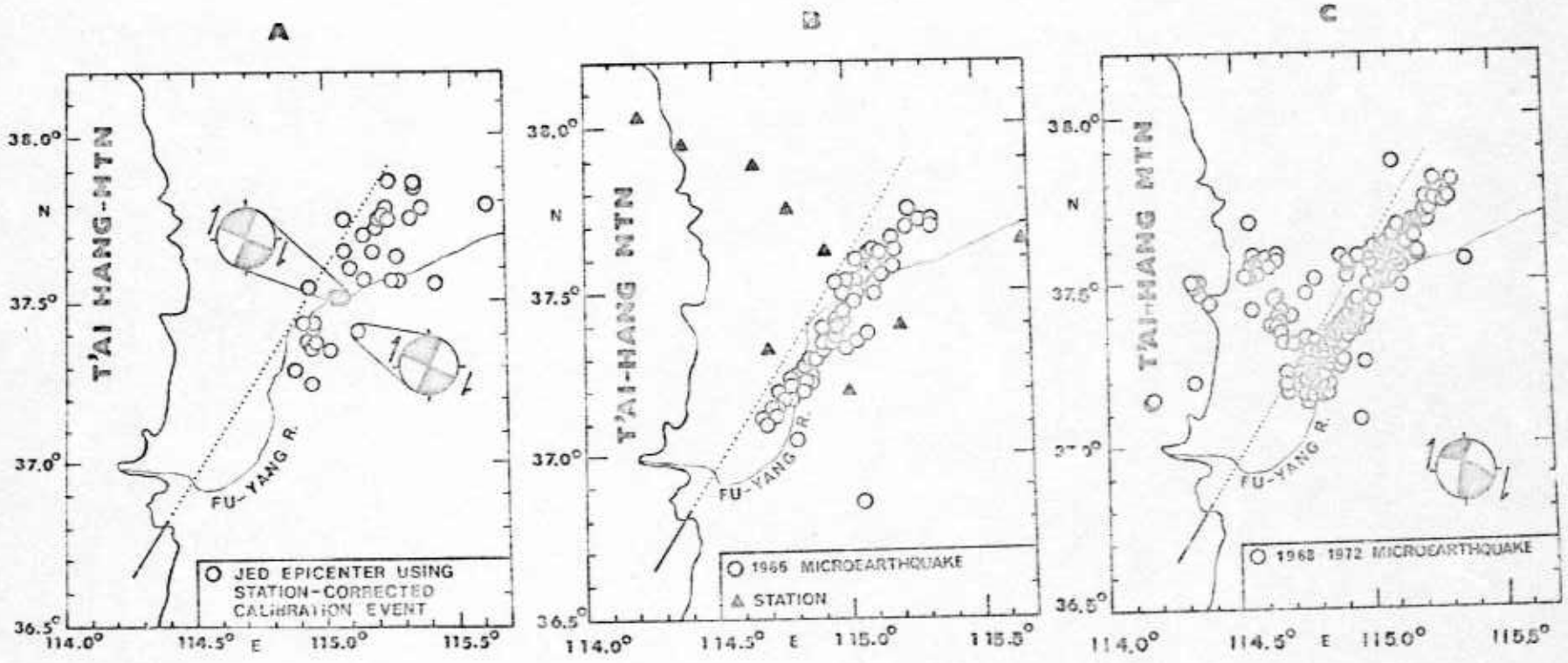
0 25 50 km.

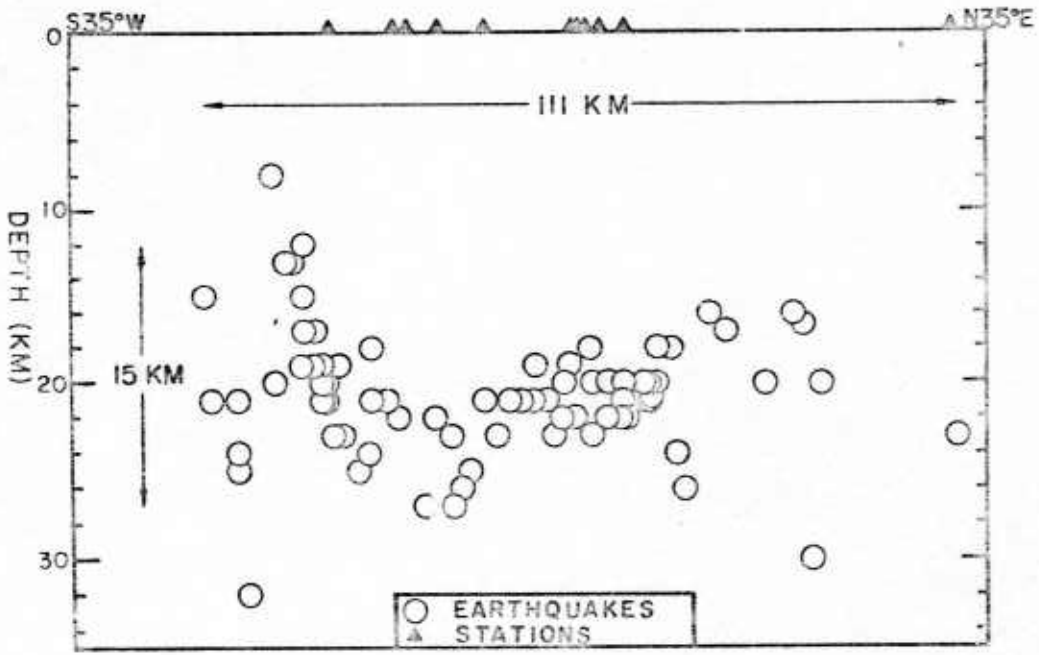

A
B
C
D
T'AI-HANG MTN
FU YANG R.
38.0°
37.5°
37.0°
36.5°
N
114.0°
114.5°
E
115.0°
115.5°
EPICENTERS
1966
1967
1968
I.S.C. EPICENTER TO BE USED IN JED RELOCATION
JED EPICENTER USING I.S.C. CALIBRATION EVENT
JED EPICENTER USING STATION-CORRECTED CALIBRATION EVENT

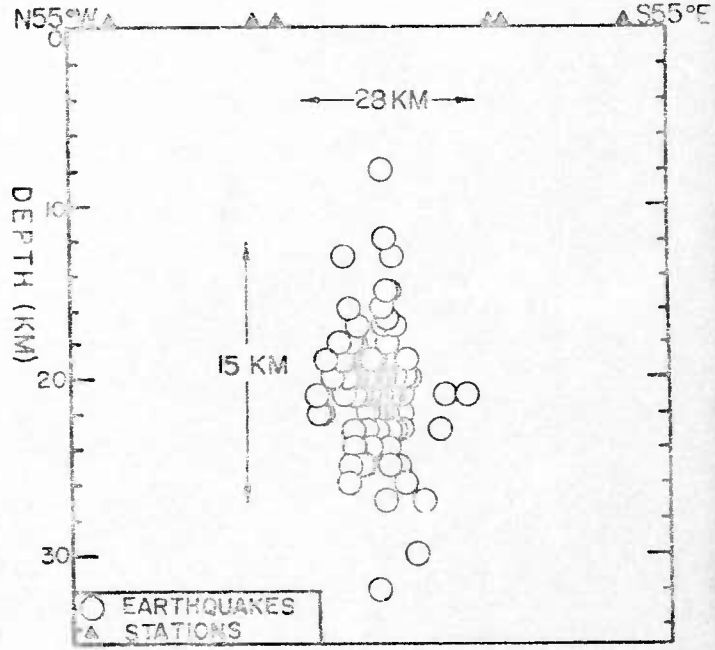

6.8 M_S
7.0 M_S
MAGNITUDE (m_b)
6.0
5.0
4.0
3.0
6
10
15
20
25
30
5
10
20
MARCH 1966
APRIL 1966


P
pP(?)
ONE MINUTE


37.60°
N
J-B
ISC
HERRIN
37.55°
STATION-
CORRECTED
37.50°
KM
0
2
4
6
8
114.95° E
115.00°
115.05°
115.10°


A
B
C
T'AI HANG-MTN
FU-YANG R.
38.0°
N
37.5°
37.0°
36.5°
114.0°
114.5°
E
115.0°
115.5°
JED EPICENTER USING STATION-CORRECTED CALIBRATION EVENT
1965 MICROEARTHQUAKE
STATION
1968 1972 MICROEARTHQUAKE


S35°W
N35°E
0
10
20
30
111 KM
15 KM
DEPTH (KM)
EARTHQUAKES
STATIONS


N55°W
S55°E
0
10
20
30
28 KM
15 KM
DEPTH (KM)
EARTHQUAKES
STATIONS

APPENDIX H

QUATERNARY FAULTING IN EASTERN TAIWAN

James E. York

Department of Geological Sciences

Cornell University

Kimball Hall

Ithaca, New York 14853

ABSTRACT

The Longitudinal Valley of eastern Taiwan probably marks the suture of a late Cenozoic collision between an island arc and the Asian continent. At present, the Longitudinal Valley represents the main active tectonic feature of the boundary between the Eurasian and Philippine plates in Taiwan. Previously published instantaneous poles of rotation indicate that this boundary in the Taiwan region is predominantly convergent with a component of left-lateral strike-slip motion, although cases of historic surface faulting suggest that the boundary is mainly strike-slip. New geologic field work provides evidence of both convergence and strike-slip motion in the Longitudinal Valley during the Quaternary. Some convergence is apparently also occurring west of the Longitudinal Valley, resulting in uplift of the Central Range and Foothill Zone.

INTRODUCTION

The island of Taiwan, lying between the Philippine Sea and mainland China, is part of the seismically active region near the ends of the Ryukyu and Manila trenches (Figure 1). The seismicity of Taiwan is concentrated in the eastern part, although earthquakes do occur throughout the island. Known historic surface faulting in Taiwan (Figure 2) and fault plane solutions near Taiwan (Wu, 1970) indicate that the tectonics of the Taiwan region is complicated, but from the geology, one main boundary in Taiwan between the Philippine and Eurasian plates appears evident. This boundary is the Longitudinal Valley (Figure 2). One main plate boundary amid a zone of active faults of different types is typical of other seismically active areas also, such as California.

Because the Longitudinal Valley separates two geologically different mountain ranges, one of which has volcanic island arc affinities, it probably represents the suture of an island arc-continent collision (Biq, 1972). The age of this collision is late Cenozoic. Earthquakes extending to depths of 100 km beneath Taiwan (Katsumata and Sykes, 1969) probably result from subduction associated with the closing of the oceanic basin which probably once existed between the two mountain ranges. From studying large earthquakes elsewhere along the Philippine-Eurasian plate boundary to determine the pole and rate of relative rotation, Fitch (1972) concluded that this boundary in Taiwan is predominantly convergent. His conclusion is in accordance with the hypothesis that the collision is still occurring. However, surface faulting in 1951 (Hsu, 1962) showed predominantly left-lateral strike-slip faulting. To help resolve the problem of the relative importance of strike-slip versus convergent motion, new geologic field work was undertaken in 1974.

Solving this problem includes the determination of the type and age of activity of major faults in and along the Longitudinal Valley. Such a study is important for evaluating seismic risk (Allen, 1975), as well as for studying the process of an island arc-continent collision (Dewey and Bird, 1970). Besides additional evidence for the strike-slip fault running through the valley, evidence for Quaternary thrusting in the southern part of the valley along a fault that may represent the main surface expression of a subduction zone was found.

GEOLOGY OF TAIWAN

The geology of Taiwan has recently been reviewed by Ho (1967), and only a brief summary will be given here. The island is separated from mainland China by the shallow (less than 100 m depth) Taiwan Straits. Taiwan consists of four main geologic provinces (Figure 2). The Coastal Range consists of Miocene andesites (Tuluanshan Formation), Miocene-Pliocene flysch (Chimei and Takangkou Formations), a Plio-Pleistocene melange (Lichi Formation) that contains exotic blocks interpreted as fragments of oceanic lithosphere, and a Plio-Pleistocene conglomerate (Pinanshan conglomerate) with clasts from the Central Range. These rock units differ considerably from most of the other rock units in Taiwan. The andesites and melange probably represent island arc volcanics and trench deposits, respectively. Eastward dipping thrust faults within the Coastal Range and the sharp boundary between the Coastal and Central Ranges together with the presence of the andesites and melange suggest that an oceanic basin once existed between the two ranges and that this basin was consumed in a subduction zone dipping eastward beneath the Coastal Range. Plate tectonic models with such an interpretation have been presented by Biq (1972), Chai (1972), and Karig (1973), although alternative interpretations, with a subduction zone dipping westward beneath the Coastal Range, have been

given by Jahn (1972) and Murphy (1973). A gravity profile across Taiwan supports the concept of an eastward dipping subduction zone (Lu and Wu, 1974). Intermediate depth earthquakes occur beneath Taiwan (Katsumata and Sykes, 1969; M.T. Hsu, 1971) but do not define a clear direction of dip, perhaps because subduction is presently occurring over a wide zone.

The Central Range contains a schist belt overlain by Paleogene slates and quartzites. The schist belt contains greenschist, marble, black schist, siliceous schist, and migmatite. Deformed fossils in the schists gives a Permo-Triassic age (Yen, 1954). Two K/Ar dates on mica give ages of 33 and 86 million years (Yen and Rosenblum, 1963), but the ages may be affected by subsequent thermal events. The topography of the Central Range is rugged and steep, despite the high rainfall and abundance of weak schists and slates. The topography probably indicates rapid Plio-Pleistocene and Recent uplift.

The Foothill zone consists mainly of Miocene sandstones and shales and Plio-Pleistocene conglomerates. The conglomerates, which are made of clasts from the Central Range, probably record the rapid uplift of that range. These conglomerates are both overlain and underthrust by the Quaternary sediments of the Coastal Plain.

LONGITUDINAL VALLEY

The linearity, narrowness, and low elevation of the Longitudinal Valley make it prominent on satellite imagery (Figure 3). In addition to this peculiar morphology, the Longitudinal Valley has exceptional thicknesses of alluvium. Thicknesses of about 2 km have been measured by seismic refraction along the western side of the valley (Tsai et al., 1974). Alluvium in the center may well be thicker. Along most of the valley,

alluvium separates the Central and Coastal Ranges by a few kilometers. Spectacular bare alluvial fans are visible on the satellite imagery (Figure 3), as well as on aerial photography (Figure 5).

At a few localities, possible contacts between the two ranges have been described. Yen (1965) described a locality near Juisui (Figure 4) where rocks of the Central Range overthrust young sediments, but these sediments show no clear resemblance to rocks of the Coastal Range. Hsu (1956) reported an outcrop or possibly a large boulder of schist near Fuli (Figure 4) within a few meters of exposures of rocks of the Coastal Range, but the contact relation could not be determined. Only in the southernmost part of the valley do the alluvial deposits narrow sufficiently for geologic contacts to be exposed and traceable across the alluvium (Figure 6).

Quaternary Fault Movements

The seismicity (Figure 1) suggests that eastern Taiwan is the most tectonically active part of Taiwan. Left-lateral strike-slip faulting (Figure 2 and F1 and F2 in Figure 4) in the Longitudinal Valley occurred during two earthquakes in 1951 (Hsu, 1962). The one reported measured strike-slip displacement was 1.63 m (Hsu, 1962). In addition to strike-slip faulting, a smaller component of vertical faulting, with the east side moving up relative to the west side, was observed at some localities in 1951. The exposed fault planes were nearly vertical. Re-triangulation showed average left-lateral movement of 3.65 m across the northern part of the Longitudinal Valley between surveys in 1971 and 1909-1942 (Chen, 1974). Hsu (1962) also described a linear scarp near Chihshang (F3 in Figure 4) with water ponded on the west side. This scarp, preserved at a drainage divide, probably represents Quaternary faulting. The high seismicity, surface

faulting, and linearity of the Longitudinal Valley are evidence for a continuous major strike-slip fault running through the valley (Allen, 1962).

To complement the field work, aerial photographs were examined during this study. In the northern third of the Coastal Range and a few kilometers east of the Longitudinal Valley, another strike-slip fault appears on air photos (Figure 5 and F4 in Figure 4). The main river in this section of the Longitudinal Valley flows northward, yet many westward flowing tributaries are offset to the south (as viewed from upstream). Such offsets are suggestive of Quaternary left-lateral strike-slip movement. The linear trace of the fault across the varying topography indicates that the fault plane is nearly vertical. Although no historic movement on this fault has been documented, it probably is part of an active system of strike-slip faulting in eastern Taiwan.

In addition to strike-slip faulting, evidence of Quaternary thrust faulting was found during this study in the southern part of the Longitudinal Valley. There a Plio-Pleistocene unit, the Pinanshan conglomerate, is exposed between the slates of the Central Range and the melange unit, the Lichi Formation, of the Coastal Range (Figure 6). The contact between the conglomerate and the melange is a thrust fault that is well exposed in river cliffs. At one locality this thrust fault cuts across a serpentine rock in the melange. At another locality, the thrust fault offsets flat-lying alluvial deposits that are probably Quaternary in age (Figure 7 and F5 in Figure 4). Because this fault separates two widely different rock units, a conglomerate with clasts derived from the Central Range and a melange probably from an oceanic trench, and because the fault offsets Quaternary alluvial deposits, it appears to be a major fault that has been

accommodating some of the convergent motion between the Philippine and Eurasian plates during the Quaternary.

West of the Pinanshan conglomerate another major fault (F6 in Figure 4) separates the conglomerate from the slates of the Central Range. A fault zone about 100 m wide is exposed at one locality, but no conclusive evidence to determine the sense of motion on the fault was found. This fault is probably a continuation of the left-lateral strike-slip fault which moved during 1951 farther north, because field work and aerial photograph investigations limit a continuous major strike-slip fault to this locality. At least several kilometers of movement has probably occurred on this fault since deposition of the Plio-Pleistocene Pinanshan conglomerate, because the source for the clasts in the Pinanshan conglomerate is not the same source which is depositing gravels presently. Besides quartzites and schists, the Pinanshan conglomerate contains marble, which is absent both from terrace gravels unconformably overlying the Pinanshan conglomerate and from Central Range rocks immediately to the west. Also, the younger terrace gravels contain predominantly slate, which is virtually absent from the older conglomerate. Thus there appear to be two major faults in the southern part of the Longitudinal Valley (Figure 6).

CONCLUSIONS

The Longitudinal Valley, remarkably linear and averaging about 4 km in width, is the major tectonic feature in eastern Taiwan. Yet alluvial fill and rapid erosion prevents unambiguous interpretations of the kind of faulting along the valley for most of its length. For example, the 1951 surface faulting occurred in the alluvium, and evidence for these breaks had been obliterated by 1974, because of the very active

erosional processes during the typhoon season. Along most of the valley the only evidence for Quaternary tectonic activity found during this study was dissected terrace gravels that have been steeply tilted at three localities (near Hualien, Juisui, and Luyeh, Figure 4) and five small hills of younger alluvium that have been tilted and dissected at the western side of the Coastal Range a few kilometers southwest of Tungli (Figure 4). Less intense erosion in western Taiwan probably accounts for the better preservation of evidence for Quaternary faulting there. Thus more Quarternary faults are found there than in eastern Taiwan (Bonilla, 1975), although the seismicity (Figure 1) indicates that eastern Taiwan is more active tectonically.

Only in the southernmost part of the valley were fault zones between major rock units seen. The thrust of the Lichi melange of the Coastal Range over the Pinanshan conglomerate, derived from the Central Range, and Quaternary alluvial deposits may represent the boundary of the island arc-continent collision. Although no historic earthquakes can definitely be attributed to this thrust, its Quaternary activity suggests that it may be a potentially active fault (Allen, 1975). The zone of collision is not simple, however, and certainly strike-slip faulting has been occurring also. The existence of a thrust fault and a probable strike-slip fault, both possibly active, spaced only a few kilometers apart (Figure 6) raises interesting questions about how they were generated, how continued activity might affect the morphology of the Longitudinal Valley, what happens at depth, and what happens farther north in the valley. At present, any answers to these questions are mainly speculative, and hence only possibilities are suggested here.

Fitch (1972) has proposed a simple model that accommodates oblique subduction by two faults, a thrust and a vertical strike-slip fault, instead of one dipping fault with oblique motion. If such a model is applicable to Taiwan, the generation of both types of faults may be explained. Whether continued thrusting will decrease the width and increase the elevation of the longitudinal Valley or not largely depends on the rate of erosional processes. Small incremental movements of the Coastal Range westward relative to the Central Range can easily be compensated for by erosion, thereby keeping the width of the valley nearly constant. However, in the southern part of the valley the surface trace of the thrust is in some places west of the main river running south through this part of the valley (Figure 6), and thus there the valley might be closing. Answers regarding what happens to the faults at depth and what type of rocks exist between the faults at depth must depend on further detailed geophysical work on land, some of which is in progress (C.P. Lu, personal communication, 1975), as well as further work on the nearby marine geology. No exposures of either the thrust fault or the strike slip fault were found north of the area in Figure 6; thus their true extent is still an oper question.

Not all of the convergent motion in Taiwan between the Philippine and Eurasian plates has been taking place in the Longitudinal Valley. The geology and seismicity of the Central Range plus the fault plane solution by Wu (1970) suggest that thrusting is also occurring there. The geologic evidence supports eastward dipping thrusts there, although right-lateral strike-slip faulting, nearly conjugate to the left-lateral faulting in the Longitudinal Valley, has also occurred near the Central Range during historic earthquakes (Figure 2). Subsequent crustal thickening and isostatic uplift may be responsible for the high topography of the Central Range.

ACKNOWLEDGMENTS

Appreciation is expressed to Biq Chingchang, T. L. Hsu, Hui-Cheng Chang, H. N. Hu, and Hsein-Ching Chang, all of the Geological Survey of Taiwan, for collaboration in doing the field work. Beneficial discussions were held with Y. B. Tsai and Chih-Ping Lu of the Chinese Earthquake Research Center. The manuscript was reviewed by M. Barazangi, D. Karig, J. Oliver, and F.T. Wu. This research was supported by the United States-Republic of China Cooperative Science Program of the National Science Foundation under Grant Number OIP-7419400 and by the Advanced Research Projects Agency of the Department of Defense and was monitored by the Air Force Office of Scientific Research under Contract Number AFOSR-73-2494. Cornell University Department of Geological Sciences Contribution Number 566.

REFERENCES CITED

Allen, C.R., 1962, Circum-Pacific faulting in the Philippines-Taiwan region: J. Geophys. Res., v. 67, p. 4795-4812.

Allen, C.R., 1975, Geological criteria for evaluating seismicity: Geol. Soc. Amer. Bull., v. 86, p. 1041-1057.

Biq, Chingchang, 1972, Dual-trench structure in the Taiwan-Luzon region: Geol. Soc. China Proc., no. 15, p. 65-75.

Biq, Chingchang, 1974, Taiwan, in Spencer, A.M., ed., Mesozoic-Cenozoic Orogenic Belts, Geological Society, London, p. 501-511.

Bonilla, M.G., 1975, A review of recently active faults in Taiwan: Open File Report 75-41, U.S. Geol. Surv., Menlo Park, Calif., 58 p.

Chai, B.H.T., 1972, Structure and tectonic evolution of Taiwan: Amer. J. Sci., v. 272, p. 389-422.

Chang, L.S., Chow, M., and Chen, P.Y., 1947, The Tainan earthquake of December 5, 1946: Taiwan Geol. Surv. Bull., no. 1, p. 11-20.

Chen, C.Y., 1974, Verification of the north-northeastward movement of the Coastal Range, eastern Taiwan, by retriangulation: Taiwan Geol. Surv. Bull., no. 24, p. 119-123.

Dewey, J.F., and Bird, J.M., 1970, Mountain belts and the new global tectonics: J. Geophys. Res., v. 75, p. 2625-2647.

Fitch, T.J., 1972, Plate convergence, transcurrent faults, and internal deformation adjacent to southeast Asia and the western Pacific: J. Geophys. Res., v. 77, p. 4432-4460.

Ho, C.S., 1967, Structural evolution of Taiwan: Tectonophysics, v. 4, p. 367-378.

Hsu, M.T., 1971, Seismicity of Taiwan and some related problems: Internatl. Inst. of Seismology and Earthquake Eng. Bull., v. 8, p. 41-160.

Hsu, T.L., 1956, Geology of the Coastal Range, Taiwan: Taiwan Geol. Surv. Bull., no. 8, p. 39-63.

Hsu, T.L., 1962, Recent faulting in the Longitudinal Valley of eastern Taiwan: Geol. Soc. China Mem., no. 1, p. 95-102.

Jahn, B.M., 1972, Re-interpretation of geologic evolution of the Coastal Range, east Taiwan: Geol. Soc. Amer. Bull., v. 83, p. 241-248.

Karig, D.E., 1973, Plate convergence between the Philippines and the Ryukyu Islands: Marine Geology, v. 14, p. 153-168.

Katsumata, M., and Sykes, L.R., 1969, Seismicity and tectonics of the western Pacific: Izu-Mariana-Caroline and Ryukyu-Taiwan regions: J. Geophys. Res., v. 74, p. 5923-5948.

Lu, C.P., and Wu, F.T., 1974, Two-dimensional interpretation of a gravity profile across Taiwan: Taiwan Geol. Surv. Bull, no. 24, p. 125-132.

Murphy, R.W., 1973, The Manila trench-west Taiwan foldbelt: a flipped subduction zone: Geol. Soc. Malaysia Bull., no. 6, p. 27-42.

Richter, C.F., 1958, Elementary Seismology, San Francisco, W.H. Freeman, 768 pp.

Tsai, Y.B., Teng, T.L., Ysiung, Y.M., and Lo, C.M., 1973, New seismic data of Taiwan region: Inst. of Physics, Academia Sinica, Ann. Rept., p. 223-237.

Tsai, Y.B., Hsiung, Y.M., Liaw, H.B., Lueng, H.P., Yao, T.H., Yeh, Y.H., and Yen, Y.T., 1974, A seismic refraction study of eastern Taiwan: Petroleum Geology of Taiwan, no. 11, p. 165-182.

Wu, F.T., 1970, Focal mechanisms and tectonics in the vicinity of Taiwan: Seism. Soc. Amer. Bull., v. 60, p. 2045-2056.

Yen, T.P., 1954, Some problems on the Tananao schist: Taiwan Geol. Surv. Bull., no. 7, p. 47-50.

Yen, T.P., 1965, A thrust fault near Juisui, eastern Taiwan: Geol. Soc. China Proc., no. 8, p. 97-99.

Yen, T.P., and Rosenblum, S., 1963, Potassium-argon ages of micas from the Tanano-schist terrain of Taiwan: Geol. Soc. China Proc., no. 7, p. 80-87.

FIGURE CAPTIONS

Figure 1: Seismicity of the Taiwan region, 1961-1972. Circles represent hypocenters less than 70 km deep; squares, 70-300 km deep. Epicenters redrawn from Tsai et al. (1973). Trench depths in km.

Figure 2: Geologic provinces of Taiwan (from Ho, 1974). Also shown are known cases of historic surface faulting (data from Chang et al., 1947; Richter, 1958; Hsu, T.L., 1962). Elevations of highest peaks in Central and Coastal Ranges in meters.

Figure 3: Mosaic of Landsat-I imagery of Taiwan. Imagery of MSS band 5, taken 1 November 1972.

Figure 4: Longitudinal Valley, Coastal Range, and part of Central Range. Fault localities are referenced in text. Contours at 400, 1000, 2000 and 3000 m.

Figure 5: Vertical aerial photograph of a fault (arrows) showing left-lateral stream offsets in the northern part of the Coastal Range. A part of the Longitudinal Valley is in the western half of the photograph; some hills of the Central Range are visible along parts of the western edge of the photograph. Fenglin (Figure 4) is in the southwestern quarter of the photograph.

Figure 6: Geologic map of the southern portion of the Longitudinal Valley. Qal - alluvium, PQp - Pinanshan Conglomerate, PQl- Lichi Formation, MPs - Chimei Formation, Ml - limestone,

Mt - Tuluanshan Formation, Eo - slate and quartzite. See text and T. L. Hsu (1956) for descriptions of rock units. The contacts between Eo and PQp and between PQp and PQl are faults, dashed where approximate and dotted where concealed. Elevations are in meters.

Figure 7: Thrust fault (arrows) separating Lichi Formation (hanging wall) from Pinanshan conglomerate and overlying alluvial deposits (footwall). Distance from top to bottom is about 5 meters.

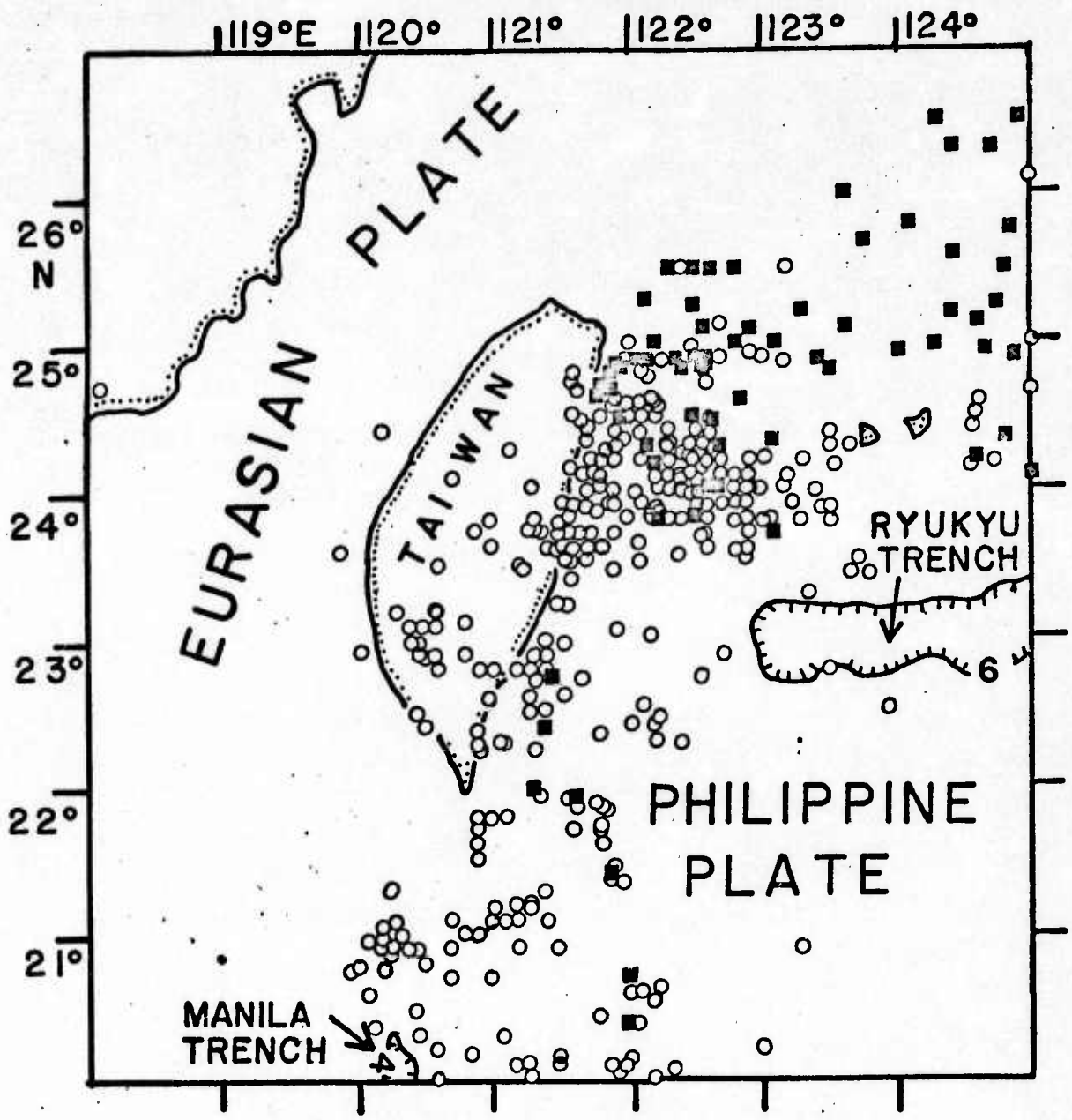

119°E
120°
121°
122°
123°
124°
26° N
25°
24°
23°
22°
21°
EURASIAN PLATE
TAIWAN
RYUKYU TRENCH
PHILIPPINE PLATE
MANILA TRENCH

Fig. 1

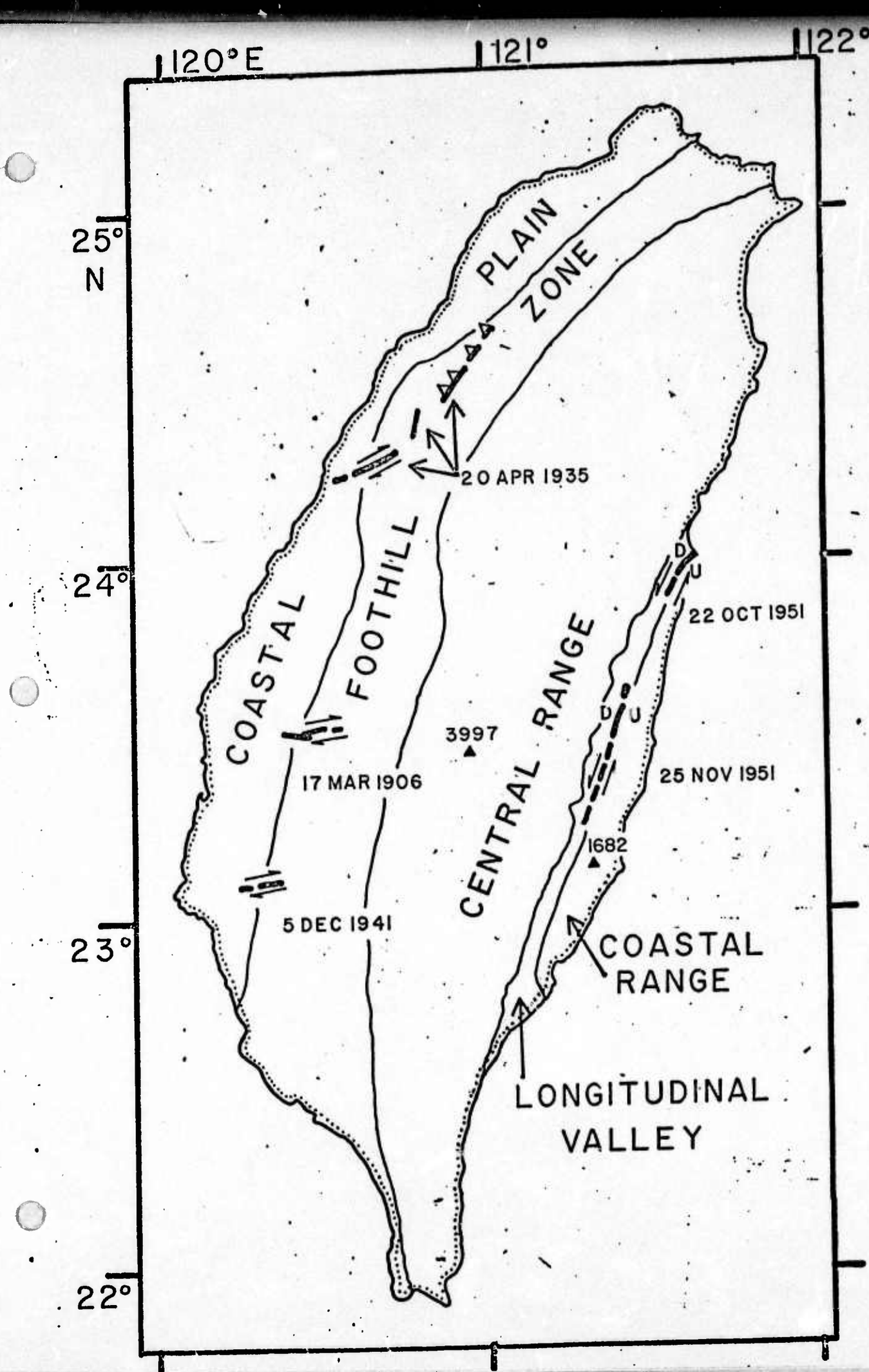

120°E
121°
122°
25° N
24°
23°
22°
PLAIN
ZONE
20 APR 1935
COASTAL
FOOTHILL
CENTRAL RANGE
22 OCT 1951
3997
17 MAR 1906
25 NOV 1951
1682
5 DEC 1941
COASTAL RANGE
LONGITUDINAL VALLEY

Fig. 2



Fig. 3

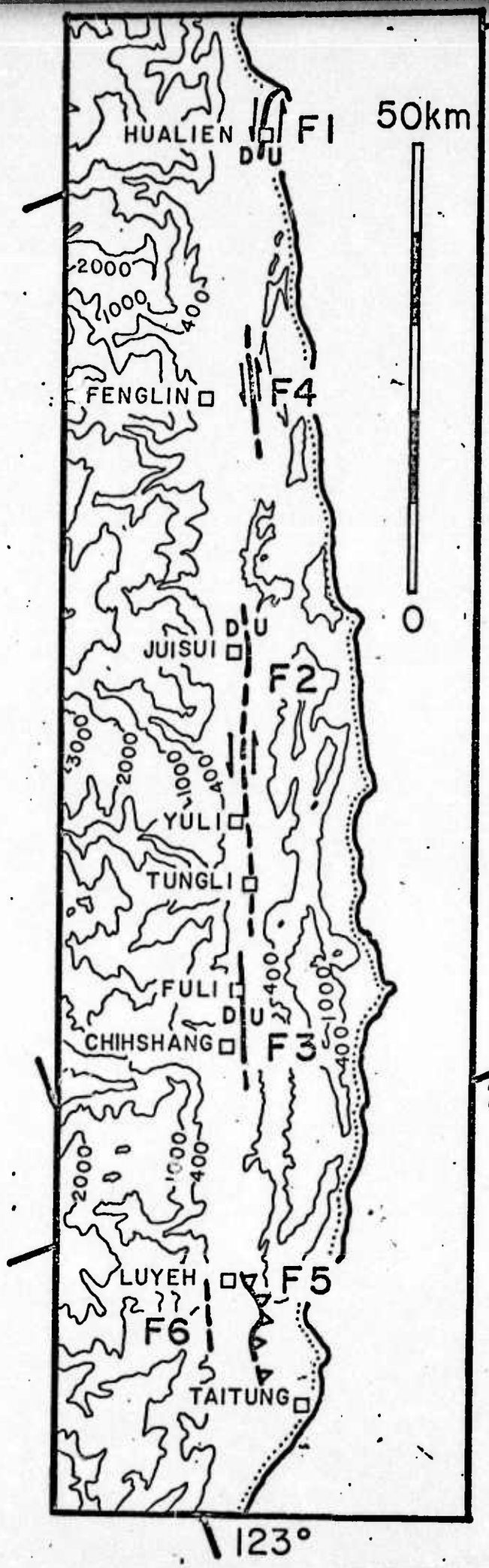

24°
HUALIEN
F1
D
U
50km
2000
1000
400
FENGLIN
F4
0
JUISUI
D
U
F2
3000
2000
1000
400
YULI
TUNGLI
FULI
D
U
400
1000
CHIHSHANG
F3
400
23°
2000
1000
400
LUYEH
F5
F6
TAITUNG
123°

Fig. 4

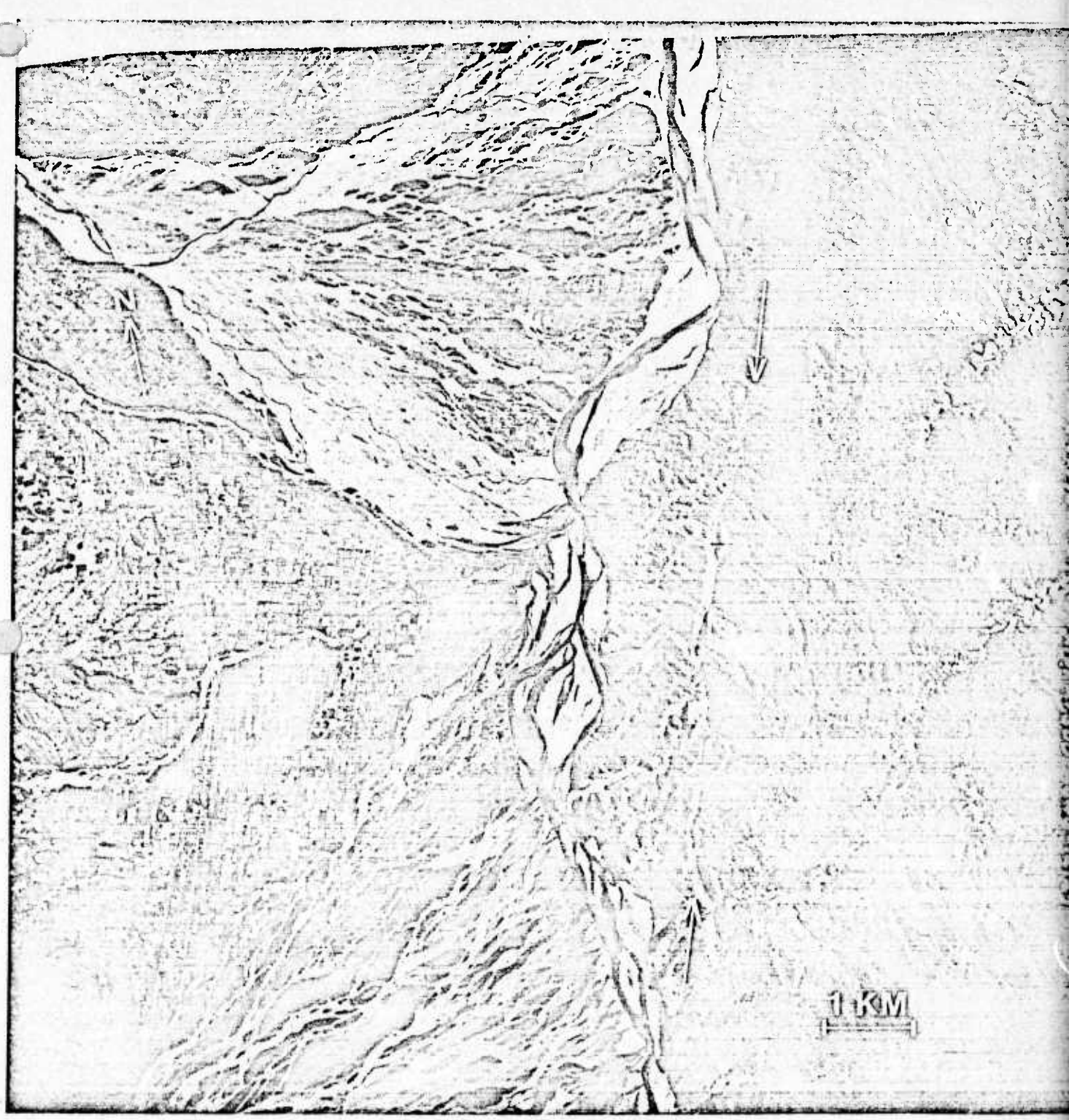


Fig. 5.

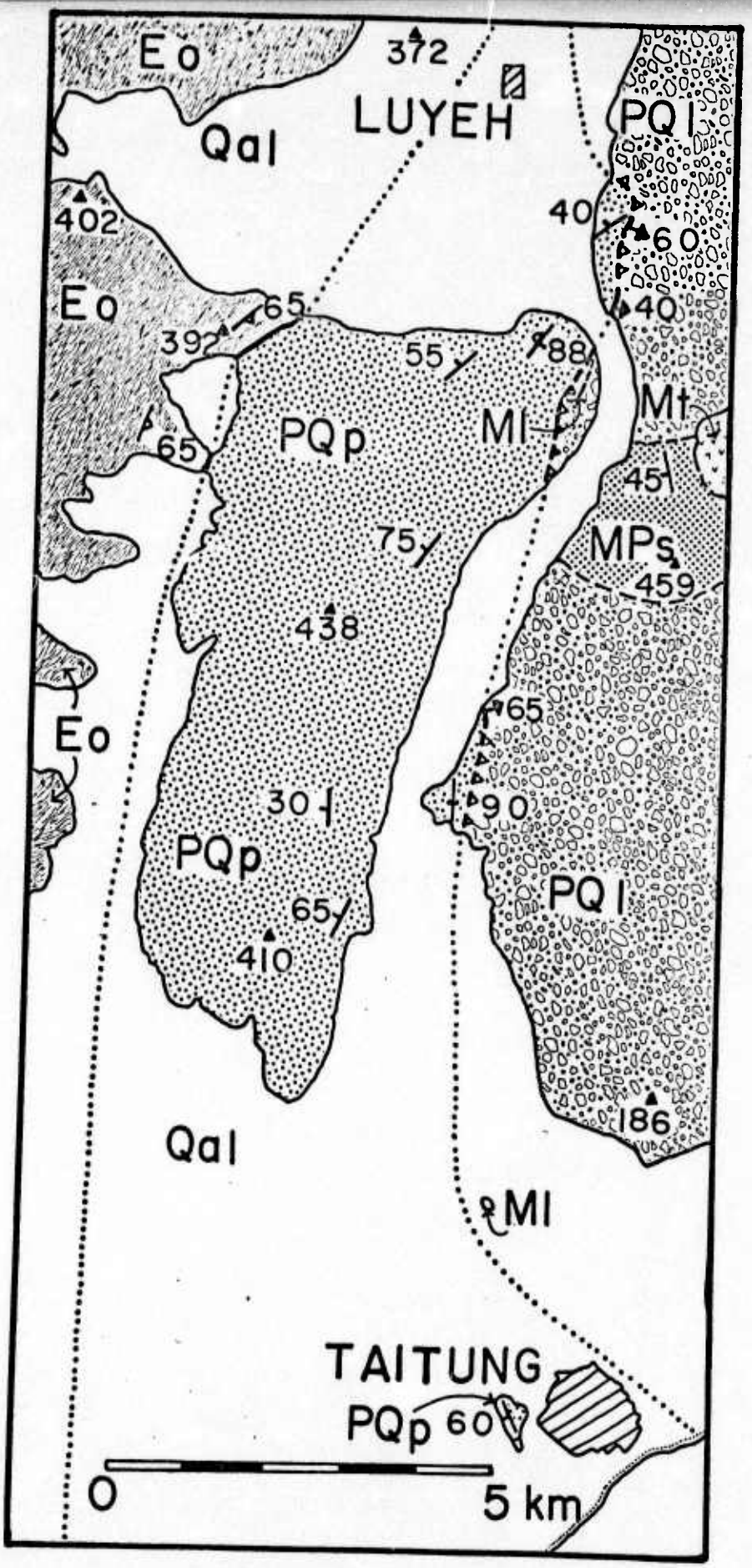

Eo
372
LUYEH
PQl
Qal
402
40
60
Eo
65
40
392
55
88
Mt
MI
PQp
65
45
75
MPs
459
438
Eo
65
90
30
PQp
PQl
65
410
186
Qal
MI
TAITUNG
PQp
60
0
5 km

Fig. 6

Fig. 7